

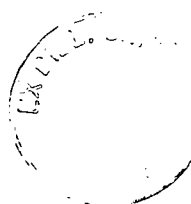
Identification of the Nitrite Reductase
from *Neisseria subflava* B19

Joanne M. Thomas

Thesis presented for the degree of Doctor of Philosophy

University of Edinburgh

September, 1998



Declaration

Except where specific reference is made to other sources, the work presented in this thesis is the original work of the author. It has not been submitted, in whole or in part, for any other degree.

Joanne M. Thomas

Acknowledgements

I have had the good fortune to work with many people throughout my Ph.D. and I would like to take this opportunity to thank them.

First and foremost I would like to thank my supervisor, Dr Bruce Ward, for his guidance and encouragement throughout my time in the lab.

Thanks are also warmly extended to past and present members of the Ward group for their friendship and good humour, namely Karen, Jason and Richard. Special thanks go to Pam whose help when I first arrived in the lab was invaluable.

For help with the *aniA* PCR I am extremely grateful to Carey Lambert, and for checks on the growth requirements of *N. subflava* strains, thank you to Darryl Lisk-Carew.

I am extremely grateful to my parents for their patience, understanding and financial assistance, particularly during the past twelve months. Without their help I would not be where I am today.

I would like to express thanks to all the people who have made my time in Edinburgh so memorable; in ICMB Darren and Simone, Anthony and Berry, Theo and Emma, Dave B and across the 'pond' in LA Dr Craig Draper and Harriet; in chemistry, Ally T and Kathy, Gideon and Vicki. Thanks also go to the many members of ICMB whom I have badgered for help and advice throughout my time in Edinburgh.

Finally, my most profound thanks go to Nick, whose constant love and support has kept me sane during the many ups and downs encountered whilst completing this work.

Table of Contents

Declaration	ii
Acknowledgements	iii
Table of Contents	iv
List of Figures	xi
List of Tables	xvii
List of Graphs	xviii
Abbreviations	xix
Abstract	xxi

Chapter One - Introduction

1.1 Denitrification	1
1.2 Denitrification gene clusters	4
1.3 Nitrate reductase	9
1.3.1 Assimilatory nitrate reductases	9
1.3.2 Periplasmic dissimilatory nitrate reductase	10
1.3.3 Membrane bound dissimilatory nitrate reductase	11
1.3.3.1 The molybdenum cofactor	12
1.3.3.2 The iron sulphur centres	14
1.3.3.3 The transmembrane (γ) subunit	14
1.3.3.4 Genes encoding nitrate reductase	16
1.4 Nitrite reductase	17
1.4.1 The product of the copper and cytochrome cd_1 nitrite reductases	18
1.4.2 Cytochrome cd_1 nitrite reductase	19
1.4.2.1 The molecular structure	19
1.4.2.2 Roles of the c-type and d_1 haems	23
1.4.2.3 The cytochrome cd_1 genes	26

1.4.3	Copper nitrite reductase	26
1.4.3.1	Biological copper centres	27
1.4.3.2	The molecular structure	27
1.4.3.3	Roles of the type I and type II copper centres	31
1.4.3.4	The copper nitrite reductase genes	33
1.4.3.5	A membrane bound copper nitrite reductase?	33
1.4.4	Electron donation to the cytochrome cd_1 and copper nitrite reductases	36
1.4.4.1	Mechanism of electron donation	37
1.5	Nitric oxide reductase	38
1.5.1	Molecular properties of nitric oxide reductase	39
1.5.2	The catalytic mechanism	42
1.5.3	Is the nitric oxide a proton pump?	42
1.5.4	Nitric oxide reductase genes	43
1.6	Nitrous oxide reductase	44
1.6.1	The electron transfer (Cu_A) centre	45
1.6.2	The catalytic (Cu_Z) centre	47
1.6.3	Electron transfer between the Cu_A and Cu_Z centres	49
1.6.4	Assembly of the copper centres	49
1.7	Electron transport chains	51
1.7.1	Topology of the denitrification pathway	52
1.7.2	Transport of nitrate and nitrite across the cytoplasmic membrane	57
1.8	Control of denitrification	58
1.8.1	Regulation of gene expression	58
1.8.1.1	FNR mediated regulation	59
1.8.1.2	N-oxide regulation of denitrification gene expression	62
1.9	Cancer of the stomach	66
1.9.1	Background	66
1.9.2	Nitrate, nitrite and <i>N</i> -nitroso compounds in food	66

1.9.3 Stomach cancer and achlorhydria - a hypothesis	68
1.9.4 Bacterial flora in the achlorhydric stomach	71
1.9.5 <i>N</i> -nitrosamine formation	72
1.9.5.1 Acid catalysed <i>N</i> -nitrosation	73
1.9.5.2 Bacterial <i>N</i> -nitrosation	75
1.9.6 Inhibition of <i>N</i> -nitrosation	80
1.9.7 <i>Helicobacter pylori</i> and gastric cancer	82
1.10 Summary	84
1.11 Aims of this study	85

Chapter Two - Materials and Methods

2.1 Bacterial strains and growth conditions, plasmids and general materials	87
2.1.1 Laboratory suppliers	87
2.1.1.1 General laboratory chemicals	87
2.1.1.2 Enzymes	87
2.1.1.3 Isotopes	87
2.1.1.4 Oligonucleotides	88
2.1.2 Growth media and buffers	88
2.1.2.1 Growth media	88
2.1.2.2 Commonly used buffers	90
2.1.3 Selection for antibiotic resistance	91
2.1.4 Plasmids	92
2.1.5 Bacterial strains	94
2.1.6 Growth of bacterial strains	95
2.1.6.1 Growth conditions of <i>N. subflava</i> B19	95
2.1.6.2 Maintenance and growth of <i>N. subflava</i> strain 163 carrying a Tn5 insertion	96
2.1.6.3 Long term storage of bacterial cultures	97

2.2 DNA techniques	98
2.2.1 Large scale preparation of chromosomal DNA	98
2.2.2 Small scale preparation of chromosomal DNA	99
2.2.3 Large scale preparation of plasmid DNA from <i>E. coli</i>	100
2.2.4 Plasmid minipreparation by alkaline lysis	102
2.2.4.1 Chloramphenicol amplification of pACYC177 plasmids in <i>E. coli</i>	104
2.2.5 Large scale preparation of bacteriophage λ DNA	105
2.2.6 Precipitation of DNA	107
2.2.7 Determination of DNA concentration	107
2.2.8 Restriction of DNA	107
2.2.8.1 Digestion of DNA using two restriction enzymes	108
2.2.9 Dephosphorylation of DNA	108
2.2.10 Agarose gel electrophoresis of DNA	109
2.2.11 Extraction of DNA from agarose gels	109
2.2.12 Ligation of DNA fragments	111
2.2.13 Preparation and transformation of competent cells (CaCl ₂ method)	111
2.2.13.1 Blue/white selection for transformant colonies	112
2.2.14 Preparation of cells for high efficiency electro- transformation	112
2.2.15 Preparation of DNA for electroporation	113
2.2.16 Electro-transformation of ligation mixtures	114
2.2.17 DNA sequencing	114
2.2.17.1 Introduction	114
2.2.17.2 Annealing of primer to double stranded template	115
2.2.17.3 Sequencing reaction	116
2.2.17.4 DNA sequencing gel electrophoresis	117
2.2.18 Automated DNA sequencing	118
2.2.18.1 Sequence analysis	119

2.2.19	Southern blotting of DNA onto nylon filters	119
2.2.20	Preparation of labelled DNA probe	121
2.2.21	Probing nylon membranes	121
2.2.22	Colony blotting plasmid mini-libraries	124
2.2.23	Stripping probes from nylon membranes	125
2.2.24	The Polymerase Chain Reaction (PCR)	125
2.3	Protein techniques	128
2.3.1	Production of whole cell lysates	128
2.3.2	Preparation of non-denaturing polyacrylamide gels	129
2.3.3	Running non-denaturing polyacrylamide gels	130
2.3.4	Silver staining polyacrylamide gels	132
2.3.5	Coomassie brilliant blue staining polyacrylamide gels	133
2.3.6	Detection of nitrite reductase activity in non-denaturing polyacrylamide gels	134
2.3.7	Whole cell nitrite reductase assay	135
2.3.8	Nitrite reductase assay with methyl viologen	137
2.3.8.1	Use of the French press	138
2.3.9	Preparation of <i>N. subflava</i> membrane	138
2.3.10	Sarosyl extraction of <i>N. subflava</i> outer membrane	139
2.3.11	Protein determination	140
2.4	Bacteriophage λ techniques	141
2.4.1	Construction of <i>N. subflava</i> B19 and 163 λ libraries	141
2.4.1.1	Partial digestion of genomic DNA	141
2.4.1.2	Ligation of EMBL 3 vector and insert DNA	142
2.4.1.3	<i>In-vitro</i> packaging of the ligated DNA	142
2.4.1.4	Estimating the titre of the λ library	143
2.4.2	Screening <i>N. subflava</i> B19 and 163 λ libraries	144
2.4.3	Picking bacteriophage λ plaques	145
2.4.4	Preparation of plate lysates from a single plaque	146

Chapter Three - Analysis of *N. subflava* Mutant 163

3.1 Background information	148
3.1.1 Production of <i>N. subflava</i> Tn5 mutants	148
3.1.2 Preliminary subcloning from <i>N. subflava</i> mutant 163	149
3.2 Initial characterisation of <i>N. subflava</i> B19 and mutant 163 strains	152
3.2.1 Confirmation of a single Tn5 insertion in <i>N. subflava</i> mutant 163	152
3.2.2 Probing chromosomal DNA with copper and <i>cd₁</i> probes	154
3.3 Genetic analysis of pZS163	163
3.3.1 Sequence analysis	163
3.3.2 Mutant 163/pZS163 deletion characterisation	170
3.3.2.1 <i>N. subflava</i> B19 library screen with the 170bp probe	175
3.3.2.2 Deletion characterisation using pJT170	180
3.4 pJT170 sequence analysis	186
3.5 Summary	196

Chapter Four - Preliminary Nitrite Reductase Protein Analysis

4.1 Background information	198!!!!
4.2 Growth tests on <i>N. subflava</i> B19 and mutant 163	198
4.3 Native PAGE analysis of <i>N. subflava</i> B19 and mutant 163	198
4.3.1 Introduction	198
4.3.2 Cell lysis	200
4.3.3 Nitrite reductase activity stain experiments on native gels	202
4.3.3.1 Comparison of <i>N. subflava</i> B19 and mutant 163 strains	202
4.3.3.2 <i>N. subflava</i> B19 nitrite reductase activity in the presence of Triton X-100	206
4.3.3.3 Nitrite reductase activity staining on native gels in the	

presence of DDC	208
4.4 Methyl viologen nitrite reductase assay on <i>N. subflava</i> B19	209
4.5 Discussion	212
4.6 Summary	216
<u>Chapter Five - PCR Amplification of the Nitrite Reductase Gene</u>	
5.1 Background information	217
5.2 PCR strategy	218
5.2.1 Primer design	218
5.2.2 PCR results	224
5.2.3 pANIA350 sequence analysis	227
5.3 <i>N. subflava</i> B19 mini-library construction and sequencing	233
5.3.1 Sequence analysis of pANIA10	241
5.3.2 Recombination in pANIA10	249
5.4 Alternative vectors for mini-library construction	252
5.4.1 pACYC177	252
5.4.1.1. pH25 sequence analysis	256
5.4.1.2 pH25-6 sequence analysis	261
5.4.2 pASHOK	265
5.5 Cloning from λ EMBL 3	268
5.6 Further <i>nir</i> cloning strategies	275
5.6.1 Cloning into <i>E. coli</i> DL795	275
5.6.2 Cloning into <i>N. subflava</i> B19	277
5.7 Summary	279
<u>Chapter Six - Concluding Discussion</u>	281
<u>Chapter Seven - Future Work</u>	288

Bibliography	293
Appendix	315

List of Figures

Chapter One

Figure 1.1	The nitrogen cycle	2
Figure 1.2	The denitrification gene clusters of <i>Ps. stutzeri</i> , <i>Ps. aeruginosa</i> and <i>P. denitrificans</i>	6
Figure 1.3	The MGD cofactor	13
Figure 1.4	Reduction of nitrate via the molybdenum cofactor	14
Figure 1.5	Position of the membrane bound nitrate reductase	15
Figure 1.6	<i>E. coli narGHJI</i> operon for the membrane bound nitrate reductase	16
Figure 1.7	X-ray structure of cytochrome cd ₁ nitrite reductase from <i>T. pantotropha</i>	21
Figure 1.8	Cytochrome cd ₁ nitrite reductase peptide alignment	22
Figure 1.9	A reaction scheme for cytochrome cd ₁ nitrite reductase	25
Figure 1.10	Molecular structure of the copper nitrite reductase	29
Figure 1.11	Copper nitrite reductase peptide alignment	30
Figure 1.12	Model of the proposed mode of nitrite binding at the subunit interface of nitrite reductase	32
Figure 1.13	Sequence alignment of the copper nitrite reductase from <i>Al. faecalis</i> and AniA from <i>N. gonorrhoeae</i>	35
Figure 1.14	Proposed electron transfer complex between the copper nitrite reductase and pseudoazurin of <i>Al. faecalis</i>	38
Figure 1.15	Structural model of haem-copper oxidase proteins and their relationship to nitric oxide reductase	41

Figure 1.16	Sequence analysis of the Cu _A binding region in nitrous oxide reductase and cytochrome oxidase	45
Figure 1.17	Models for the ligation of the Cu _A site	46
Figure 1.18	Model of the spectroscopic states of the Cu _A and Cu _Z centres of nitrous oxide reductase	48
Figure 1.19	Topology of the apparatus for copper insertion into nitrous oxide reductase	50
Figure 1.20	Organisation of the electron transport components in <i>P. denitrificans</i>	52
Figure 1.21	The denitrification respiratory chain of <i>P. denitrificans</i>	55
Figure 1.22	The denitrification respiratory chain of <i>Ps. stutzeri</i>	56
Figure 1.23	The regulatory circuit of denitrification in <i>Ps. stutzeri</i>	62
Figure 1.24	Hypothesis of gastric cancer etiology	70
Figure 1.25	Representation of the <i>N</i> -nitrosation reaction	73
Figure 1.26	Acid catalysed formation of <i>N</i> -nitrosating agents	74
Figure 1.27	Diagram showing the connection between <i>N</i> -nitrosation and denitrification	76
Figure 1.28	Reaction evolving nitrous oxide via N-N bond formation by nitrite and nitric oxide reductases	77
Figure 1.29	Reduction of nitrous acid to nitric oxide by ascorbic acid	80

Chapter Three

Figure 3.1	Plasmid map of pZS163	150
Figure 3.2	Plasmid map of pZS55	151
Figure 3.3	Southern hybridisation of <i>N. subflava</i> mutant 163 genomic DNA to the 1.86kb cassette of pZS55	153
Figure 3.4	PCR strategy to produce the 717bp cd ₁ probe	155
Figure 3.5	Southern hybridisation of denitrifying bacteria to the cd ₁ probe of <i>Ps. stutzeri</i>	156

Figure 3.6	Restriction map of pNIR201	157
Figure 3.7	Southern hybridisation of denitrifying bacteria to the nir3 copper probe of <i>Al. faecalis</i>	158
Figure 3.8	Topology tree of the eubacteria	160
Figure 3.9	Alignment of the N-terminal regions of the <i>Al. faecalis</i> and <i>N. gonorrhoeae</i> nitrite reductase enzymes	161
Figure 3.10	Linearised representation of pZS163 showing fragments at the IS50 _R end of Tn5 subcloned for sequencing	164
Figure 3.11	Linearised representation of pZS163 showing fragments at the IS50 _L end of Tn5 subcloned for sequencing	166
Figure 3.12	pZS163 consensus sequence	168
Figure 3.13	Comparison of the translated amino acid sequence obtained from the pZS163 consensus sequence to the amino acid sequence of DNA topoisomerase III from <i>H. influenzae</i>	169
Figure 3.14	Linearised representation of pZS163 showing the positions of the 170 and 280bp probes	172
Figure 3.15	Diagram of the 1.6kb <i>Pst</i> I fragment expected to hybridise to the 280bp probe in pZS163	174
Figure 3.16	Plasmid map of pJT170	179
Figure 3.17	Linearised representation of pJT170 showing the position of the FP26 sequencing primer	180
Figure 3.18	Alignment of sequence from pJT170 and pZS163	181
Figure 3.19	Hypothetical looping out mechanism which led to the deletion of DNA in pZS163	183
Figure 3.20	Relationship between plasmids pZS163 and pJT170	184
Figure 3.21	Linearised representation of pJT170 illustrating fragments subcloned for sequencing	187
Figure 3.22	pJT170 consensus sequence	189
Figure 3.23	Sequence from pJT13 using the Reverse primer	190

Figure 3.24	Comparison of the translated amino acid sequence from pJT170 Reversed primed sequence to the amino acid sequence of adenylosuccinate synthetase from <i>H. influenzae</i>	191
Figure 3.25	Comparison of the translated amino acid sequence from pJT170 consensus sequence to the amino acid sequence of acetoacetyl-CoA reductase from <i>Acinetobacter</i> spp.	192

Chapter Four

Figure 4.1	Illustration of the chemistry involved in the nitrite reductase specific methyl viologen native gel activity stain	200
Figure 4.2	Coomassie stained native polyacrylamide gel of whole cell lysates of a number of denitrifying bacteria	202
Figure 4.3	Nitrite reductase activity stain of denitrifying bacteria on a native gel	203
Figure 4.4	Nitrite reductase activity stain of denitrifying bacteria on a Triton X-100 native gel	208
Figure 4.5	Nitrite reductase activity stain of <i>N. subflava</i> B19 and mutant 163 in the presence of DDC	210
Figure 4.6	Hypothetical organisation of the electron transport system in the denitrification pathway of <i>N. subflava</i>	216

Chapter Five

Figure 5.1	PILEUP of the copper nitrite reductases from a number of different denitrifying organisms	220
Figure 5.2a	Design of AniA1 PCR primer	222
Figure 5.2b	Design of AniA2 PCR primer	223

Figure 5.3	Codon usage table of <i>N. gonorrhoeae</i>	224
Figure 5.4	Agarose gel electrophoresis of the AniA PCR	226
Figure 5.5	Plasmid map of pANIA350	227
Figure 5.6	DNA sequence from pANIA350	229
Figure 5.7	Peptide alignment of the AniA nitrite reductase from <i>N. gonorrhoeae</i> and the ORF obtained from pANIA350	230
Figure 5.8a	Peptide alignment of the pANIA350 ORF and the nitrite reductase from <i>A. cycloclastes</i>	231
Figure 5.8b	Peptide alignment of the pANIA350 ORF and the nitrite reductase from <i>Al. faecalis</i>	232
Figure 5.9	Southern hybridisation of <i>N. subflava</i> B19 chromosomal digests to the 350bp probe	235
Figure 5.10	Southern hybridisation of <i>N. subflava</i> mutant 163 chromosomal digests to the 350bp probe	236
Figure 5.11	Results of the pBR325/ <i>Hind</i> III mini-library screen with the 350bp probe	240
Figure 5.12	<i>AniA</i> PCR results from pANIA10	241
Figure 5.13	DNA sequence from pANIA350 showing the positions of AniA3 and AniA4	243
Figure 5.14	DNA sequence from pANIA10	245
Figure 5.15	Alignment of the nitrite reductase peptide from <i>N. subflava</i> and the AniA peptide from <i>N. gonorrhoeae</i>	248
Figure 5.16a	Alignment of the nitrite reductase peptides from <i>N. subflava</i> and <i>Al. faecalis</i>	249
Figure 5.16b	Alignment of the AniA nitrite reductase from <i>N. gonorrhoeae</i> and the soluble nitrite reductase from <i>Al. faecalis</i>	250
Figure 5.17	Proposed deletion mechanism in pANIA10	252
Figure 5.18	pANIA10 <i>Hind</i> III restriction digests	253
Figure 5.19	<i>AniA</i> PCR on pACYC177 transformants	256

Figure 5.20	Putative map of transformant pH25	257
Figure 5.21	Transformation screen of the 2.0kb fragment from pH25 cloned into pUC19	261
Figure 5.22	<i>AniA</i> PCR on pH25/pUC19 transformants	262
Figure 5.23	Sequence produced from pH25-6	264
Figure 5.24	Peptide alignment of ORF 1 from pH25-6 and the Ychb peptide of <i>Ps. aeruginosa</i>	265
Figure 5.25	The C5 pathway for the formation of ALA	266
Figure 5.26	Arrangement of the <i>hemA-prs</i> operon	266
Figure 5.27	Results of pASHOK/ <i>Hind</i> III mini-library screen	269
Figure 5.28	<i>AniA</i> PCR on λ 350-5 and λ 350-9	271
Figure 5.29	Map of λ 350-9	274
Figure 5.30	Putative map of the nitrite reductase gene from <i>N.</i> <i>subflava</i> B19	275
Figure 5.31	<i>Stu</i> I/ <i>Hind</i> III mini-library screen with the 350bp probe	279

Appendix

Figure A1	Map of Tn5	318
Figure A2	Plasmids constructed for sequencing pZS163	319
Figure A3	Plasmids constructed for sequencing pJT170	320
Figure A4	Plasmid map of pBR325	321
Figure A5	Plasmid map of pACYC177	322
Figure A6	Plasmid map of pASHOK	323
Figure A7	Plasmid map of pSL1190	324
Figure A8	Plasmid map of pKT231	325
Figure A9	Plasmid map of pUC19	326
Figure A10	Plasmid map of pBluescript KS ⁻	327

List of Tables

Chapter One

Table 1.1 Genes for the denitrification proteins and their functions	7
Table 1.2 Structural elements and specificity of co-existent FNR-like factors found in denitrifiers	61

Chapter Two

Table 2.1 Antibiotic solutions used in this study	91
Table 2.2 Plasmids used and constructed during this study	92
Table 2.3 Bacterial strains used in this study	94

Chapter Three

Table 3.1 Characteristics of <i>Neisseria</i> spp.	160
Table 3.2 List of the most common sequencing primers used in this study	164
Table 3.3 Summary of the subclones produced from pZS163	167
Table 3.4 Summary of the B19 and mutant 163 DNA fragments hybridising to the 170 and 280bp probes	172
Table 3.5 Summary of the λ 170-3 and λ 170-5 fragments hybridising to 170 and 280bp probes	176
Table 3.6 Comparison of fragment sizes hybridising to the 170bp probe in λ and genomic DNA isolates	178
Table 3.7 Summary of the subclones produced from pJT170	188

Chapter Five

Table 5.1 Primers used in the sequence analysis of pANIA10	242
Table 5.2 Primers designed for the sequence analysis of pH25	258
Table 5.3 Fragments from <i>N. subflava</i> B19 and λ 350-9 positive to the 350bp probe	273

List of Graphs**Chapter Four**

Graph 4.1 Graph comparing cell lysis of anaerobic cultures of <i>N.</i> <i>subflava</i> B19 and <i>Ps. stutzeri</i>	201
---	-----

Abbreviations

Δp	proton motif force
A	absorbance
Amp	ampicillin
BBL	Bethesda Biological Laboratory
BHI	Brain Heart Infusion
bp	base pairs
BSA	bovine serum albumin
Chl	chloramphenicol
COX	cytochrome c oxidase
cps	counts per second
CTAB	hexadecyltrimethyl ammonium bromide
dATP	dideoxyadenosine triphosphate
dCTP	dideoxycytidine triphosphate
DDC	diethyldithiocarbamate
dGTP	dideoxy guanosine triphosphate
DNA	deoxyribonucleic acid
dNTP	dideoxynucleotide triphosphate
dTTP	dideoxythymidine triphosphate
EDTA	ethylenediaminetetraacetate
EMBL	European Molecular Biology Laboratory
EPR	Electron Paramagnetic Resonance
HEPES	N-[2-Hydroxyethyl]piperazine-N'-[2-ethanesulphonic acid]
IHF	integration host factor
IPTG	isopropyl- β -D-thiogalactopyranoside
Kan	kanamycin
kb	kilobase
kDa	kiloDalton
L-broth	Luria-Bertani broth
Mb	megabase
MCS	multiple cloning site
MGD	molybdopterin guanine dinucleotide
Mr	relative molecular mass
Nal	nalidixic acid
NaP	periplasmic nitrate reductase
NaR	nitrate reductase
NiR	nitrite reductase
NoR	nitric oxide reductase
NoS	nitrous oxide reductase
OD	optical density
ORF	open reading frame
PAGE	polyacrylamide gel electrophoresis

PCR	Polymersae Chain Reaction
PEG	polyethylene glycol
pfu	plaque forming unit
psi	pounds per square inch
rpm	rotations per minute
RNA	ribonucleic acid
RP	Reverse primer
SAP	shrimp alkaline phosphatase
SDS	sodium dodecylsulphate
SSC	sodium chloride with sodium citrate
Strep	streptomycin
TAE	Tris acetate with EDTA
TBE	Tris borate with EDTA
TE	Tris-EDTA
TEMED	N, N, N' ,N' -tetramethylethylenediamine
Tet	tetracycline
T _m	melting temperature
Tris	tris (hydroxymethyl) aminomethane
TTC	triphenyl tetrazolium chloride
UP	Universal primer
UQ	ubiquinol
UQH ₂	ubiquinone
UV	ultraviolet
X-gal	5-Bromo-4-chloro-3-indoyl-β-D-galactopyranoside

Abstract

Neisseria subflava is a commensal organism of the oral cavity, which is able to colonise the gut when the stomach becomes achlorhydric. *N. subflava* is believed to have the ability to catalyse *N*-nitrosation reactions, producing carcinogenic *N*-nitroso compounds. It has been postulated that *N. subflava* uses breakdown products from foodstuffs to catalyse these reactions, although it is unknown whether *N. subflava* achieves this catalysis directly or whether a secondary chemical reduction is involved also. *N*-nitroso compounds initiate changes to the stomach lining and eventually cause cancer. It is thought that this explains the high incidence of gastric cancer in patients suffering from achlorhydria.

The work in this thesis covers the characterisation of the nitrite reductase enzyme of *N. subflava*. Nitrite reductases have previously been discounted as having a direct role in *N*-nitrosation catalysis but do produce nitric oxide, an immediate precursor of *N*-nitroso compounds. A basic understanding of the enzyme was required before further analysis of the nitrite reductase/*N*-nitrosation reaction hypothesis could progress.

Degenerate oligonucleotide primers designed from sequence alignments of a number of well characterised nitrite reductase enzymes were used to amplify a 350bp fragment from wild type *N. subflava* DNA using PCR. Sequence analysis and database comparisons on this DNA led to the conclusion that the nitrite reductase gene had been identified. When translated, the enzyme was found to contain copper in its active site and was proposed to be unusually associated with the outer membrane. This contrasts with the known periplasmic location. A number of unsuccessful attempts were made to clone the 5' end of the gene. It was postulated that a high degree of DNA secondary structure upstream of, or within, the 5' end of the gene was preventing cloning of the entire nitrite reductase gene.

Sequence and probing analysis on a Tn5 insertion mutant of *N. subflava*, lacking the ability to reduce nitrite, showed that Tn5 had not inserted into a structural or regulatory gene for nitrite reduction, but affected the nitrite reductase gene

distally. From studies on native polyacrylamide gels an outer membrane location for the electron donor protein was also postulated. The presence of an azurin like protein attached to the outer membrane has been identified in *N. gonorrhoeae* which is thought to act as donor to the gonococcal membrane bound nitrite reductase. However it is anticipated that the donor protein in *N. subflava* will differ from this as attempts to PCR an azurin gene from *N. subflava* were repeatedly unsuccessful (Lambert, 1997). The presence of outer membrane associated nitrite reductase and electron donor proteins in *N. subflava* indicate that a novel arrangement of the denitrification pathway may exist in this organism which spans the periplasmic space. This periplasmic arrangement is proposed to be unique to *Neisseria* spp.

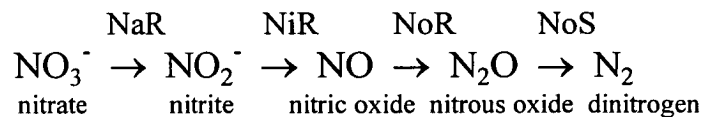
Chapter One

Introduction

The first part of the introduction outlines current understanding of the denitrification respiratory pathway. A detailed knowledge of denitrification is necessary to understand the mechanisms by which nitrate and nitrite reducing organisms may act as potential pathogens in the development of gastric cancer when bringing the context of this thesis into focus.

1.1 Denitrification

Nitrogen in the environment exists in a number of oxidation states. Interconversion between these oxidation states results in a process known as the nitrogen cycle (Figure 1.1). Nitrogen is introduced into the biosphere by biological and chemical fixation of dinitrogen and removed by denitrification. Denitrification is predominantly a biological process and the bacteria involved are nearly always facultative aerobes. The processes involved in denitrification entail respiratory reduction of nitrate to dinitrogen via nitrite, nitric oxide and nitrous oxide. Each step of this reductive pathway is catalysed by a specific oxidoreductase enzyme:



NaR = nitrate reductase

NiR = nitrite reductase

NoR = nitric oxide reductase

NoS = nitrous oxide reductase

(Berks, *et al.*, 1995a)

These enzymes are arranged in association with the cytoplasmic membrane enabling an electrochemical gradient to be generated thereby coupling denitrification to

electron transport phosphorylation. Some of the denitrification pathway intermediates are cytotoxic, particularly nitric oxide, and a tight mechanism of cellular regulation governs expression and activity of each of the reductase enzymes to ensure the toxic intermediates cannot accumulate and affect cell viability.

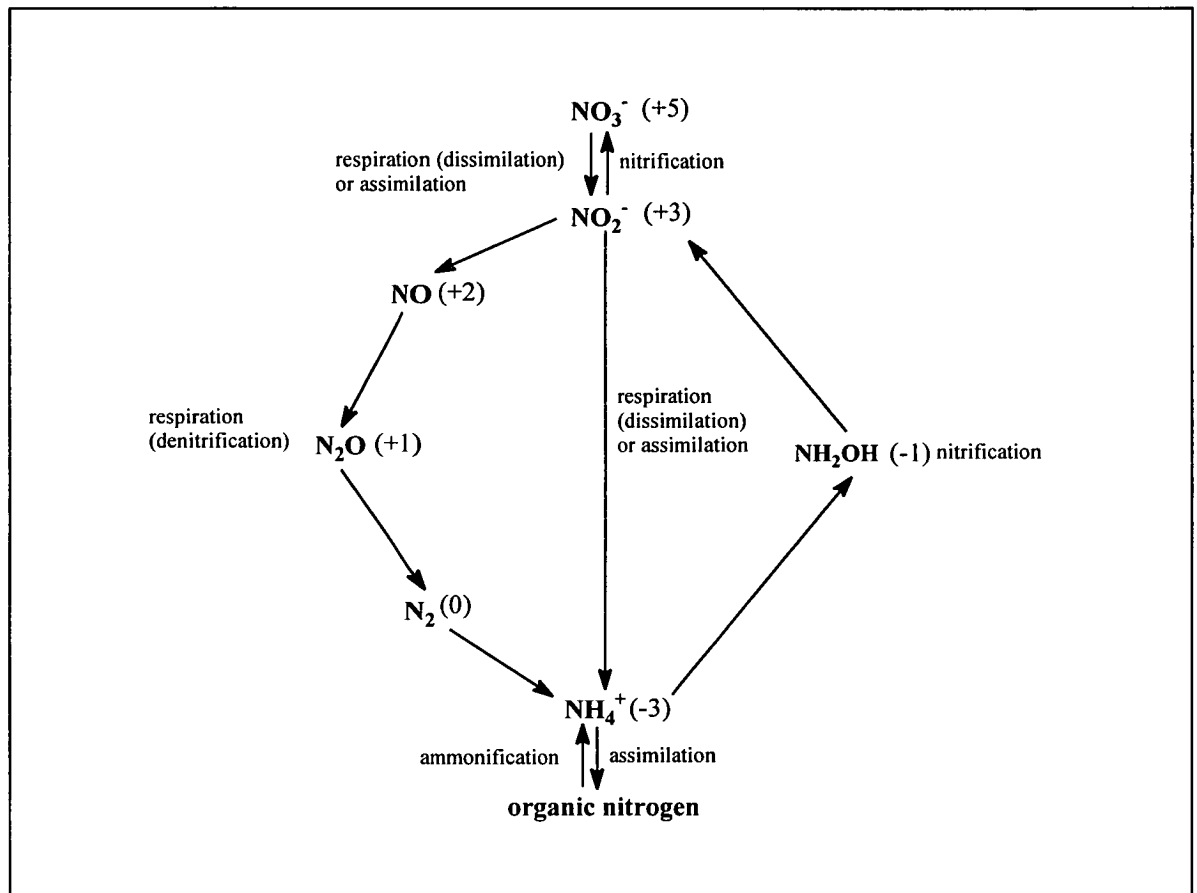


Figure 1.1. The nitrogen cycle. The oxidation state of nitrogen is given in brackets for each intermediate. The terms respiration and dissimilation are often used interchangeably. The oxidation of ammonia (NH₄⁺) to nitrite (NO₂⁻) via hydroxylamine (NH₂OH), and the oxidation of nitrite to nitrate (NO₃⁻) are both considered reactions of nitrification but have never been found in a single bacterial species. Taken from Berks *et al.*, 1995a.

The distribution of denitrification amongst prokaryotes is widespread amongst the Eubacteria and has been identified in a broad variety of groups including: Rhodospirillaceae, Pseudomonaceae, Rhizobiaceae, Halobacteriaceae,

Neisseriaceae and Bacillaceae. The ability to denitrify has also been identified in the Archaea (Völkl, *et al.*, 1993).

Organisms that can denitrify preferentially grow in aerobic environments but have an alternate capacity to use nitrogen oxides as respiratory electron acceptors when oxygen becomes depleted. Oxygen therefore acts as a non-competitive inhibitor of nitrate reductase by withdrawing electrons from the denitrification respiratory chain.

Carlson and Ingraham (1983) compared denitrification in three different bacteria (*Pseudomonas stutzeri*, *Pseudomonas aeruginosa* and *Paracoccus denitrificans*). In all three organisms nitrate was reduced to dinitrogen but the rates at which this occurred and the products of the reactions varied. *Ps. stutzeri* produced only dinitrogen whereas the other two organisms produced more nitrous oxide. *Ps. stutzeri* and *P. denitrificans* were able to reduce nitrate, nitrite and nitrous oxide readily and grow anaerobically with any of these nitrogen oxides. But *Ps. aeruginosa* reduced these oxides slowly and was unable to grow at all in the presence of nitrous oxide. This study demonstrated the diversity of denitrification and how the control of denitrification enzymes and the organisms responses to their environments can differ greatly.

Usually denitrification is inhibited by oxygen but *Thiosphaera pantotropha* has been identified as a fully aerobic denitrifier (Robertson and Kuenen, 1984). Bell *et al.*, (1990) showed that this organism has two distinct nitrate reductase enzymes; one found in the cytoplasmic membrane and one in the periplasm. The membrane bound enzyme is the dominant form expressed after anaerobic growth and is only active under anaerobic conditions. The periplasmic nitrate reductase is expressed preferentially when cells are grown under aerobic denitrifying conditions but has activity when exposed to aerobic or anaerobic growth conditions. It is thought that the periplasmic nitrate reductase enables bacterial cells to adapt quickly to changes in oxygen tension as a survival mechanism. Studies using Tn5 mutagenesis discovered that the membrane bound and periplasmic nitrate reductases are subject to different regulatory mechanisms within the cell (Bell *et al.*, 1993). When the gene for the membrane bound nitrate reductase was knocked out elevated levels of the

periplasmic enzyme were found even under anaerobic growth conditions. These mutants were found to have lower growth rates than wild type cells, when grown anaerobically (Bell *et al.*, 1993). Under aerobic conditions it is necessary for the cell to express a periplasmic nitrate reductase to overcome the regulatory effect that oxygen has on the membrane bound nitrate reductase. This is because oxygen is believed to inhibit nitrate transport across the cytoplasmic membrane to the periplasmic active site of the enzyme. It has been postulated that the reduced growth rate of membrane bound nitrate reductase mutants is due to the periplasmic nitrate reductase acting as an electron sink. The reduction reaction carried out by this enzyme is believed to be uncoupled from the proton motive force (Δp), (Nicholls and Ferguson, 1992). Therefore it is bioenergetically favourable to express the membrane bound nitrate reductase during anaerobic growth, when nitrate respiration is required to be the major generator of Δp .

To summarise: it can be seen that denitrification is a highly divergent respiratory pathway subject to stringent and varied control between different bacterial species. The following sections discuss the individual enzymes involved in denitrification in detail together with information on the associated electron transport and regulatory mechanisms.

1.2 Denitrification gene clusters

The genes for denitrification, encoding functions for nitrate respiration (*nar*), nitrite respiration (*nir*), nitric oxide respiration (*nor*) and nitrous oxide respiration (*nos*), are found assembled in clusters. The gene clusters have been particularly well characterised in *Ps. stutzeri* (Jüngst *et al.*, 1991; Braun and Zumft, 1992), *Ps. aeruginosa* (Arai *et al.*, 1995) and *P. denitrificans* (deBoer *et al.*, 1994; deBoer *et al.*, 1996). Figure 1.2 shows the comparative denitrification gene clusters from these three organisms. The *nir-nor* gene clusters contain the structural information for both reductases and also functions for metal processing, cofactor synthesis, protein maturation, assembly processes and regulation. Genes encoding electron donors to

the reductases are not necessarily part of the denitrification gene clusters. Only in *Ps. stutzeri* are the *nos* genes linked with the *nir* and *nor* genes forming a supraoperon structure of about 30kb comprising over 30 genes. The presence of several more genes is indicated in the *Ps. stutzeri* supraoperon as several uncharacterised proteins have been identified that are dependent on denitrification for expression (Zumft, 1997). It is thought that these genes will map to the unidentified ORFs located between the *nos* and *nir* gene clusters. A brief summary of the principal genes involved in denitrification can be found in Table 1.1.

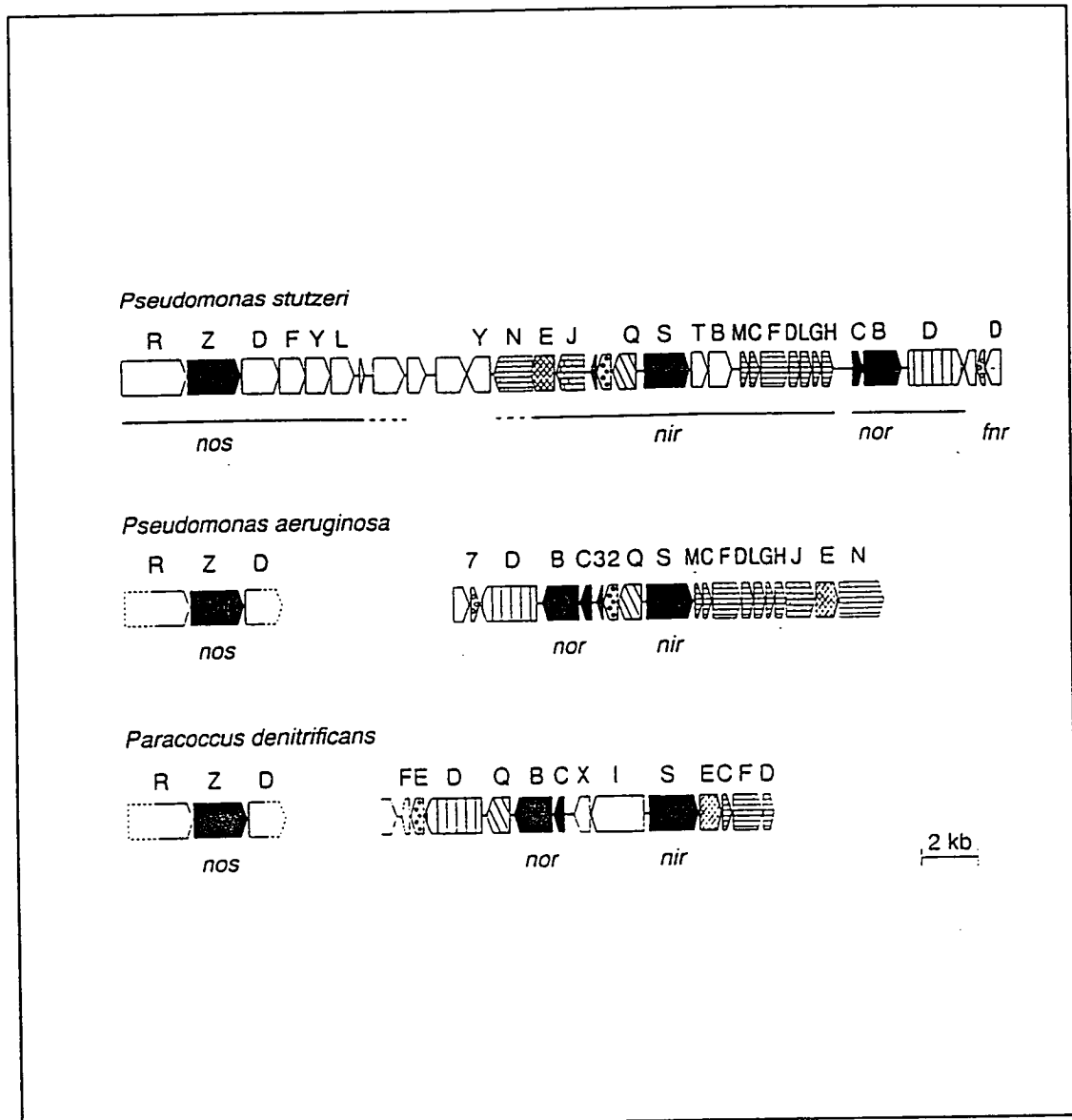


Figure 1.2. Comparative organisation of denitrification genes amongst cytochrome cd_1 synthesising denitrifiers. The approximate size and transcriptional direction of genes are given by the arrow boxes. Homologous genes within the *nir* and *nor* regions are shown by the same graphic patterns: open boxes have no homologs. Solid boxes represent the structural genes for nitrous oxide reductase (*nosZ*), nitrite reductase (*nirS*) and nitric oxide reductase (*norCB*). Boxes with broken lines denote genes that are only partially sequenced. The gene clusters are aligned with respect to the position and transcriptional organisation of *nirS*. Taken from Zumft (1997).

Category of affected process	Gene or locus*	Encoded gene product, function or observation	Reference(s)
Nitrate respiration	<i>narG</i>	α subunit of nitrite reductase - binds MGD	Philipott <i>et al.</i> , 1997 ^a
	<i>narH</i>	β subunit of nitrite reductase - binds Fe-S clusters	Berks <i>et al.</i> , 1995b ^b
	<i>narI</i>	Cytochrome b subunit of nitrate reductase	Berks <i>et al.</i> , 1995b ^b
	<i>narJ</i>	Protein necessary for nitrate reductase assembly	Berks <i>et al.</i> , 1995b ^b
Nitrite respiration	<i>nirB</i>	Cytochrome c_{552}	Jüngst <i>et al.</i> , 1991 ^c
	<i>nirC</i>	Monohaem cytochrome c. Function in NirS maturation	Jüngst <i>et al.</i> , 1991 ^c
	<i>nirK, nirU</i>	Copper containing nitrite reductase	Glöckner <i>et al.</i> , 1993 ^e Nishiyama <i>et al.</i> , 1993 ^d
	<i>nirN, orf507</i>	Affects <i>in vivo</i> nitrite reduction	Kawasaki <i>et al.</i> , 1997 ^e
	<i>nirQ</i>	Gene product affects function of NirS and NorCB	Jüngst and Zumft, 1992 ^c
	<i>nirS</i>	Cytochrome cd_1 nitrite reductase	Jüngst <i>et al.</i> , 1992 ^c deBoer <i>et al.</i> , 1994 ^f
Haem d_1 biosynthesis	<i>nirD</i>	Gene product affects haem d_1 biosynthesis or processing	deBoer <i>et al.</i> , 1994 ^f
	<i>nirE</i>	Has methyl transferase activity	deBoer <i>et al.</i> , 1994 ^f
	<i>nirF</i>	Required for haem d_1 biosynthesis	deBoer <i>et al.</i> , 1994 ^f
	<i>nirG</i>	Gene product affects haem d_1 biosynthesis or processing	Kawasaki <i>et al.</i> , 1997 ^e
	<i>nirH</i>	Gene product affects haem d_1 biosynthesis or processing	Kawasaki <i>et al.</i> , 1997 ^e
	<i>nirJ, orf393</i>	Affects haem d_1 biosynthesis or processing	Kawasaki <i>et al.</i> , 1997 ^e
	<i>nirL</i>	Gene product affects haem d_1 biosynthesis or processing	Kawasaki <i>et al.</i> , 1997 ^e
Nitric oxide respiration	<i>norB</i>	Cytochrome b subunit of nitric oxide reductase	Arai <i>et al.</i> , 1995 ^e deBoer <i>et al.</i> , 1996 ^f
	<i>norC</i>	Cytochrome c subunit of nitric oxide reductase	Arai <i>et al.</i> , 1995 ^e deBoer <i>et al.</i> , 1996 ^f
	<i>norD, orf6</i>	Affects viability under denitrifying conditions	Arai <i>et al.</i> , 1995 ^e deBoer <i>et al.</i> , 1996 ^f
	<i>norE, orf2, orf175</i>	Membrane protein, homologous with COX III	deBoer <i>et al.</i> , 1996 ^f
	<i>norF</i>	Affects nitric oxide and nitrite reduction	deBoer <i>et al.</i> , 1996 ^f
	<i>norQ</i>	Affects NirS and NorCB function	deBoer <i>et al.</i> , 1996 ^f

Nitrous oxide respiration	<i>nosA, oprC</i>	Channel forming outer membrane protein; affects copper processing for NosZ	Lee <i>et al.</i> , 1991 ^c
	<i>nosD</i>	Involved in copper insertion for NosZ	Zumft <i>et al.</i> , 1990 ^c
	<i>nosF</i>	ATP binding protein involved in copper insertion into NosZ	Zumft <i>et al.</i> , 1990 ^c
	<i>nosL</i>	Putative outer membrane lipoprotein	Chan <i>et al.</i> , 1997 ^b
	<i>nosY</i>	Inner membrane protein involved in copper processing for NosZ	Zumft <i>et al.</i> , 1990 ^c
	<i>nosZ</i>	Nitrous oxide reductase	Hoeren <i>et al.</i> , 1993 ^f
Periplasmic nitrate reduction	<i>napA</i>	Large subunit of periplasmic nitrate reductase - binds MGD and Fe-S cluster	Berks <i>et al.</i> , 1995 ^c
	<i>napB</i>	Small subunit of periplasmic nitrate reductase - a dihaem cytochrome c	Berks <i>et al.</i> , 1995 ^c
	<i>napD</i>	Cytoplasmic protein with presumed maturation function	Berks <i>et al.</i> , 1995 ^c
	<i>napE</i>	Putative membrane protein	Berks <i>et al.</i> , 1995 ^c

Table 1.1. Genes for the denitrification proteins and their functions. * mnemonics for gene designations: *nap*, nitrate reductase, periplasmic; *nar*, nitrate respiration; *nir*, nitrite respiration; *nor*, nitric oxide respiration; *nos*, nitrous oxide respiration. Key to organisms genes identified in: ^a *Ps. fluorescens*, ^b *T. pantotropha*, ^c *Ps. stutzeri*, ^d *Al. faecalis*, ^e *Ps. aeruginosa*, ^f *P. denitrificans*, ^g *R. meliloti*.

The denitrification gene clusters represented in Figure 1.2 are from organisms that have cytochrome *cd₁* nitrite reductase enzymes. It appears that the genetic arrangement of the denitrification gene clusters in strains that contain copper nitrite reductases differ as the *nir* and *nor* genes in these organisms are believed to be separated (Bartnikas *et al.*, 1997; Tosques *et al.*, 1997); however the extent of this separation is unknown at present. The *nir* and *nor* gene clusters of *Rhodobacter sphaeroides* f. sp. *denitrificans* (a copper nitrite reductase strain) are subject to control by the same regulatory membrane bound protein, NnrR. This indicates the requirement for global regulators of anaerobic gene expression in this organism (Bartnikas *et al.*, 1997).

Of the genes found in the *Ps. stutzeri* denitrification gene cluster 23 are transcribed in the same direction. Transcript initiation sites have been mapped for a number of genes including *nosR*, *nosZ* and *nosD* (Cuypers *et al.*, 1995) and *norCB* (Zumft *et al.*, 1994). This revealed that certain genes are transcribed from more than one promoter. As denitrification is an environmentally regulated process the use of

multiple promoters may be a means of altering global gene expression differentially with respect to external factors such as oxygen supply and the presence of N-oxides. The regulatory mechanisms involved in the control of denitrification are discussed in more detail in section 1.8.

1.3 Nitrate Reductase

A number of classes of nitrate reductases have been identified; the bacterial membrane bound and periplasmic dissimilatory enzymes discussed briefly in section 1.1 and the distinct cytoplasmic assimilatory enzymes of both bacteria and eukaryotes. All four types of enzyme have a molybdopterin cofactor at their active sites. The bacterial nitrate reductases contain a variant of the molybdopterin cofactor in which the cofactor is bound to guanosine monophosphate. This was termed molybdopterin guanine dinucleotide (MGD) by Rajagopalan and Johnson (1992). Amino acid comparison of all MGD binding proteins enabled the structural relatedness of the proteins to be determined. Although related to each other the MGD binding proteins are structurally distinct from proteins binding other forms of molybdopterin cofactor (Berks *et al.*, 1995a).

For the purposes of this study the membrane bound dissimilatory nitrate reductase will be discussed in the greatest detail as this enzyme is most commonly associated with denitrification. However a brief overview of the other enzymes will also be included.

1.3.1 Assimilatory nitrate reductases

Assimilatory nitrate reducers are microorganisms capable of growth using nitrate as the sole source of cellular nitrogen because they can convert nitrate to ammonia. The eukaryotic assimilatory nitrate reductase is composed of two proteins one of which is a cytoplasmic, NAD(P)H linked enzyme possessing haem (cytochrome b) and FAD as noncovalently bound cofactors (Solomonson and Barber,

1990). Reduction occurs as the FAD cofactor transfers electrons from the bound NAD(P)H electron donor of one protein to the molybdopterin cofactor on the second protein. The two electron reduction to nitrite takes place at the molybdopterin site. Nitrite is then reduced to ammonia which is assimilated as a source of cell nitrogen (Smith, 1994).

Bacterial assimilatory nitrate reductases (Nas) are single sub-unit cytoplasmic enzymes. Sequence analysis demonstrated that they bind MGD, an N-terminal [4Fe-4S] cluster and at least one [2Fe-2S] cluster in the C-terminal (Berks *et al.*, 1995a). The iron sulphur centres transfer electrons to MGD for reduction of nitrate to occur. Unlike the eukaryotic assimilatory nitrate reductase the bacterial enzymes do not use NAD(P)H as an electron donor. The *nasC* gene in *Klebsiella pneumoniae* codes for a protein with sequence similarity to NADH-dependent reductases, (Lin *et al.*, 1994). Consequently NasC is thought to be the electron donor to the assimilatory nitrate reductase in this organism.

1.3.2 Periplasmic dissimilatory nitrate reductase

Periplasmic nitrate reductases have been purified from a number of closely related bacteria, *Rhodobacter capsulatus* (McEwan *et al.*, 1987), *R. sphaeroides* f. sp. *denitrificans* (Sato, 1981), *Thiosphaera pantotropha* (Berks *et al.*, 1994), *Alcaligenes eutrophus* (Siddiqui *et al.*, 1993), *P. denitrificans* (Sears *et al.*, 1995) and *Ps. stutzeri* (Zumft, 1997). Periplasmic nitrate reductases are responsible for catalysing aerobic nitrate reduction and the role of the periplasmic nitrate reductases in aerobic denitrification was discussed in section 1.1.

The periplasmic nitrate reductase exists as a heterodimer. The catalytic subunit (NapA) is 90kDa and binds MGD and [4Fe-4S] as cofactors whereas the second subunit (NapB) is a 16kDa dihaem cytochrome c_{552} (Berks *et al.*, 1995c). The interaction between the two subunits is predominantly hydrophobic and some dissociation of the subunits can occur during purification (Richardson *et al.*, 1990). In contrast to the membrane bound nitrate reductase the periplasmic enzyme shows

complete specificity for nitrate as substrate whereas the membrane bound enzyme will also reduce chlorate (Bell *et al.*, 1990).

A total of five genes for the periplasmic nitrate reductase have been identified, *napA*, *napB*, *napC*, *napD* and *napE*, present in an *napEDABC* operon structure (Berks *et al.*, 1995c). *NapA* encodes the larger MGD binding catalytic subunit whereas *napB* codes for the smaller peptide containing dihaem cytochrome c for electron transfer. *NapC* encodes a membrane anchored tetrahaem protein which is proposed to transfer electrons to NapAB. The exact functions of the *napD* and *napE* gene products are unknown although it is likely they are involved in NapAB assembly or in the mediation of interactions between NapC and a quinol oxidase. NapA shows a high degree of sequence similarity to the gene product of the *E. coli aeg-46.5* operon (Berks *et al.*, 1995c). This locus is subject to tight control by two regulatory proteins, NarP and NarQ, (Stewart, 1993). Regulation via these two proteins is analogous to that controlling expression of the membrane bound nitrate reductase gene, a full description of which is given in section 1.8.1.2.

1.3.3 Membrane bound dissimilatory nitrate reductase

The membrane bound nitrate reductase (NaR) has been found in many bacteria including the denitrifiers *P. denitrificans* (Craske and Ferguson, 1986), *Ps. aeruginosa* (Carlson *et al.*, 1982), *Ps. stutzeri* strain ZoBell (Blumle and Zumft, 1991) and *R. capsulatus* (Richardson *et al.*, 1994). It has also been identified in *E. coli* (Garland *et al.*, 1975). The isolated enzymes were found to vary in molecular weight due to the different methods employed to release the membrane bound enzyme. A molecular weight of 60kDa was reported for *Ps. stutzeri* (Blumle and Zumft, 1991), compared to 260kDa for *Ps. aeruginosa* (Carlson *et al.*, 1982). Difficulties encountered when solubilising the enzyme from the membrane may also explain the contradictory results reported when primarily identifying the number of subunits present in the intact enzyme. It is now accepted that the membrane bound nitrate reductase is generally composed of three subunits (α , β and γ). The α subunit is 140kDa and contains molybdenum as a cofactor plus a number of [4Fe-4S] iron

sulphur clusters (Chaudry and MacGregor, 1983). The β subunit is 60kDa and is involved in maintaining quaternary structure by mediating subunit interactions and

membrane association. These two subunits are bound to the membrane by the γ subunit which is an integral membrane protein with a b-type cytochrome associated as an apoprotein. Electron donation to the nitrate reductase enzyme complex comes from the cellular ubiquinone pool to the b-type cytochrome of the γ subunit and from there to the active site (Ferguson, 1988; Zumft *et al.*, 1988). The position of the subunits is important in generating Δp across the cytoplasmic membrane. Further details of the reactions involved in Δp generation are discussed in section 1.7.

Notable exceptions to the above nitrate reductase subunit organisation exist. In *R. sphaeroides* f. sp. *denitrificans* a soluble molybdoprotein exists which is found localised in the periplasm associated with haem c (Satoh, 1981). Also, as discussed in sections 1.1 and 1.7.1, *T. pantotropha* possesses two nitrate reductases, one in the periplasm and one associated with the cytoplasmic membrane (Bell *et al.*, 1990).

1.3.3.1 The molybdenum cofactor

As defined in section 1.3 a variant of the molybdenum cofactor exists in bacteria in which the cofactor is bound to guanosine monophosphate. This molybdopterin guanine dinucleotide (MGD) molecule is believed to exist as a bis(pterin)-molybdenum complex as identified in the dimethyl sulfoxide reductase of *R. sphaeroides* f. sp. *denitrificans* (Hilton and Rajagopalan, 1996). This is illustrated in Figure 1.3. For reference MGD and molybdenum cofactor both refer to the active site of the α subunit and will be used interchangeably in the text.

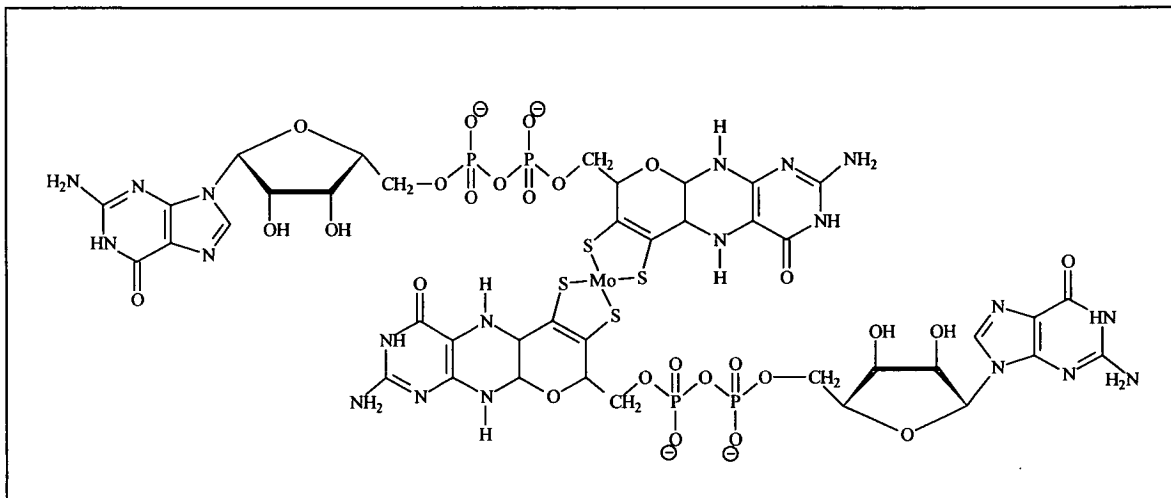


Figure 1.3. The bis(MGD)molybdenum cofactor (Hilton and Rajagopalan, 1996).

Purified nitrate reductase contains one atom of molybdenum per monomer forming the active site for nitrate reduction by coupled proton and electron transfer. It was proposed by Stoutamer (1988) that molybdenum in oxidation state IV interacts with nitrate, causing the molybdenum IV to be oxidised by two electrons to molybdenum VI. The donor atom (XH) then becomes acidic and transfers its protons to nitrate causing cleavage to nitrite and hydroxide. The molybdenum VI is then reduced back to the IV state by electron transfer from one of the [4Fe-4S] clusters present in the α subunit (Figure 1.4).

The assembly of the molybdenum cofactor, including insertion into the cytoplasmic membrane, is coded for by five distinct regions on the *E. coli* chromosome; *moa*, *moe*, *mob*, *mod* and *mog* participate in establishing a functional molybdoenzyme (Shanmugam *et al.*, 1992). Significant discrepancies in EPR spectra from the periplasmic nitrate reductase of *T. pantotropha* suggest that there are major structural differences in the molybdenum centres in both the membrane bound and periplasmic nitrate reductases (Bennett, *et al.*, 1994).

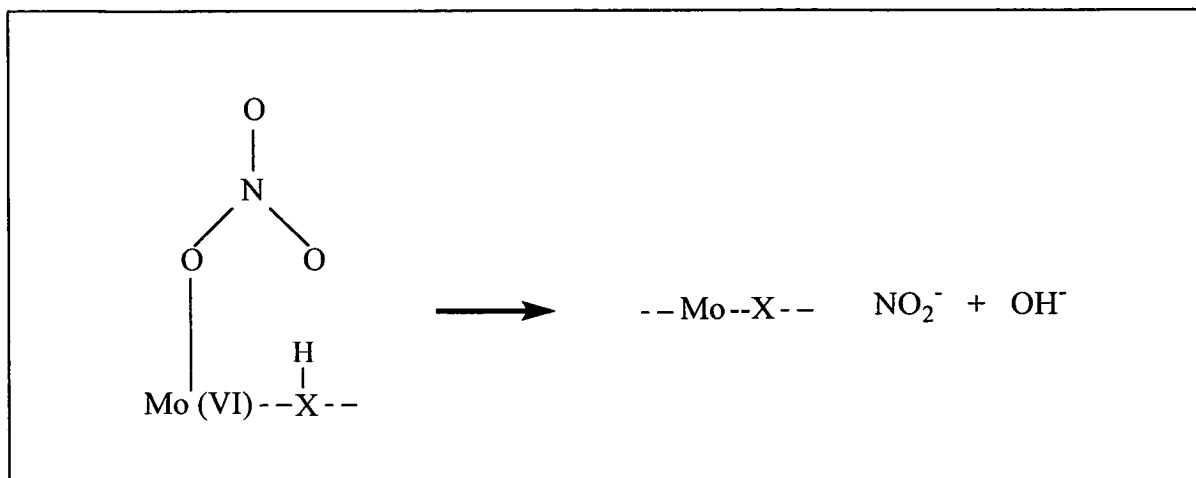


Figure 1.4. Reduction of nitrate via the molybdenum cofactor.

1.3.3.2 The iron sulphur centres

A single [3Fe-4S] cluster and three [4Fe-4S] clusters have been identified in the *E. coli* $\alpha\beta$ complex (Johnson *et al.*, 1985). They have a role in electron transfer despite having very low mid-point potentials (Berks *et al.* 1995a). They achieve this by localisation of the electron over the centre which enhances electron transfer due to the exponential dependence that electron transfer rate has on the distance to be travelled (Canters and van de Kamp, 1992). This means the greater the distance for the electron to travel the faster it will do so. The protein coat surrounding the iron sulphur clusters acts as a tunnelling bridge channelling electrons towards the clusters whilst also serving as an insulator protecting the reducing equivalents against short circuiting (Canters and van de Kamp, 1992).

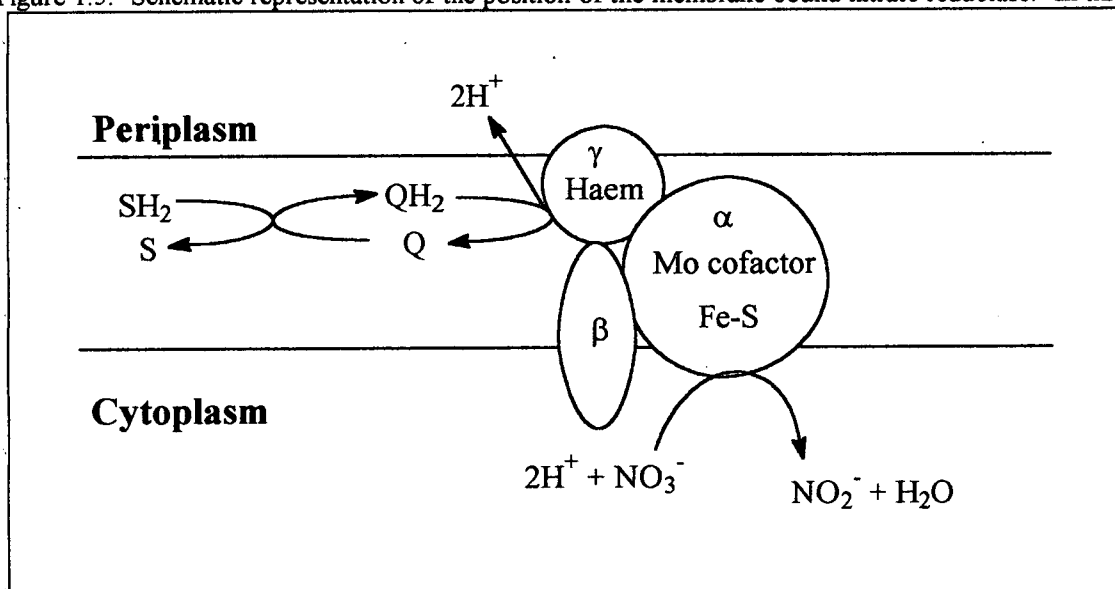
1.3.3.3 The transmembrane (γ) subunit

The membrane bound nitrate reductase is believed to generate a proton electrochemical gradient due to the oxidation of quinol at the periplasmic side of the membrane with the electrons produced being transferred across the membrane to the cytoplasmic side for nitrate reduction (Nicholls and Ferguson, 1992). Transfer of

spaced redox centres. Two b-type haems (b_{557}) have been identified in the purified *P. denitrificans* enzyme that are proposed to fulfil this role. These haems are reduced by the ubiquinol analogue duroquinol and are reoxidised by nitrate (Ballard and Ferguson, 1988).

Sequence comparisons on the *E. coli* and *T. pantotropha* peptides have enabled a structural model of the γ subunit to be elucidated (Berks *et al.*, 1995a). The subunit is predicted to consist of five transmembrane helices with the N-terminal periplasmic and the C-terminal cytoplasmic. Four conserved histidine residues have been identified as potential b-type haem binding ligands. The distribution of the haem ligands is such as to allow placement of the haems in different halves of the membrane bilayer for efficient transfer of electrons to the catalytic α subunit in the cytoplasm. A proposed arrangement of the position of the membrane bound nitrate reductase is illustrated in Figure 1.5.

Figure 1.5. Schematic representation of the position of the membrane bound nitrate reductase. In this



example SH_2 is oxidised by specific dehydrogenases coupled to the reduction of quinol (Q) to quinone (QH_2). Quinone oxidation is coupled to nitrate reduction.

1.3.3.4 Genes encoding nitrate reductase

The genes encoding nitrate reductase have been extensively studied in *E. coli* and a comprehensive review was published by Stewart (1993). The *Ps. aeruginosa* nitrate reductase operon has also been determined but to a lesser degree (Zumft *et al.*, 1988). In *E. coli* seven genetic loci have been identified which are involved in assembly of the active enzyme. The genes responsible for the structural elements of the nitrate reductase enzyme are *narG*, *narH* and *narI* encoding the α , β and γ subunits respectively. A fourth gene, *narJ*, involved in assembly of the nitrate reductase enzyme is placed with the structural genes in the operon order GHJI, *narG* being closest to the promoter (Figure 1.6).

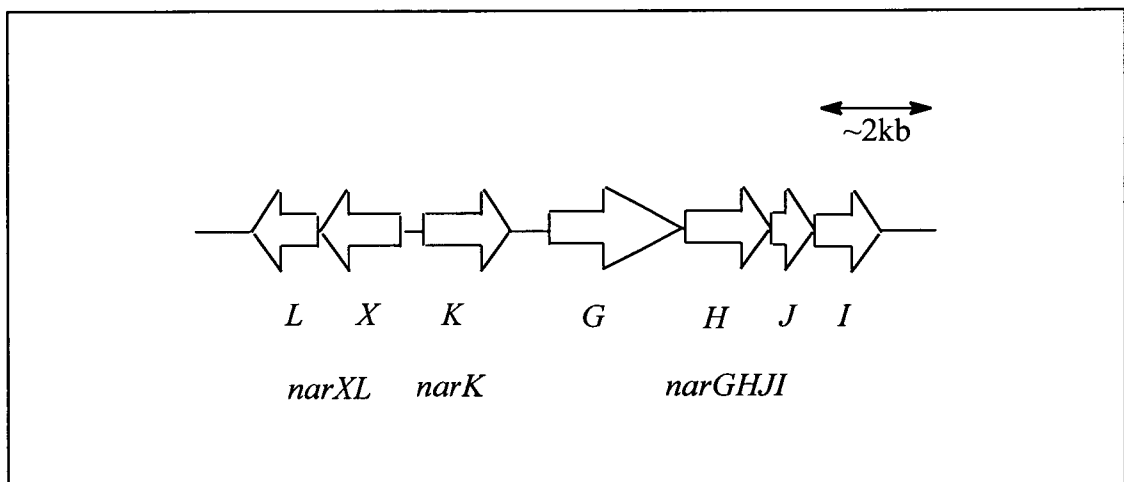


Figure 1.6. *E. coli narGHJI* operon locus for the membrane bound nitrate reductase (NarA) showing the position of the *narKLX* genes. *NarGHI* are the structural genes for the α , β and γ sub-units, *narJ* codes for a protein involved in the assembly of the mature nitrate reductase, *narK* for a nitrite exporter and *narXL* encodes a two component regulatory system that sense nitrate and nitrite.

Other genes associated with nitrate reductase and its control are *narL*, *narX* and *narK*. The product of *narK* is an integral membrane protein and is proposed to be involved in the removal of nitrite from the cytoplasm once it has been produced by the nitrate reductase (Nicholls and Ferguson, 1992). The *narXL* genes were identified as encoding a two component nitrate responsive positive regulator of

nitrate reductase operon expression. The NarL protein activates the expression of genes associated with nitrate respiration such as *narG* (nitrate reductase α subunit) and *narK* (nitrate/nitrite uptake), and represses expression of operons encoding alternative anaerobic respiratory enzymes such as *frdA*, fumarate reductase and *dmsA*, dimethylsulphoxide reductase (Stewart, 1992). A second two component regulator of nitrate reductase gene expression also exists, NarPQ. A more detailed discussion of both NarXL and NarPQ can be found in section 1.8.1.2.

1.4 Nitrite Reductase

The second stage in the denitrification process is the reduction of nitrite. Denitrification nitrite reductases tend to be periplasmic proteins and have been studied from many different organisms. They fall into two distinct groups: One group have a nitrite reductase which is a cytochrome, containing both c and d₁ type haems (section 1.4.2), and the other group have an enzyme which contains copper in its active site (section 1.4.3). Two other classes of nitrite reductase also exist but are not associated with denitrification. These are the cytochrome c respiratory nitrite reductase and the cytoplasmic sirohaem nitrite reductase which both reduce nitrite to ammonia.

The cytochrome c nitrite reductases are single polypeptides of 50-70kDa containing between four and six c-type haems. A 'hexahaem' nitrite reductase was an exciting proposition because the reduction of nitrite to ammonia requires six electrons but the amino acid sequence of the *E. coli* cytochrome c nitrite reductase contains only four consecutive c-type haem binding motifs (Cys-Xaa-Xaa-Cys-His), (Darwin *et al.*, 1993).

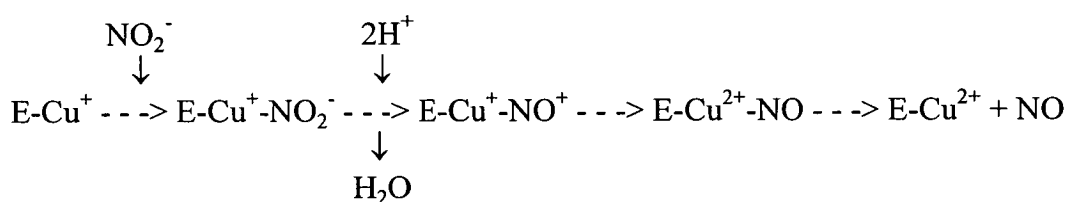
The sirohaem nitrite reductase is a homo-dimer of 90-100kDa polypeptides. The prosthetic groups are FAD, an iron-sulphur cluster(s) and sirohaem which is the site of nitrite reduction. In *E. coli* nitrite reduction via this enzyme is not coupled to energy conservation. It is thought that the main role of the sirohaem nitrite reductase

may be the removal of nitrite which is toxic in the cell at high levels (Page *et al.*, 1990).

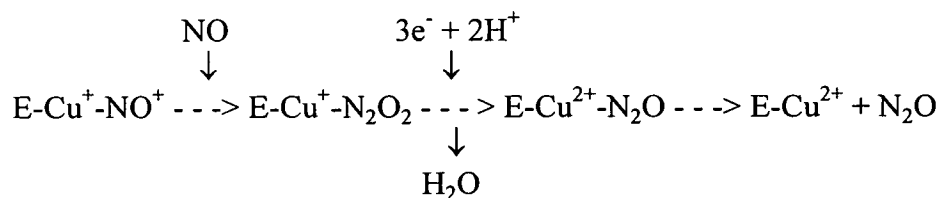
In vivo the denitrifying nitrite reductases reduce nitrite to nitric oxide and no organism has yet been identified that can express both the haem and copper enzymes. The presence of the copper nitrite reductase in an organism can be identified in intact cells and cell extracts by monitoring the sensitivity of nitrite reduction in the presence of the copper chelator diethyldithiocarbamate (DDC), (Shapleigh and Payne, 1985). However artificial electron donors must be used in these experiments as DDC could also chelate copper from cupredoxins which may be serving as electron donors to nitrite reductase. Polyclonal antibodies and gene probes have also been used to characterise the type of nitrite reductase present in denitrifying bacterial species (Coyne *et al.*, 1989; Ward *et al.*, 1993; Ye *et al.*, 1993).

1.4.1 The product of copper and cytochrome cd_1 nitrite reductases

Both nitric oxide and nitrous oxide have been detected as reaction products from the cytochrome cd_1 and copper nitrite reductases using a variety of physiological and artificial electron donors. It is now generally accepted that reduction of nitrite by both types of enzyme proceeds via an enzyme bound nitrosyl intermediate (Hulse *et al.*, 1989; Shearer and Kohl, 1988). When nitric oxide is the reaction product for copper nitrite reductase the reaction may proceed as follows:



However nitric oxide accumulation affects the reaction product obtained from the copper nitrite reductase. In the presence of excess nitric oxide nitrous oxide is formed as the reaction product through a nitric oxide rebinding mechanism (Jackson *et al.*, 1992):



The major product of the cytochrome cd_1 nitrite reductase *in vivo* is nitric oxide and the nitric oxide rebinding side reaction to produce nitrous oxide is of little physiological relevance. The reasons for this will be explained in section 1.4.2.2.

1.4.2 Cytochrome cd_1 nitrite reductase

Cytochrome cd_1 nitrite reductases have been isolated from a number of denitrifying organisms including *Ps. aeruginosa* (Gudat *et al.*, 1973), *P. denitrificans* (Lam and Nicholas, 1969), *Ps. stutzeri* (Zumft *et al.*, 1988), *T. pantotropha* (Moir *et al.*, 1993) and *A. eutrophus* (Sann *et al.*, 1994). The nitrite reductases from these organisms are periplasmic, have a subunit molecular mass of 120 kDa and are dimeric in structure. Each subunit contains one covalently bound c-type haem and one non-covalently bound molecule of a unique d_1 haem prosthetic group.

1.4.2.1 The molecular structure

The X-ray structure of the *T. pantotropha* crystallised cytochrome cd_1 nitrite reductase has been determined (Fülop *et al.*, 1993; Fülop *et al.*, 1995). This revealed that each monomer of the enzyme is organised into two domains (Figure 1.7). The N-terminal (top) domain consists of α -helices and binds the c-type haem. Unexpectedly the c-type haem is liganded by two histidine residues. Usually *bis*-His liganded cytochromes have low redox potentials whereas the cytochrome cd_1 enzyme is required to have a redox potential of +200 to +300mV in order to accept electrons from cytochrome c_{550} or pseudoazurin (Moir *et al.*, 1993). The C-terminal (bottom) domain forms an eight bladed β -propellor structure surrounding the d_1 haem. The haem iron is liganded by a histidine residue from the β -propellor domain and a tyrosine residue (Tyr-25) from the α -helical domain. In addition to the tyrosine

residue the two domains are connected by approximately 20 hydrogen bonds. Sequence conservation between the different cd_1 nitrite reductases is high (~70%) and groups the proteins together as members of a single family. Figure 1.8 demonstrates the high degree of sequence similarity between three cd_1 containing nitrite reductase enzymes from three representative bacterial strains. However structural diversity is observed to exist between members of the cytochrome cd_1 nitrite reductase family as the *Ps. aeruginosa* c-type haem is His-Met liganded instead of bis-His (Silvestrini *et al.*, 1989). Also the presence of a long deletion in the *Ps. stutzeri* peptide sequence spanning the Tyr-25 ligand region means this residue cannot coordinate to haem d_1 in this organism (Jüngst *et al.*, 1991; Smith and Teidje, 1992).

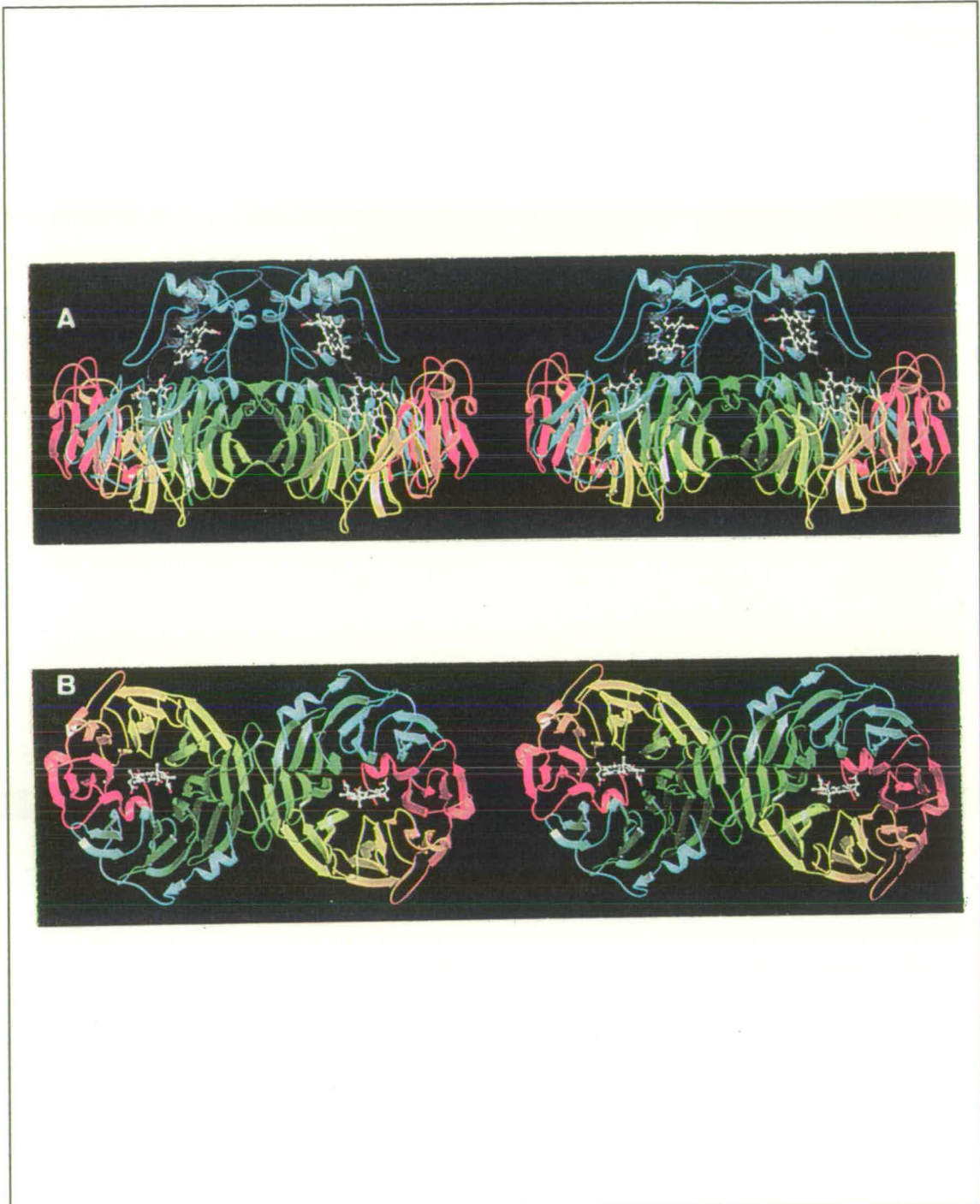


Figure 1.7. X-ray structure of crystallised cytochrome cd₁ nitrite reductase from *T. pantotropha*. (Fülöp et al., 1993; Fülöp et al., 1995). The protein chain is rainbow coloured with the N-terminus in blue and finishing at residue 567 at the C-terminus in red. The c type cytochrome (blue in A), containing the covalently linked c haem, has been removed in (B) to reveal the location of the d₁ haem in the middle of an eight-bladed β propellor structure in the d₁ domain. The d₁ haem is the site of nitrite reduction. Taken from Fülöp *et al* (1995).

	1				50
Psaer	..	.MPFGKP	LVGTLLASLT	LLGLATAHAK	DDMKAAEQYQ GAASAV....
Paden		MRQRTPFARP	...GLLASAA	LALVLGPLAV	AAQEQAAPPK DPAAALEDHK
Psstu	..	MSTIGKP	VIGLFAGMSN	LLGMAVAHA.
	51				100
PsaerDPA	HVVRTNGAPD	MSESEFNKAK	QIYFQRCAGC
Paden		TKTDNRYEPS	LDNLAQQDVA	ALGAPEGIPA	LSDAQYNEAN KIYFERCAGC
PsstuAAPD	MTAEEKEAAK	KIYFERCAGC
	101				150
Psaer		HGVLRKGATG	KPLTPDI....T	QQRGQQYLEA LITYGTPLGM
Paden		HGVLRKGATG	KALTPDL....T	RDLGFDYLS FITYGSPAGM
Psstu		HGVLRKGATG	KNLEPHWEKT	EDGKKIEGGT	LKLGTKRLEN IIAFGTEGGM
	151				200
Psaer		PNWGSSGELS	KEQITLMAKY	IQHTPPQPPE	WGMPEMRESW KVLVKPEDRP
Paden		PNWGTSGELT	AEQVDLMANY	LLLDPAAPPE	FGMKEMRESW QVHVAPEDRP
Psstu		VNYD..DILT	AEEINLMARY	IQHTPDIPPE	FSLQDMKDSW NLIVPVERR.
	201				250
Psaer		KKQLNDLDP	NLFSVTLRDA	GQIALVDGDS	KKIVKVIDTG YAVHISRMSA
Paden		TQQENDWLE	NLFSVTLRDA	GQIALIDGTT	YEIKSVLDTG YAVHISRMSA
Psstu		.RQMNKVNLE	NVFAITLRDA	...QLWDGDT	HEIWKILDTG YAVHISRMSA
	251				300
Psaer		SGRYLLVIGR	DARI.DMIDL	WAKEPTKVAE	IKIGIERSV ESSKFKGYED
Paden		SGRYLFVIGR	DGKV.NMIDL	WMKEPATVAE	IKIGSEARSI ETSKMEGWED
Psstu		SGR..MSTPS	AGWLTTIIDM	WYPEPTTVAT	VRLG.PIRSV DVSKFKGYED
	301				350
Psaer		RYTIAGAYWP	PQFAIMDGET	LEPKQIVSTR	GMTVDTQTYH PEPRVAIIA
Paden		KYAIAGAYWP	PQYVIMDGET	LEPMKIQSTR	GMIYDEQEYH PEPRVAAILA
Psstu		KYLIGGTYWP	PQYSIMDGET	LEPMKVSTR	GQTVVDG.YH PEPRVASIVA
	351				400
Psaer		SHEHPEFIVN	VKETGKVLV	NYKDIDNLTV	TSIGAAPFLH DGGWDSSHRY
Paden		SHYRPEFIVN	VKETGKILLV	DYTDLKNLKT	TEIEAERFLH DGGLDGSHRY
Psstu		SHIKPEWVVN	VKETGQIMLV	DYTDIKNLKT	TTIESAKFLH DGGWDASHRY
	401				450
Psaer		FMTAANNSNK	VA.VIDSKDR	RLSALVD.VG	KTPHPGRGAN FVHPKYGPVW
Paden		FITAANARNK	LV.VIDTKEG	KLVAIEDTGG	QTPHPGRGAN FVHPTFGPVW
Psstu		FMVAANASNK	AAPAVDTKTG	KLAALIDTA.	..KIRTRTRN FVHPQFGPVW
	451				500
Psaer		STSHLGDGSI	SLIGTDPKN.HPQYAW	KKVAELQGQG GGSLFIKTHP
Paden		ATSHMGDDSV	ALIGTDPEG.HPDNAW	KILDSFPALG GGSLFIKTHP
Psstu		STGHLGDDVV	SLISTPSDES	KYAKYKEHNW	KVVQELKMPG AGNLFVKTHP
	501				550
Psaer		KSSHLYVDTT	FNP DARISQS	VAVFDLKNL.DAKYQV LPIAEWADLG
Paden		NSQYLYVDAT	LNPEAEISGS	VAVFDTKAMT	GDGSDPEFKT LPIAEWAGIA
Psstu		KSKHFWADAP	MNPEREVAES	VYVFDMNDLS	KAPTQ..... LNVAKDSGLP

```

                    551                                600
Psaer  EGA. .KRVVQ PEYNKRGDEV WFSVWNGKND SSALVVVDDK TLKLKAVVKD
Paden  EGQ. .PRVVQ GEFNKDGTEV WFSVWNGKDQ ESALVVVDDK TLELKHVIKD
Psstu  ESKAIRGAVQ PEYNKAGDEV WISSGAGKTD QSAIVIYDDK TLKLKRVITD

                    601                                620
Psaer  PRLITPTGKF NVYNTQHDVY
Paden  ERLVTPPTGKF NVYNTMTDTY
Psstu  PAVVTPPTGKF NVFNTMNDVY

```

Figure 1.8. Sequence alignment of the peptide sequences from three cytochrome cd_1 nitrite reductases. Key: Psaer - *Ps. stutzeri*; Paden - *P. denitrificans*; Psstu - *Ps. stutzeri*. The haem c binding motif (Cys-Xaa-Xaa-Cys-His) is illustrated in bold. Alignment was done using the PILEUP programme on the GCG9 package. Peptide sequences were obtained from SwissProt.

1.4.2.2 Roles of the c-type and d_1 haems

It is broadly agreed that the d_1 haem is the site of nitrite reduction, while the c-type haem transfers electrons from the donor protein to the site of catalysis. An apoprotein of *Ps. stutzeri* nitrite reductase was produced which lacked haem d_1 . Without haem d_1 the apoprotein did not exhibit any nitrite reductase activity; activity was restored when the enzyme was reconstituted with native and synthetic haem d_1 (Weeg-Aerssens *et al.*, 1991). The first reliable crystal structure of cytochrome cd_1 nitrite reductase from *T. pantotropha* was elucidated in 1993 (Fülöp *et al.*, 1993). Studies on the crystal structure unambiguously identified haem d_1 as the site of nitrite reduction. The nitrite substrate molecule was identified tightly bound to the haem d_1 active site (Fülöp *et al.*, 1995).

The physiological electron donor to the cytochrome cd_1 nitrite reductase in *Ps. aeruginosa* is thought to be cytochrome c_{551} rather than azurin, as cytochrome c_{551} has a higher affinity for cytochrome cd_1 than the cupredoxin (Timkovich *et al.*, 1982). However both proteins can donate electrons to cytochrome cd_1 (Parr *et al.*, 1977). Pseudoazurin has also been observed to donate electrons to cytochrome cd_1 in this organism (Moir and Ferguson, 1993).

The reductive mechanism of haem d_1 is complicated but is thought to occur in *P. denitrificans* as illustrated in Figure 1.9. Basically reduction of the cytochrome cd_1 enzyme displaces the Tyr-25 ligand from the d_1 haem iron allowing nitrite to bind to the reduced enzyme. Once nitrite is reduced to nitric oxide a refolding of the haem c domain occurs resulting in a change of c haem iron coordination. This change is thought to affect the redox potentials of the c and d_1 haems which forces the reduced nitric oxide product to leave active site. This occurs to prevent the irreversible binding of nitric oxide to FeII which would effectively block the enzyme (Fülop *et al.* 1995; Williams *et al.*, 1997). In organisms which lack the Tyr-25 residue, such as *Ps. stutzeri*, it is assumed that different ligands play a role in catalysis. Proof of this assumption came from studies on *Ps. aeruginosa* (Cutruzzolà *et al.*, 1997; Nurizzo *et al.*, 1998). In sequence alignments of the cytochrome cd_1 nitrite reductase the catalytically important Tyr25 residue in *P. denitrificans* is found at amino acid position number 10 in *Ps. aeruginosa*. Mutagenesis experiments were used to change this Tyr10 residue to Phe and the catalytic activity of the nitrite reductase enzyme determined (Cutruzzolà *et al.*, 1997). It was found that in *Ps. aeruginosa* NiR substitution of Tyr10 with Phe had no effect on the activity, optical spectroscopy and electron transfer kinetics of the enzyme. Further experiments have suggested that Tyr10 coordinates to FeIII via a hydroxide intermediate (Nurizzo *et al.*, 1998). As a result of this difference in coordination the conformational changes observed in the *Ps. aeruginosa* NiR are less extensive than those in *P. denitrificans*. The implications of this are that the conformational changes involved in NiR catalysis between species are considerably diverse.

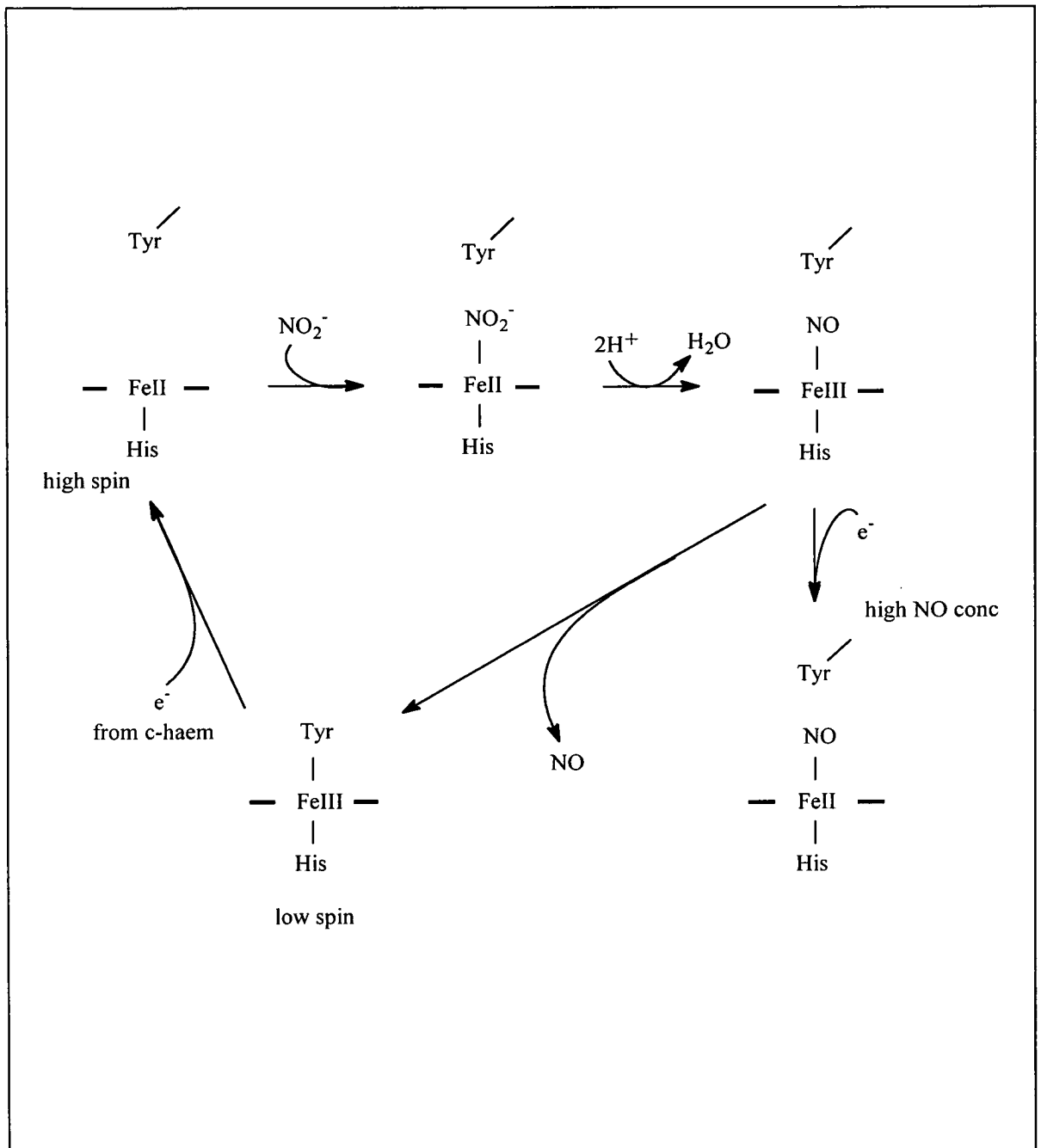


Figure 1.9. A reaction scheme for cytochrome cd_1 nitrite reductase. The tyrosine coordinates the haem iron only in the oxidised (Fe^{III}) state and nitrite binds to reduced (Fe^{II}) haem d_1 . The formation of a species in which nitric oxide is irreversibly bound to the reduced form of the d_1 haem occurs as result of electron transfer from the c-type haem under conditions of high nitric oxide concentration. Taken from Berks *et al* (1995a).

1.4.2.3 The cytochrome cd_1 genes

The *nirS* structural cytochrome cd_1 gene is found in clusters with genes encoding electron transport proteins and enzymes involved in haem d_1 biosynthesis. This is true for *Ps. aeruginosa* and *P. denitrificans* but the gene cluster of *Ps. stutzeri* is particularly well characterised (Jüngst *et al.*, 1991). In *Ps. stutzeri* the *nirS* gene is followed by *nirT* encoding a tetra-haem c electron transport protein, *nirB* codes for a di-haem cytochrome c_{552} , *nirM* encodes a mono-haem cytochrome c_{551} and *nirC* which codes for a small haem type cytochrome. NirQ regulates the catalytic activity of NirS (Jüngst and Zumft, 1992). A number of genes involved in haem d_1 biosynthesis have also been identified downstream of the *nirQSTBMC* gene cluster (Kawasaki *et al.*, 1997). The complete gene clusters of *Ps. aeruginosa*, *P. denitrificans* and *Ps. stutzeri* are represented diagrammatically in Figure 1.2.

1.4.3 Copper nitrite reductase

Copper nitrite reductases have been isolated from a number of bacterial species including *Alcaligenes. faecalis* (Kakutani *et al.*, 1981), *Achromobacter cycloclastes* (Iwasaki and Matsubara, 1972), *Alcaligenes xylosoxidans* (Abraham *et al.*, 1993), *Pseudomonas aureofaciens* (Zumft *et al.*, 1987) and *R. sphaeroides* f. sp. *denitrificans* (Sawada *et al.*, 1978). The presence of the copper nitrite reductase appears to be widespread as a copper containing nitrite reductase gene probe from *Pseudomonas* sp. G-179 has been used diagnostically to detect this gene in a number of other denitrifying strains (Ye *et al.*, 1993). In all cases the enzymes are homotrimers with a subunit mass of 36kDa. Each subunit binds one type I and one type II copper centre. The structural gene has been sequenced from *Al. faecalis* (Nishiyama *et al.*, 1993), *Pseudomonas* sp. G-179 (Ye *et al.*, 1993) and *Ps. aureofaciens* (Glöckner *et al.*, 1993). Crystallisation of the protein from *A. cycloclastes* by Godden and co-workers in 1991 provided a wealth of information enabling the actual reductive mechanism to be elucidated, see sections 1.4.3.2 and 1.4.3.3.

1.4.3.1 Biological copper centres

Copper proteins have been classified according to their spectroscopic state as type I, II or III (Malkin and Malmström, 1970).

Type II copper centres contain a single copper atom and are involved in catalysis at the active site. Ligation of the copper is mainly by histidine residues with at least one water derived ligand that can be displaced by either substrate or other exogenous ligands. Cysteine ligation is absent (Berks *et al.*, 1995a).

'Blue copper' or type I copper are mononuclear centres with cysteine ligation. They are named blue copper centres as they have a very intense absorption near 600nm. Two histidine and one cysteine form strong bonding interactions with the copper atom whereas the axial ligand interaction is weak and provided usually by methionine. Type I copper centres are involved in electron transfer rather than catalytic reactions.

Type III copper centres are dinuclear and exist in an EPR silent Cu(II)-Cu(II) state. Type III centres are involved in ligand binding and/or catalysis. An unusual catalytic type III copper centre containing a cysteine sulphur bridge (Cu₂) is found in nitrous oxide reductase. This is considered in more detail in section 1.6.2.

A fourth type of copper centre, the Cu_A centre, has been detected in cytochrome oxidase and nitrous oxide reductase. This copper centre acts solely as an obligate one electron carrier.

1.4.3.2 The molecular structure

The copper nitrite reductase was initially crystallised from *A. cycloclastès* (Godden *et al.*, 1991). The crystal structures of the *Al. faecalis* and *A. xylooxidans* enzymes have since been determined (Grossman *et al.*, 1993; Kukimoto *et al.*, 1994). In all cases the enzyme was found to be a homotrimer which binds three type I and three type II copper centres. Each monomer forms two β barrel domains. The monomer domains are stabilised by a bridging helical region between them. The type I copper centre is completely liganded by residues within domain one, His-95,

His-145, Met-150 and Cys-136. The type II copper centre has a more complex set of ligands arranged in a regular tetrahedron. His-100 and His-135 coordinate from domain one whereas His-306 coordinates from domain two of a different subunit (Figure 1.10). The fourth ligand to the type II copper is a solvent, probably water. Site directed mutagenesis on these ligands in *Al. faecalis* conclusively enabled the proposed roles of the two copper centres to be confirmed (Kukimoto, 1994).

All the type I and type II copper ligands are conserved in the sequenced copper nitrite reductases. Figure 1.11 shows a sequence alignment of three well characterised copper nitrite reductase peptides with the conserved copper ligands highlighted. A high degree of sequence conservation over the entire length of the peptides is observed (~80%). Due to this high degree of sequence conservation a trimeric arrangement is expected for all copper nitrite reductases.

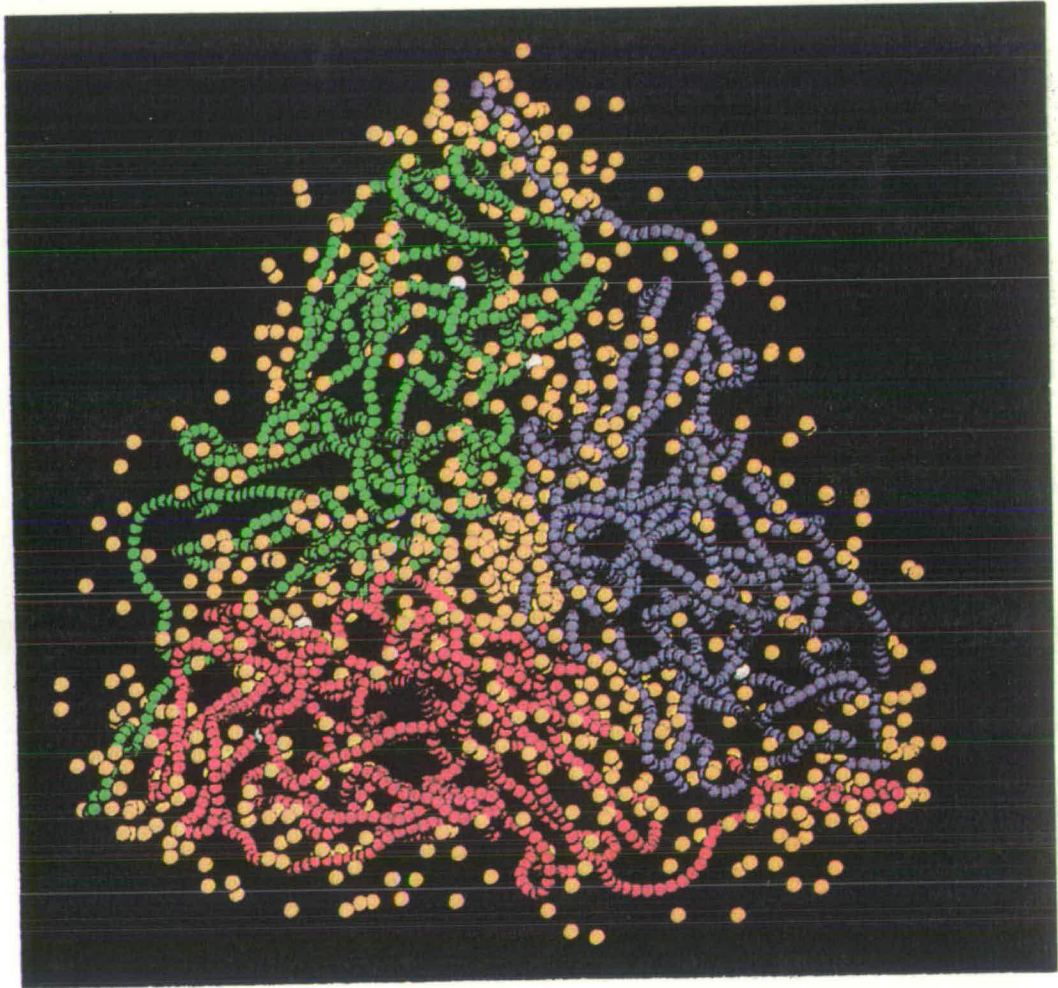


Figure 1.10. Crystal structure showing the trimeric arrangement of the hydrated copper nitrite reductase from *A. cycloclastes*. The monomers are represented by their smoothed backbone structures using different colours (red, green and blue). Water oxygens are shown as yellow spheres. The copper atoms are shown as white spheres. Taken from Grossman *et al* (1993).

	1					50
Afnir	MAEQMQISRR	TILAGAALAG	ALAPVLATTS	AWGQGAVRK.	..ATAAEIAA	
CyclonirAA	GAAPV.....DIST	
Panirax	MSEQFRLTRR	SMLAGAAVAG	ALAPVVTSVA	HAEGGGIKTN	SAATAANIAT	
	51					100
Afnir	LPRQKVELVD	PPFVHAHSQV	AEGGPKVVEF	TMVIEEKKIV	IDDAGTEVHA	
Cyclonir	LPRVKVDLVK	PPFVHAHDQV	AKTGPRVVEF	TMTIEEKKLV	IDREGTEIHA	
Panirax	LERVKVELVK	PPFVHAHTQK	AEGEPKVVEF	KMTIQEKKIV	VDDKGTEVHA	
	101			I	II	150
Afnir	MAFNGTVPGP	LMVVHQDDYL	ELTLINPETN	TLMHNIDFHA	ATGALGGGGL	
Cyclonir	MTFNGSVPGP	LMVVHENDYV	ELRLINPDTN	TLLHNIDFHA	ATGALGGGAL	
Panirax	MTFDGSVPGP	MMIVHQDDYV	ELTLVNPDTN	ELQHNIDFHS	ATGALGGGAL	
	151		III	I	I	200
Afnir	TEINPGEKTI	LRFKATKPGV	FVYHCAPPGM	VPWHVVS GMN	GAIMVLPREG	
Cyclonir	TQVNPGEETT	LRFKATKPGV	FVYHCAPEGM	VPWHVTS GMN	GAIMVLP RDG	
Panirax	TVVNP GD TAV	LRFKATKAGV	FVYHCAPAGM	VPWHVTS GMN	GAIMVLP RDG	
	201					250
Afnir	LHDGKGKALT	YDKIYYVGEQ	DFYVPRDENG	KYKKYEAPGD	AYEDTVKVMR	
Cyclonir	LKDEKGQPLT	YDKIYYVGEQ	DFYVPKDEAG	NYKKYETPGE	AYEDAVKAMR	
Panirax	LKDHKGHEL V	YDKVYYVGEQ	DFYVPKDENG	KFKKYESAGE	AYPDVLEAMK	
	251					300
Afnir	TLTPTHVVFN	GAVGALTGDK	AMTAAVGEKV	LIVHSQANRD	TRPHLIGGHG	
Cyclonir	TLTPTHIVFN	GAVGALTGDH	ALTAAVGERV	LVVHSQANRD	TRPHLIGGHG	
Panirax	TLTPTHVVFN	GAVGALTGDN	ALQAKVGDRV	LILHSQANRD	TRPHLIGGHG	
	301				I	350
Afnir	DYVWATGKFN	TPPDVDQETW	FIPGGAAGAA	FYTFQQPGIY	AYVNHN LIEA	
Cyclonir	DYVWATGKFR	NPPDL DQETW	LIPGGTAGAA	FYTFRQPGVY	AYVNHN LIEA	
Panirax	DYVWATGKFA	NPPELDQETW	FIPGGAAGAA	YYTFQQPGIY	AYVNHN LIEA	
	351		380			
Afnir	FELGAAA HFK	VTGEWNDDL M	TSVLAPSGT*			
Cyclonir	FELGAAG HFK	VTGEWNDDL M	TSVVKPASM.			
Panirax	FELGAAG HFK	VTGDWNDDL M	TAVVSPTSG.			

Figure 1.11. Sequence alignment of three copper nitrite reductase peptides. The conserved type I and type II copper binding ligands are shown in bold. Key to organisms: Afnir = *Al. faecalis*, Cyclonir = *A. cycloclastes*, Panirax = *Ps. aeruginosa*. The copper ligands have different positions in the above sequence alignment than are mentioned in the text due to the presence of signal sequences for secretion at the N-terminals of the *Al. faecalis* and *Ps. aeruginosa* peptides (Nishiyama *et al.*, 1993).

1.4.3.3 Roles of the type I and type II copper centres

The type I copper centre transfers electrons from donor proteins (cupredoxins and cytochromes) to the type II centre. This is analogous to c-type haem in the cytochrome cd_1 nitrite reductase. As type II copper centres commonly form catalytic sites they are probably the site of nitrite reduction. It has been shown that the activity of the copper nitrite reductase is proportional to the type II copper content with zero activity observed when the type II copper is completely depleted (Libby and Averill, 1992).

Nitrite binds to the reduced form of the enzyme at the type II copper site by replacing the solvent ligand (Godden *et al.*, 1991; Adman *et al.*, 1995; Strange *et al.*, 1995). Two ligands (Asp-98 and His-255) are important in maintaining the interaction of nitrite with the type II copper centre. When nitrite displaces water it is suggested that Asp-98 becomes protonated so that only OH^- is actually displaced, not H_2O as previously described. The protonated Asp-98 steadies the displaced solvent ligand via hydrogen bonding. The unstable Cu-ONO nitrosyl intermediate first suspected by Suzuki and coworkers in 1989 is stabilised due to hydrogen bonding from His-255 so that it can receive electrons from the type I copper site. The protonated Asp-98 also helps to break one of the NO bonds of the nitrosyl intermediate leaving one of the nitrite oxygens still attached to the copper. The type II copper is regenerated by the replacement of the solvent ligand (OH^-) and nitric oxide leaves the active site (Adman *et al.*, 1995; Strange *et al.*, 1995). Figure 1.12 illustrates this in more detail.

Evidence for the type I copper centre being involved in electron transport came from studies on *Al. faecalis*. Substitution of the type I copper ligand Met-150 with glutamine resulted in a type I copper deficient protein that lost 95% of the wild type activity when methyl viologen was used as an exogenous electron donor, (Kukimoto *et al.*, 1994). It has been suggested that electrons may pass from the type I copper to the active site across the bond connecting the two adjacent residues involved in the type I and type II coordination of copper, Cys-136 and His-135, (Berks *et al.*, 1995a), although a mechanism for this has not yet been proposed. The

type I copper centre also has to receive electrons from donor proteins. Other cupredoxins such as amicyanin achieve this by means of a surface exposed histidine copper ligand (Chen *et al.*, 1992). However the nitrite reductase type I copper centre is buried beneath the enzyme surface and the presence of solvent molecules and the shape of the enzyme itself could effectively block access of any potential donor molecules. The actual mechanism by which the type I copper receives electrons from an assortment of electron donors is discussed in more detail in section 1.4.4.

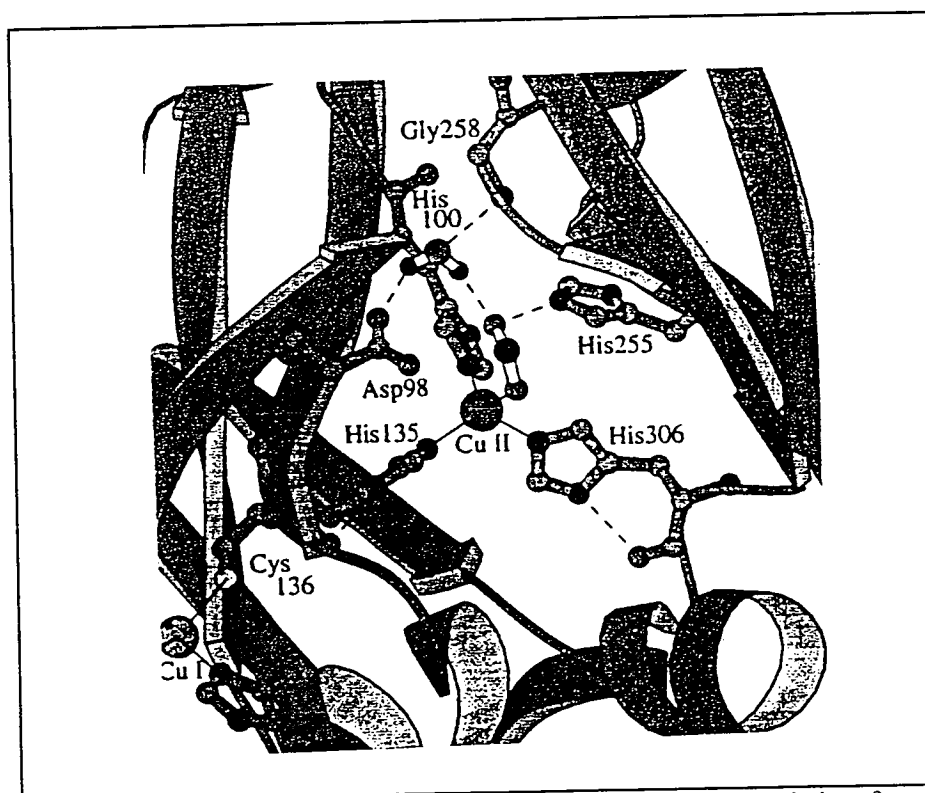


Figure 1.12. Model of the proposed mode of nitrite binding at the subunit interface in nitrite reductase. The positions of the two copper ligands are illustrated as are the nitrite stabilising residues, Asp-98 and His-255, in the copper cavity. The displaced solvent ligand pictured here hydrogen bonded to Asp-98 has also been proposed to be displaced as OH^- not H_2O (Adman *et al.*, 1995), see text. Taken from Strange *et al* (1995).

1.4.3.4 The copper nitrite reductase genes

The structural gene for copper nitrite reductase, *nirK*, was identified in *Pseudomonas* sp. G-179 by Tn5 mutagenesis (Ye *et al.*, 1993), in *Al. faecalis* by using protein derived oligonucleotides as screening probes (Nishiyama *et al.*, 1993) and in *Ps. aeruginosa* by screening an expression library with an anti-NirK anti-serum (Glöckner *et al.*, 1993). The gene from *Ps. aeruginosa* encodes a polypeptide of 363 amino acids including a signal sequence of 24 amino acids for protein export (Figure 1.11). This gene showed 63.8% similarity to the *nirK* gene from *A. cycloclastes*. No other genes associated with copper nitrite reductase enzyme assembly or electron transport located with *nirK* have been identified at present. Nevertheless the presence of a copper nitrite reductase gene cluster analogous to those for the cytochrome cd_1 enzymes cannot be discounted and it is assumed that a comparable gene cluster will exist. Recently the *nnrR* gene of *R. sphaeroides* f. sp. *denitrificans* was characterised. The NnrR gene product is believed to activate transcription of the copper nitrite reductase structural gene and also the nitric oxide reductase genes in response to nitric oxide concentration (Tosques, *et al.*, 1996). However the *nnrR* gene is found immediately upstream from *norC* and the *nor* and *nir* gene clusters in copper nitrite reducing organisms are not believed to form supraoperon structures characteristic of denitrifiers containing cd_1 nitrite reductases (Tosques, *et al.*, 1997).

1.4.3.5 A membrane bound copper nitrite reductase?

In addition to the copper nitrite reductase enzymes outlined above the *aniA* gene product of *Neisseria gonorrhoeae* has been identified as a membrane bound copper nitrite reductase (Berks *et al.*, 1995a; Mellies *et al.*, 1997). The gene is induced anaerobically in the presence of nitrite (Hoehn and Clark, 1992a), and the gene product has been localised to the outer membrane. This suggests that nitrite reduction may occur extracellularly although this would be problematic for the cell if the nitrite reductase electron donors and substrates ordinarily found in the periplasm

were present in *N. gonorrhoeae*. The AniA protein can be detected immunologically in patient sera implying that adaptation to anaerobiosis with associated nitrite reduction is important in successful gonococcal infection. *N. subflava* was observed to react to the anti-AniA anti-serum (Hoehn and Clark, 1990).

The AniA sequence contains N and C-terminal motifs characteristic of gonococcal lipoproteins (Hoehn and Clark, 1992b). At the N-terminal the consensus sequence, Ala-Leu-Ala-Ala-Cys, is present. This pentapeptide is recognised and processed by the enzyme signal peptidase II which cleaves between Ala and Cys. The Cys residue becomes modified with glycerol and fatty acid to form the anchor point of the peptide into the outer membrane (Hussain *et al.*, 1982; Pugsley *et al.*, 1986). At the C-terminal AniA has four direct contiguous copies of another pentapeptide, Ala-Ala-Ser-Ala-Pro. The region between these motifs reveals significant similarity to copper nitrite reductases (Figure 1.13). Overall ~30% identity exists between AniA and all of the characterised copper nitrite reductase proteins with complete conservation of all the type I and type II copper binding ligands.

An azurin like protein also located in the outer membrane has been identified in *N. gonorrhoeae* (Gotschlich and Seiff, 1987). It is suggested that this is the electron donor to AniA (Berks *et al.*, 1995a). If this is the case then a highly modified arrangement of the denitrification pathway outlined in section 1.7.1 must be present in *N. gonorrhoeae* for denitrification to occur.

```

10 TILAGAALAGALAPVLATTSAWGQGAVRKATAAEIAALPRQKVELVDPPF 59
   .: | | | | | . . . | | | . . .: |
12 SLFALAACGGEQAAQAPAETPAASAEAASSAAQATAETPAGELPVIDAVT 61
   . . . . .
60 VHAHS...QVAEGGPKVVEFTMVIIEKKIVIDDAGTEVHAMAFNGTVPGP 106
   || : | | | | | | | . || | | | | | | | |
62 THAPEVPPAIDRDYPAKVRVKMETVEKTMKDD.GVEYRYWTFDGDVPGR 110
   . . . . .
                                     I   II .
107 LMVVHQDDYLELTLINPETNTLMHNIDFHAATGALGGGGLTEINPGEKTI 156
   :. | : | .|. | ..|. ||:||||||| | | | | |
111 MIRVREGDTEVEFEFSNNPSSSTVPHNVDFHAATGQGGGAAATFTAPGRTST 160
   . . . . .
                                     III . I   I
157 LRFKATKPGVFVYHCAPPGMVPWHVVSGMNGAIMVLPREGLHDGK GKALT 206
   ||| .||:| ||| | | : .|| | | :| | :|||
161 FSFKALQPLGIYIYHCA.VAPVGMHIANGMYGLILVEPKGLP.....K 202
   . . . . .
207 YDKIYYVGEQDFYVPRDENGKYYKYEAPGDAYEDTVKVMRTLTPTHVVFN 256
   || :|: : ||| | | | | | | . | :|||
203 VDKEFYIVQGDFYTK.....GKKGAQGLQPFDMDKAVAE.QPEYVVFN 244
   . . . . .
257 GAVGALTGDKAMTAAVGE..KVLIVHSQANRDTRPHLIGGHGDYVWATGK 304
   | ||:| | | :| | | | . . . | . |.|| | | :| |
245 GHVGSIAGDNALKAKAGETVRMYVGNPVLVSSSFHVIGEIFDKVYVEGG 294
   . . . . .
                                               II .
305 FNTPPDQDETWFIPGGAAGAAFYTFQQPGIYAYVNHNLIEAFELGAAAH 354
   .| :. :| | . : | | | | .|. : | | | |
295 KLINENV..QSTIVPAGGSAIVEFKVDIPGSYTLVDHSIFRAFNKGALGQ 342
   . . . . .
355 FKVTGEWNDDLMTSVLA 371
   || | | :| | | .
343 LKVEGAENPEIMTQKLS 359

```

Percent identity: 33.5%

Figure 1.13. Sequence alignment of the copper nitrite reductase peptide from *Al. faecalis* and AniA from *N. gonorrhoeae*. The conserved type I and type II copper ligands are illustrated. The top peptide corresponds to *Al. faecalis* and the bottom to *N. gonorrhoeae*.

1.4.4 Electron donation to the cytochrome cd_1 and copper nitrite reductases

It was originally believed that electron donors containing copper would only donate electrons to proteins that also contained copper. However Glöckner and coworkers (1993) expressed the copper nitrite reductase protein of *Ps. aeruginosa* in a *Ps. stutzeri* mutant deficient in cytochrome cd_1 . Surprisingly *Ps. stutzeri* was able to donate electrons to the copper nitrite reductase even though it does not express a cupredoxin such as azurin or pseudoazurin (Glöckner *et al.*, 1993). More recently pseudoazurin has been identified as the preferred electron donor to the cd_1 nitrite reductase in *T. pantotropha* (Williams *et al.*, 1995). This suggests that there are different types of electron donor to nitrite reductase enzymes in most of the nitrite reducing organisms identified so far.

Cytochrome cd_1 has a dual electron acceptor specificity for cytochrome c_{551} and azurin *in vitro* (Wharton *et al.*, 1973; Parr *et al.*, 1997). However *in vivo* one electron donor tends to be favoured over the other and this depends on the denitrifying bacterial species. A mutation in the structural azurin (*azu*) gene in *Ps. aeruginosa* is silent with respect to nitrite reduction; the cellular growth rate is only affected in an azurin-cytochrome c_{551} double mutant (Vijgenboom *et al.*, 1997). Also in *P. denitrificans* a mutation in cytochrome c_{550} does not affect nitrite reduction (van Spanning *et al.*, 1990). Cytochrome cd_1 from *P. denitrificans* GB17 accepts electrons from both its indigenous pseudoazurin and from cytochrome c_{550} (Moir *et al.*, 1993). It seems that with the cytochrome cd_1 nitrite reductases there is some degree of redundancy in the recognition of electron donors.

The principle electron donors to copper nitrite reductases are azurin and pseudoazurin. Both proteins are members of the cupredoxin family of small (12 to 14kDa) electron transfer proteins with a single type I copper atom (Adman, 1991). Azurin acts as electron donor to the copper nitrite reductases found in *P. aureofaciens* and *Al. xylosoxidans* (Zumft *et al.*, 1987; Dodd *et al.*, 1995), whereas pseudoazurin donates electrons to *Al. faecalis* and *A. cycloclastes* (Kakutani *et al.*, 1981; Liu *et al.*, 1986). The X-ray structures of pseudoazurin and azurin are almost superimposable despite the fact that there is as little as 11% sequence similarity

between the two peptides. However the azurin of *P. aeruginosa* reacts poorly with the copper nitrite reductase from *Al. faecalis* (Kukimoto *et al.*, 1996).

1.4.4.1 Mechanism of electron donation

The interaction of electron donor with its related nitrite reductase is believed to be electrostatic. Site-directed mutagenesis on the pseudoazurin-copper nitrite reductase pair from *Al. faecalis* identified a ring of complementary charges on the two proteins (Kukimoto *et al.*, 1995; Kukimoto *et al.*, 1996). Four basic lysine residues (Lys-10, Lys-38, Lys-57 and Lys-77) on the surface of pseudoazurin surround a type I copper site and interact with four exposed surface residues on the copper nitrite reductase (Glu-197, Asp-205, Glu-204 and Glu-118 respectively). This electrostatic hydrophobic patch pairing brings the two type I copper centres of each protein 14-15Å away from each other to facilitate electron transfer via a network of stabilising hydrogen bonds, (Figure 1.14). A similar interaction is proposed to occur between pseudoazurin and the haem c domain of cytochrome cd_1 nitrite reductase in *T. pantotropha* (Williams *et al.*, 1995). However the surface of azurin lacks these conserved lysine residues and it is expected that azurin forms an electron transferring complex with its redox partner in a different and as yet undefined manner (Kukimoto *et al.*, 1996). The hydrophobic patch concept for recognition amongst electron transfer partners is also proposed to be the mechanism which facilitates electron transfer from the c-type cytochromes (Williams *et al.*, 1995). This may help to explain why haem cd_1 nitrite reductase proteins are able to accept electrons from donors other than their indigenous redox partner and why there is a lower degree of redundancy between copper nitrite reductases and their electron donor proteins.

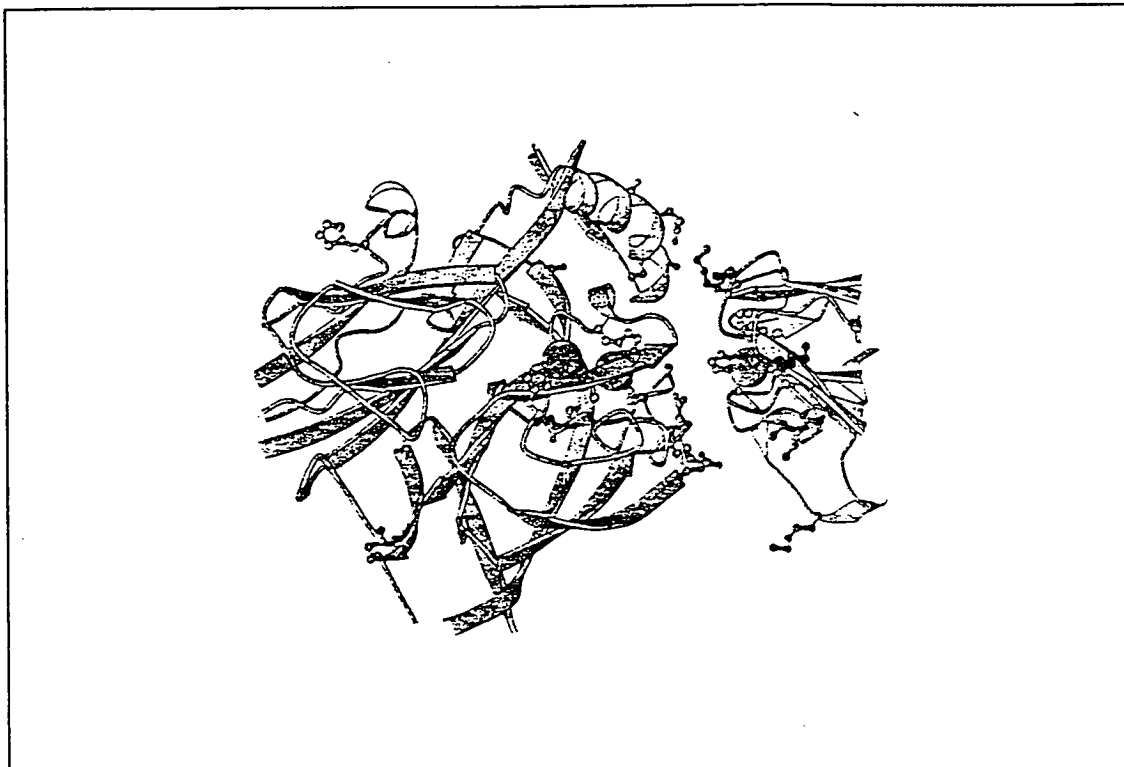


Figure 1.14. Proposed electron transfer complex between the copper nitrite reductase and pseudoazurin of *Al. faecalis*. A single subunit of NiR is on the left and pseudoazurin on the right. The amino acid residues forming the hydrophobic patch are represented as ball and stick structures. Taken from Kukimoto *et al* (1996).

1.5 Nitric oxide reductase

This reductase was the last of the enzymes of denitrification to be identified. For many years there was debate as to whether nitric oxide was a freely diffusible intermediate in denitrification. Identification was hampered as nitric oxide is highly cytotoxic; enzymes which use it as their substrate have such a high affinity for it ($k_m \sim 10\text{-}60\mu\text{M}$) that any free nitric oxide is effectively scavenged by these enzymes, before it has a chance to accumulate and be detected. However in the late 1980s this debate was finally ended with the isolation of free nitric oxide from *A. cycloclastes* (Goretski and Hollocher, 1988). A spectrophometric technique was employed in which extracellular haemoglobin was used to trap nitric oxide released during denitrification as nitrosyl haemoglobin. As nitric oxide was found to exist as a

free denitrification individual it seemed sensible to assume that a nitric oxide reductase enzyme would be present also. Evidence for the existence of such an enzyme came from studies on a mutant of *Ps. stutzeri* which lacked cd_1 nitrite reductase but was still able to reduce nitric oxide (Zumft *et al.*, 1988). It was also found that deletion of the copper nitrite reductase from *Pseudomonas* sp. G-179 did not abolish nitric oxide reductase activity (Ye *et al.*, 1992). This established that a distinct nitric oxide reductase enzyme was present irrespective of the type of nitrite reductase.

1.5.1 Molecular properties of nitric oxide reductase

Nitric oxide has been purified from *Ps. stutzeri* (Heiss *et al.*, 1989), *P. denitrificans* (Carr and Ferguson, 1990; Dermastia *et al.*, 1991) and *A. cycloclastes* (Jones and Hollocher, 1993). The enzyme is a heterodimer with a 17kDa c-type cytochrome subunit (NorC) and a 53kDa polypeptide that binds haem b (NorB).

NorC is predicted to have a single N-terminal transmembrane helix anchoring the protein to the cytoplasmic membrane at the periplasmic side. A single [Cys-Xaa-Xaa-Cys-His] c-type haem binding motif is present in this domain.

Analysis of NorB has revealed sequence similarity to the catalytic subunits of the haem-copper oxidase family, (Saraste and Castresana, 1994; van der Oost *et al.*, 1994). Subunit I of the haem copper oxidase proteins is the catalytic centre and forms 12 transmembrane helices. Six invariant histidine residues have been identified in helices II, VI, VII, and X. These provide two ligands to a low spin haem, one ligand to a high spin haem and three ligands to a copper ion (Cu_B). The copper ion and the high spin haem form a dinuclear centre where oxygen is reduced (Figure 1.15a). Subunit II possesses a second copper centre (Cu_A) which is believed to be the site of electron entry (van der Oost, *et al.*, 1994). Therefore electron flow goes from the Cu_A centre of subunit II to the low spin haem of subunit I. The electron is then transferred to the high spin haem and then to Cu_B where oxygen is reduced. The crystallisation of cytochrome c oxidase (COX) from *P. denitrificans*, a member of

the haem copper oxidase family, confirmed the helical arrangement of subunit I (Iwata *et al.*, 1995).

The histidine ligands in subunit I are conserved in the NorB subunit of nitric oxide reductase. This suggests that a similar arrangement of the redox centres is present. Helices II and X would provide histidine ligands to a low spin haem, helix X to a high spin haem and helices VI and VII to a metal ion, presumably haem b (Figure 1.15b). By analogy to the haem copper oxidases the low spin haem would be involved in mediating electron transfer (from NorC) to the dinuclear centre which would be the site of nitric oxide reduction. Unfortunately experimental evidence does not completely support the haem copper oxidase model of nitric oxide reduction. EPR studies have found signals corresponding to high and low spin haem (Heiss *et al.*, 1989; Kastrau *et al.*, 1994), but only two rather than three haems have been reported per NorCB complex (Carr and Ferguson, 1990; Heiss *et al.*, 1989). The presence of a non-haem iron in the enzyme was detected by Heiss and coworkers in 1989. Perhaps this indicates the dinuclear centre in NorB is haem/non-haem iron rather than haem/copper.

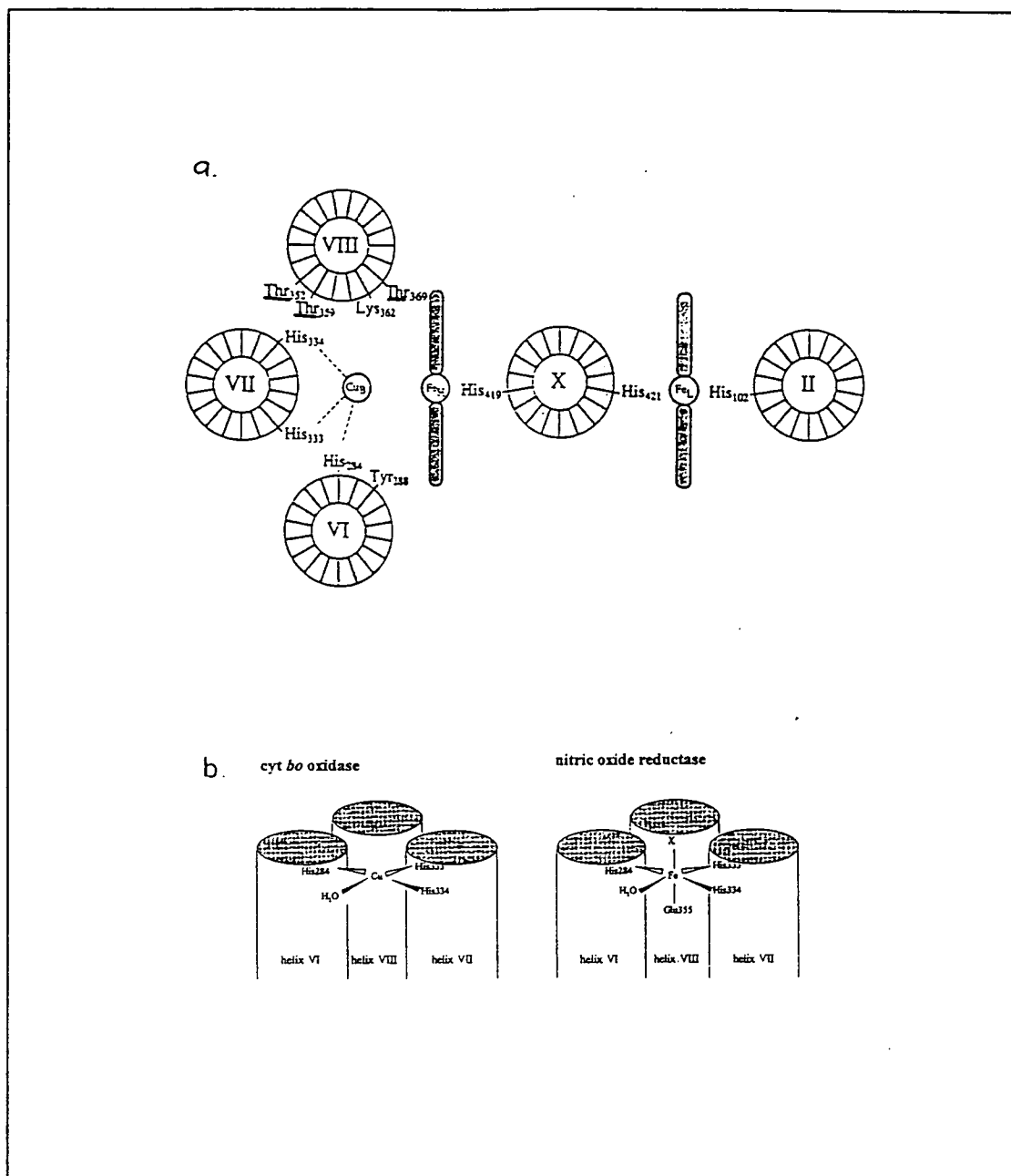


Figure 1.15. Structural models of haem copper oxidase proteins and their relationship to nitric oxide reductase. a) Helical wheel model of haem copper oxidase subunit I. Indicated are the transmembrane helices II, VI, VII and X that contain the histidine ligands of low spin haem (Fe_L) and of the dinuclear centre consisting of high spin haem (Fe_H) and copper (Cu_B). Taken from van der Oost (1994). b) A possible mononuclear iron site in nitric oxide reductase based on the coordination site of copper in the *E. coli* cytochrome bo oxidase. The ligand Glu-355 is conserved in nitric oxide reductase but is absent from the oxidases. The ligand is proposed to create an octahedral coordination site that favours iron rather than copper insertion. Ligand X could be a solvent or amino acid molecule. The amino acid numbering is taken from the *E. coli* cytochrome bo oxidase. Taken from Berks *et al* (1995).

1.5.2 The catalytic mechanism

Nitric oxide reductase catalyses the reduction of nitric oxide to nitrous oxide. This reaction involves the dimerisation of a mononitrogen species to form the N-N bond. A number of haem copper oxidase enzymes also have the ability to reduce nitric oxide. In these cases the reduced oxidase enzyme binds two molecules of nitric oxide in close proximity at the binuclear catalytic site as Fe(II)-NO and Cu_B(I)-NO. These nitric oxide molecules are presumably reduced by electrons from the iron and copper metal centres resulting in the formation of two metal-nitroxyl (M-NO[•]) species. Nitrous oxide and water are then proposed to be formed by dimerisation of the two nitroxyls (Berks *et al.*, 1995a).

EPR studies have shown that on addition of nitric oxide to nitric oxide reductase the formation of a haem nitrosyl is observed (Kastrau *et al.*, 1994). The formation of a non-haem iron dinitrosyl complex similar to that found in the cytochrome oxidase enzyme has been proposed at the active site of NorB (Ye *et al.*, 1994). This model for the formation of two nitrosyl groups is particularly appealing as it brings two nitric oxide molecules close together for N-N bond formation which would not be possible at a monohaem site.

Current models would suggest that nitric oxide reductase has evolved a dinuclear haem/non-haem iron active site in NorB to enable two nitric oxide molecules to come together to dimerise and form nitrous oxide.

1.5.3 Is the nitric oxide reductase a proton pump?

The nitric oxide reductase is an integral protein of the cytoplasmic membrane and reduces nitric oxide in the periplasm. This is thought to protect the cell from nitric oxide toxicity by providing a nitric oxide sink at the cell envelope. Although nitric oxide reductase has structural similarity to the cytochrome oxidase it is believed not to act as a proton pump. Most of the residues involved in proton movement in haem copper oxidases are not conserved in nitric oxide reductase

(Wikström *et al.*, 1994); proton uptake from the periplasm is associated with nitric oxide reduction (Shapleigh and Payne, 1985); a lack of build up of a membrane potential is observed when electrons are supplied from the periplasm to nitric oxide reductase (Bell *et al.*, 1992), and no charge movement is detected when nitric oxide reductase undergoes catalysis (Carr and Ferguson, 1990). These lines of evidence demonstrate that the catalytic site is accessible to protons from the periplasm but not the cytoplasm. The membrane bound nitric oxide reductase therefore does not act as a proton pump.

1.5.4 Nitric oxide reductase genes

The genes for NorC and NorB have been cloned from *Ps. stutzeri*, *P. aeruginosa*, *P. denitrificans* and *R. sphaeroides* f. sp. *denitrificans* (Arai *et al.*, 1995; Bartnikas *et al.*, 1997; deBoer *et al.*, 1994; Zumft *et al.*, 1994). In *Ps. stutzeri* the genes are transcribed on a single transcript in the order *norCB* separated by ~40bp. A number of other genes associated with nitric oxide reductase have been identified adjacent to the *norCB* structural genes. In *P. denitrificans* a six gene cluster has been identified (*norCBQDEF*) (deBoer *et al.*, 1996). *NorQ* encodes a protein with an ATP binding motif, *norE* codes for a protein with five putative transmembrane α helices and *norF* encodes a small protein with two putative transmembrane α -helices. Mutational analysis of these genes revealed that *norE* and *norF* may have a role in regulation of nitric oxide reductase activity. However, inactivation of *norE* and *norF* does not affect expression levels of the enzyme. It has also been hypothesised that the *norE* and *norF* gene products form a third and fourth subunit of nitric oxide reductase (deBoer *et al.*, 1996). Although evidence for this has not been demonstrated as NorE and NorF have not yet been found to purify with nitric oxide reductase. Further analysis on *norQ* and *norD* in *R. sphaeroides* f. sp. *denitrificans* demonstrated that these two genes are required for expression of an active Nor complex (Bartnikas *et al.*, 1997). It is interesting to note that in all organisms characterised so far the *nor* gene cluster is found next to a gene cluster for nitrite reductase. In *Ps. stutzeri* the *nor* genes are found downstream of the nitrite reductase

genes whilst in *Ps. aeruginosa* and *P. denitrificans* the nitric oxide genes are found upstream (section 1.2).

1.6 Nitrous oxide reductase

Nitrous oxide reductase has been isolated from *Ps. stutzeri* (Coyle *et al.*, 1985), *R. sphaeroides* f. sp. *denitrificans* (Michalski *et al.*, 1986), *P. denitrificans* (Snyder and Hollocher, 1987), *T. pantotropha* (Berks *et al.*, 1993), *A. cycloclastes* (Hulse and Averill, 1990) and *Ps. aeruginosa* (SooHoo and Hollocher, 1991). In all cases the enzyme is found in the periplasm as a homodimer with a subunit mass of 66-68kDa. The enzyme has a stoichiometry of four copper atoms per polypeptide. Two types of copper centre are known to exist: the Cu_A site mediates electron transfer between the external electron donor and the catalytic site, and the catalytic site itself, Cu_Z. (This site has also been designated Cu_C and Cu_B but Cu_Z is the term used here.)

Different spectral forms of the enzyme are isolated depending upon whether purification is carried out anaerobically or aerobically. These are referred to as the 'purple' or N₂ORI form (anaerobic purification) and the 'pink' or N₂ORII (oxygen affected) form. Both of these spectral forms can be converted to a 'blue' or N₂ORIII form under reducing conditions in the absence of oxygen. On average the purple form has 2.5 times more activity than the pink form (Coyle *et al.*, 1985). It is believed that the reduced activity of the pink form is due to oxidation during purification. Whether the enzyme is present as a pink form *in vivo* is unknown. In *T. pantotropha* the same type of nitrous oxide reductase is expressed and active under anaerobic and aerobic growth conditions but when purified under aerobic conditions the pink oxygen affected form is always isolated (Bell and Ferguson, 1991; Berks *et al.*, 1993).

1.6.1 The electron transfer (Cu_A)centre

This copper centre is so named as it has similarities to the Cu_A site of mitochondrial-type cytochrome c oxidase complex (complex IV). It has a distinctive colour and is also called the 'purple copper centre'. In cytochrome c oxidase the Cu_A site acts as an obligate one electron carrier between periplasmically located electron donors and a low spin cytochrome. It has no role in proton pumping or catalysis (Hill, 1991; Hill, 1993). An analogous role for the Cu_A centre of nitrous oxide reductase is expected.

Amino acid alignment of nitrous oxide reductase and cytochrome c oxidase subunit II reveals a number of conserved residues believed to be the copper ligands (Zumft *et al.*, 1992). Potential candidates include two histidines, two cysteines, a methionine and an aspartic acid found in a 50 amino acid span at the C-terminal of nitrous oxide reductase (Figure 1.16).

	10	20	30	40	50	60
1.	S.....	..P.....	.G.....Y...	.A...G....
2.	.. DV.H K G .	C.E.CG..H .	.M
3.	I.D..HGF V ..	PQ.T.S.TF .	A..PG..W.Y	C..FCHALH .	EM..RM.VE .
4.	.. D..H	C...C...H .	.M
5. H	C-----TPHP	F

Figure 1.16. Sequence analysis of the Cu_A binding region in nitrous oxide reductase and cytochrome oxidase. The amino acid numbering scheme is arbitrary. All conserved residues are shown in bold. Key to peptide sequences: 1. = ubiquinol oxidase, 2. = cytochrome c oxidases, 3. = nitrous oxide reductases, 4. = consensus Cu_A site, 5. = synthetic type I Cu site. Ubiquinol oxidases are included for comparison as they do not contain Cu_A. Taken from Berks *et al* (1995a).

Mutagenesis experiments on *P. denitrificans* have demonstrated that the conserved aspartate residue is not required for Cu_A coordination (Lappalainen and Saraste, 1994). The ligands involved in binding to Cu_A are very similar to those involved in

type I copper coordination. It has been suggested that the fold of the Cu_A domain may resemble that of the cupredoxins (van der Oost *et al.*, 1992).

The oxidised Cu_A centre has an unusual EPR spectrum that arises from a single electron delocalised over two equivalent copper atoms (Coyle *et al.*, 1985; Kroneck *et al.*, 1989; Kroneck *et al.*, 1989). This novel dinuclear copper centre in nitrous oxide reductase does not conform to the previous characterisation of copper centres as type I, type II and type III (Malkin and Malström, 1970). Two structural models for ligation to the Cu_A site have been proposed with two copper atoms in close proximity to allow electron delocalisation (Blackburn *et al.*, 1994; Lappalainen and Saraste, 1994). Figure 1.17 illustrates these two models.

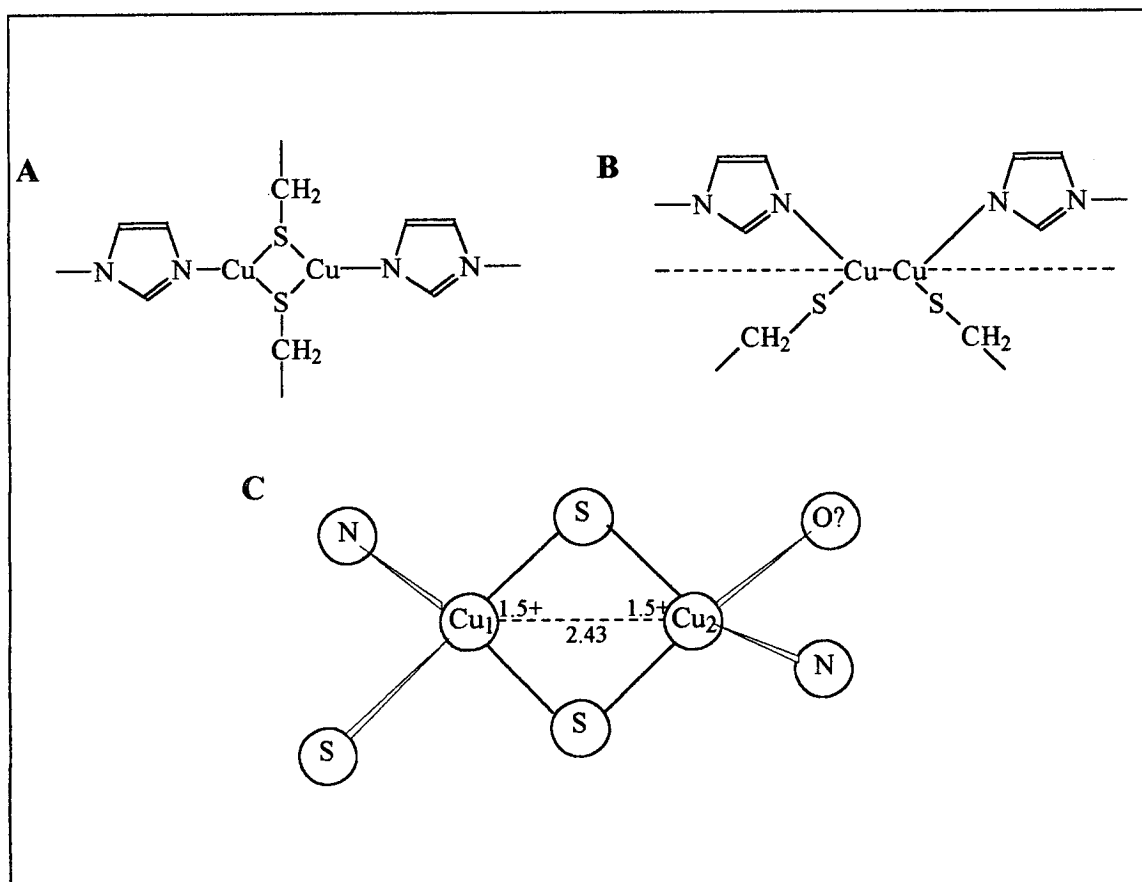


Figure 1.17. Models for the ligation of the Cu_A site. A = Lappalainen and Saraste, (1994) and B = Blackburn *et al.*, (1994). C shows the spatial arrangement of the copper atoms and ligands. The ligands are assigned by site directed mutagenesis. Taken from Zumft (1997).

In the model by Lappalainen and Saraste electron delocalisation occurs over two bridging cysteine ligands. In the model by Blackburn and coworkers the electron is delocalised by a direct copper-copper bond. However the recent crystallisation of cytochrome oxidase from *P. denitrificans* supported the double cysteine-bridged structure (Iwata *et al.*, 1995).

1.6.2 The catalytic (Cu_Z) centre

It has been assumed that the copper atoms not involved in forming the Cu_A centre form the site of nitrous oxide reduction. Characterisation of the catalytic Cu_Z centre was made difficult due to the confusing EPR spectra detected but a dinuclear structural model was proposed by Farrar *et al.* (1991) that accounted for all observed spectroscopic features. It is believed that the novel type III Cu_Z centre exists in at least two forms which correspond to an active and inactive or blocked form. Centre Z has no catalytic activity when it exists in the mixed-valence state Cu(I)/Cu(II) but activity can be restored by re-oxidation. In the absence of substrate some Cu_Z can be reduced to the inactive mixed-valence state suggesting that other molecules such as OH⁻ or carboxylate can bind to the Cu_Z active site as well as nitrous oxide. As well as confusing EPR spectra corresponding to the many forms of the Cu_Z centre the dinuclear Cu_A centre also generates EPR signals of its own. A brief overview of a modified Farrar model for the spectroscopic states of the Cu_A and Cu_Z centres of nitrous oxide reductase is represented in Figure 1.18.

Eight histidines at positions 129, 130, 132, 178, 326, 382, 433 and 494 (*Ps. stutzeri* count) are conserved in all known primary structures and are thought to have a role in coordination to the Cu_Z centre. Unpublished results by Zumft demonstrate that mutagenesis of His-494 results in an inactive enzyme.

The actual mechanism for the reduction of nitrous oxide at the Cu_Z site is unknown. It must be assumed that the dinuclear nature of the active site is crucial to catalysis. Most likely is the activation of the N-O bond of nitrous oxide for cleavage by forming a bonding interaction between the substrate and both of the Cu_Z copper atoms. Effectively nitrous oxide would be bound as a bridging ligand between both

Cu_Z copper atoms and when reduced dinitrogen would be released from the active site. However direct interaction of nitrous oxide with Cu_Z has not been demonstrated (Zumft, 1997).

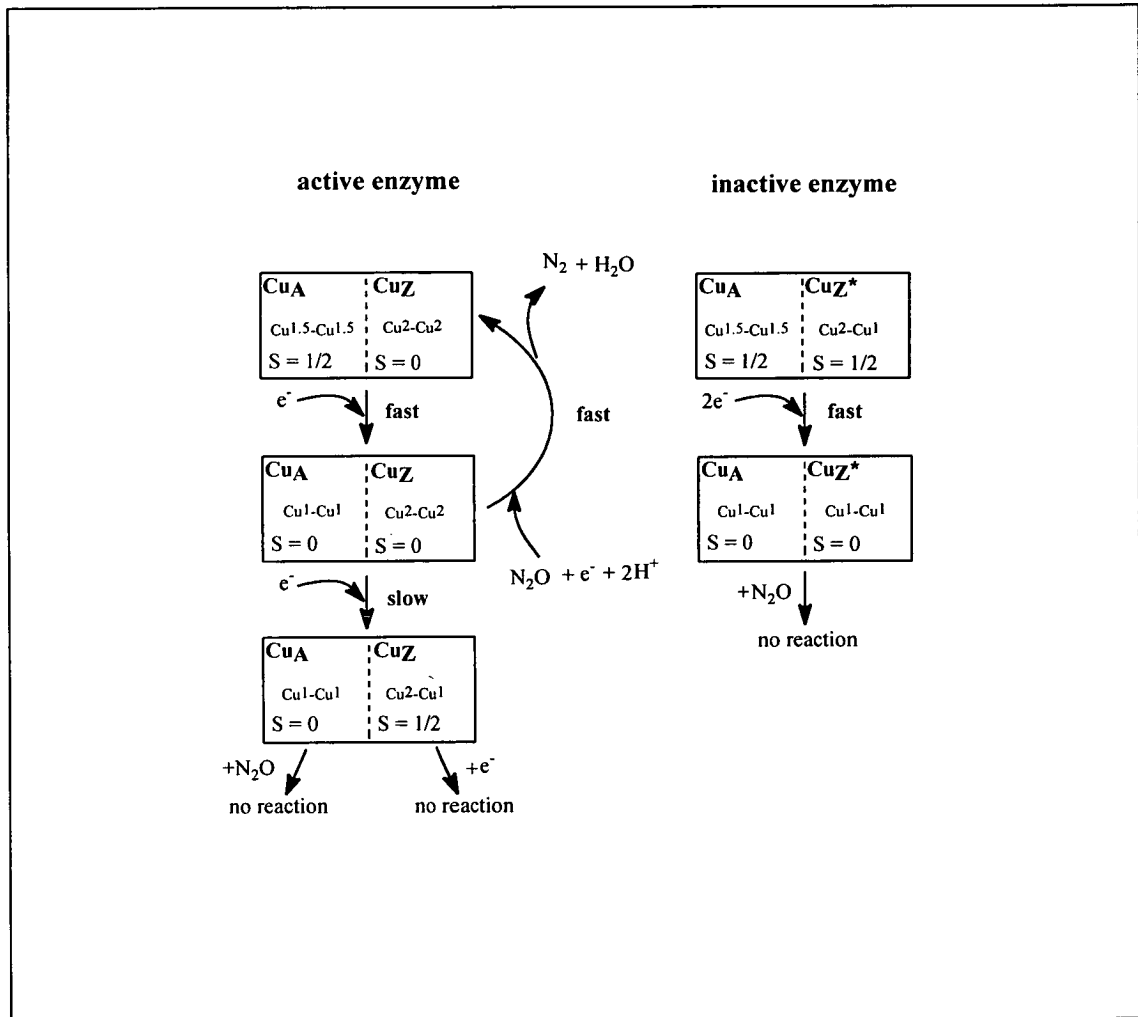


Figure 1.18. Model of the spectroscopic states of the Cu_A and Cu_Z centres of nitrous oxide reductase and the possible relation of these states to the catalytic cycle. Based on the model proposed by Farrar *et al* (1991). Cu_Z^* denotes the Cu_Z centre in the inactive enzyme. Taken from Berks *et al* (1995a).

1.6.3 Electron transfer between the Cu_A and Cu_Z centres

It was initially believed that the extra length of the unusual dinuclear Cu_A centre was necessary to facilitate electron transfer to the Cu_Z catalytic site as is thought to occur in the cytochrome c oxidase enzymes (Berks *et al.*, 1995a). However it has now been suggested that electron transfer occurs via an adjacent covalent bond mechanism similar to that proposed for transfer between type I and type II copper in the copper nitrite reductase enzymes, see section 1.4.3.3. In nitrous oxide reductase a histidine residue (His-46) that is not conserved in the cytochrome c oxidases immediately follows the putative second cysteine ligand for the Cu_A centre (Cys-45; Figure 1.15). If this histidine is determined to be a Cu_Z centre ligand a route for electron transfer analogous to that in the copper nitrite reductases would be possible (Hoeren *et al.*, 1993).

1.6.4 Assembly of the copper centres

In *Ps. stutzeri* the *nosDFY* operon is found immediately downstream of the structural nitrous oxide gene, *nosZ*. The products of these genes are predicted to form a putative copper insertion complex with components on either side of the inner membrane (Figure 1.19). NosF forms a cytoplasmic component with the ability to hydrolyse ATP whilst NosD is a periplasmic binding protein (Cuypers *et al.*, 1995). NosY is highly hydrophobic and forms an integral membrane protein with six predicted transmembrane helices. Transposon mutagenesis was used to determine where assembly of the catalytic centre occurred (Zumft *et al.*, 1985; Zumft *et al.*, 1990). The partially assembled nitrous oxide reductases produced by these *nosDFY* mutants all lacked a Cu_Z site but contained Cu_A and were found located in the periplasm. A periplasmic location for assembly of the Cu_Z centre was postulated. It is also understood that copper passes through the outer membrane for periplasmic assembly into the mature nitrous oxide reductase enzyme via a pore formed by the NosA protein (Lee *et al.*, 1991). It has been proposed the NosD protein functions to insert copper into the catalytic site although sequence analysis has revealed no

peptide motifs for copper coordination. It has been postulated that NosD receives the energy required to perform this task via ATP hydrolysis by NosF (Zumft *et al.*, 1990).

Expression of nitrous oxide reductase is regulated by NosR, a membrane bound regulatory protein with seven membrane spanning domains. NosR is believed to act as a transcriptional activator although homology to other transcriptional activators such as ToxR and FecI is not apparent. The gene encoding NosR is located directly upstream from *nosZ* (Cuypers *et al.*, 1992). The position of the NosR protein in relation to NosZ is illustrated in Figure 1.19.

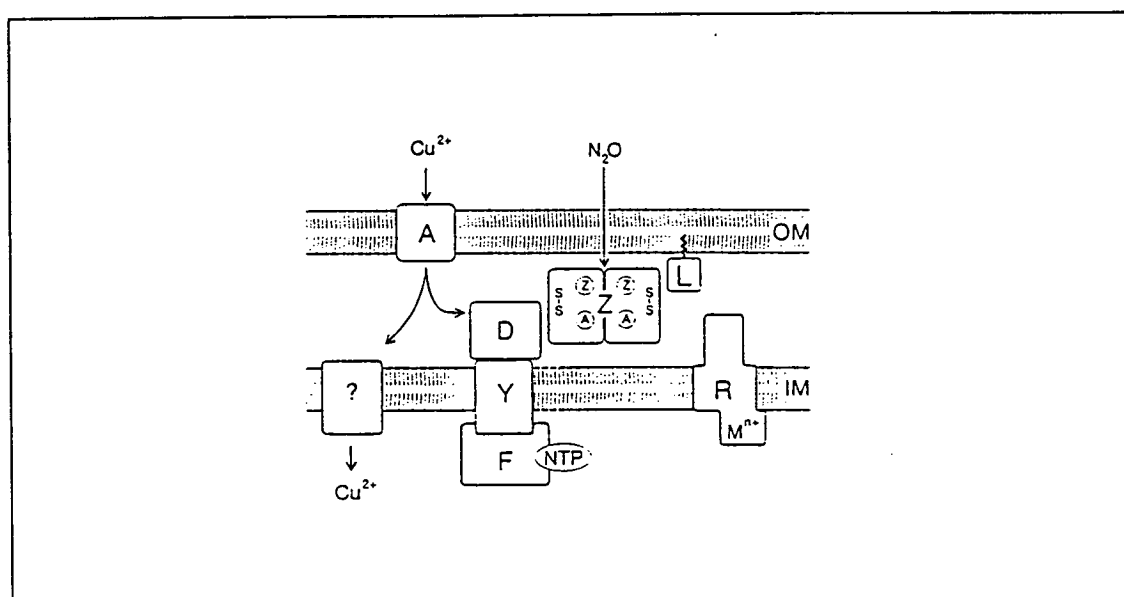


Figure 1.19. Topology of the apparatus for copper insertion into nitrous oxide reductase. A, D, F, L, R, Y and Z denote the proteins NosA, NosD, NosF, NosL, NosR, NosY and NosZ respectively. The encircled small capitals A and Z represent the two types of copper centres, Cu_A and Cu_Z . The question mark symbolises a presumed copper transporter. OM and IM, outer and inner membranes respectively. NTP, nucleotide binding site of NosF; M^{n+} , putative metal binding site of NosR. A detailed discussion is provided in the text. Taken from Zumft (1997).

The individual components of the denitrification system have been described in the preceding sections. However it is also necessary to understand how the components interact to form an efficient energy generating pathway. The spatial arrangement of the enzymes in relation to the cytoplasmic membrane will be discussed as will some aspects of the complex regulatory network that controls denitrification in response to environmental stimuli.

1.7 Electron transport chains

Electron transport in bacteria is diverse due to the many different sources and acceptors of electrons used by various organisms. Also the components in electron transfer from a donor to a given acceptor can also differ markedly between organisms - or even within the same organism depending on growth conditions. Figure 1.20 shows the organisation of the electron transfer components in *P. denitrificans*, a facultative aerobe with a versatile metabolism which can grow using a number of final electron acceptors other than oxygen. From this diagram it can be seen that there are many different respiratory chain components induced by specific growth conditions which are unlikely to be present at the same time. The respiratory chain arrangement of the denitrification pathway in *P. denitrificans* will be discussed in detail to link together the information provided in sections 1.1 - 1.6.



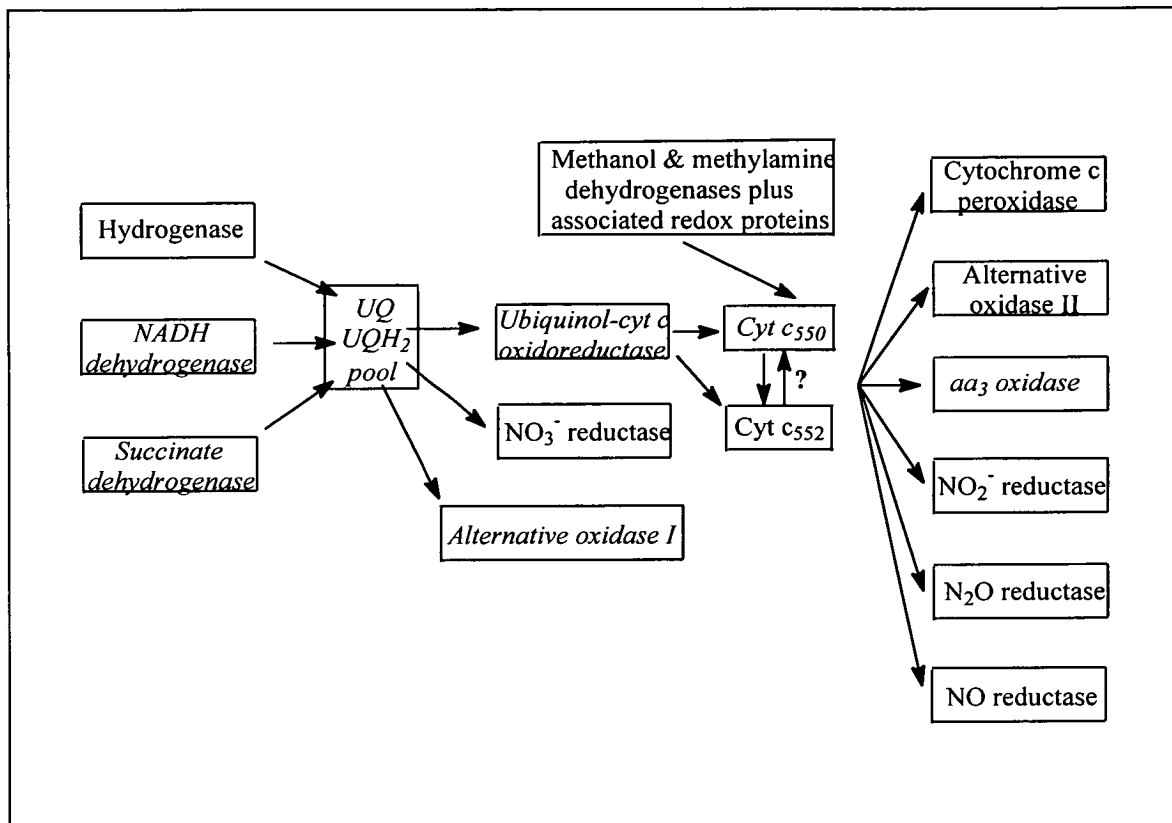


Figure 1.20. Organisation of the electron transport components in *P. denitrificans*. The components in italics are thought to be constitutive and expressed all the time. The other components are induced by appropriate growth conditions and it is unlikely that they are present all at once. Dark boxes indicate integral membrane components; pale lines represent periplasmic components. Taken from Nicholls and Ferguson (1992).

1.7.1 Topology of the denitrification system

Details of the electron transport pathways involved in N-oxide respiration are only available for a limited number of microorganisms. Denitrification electron transport in *P. denitrificans* is discussed in detail as the denitrifying pathway in this organism is particularly well understood. A comparison to denitrification in *Ps. stutzeri* is also illustrated to highlight the similarities that exist between the two organisms in this well defined reductive pathway.

Figure 1.21 shows the arrangement of the N-oxide reductases in and around the cytoplasmic membrane of *P. denitrificans*. The four denitrifying reductase enzymes receive electrons from the electron transport system used in aerobic respiration as, even during anaerobic growth, *P. denitrificans* employs a standard tricarboxylic acid cycle. This means the electron donors to the denitrification electron transport chain are primarily NADH and succinate. The reductases for nitrite and nitrous oxide are soluble periplasmic proteins, while the nitric oxide reductase and membrane bound nitrate reductase are integral membrane proteins.

The membrane bound nitrate reductase receives electrons from UQH₂ on the periplasmic side of the membrane and 2H⁺/UQH₂ are released to the periplasm generating Δp . Two electrons also pass inwards across the cytoplasmic membrane via two b-type haems to the site of nitrate reduction at the molybdenum cofactor on the cytoplasmic surface. In contrast, electrons from ubiquinol are delivered to the nitrite, nitric oxide and nitrous oxide reductases via the cytochrome bc₁ complex and individual periplasmic electron donor proteins. Transfer of electrons from UQH₂, via cytochrome bc₁, to nitrite, nitric oxide and nitrous oxide contributes to the generation of Δp across the membrane associated with these reactions (Nicholls and Ferguson, 1992).

The cytochrome bc₁ complex is obligatory for nitrite, nitric oxide and nitrous oxide reduction. However no single periplasmic electron carrier has been identified as essential for these processes. *P. denitrificans* possesses a periplasmic cytochrome c₅₅₀ which shows a marked increase in expression when grown under denitrifying conditions. It seemed likely that this cytochrome would be involved in electron transfer between cytochrome bc₁ and the terminal reductases. However a mutant of *P. denitrificans* lacking in cytochrome c₅₅₀ was found to still have the ability to denitrify (Moir and Ferguson, 1994). This implied that cytochrome c₅₅₀ was not an obligatory component of the denitrification electron transport chain. It was also found that electron transfer to the terminal N-oxide reductases in the cytochrome c₅₅₀ mutant was abolished by DDC (Moir and Ferguson, 1994), suggesting that electrons could be carried between the bc₁ complex and the terminal reductases by cytochrome c₅₅₀ and one or more copper proteins. The most likely candidate for the proposed

copper protein is pseudoazurin which has been shown to act as electron donor to nitrite and nitrous oxide reductases *in vitro* in *T. pantotropha* (Moir *et al.*, 1993).

For comparison a second denitrification respiratory chain from *Ps. stutzeri* is illustrated in Figure 1.22. *Ps. stutzeri* is another facultative aerobe capable of anaerobic growth under denitrifying conditions. It can be seen that the denitrification respiratory chains in *P. denitrificans* and *Ps. stutzeri* are highly homologous. Both contain membrane bound nitrate and nitric oxide reductases and periplasmic nitrite and nitrous oxide reductases. All have comparable locations in association with the cytoplasmic membrane. In both organisms the presence of a second type of respiratory nitrate reductase expressed during aerobic growth and located in the periplasm is proposed (Sears *et al.*, 1995; Zumft, 1997; sections 1.1 and 1.3.2). This enzyme is thought to receive electrons from the quinol pool by a cytochrome bc_1 independent route. It is believed that UQH_2 is oxidised at the periplasmic face of the cytoplasmic membrane with the release of two protons into the periplasm. Two electrons also pass directly into the periplasm and together with the two protons are used to reduce nitrate. This is therefore an electroneutral process. It means that the cytochrome component acting as a quinol oxidase before the periplasmic nitrate reductase does not function as a proton pump, whereas the quinol oxidase associated with the membrane bound nitrate reductase does. This effectively uncouples periplasmic nitrate reduction from Δp and cellular energy generation with the enzyme acting as an electron sink. This relates back to work described in section 1.1 in which anaerobically grown membrane bound nitrate reductase mutants of *T. pantotropha* showed reduced growth rates and yields due to expression of the periplasmic nitrate reductase enzyme (Bell *et al.*, 1990).

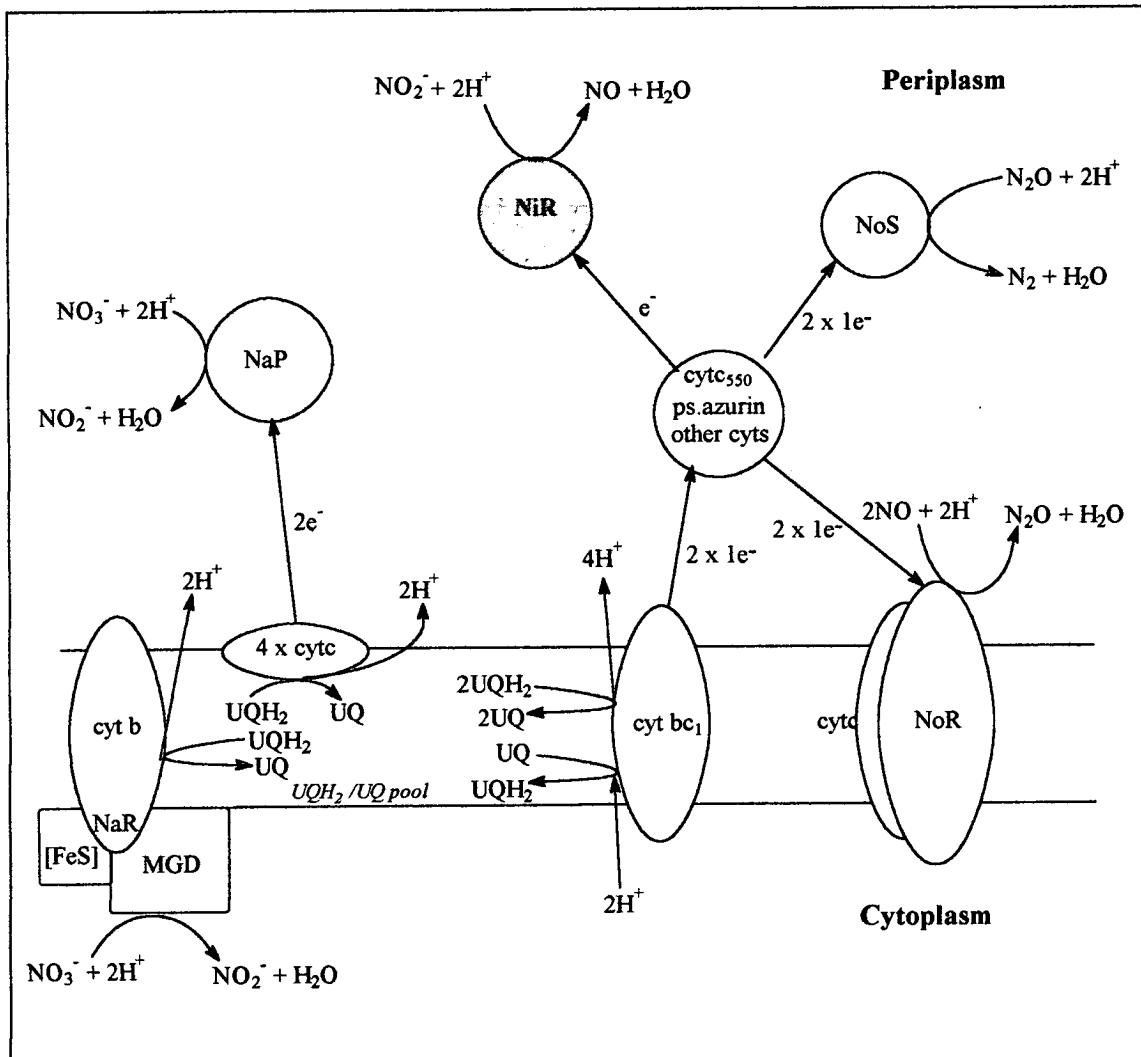


Figure 1.21. Organisation of the electron transport system from ubiquinol to the reductases from nitrate, nitrite, nitric oxide and nitrous oxide in *P. denitrificans*. Ubiquinol is reduced by NADH and succinate dehydrogenase. The flow of electrons from ubiquinol to nitrate via the membrane bound nitrate reductase involves the net movement of two positive charges out of the cell, the same stoichiometry as associated with electron movement to nitrite, nitric oxide and nitrous oxide reductases. Key: NaR - membrane bound nitrate reductase, NaP - periplasmic nitrate reductase, NiR - nitrite reductase, NoR - nitric oxide reductase, NoS - nitrous oxide reductase, cyt bc₁ - cytochrome bc₁ complex, ps.azurin - pseudoazurin.

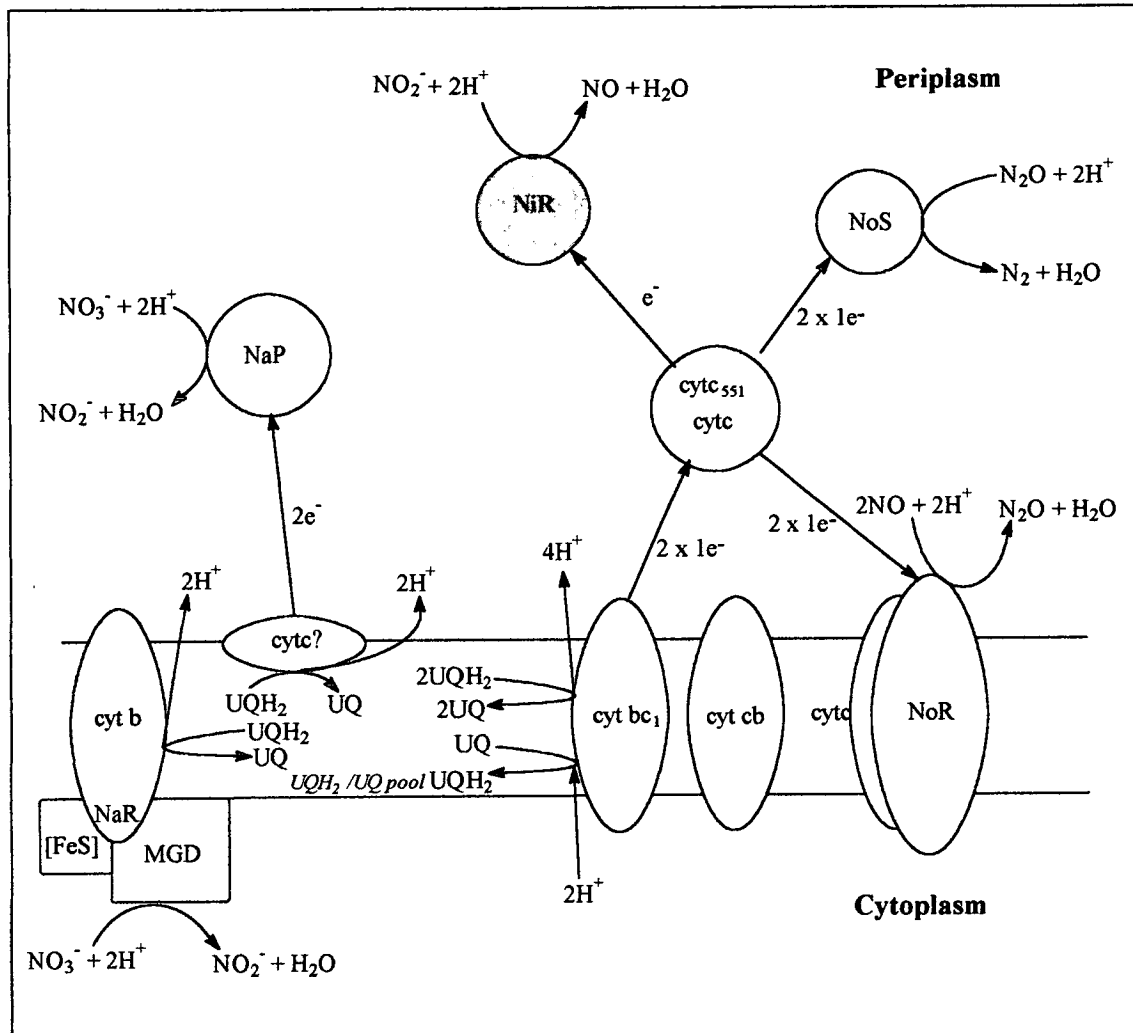


Figure 1.22. Organisation of the electron transport system from ubiquinol to the reductases for nitrate, nitrite, nitric oxide and nitrous oxide in *Ps. stutzeri*. The pathway is homologous to the denitrification pathway of *P. denitrificans*, see Figure 1.21, except that different electron donors are involved in the transfer of electrons to the terminal N-oxide reductases. Key: NaR - membrane bound nitrate reductase, NaP - periplasmic nitrate reductase, NiR - nitrite reductase, NoR - nitric oxide reductase, NoS - nitrous oxide reductase, cytc - unspecified c-type cytochromes acting as electron acceptors, cytc₅₅₁ - cytochrome c₅₅₁.

1.7.2 Transport of nitrate and nitrite across the cytoplasmic membrane

A consequence of the locations of the active sites of the nitrate and nitrite reductase enzymes is that nitrate has to be transferred across the lipid bilayer against a membrane potential to act as substrate for the nitrate reductase enzyme. Subsequently nitrite has to be delivered back across the membrane to act as substrate for the periplasmic nitrite reductase (Figures 1.21 and 1.22). Early work on *P. denitrificans* showed that intact cells were able to discriminate against nitrate and chlorate for uptake and utilisation by the cells (Alefounder and Ferguson, 1980), implying the presence of a selective transport system for nitrate uptake. Whether this nitrate and nitrite transport system is an active or passive process is a source of much debate.

In *E. coli* genes coding for the major membrane bound nitrate reductase are found clustered with the *narK* gene also (Figure 1.6). This gene codes for a hydrophobic protein that is expected to contain twelve membrane spanning helices (Noji *et al.*, 1989). Mutants lacking *narK* are not prevented from growing anaerobically with nitrate as electron donor but an increase in intracellular nitrite concentration is observed (Noji,*et al.*, 1989), along with a decrease in extracellular nitrite concentration (DeMoss and Hsu, 1991). This is consistent with the NarK protein acting as a nitrite efflux porter passively allowing nitrite to flow through the cytoplasmic membrane after production at the nitrate reductase active site to act as a substrate for the periplasmic nitrite reductase. Another possible nitrite transporter has been identified in *E. coli* encoded for by the *nirC* gene (Peakman *et al.*, 1990). The NirC protein shows high sequence similarity to the *E. coli* FocA protein. FocA was shown to be a bidirectional formate specific transporter (Suppman and Sawers, 1994).

A number of mechanisms for nitrate transport have also been considered including a passive nitrate uniport, an ATP dependent uniport, a Δp -dependent NO_3^-/H^+ symport and a nitrate/nitrite antiport. A nitrate uniport can be easily dismissed because in respiring bacteria a Δp of $\sim 200\text{mV}$ (periplasm positive with respect to the cytoplasm) would limit the flux of nitrate into the cytoplasm. Also the rate at which

such a uniport system could supply nitrate to its reductase would be too slow for the nitrate reductase to react optimally (Berks, 1995a). An NO_3^-/H^+ symport is though unlikely as it would consume Δp leading to reduced cell growth (Parsonage *et al.*, 1985). The energetic cost to the cell of an ATP hydrolytic uniport would also be detrimental. It is assumed that one ATP would be hydrolysed per nitrate ion translocated across the membrane and that 3H^+ from Δp would be needed to synthesise a replacement ATP molecule (Nicholls and Ferguson, 1992). Effectively three protons would be needed to translocate a single nitrate ion into the cytoplasm - this is not energetically attainable.

For many years a nitrate/nitrite antiporter was considered to be the most likely candidate for movement of nitrate and nitrite ions across the cytoplasmic membrane as it would involve no net charge movement. It was proposed by Boogerd *et al.* in 1983 that nitrate respiration is started initially by a nitrate/proton symport and the subsequent intracellular accumulation of nitrite is needed to drive the antiport. However if this was the case the symport would not operate in the absence of Δp .

1.8 Control of denitrification

1.8.1 Regulation of gene expression

The presence of both oxygen and N-oxides during growth of bacteria can regulate expression and *in vivo* activity of the N-oxide reductases. On the whole the enzymes are not expressed under aerobic conditions ensuring that respiration of oxygen, which is more productive energetically, occurs in preference to denitrification. The cell has a number of mechanisms by which this is achieved and these are discussed in detail.

1.8.1.1 FNR mediated regulation

In *E. coli* the transcription modulator FNR has a central role in the global activation of genes involved in anaerobic respiration, including the denitrification *nar* and *nir* gene clusters (Spiro and Guest, 1990; Spiro, 1994). The *E. coli* FNR binding motif (TTGAT-N₄-ATCAA; 'FNR box') is found 35 to 50 bases upstream of the transcriptional start point of FNR regulated genes. Sequences which resemble the *E. coli* FNR box have been found upstream of FNR regulated genes in other organisms too (Spiro, 1994). The FNR protein has a cluster of cysteine residues at its N-terminal which are involved in sensing oxygen concentration (Unden and Trageser, 1991). Upon activation by anoxia FNR dimerises allowing each subunit to bind to one of the two inverted repeat sequences in the FNR box. Activation of RNA polymerase is thought to occur via direct physical contact between the DNA-FNR complex and the polymerase enzyme (Lazizzera *et al.*, 1993).

Sequences with similarity to the *E. coli* 'FNR-box' consensus sequence have been identified upstream of genes involved in anaerobic nitrogen oxide respiration in a number of denitrifying bacteria (Jüngst *et al.*, 1991; Smith and Teidje, 1991; Zumft *et al.*, 1992; Nishiyama *et al.*, 1993; Ye *et al.*, 1993; Spiro, 1994). Similarly evidence for the presence of FNR-like proteins has been identified in a number of denitrifying bacteria including *Pseudomonas* sp. G-179 (Ye *et al.*, 1993), *Al. faecalis* (Nishiyama *et al.*, 1993) and *P. denitrificans* (Spiro, 1992).

In *Ps. aeruginosa* an alternative to FNR is the ANR protein. It was found that the *Ps. aeruginosa anr* gene could functionally complement an *fnr* mutation in *E. coli*. The *anr* gene was compared to the *E. coli fnr* gene and 51% identity was found to exist between them (Zimmerman *et al.*, 1991). Also, the cysteine gene cluster characteristic of FNR proteins was found to be present at the N-terminal of ANR. The *anr* gene was found to be essential for anaerobic activation of the denitrification pathway in *Ps. aeruginosa* (Ye *et al.*, 1995). A second gene, designated *dnr*, has also been identified in *Ps. aeruginosa* upstream of a number of denitrification structural genes including *nirS*, *norCB* and *nirQ*. This gene encodes another homolog of the FNR family of transcriptional regulators (Arai *et al.*, 1995).

It has also been reported that *Ps. stutzeri* may possess two FNR-like systems one of which is specific for denitrification. Cuypers and Zumft (1993) demonstrated that anaerobic control of denitrification in this organism escaped mutagenesis of an FNR-like gene. Using the *anr* gene of *Ps. aeruginosa* a homolog of the *fnr* gene was isolated from *Ps. stutzeri*. The gene was designated *fnrA* and the corresponding peptide was found to have 51.2% identity to the FNR protein of *E. coli* and 81.6% identity to the ANR protein of *Ps. aeruginosa*. The second FNR homolog in *Ps. stutzeri* was found when DNA upstream of *norCB* was sequenced (Vollack *et al.*, unpublished). This gene has been designated *fnrD*. Subsequent work on a number of other denitrifying bacteria have identified a considerable number of proteins related to FNR that are involved in the regulation of denitrification genes. The proteins are all divided into two classes: FNR and FixK. Proteins in the FixK class are structurally analogous to FNR but differ as they lack the N-terminal cysteine cluster characteristic of FNR proteins which is required for signal sensing. All FNR and FixK proteins recognise a specific sequence motif in the upstream promoter regions of the genes they regulate (Table 1.2).

Bacterial cells can also employ another regulatory mechanism which responds to oxygen. The ArcA/ArcB two component sensor/regulator system is distinct to FNR. This system has been particularly well characterised in *E. coli*. ArcB usually exists in the cellular membrane and detects changes in oxygen concentration. This causes a conformational change in ArcB which is detected by ArcA. ArcA becomes phosphorylated and regulates expression of the target genes (Spiro and Guest, 1991). Binding sites for ArcA have been identified upstream of a number of genes whose products are involved in the tricarboxylate acid cycle, including succinate dehydrogenase and fumarase (Park *et al.*, 1995; Park and Gunsalas, 1995). ArcA downregulates these genes so that anaerobic energy generating pathways can be used more efficiently for cell growth. However the presence of ArcA binding sites upstream of genes associated with denitrification has yet to extensively demonstrated. The ArcA/ArcB system is believed to be transcriptionally activated by FNR (Compan and Touati, 1994).

To summarise: it appears that denitrifying organisms use complex anaerobic regulatory mechanisms and do not depend on just a single FNR-like regulator to control gene expression. An example of the complexity of denitrification gene regulation in *Ps. stutzeri* is shown in Figure 1.23.

Source and factor	Class	Gene with FNR box	Sequence of recognition motif
<i>Ps. aeruginosa</i>			
ANR	FNR	<i>nosZ</i>	caactTGATtcccgcCgtc
		<i>narG</i>	?
DNR	FixK	<i>nirS</i>	atcTTGATtccggTCAAg
		<i>norC</i>	atcTTGATtgccATCAAg
<i>Ps. stutzeri</i>			
FnrA	FNR	<i>fnrA</i>	None
FnrD	FixK	<i>arc</i>	?
		<i>nirS</i>	ctcTTGATtgccgTCAAg
		<i>norC</i>	ttcTTGATtgccATCAAg
		<i>nosR</i>	gcgaaGATggaaATCAAg
		<i>nosZ</i>	actTTGAcgatcATCAAg
<i>P. denitrificans</i>			
FnrP	FNR	<i>narG</i>	?
<i>R. sphaeroides</i>			
FnrL	FNR	<i>fnrL</i>	gctTTGATtcagATCAAg
NnrR	FixK	<i>nirK</i>	ttgTTGcgcaaccgCAAA
		<i>norC</i>	tcaTTGtgctgccgCAAA
<i>E. coli</i>			
FNR	FNR	Consensus <i>fnr</i>	a--TTGAT--a-ATCCat aaaTTGAcAAATCAAT

Table 1.2. Structural elements and specificity of co-existent FNR-like factors found in denitrifiers. For a description of FNR and FixK see text.

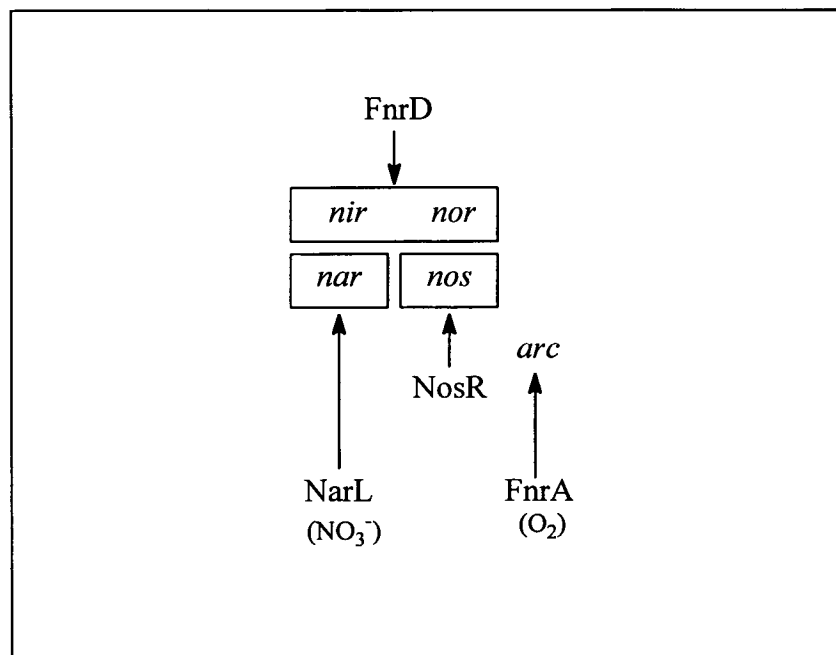


Figure 1.23. The regulatory circuit of denitrification in *Ps. stutzeri*. Arrows point to a boxed group of target genes or individual operons under the control of a given regulator. Exogenous nitrate and oxygen signals are in brackets. The NosR and NarL regulators are operon specific. NosR (section 1.6.4) is believed to be activated by an FNR-like protein whilst NarL responds directly to nitrate concentration. For details on NarL see section 1.8.1.2.

1.8.1.2 N-oxide regulation of denitrification gene expression

Genetic studies on *E. coli* have identified the presence of at least four genes whose products are involved in mediating nitrate and nitrite control of anaerobic respiratory gene expression. The products of these genes effectively provide another level of control over expression of FNR induced genes. The *narL* and *narP* products are homologous response regulators that activate or repress target operon expression in response to nitrate. The *narX* and *narQ* products are homologous histidine protein kinase sensors that inform the NarL and NarP proteins of nitrate availability (Stewart, 1992). The NarXL and NarPQ proteins act as two component regulatory systems inducing the *narGHIJ* structural operon and the *narK* gene for nitrite export. The NarPQ proteins also regulate expression of the periplasmic nitrate reductase.

A significant degree of redundancy exists between these two regulatory systems. Either of the two sensor-transmitter proteins, NarX and NarQ, can activate

the response-regulator proteins, NarL and NarP (Chiang *et al.*, 1997). In the presence of nitrate the NarX protein acts as a positive regulator of both NarL and NarP activity. In the presence of nitrite, the NarX protein acts as a negative regulator of NarL activity but remains a positive regulator of NarP activity (Williams and Stewart, 1997). The periplasmic domain of NarX was identified as the region involved in the differential response to nitrate and nitrite. In this region 17 conserved amino acids are found, called the 'P-box'. Mutations in a number of these conserved amino acids significantly affected the observed pattern of regulation by NarX in response to nitrate and nitrite (Cavicchioli *et al.*, 1996; Chiang *et al.*, 1997). A consensus DNA binding site for the response regulators NarL and NarP has been proposed by Tyson *et al.* (1994). This is known as the 'NarL heptamer' and consists of TACY-KT (Y = C or T, K = A or C). This heptamer has been found in tandem or inverse orientation upstream of a variety of NarL regulated genes (Stewart, 1993). DNA footprinting experiments have revealed that NarP only binds to heptamer sequences organised as an inverted repeat with a 2bp spacing (7-2-7 sites). The NarL protein also binds to these 7-2-7 sites but, unlike NarP, also recognises heptamers in other arrangements (Darwin *et al.*, 1997). This may help to explain why there are different effects of NarP and NarL at common target genes such as *nirB* (Darwin *et al.*, 1997).

In the denitrifying organism *Ps. stutzeri*, the presence of a NarXL/NarPQ type regulatory system has recently been proposed. Sequences resembling NarP/L heptamers have been located upstream of a number of denitrification genes including *nosZ* and *norC*, although they appear to be inactive (Cuypers *et al.*, 1995). Also, a *narL* homolog required for the cellular nitrate and nitrite response has been identified (Härtig and Zumft, unpublished). The derived NarL protein has 51% identity to NarL from *E. coli*, including the key amino acids in the 'P-box', namely Asp46 and Arg50. *NarL* of *Ps. stutzeri* overlaps with a gene that is a homolog of *narX* from *E. coli* (Zumft, unpublished). Both genes are linked to the *nar* locus as is also the case in *E. coli*, where *narLX* is adjacent to *narKGHJI*.

A switch in transcriptional pattern may also be required for anaerobic and N-oxide dependent expression of denitrification. This could be attributed to an

alternative sigma factor. A potential binding site for σ^{54} has been identified upstream of *nirU* in *Pseudomonas* spp. (Ye *et al.*, 1993). However, *nirU* is thought to be regulated by FNR and control of FNR-dependent genes by σ^{54} is thought to be unlikely. Nevertheless mutagenesis on *rpoN* (the structural gene for σ^{54}) in *Ps. stutzeri* has shown that decreased expression of *nirS* and *norCB*, and corresponding enzyme activities, results (Härtig and Zumft, 1998). No clear consensus sequences for σ^{54} were found in the promoters of *norC* and *nirS*. This indicates that the involvement of σ^{54} in the denitrification of *Ps. stutzeri* must be indirect. Transcription of *nirS* and *norC* occurred as in wild type cells so it must be assumed that a post-translational process for NirS and NorC affects wild type activity which is dependent on σ^{54} .

For σ^{54} to be involved in the regulation of denitrification genes another factor must also be involved to bring the sigma factor into contact with the DNA to be regulated. Integration host factor (IHF) accomplishes this by looping out intervening DNA to bring σ^{54} closer to the transcription initiation start. IHF is a small heterodimeric protein that specifically binds to DNA and functions as an architectural factor in many cellular processes in prokaryotes (Rice *et al.*, 1996). Most of the σ^{54} -dependent promoters also have the target sequence for IHF. The IHF gene has been identified in *Ps. aeruginosa* (Cutruzzolà *et al.*, 1997) and an IHF binding motif has been suggested for *nosZ* (Cuypers *et al.*, 1995).

Studies have also reported a degree of co-regulation of the nitrite and nitric oxide reductases in denitrifying bacteria. The nitrite reductase gene clusters of *P. denitrificans*, *Ps. stutzeri* and *Ps. aeruginosa* contain a proposed regulatory gene *nirQ* (Arai *et al.*, 1991; deBoer *et al.*, 1994; Jüngst and Zumft, 1992). Sequence analysis of the NirQ peptide reveals it has similarity to the NtrC family of transcriptional activators with the strongest degree of sequence conservation found within the nucleotide binding regions (Jüngst and Zumft, 1992). Studies on a *Ps. stutzeri* mutant lacking *nirQ* demonstrated that both the nitrite and nitric oxide reductase activities were lost *in vivo* although the enzymes were still synthesised (Jüngst and Zumft, 1992).

In short, it can be seen that regulation of nitrogen oxide respiration is very complicated. The primary regulation of the anaerobically induced genes by FNR is modulated further by gene specific transcription factors which establish a hierarchy governing all anaerobic gene expression.

1.9 Cancer of the Stomach

1.9.1 Background

In 1980 stomach cancer was estimated to be the most common cancer in the world whilst in 1989 it was still second only to lung cancer. Figures published in 1991 by the Cancer Research Campaign reported that in 1985 stomach cancer was the sixth most common cancer found in men and women in the UK with 6,110 cases in men and 4,080 cases in women (Anon., 1991). The survival rate from stomach cancer is poor. Nearly 70% of patients die within one year of prognosis and there is only a 5 year survival rate of ~10% for both males and females. However recent advances in diagnosis and the treatment of cancers are helping to improve these statistics.

As the stomach is the first place where ingested food and drink remain in the body for a prolonged period the relationship between diet and stomach cancer has been thoroughly investigated. The highest recorded incidence rates occur in Japan, Eastern Asia and China with much lower rates in the USA and Great Britain. Stomach cancer is rare in Africa (Anon., 1991). Migrant studies have demonstrated that immigrants assume the risk of the host country for stomach cancer, implicating a dietary involvement (Mirvish *et al.*, 1983).

When the diets of the high incidence groups were studied it was found that they were high in nitrates and nitrites. The sources of these salts included water, cured meats and fish, and vegetables. When the decline in the incidence of stomach cancer in the United States was studied it was seen to be associated with a decline in the consumption of salted and pickled food, along with a reduction in the nitrate and nitrite levels used in curing (Weisburger, 1986).

1.9.2 Nitrate, nitrite and *N*-nitroso compounds in foods

Acid catalysed formation of *N*-nitroso compounds is well understood (Mirvish, 1975; Mirvish, 1995), but the potential involvement of nitrate and nitrite in

the production of carcinogenic *N*-nitroso compounds under the acidic conditions present in the stomach was only postulated by Shuker (1988). Consequently many investigations into the presence of these compounds in foodstuffs have been undertaken. A report by MAFF (Ministry of Agriculture Fisheries and Food) published in 1992 summarised that the intake of nitrate and nitrite in the diet predominantly comes from potatoes, green vegetables and other vegetables whilst *N*-nitroso compounds are found in cured meat and fish, beer and cheese (Anon., 1992). The survey showed that the mean intake of nitrate is 54mg/person/day of which 76% is found in vegetables. The figure for nitrite intake is lower at a mean of 4.2mg/person/day with 50% of the intake from vegetables. It is estimated that 5% of daily nitrate consumption is converted to nitrite.

Dietary nitrate concentration is measured by monitoring the diet and the recovery of nitrate from urine samples. When the effects of reduced gastric acid secretion on urinary nitrate was investigated it was found that in the normal stomach (pH 2) 56% of nitrate was recovered compared to 33% in the achlorhydric stomach (pH 7). People suffering from achlorhydria have reduced gastric acid secretion and are found to be fifty times more likely than the normal population to develop stomach cancer (Kinlen *et al.*, 1985). Due to the permissive gastric pH large numbers of bacteria have been found to colonise the achlorhydric stomach (Forsythe *et al.*, 1988).

Evidence in the MAFF report clearly showed that *N*-nitroso compounds can be detected in human gastric juice and that they can be formed in both the normal and achlorhydric stomach. However, increased accumulation is found at the more neutral pH values associated with achlorhydria (Reed *et al.*, 1984; Stockbrugger *et al.*, 1984; Sobala *et al.*, 1991). As well as dietary intake of *N*-nitroso compounds (35µg/person/day) they can be formed via a pH dependent reaction with the rate of formation of *N*-nitroso compounds decreasing with an increase in pH. However results from patients with achlorhydria indicate that nitrite and *N*-nitroso compounds are also formed at neutral pH and constitute an increased cancer risk for achlorhydria. Acid catalysed *N*-nitrosation is unlikely at neutral pH and an alternative bacterial

mechanism of *N*-nitrosation has been proposed. This is discussed sections 1.9.4 and 1.9.5.

1.9.3 Stomach cancer and achlorhydria - a hypothesis

The correlation between reduced gastric acid secretion (achlorhydria) and bacterial growth in the stomach has been well documented and debated, as has the correlation between achlorhydria, the presence of *N*-nitroso compounds and the increased incidences of stomach cancer (Ruddell *et al.*, 1978; Stockbrugger *et al.*, 1982; Coggon and Acheson, 1984; Møller *et al.*, 1989; Chyou *et al.*, 1990; Calam *et al.*, 1991; Lechago and Correa, 1993; Dolby *et al.*, 1994). Investigations to understand how the presence of these *N*-nitroso compounds could lead to the physiological changes associated with stomach cancer have been undertaken. A comprehensive summary is provided below.

Under normal conditions in a healthy acidic gut, a basal level of *N*-nitroso compound formation occurs via an acid catalysed mechanism. The carcinogenic compounds produced are unable to reach the gastric epithelial cells as they cannot pass through the protective mucous barrier. Also their synthesis can be inhibited by antioxidants such as ascorbic acid (vitamin C) and α -tocopherol (vitamin E) found in food. However the mucous barrier can be easily overcome by irritants such as NaCl and aspirin. In these instances the glandular epithelium becomes exposed to the acid catalysed *N*-nitroso compounds and is mutated. The gastric mucosa changes by becoming inflamed. Loss of cellular differentiation is observed as well as atrophy (gland loss). Reduced gastric acid secretion occurs as a result of these changes. This leads to elevated pH levels which favour bacterial proliferation and growth. Greater concentrations of carcinogenic *N*-nitroso compounds, such as *N*-nitrosamines, are subsequently found in the stomach and are most likely produced via a bacterial catalytic mechanism (Correa, 1988; Figure 1.24).

It has been proposed that achlorhydria may play another role in the development of gastric cancer (Seery, 1991). Normal acidic gastric secretions are involved in removing carcinomatous cells from the stomach epithelium. These cells

are characterised as they are dedifferentiated and lack cellular adherence. In the absence of acid these cells might survive. A given amount of carcinogen (*N*-nitroso compound) would therefore be more potent in the achlorhydric stomach due to the presence of increased numbers of carcinomatous cells.

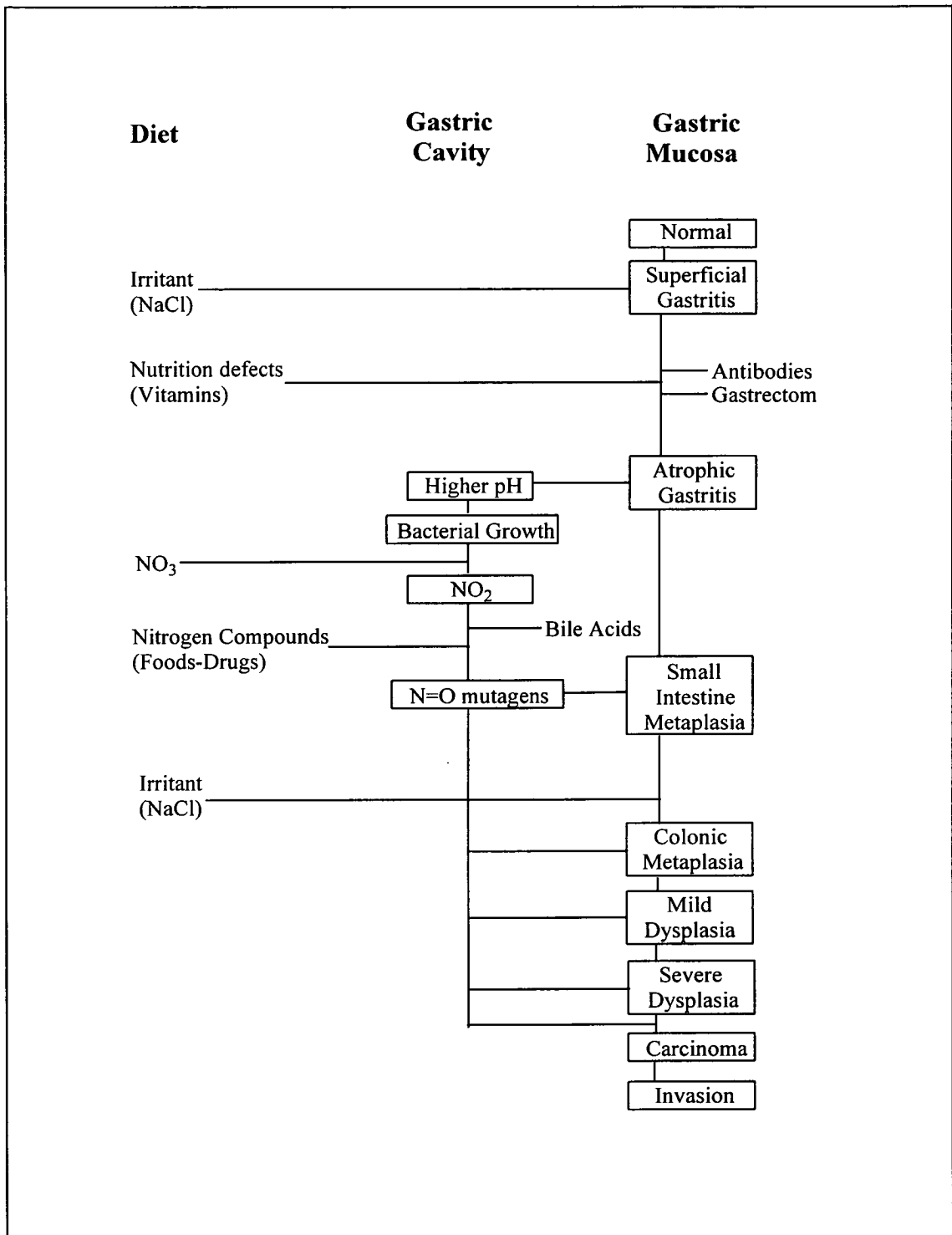


Figure 1.24. Hypothesis of gastric cancer etiology. Taken from Correa (1988).

1.9.4 Bacterial flora in the achlorhydric stomach

One of the problems in trying to identify which bacteria, if any, had a role in the formation of *N*-nitroso compounds in the achlorhydric stomach was complicated by the sheer variety of organisms identified. Initially samples of gastric juice were placed into an anaerobic cabinet so as to select specifically for organisms capable of growth in the absence of oxygen. Total anaerobic viable counts were obtained on BHI blood agar incubated at 37°C for 5 days. To select specifically for nitrate and nitrite reducing organisms BHI broth was supplemented with potassium nitrate (1mM) and sodium nitrite (0.1mM), (Forsythe *et al.*, 1988).

When comparing total cell counts to most probable numbers of nitrate and nitrite reducing organisms a high proportion of nitrogen oxide reducing organisms were found including *Veillonella*, *Neisseria*, *Haemophilus*, staphylococci, streptococci and lactobacilli (Forsythe *et al.*, 1988). When these organisms were tested for their nitrate and nitrite reducing abilities it was found that *Veillonellae* and haemophili had very high nitrate reducing activities but were not efficient nitrite reducers. In contrast *Neisseria* spp. were the most efficient reducers of nitrite but could not reduce nitrate. This situation was further complicated as the metabolic products from one particular organism were found to act as the substrate for another. In experiments using binary cultures it was discovered that the nitrite produced by *V. parvula* or *H. influenzae* could be reduced by *N. subflava* to produce gaseous products (Forsythe and Cole, 1987). As these organisms were isolated from the achlorhydric stomach this was the first instance in which a link between accumulated nitrate and nitrite levels and denitrification was proposed. It seemed reasonable to assume that one of the enzymes involved in, or one of the products of, denitrification could react with amines to produce nitrosamines via a mechanism other than the acid catalysed chemical reaction. If correct, this would account for the increase in *N*-nitrosamine concentration in the achlorhydric stomach and also the increased gastric cancer risk associated with this. Subsequent work has demonstrated that it is the *N*-nitrosation of peptides and proteins in the stomach which allows *N*-nitrosamine formation via direct attack of the $-\text{COO}^-$ group in the amino acid by the *N*-nitrosating

agents (Gil *et al.*, 1994). The experiments used to deduce this were done *in vitro* with chemical nitrosating agents but an analogous enzymatic role cannot be dismissed at this stage.

Studies were then carried out to establish whether the bacteria colonising the achlorhydric stomach were responsible for the formation of the carcinogenic *N*-nitroso compounds via direct or indirect catalysis. Leach *et al.*, (1987) measured the *N*-nitrosating ability of various different denitrifying bacteria. It was found that strains with the capability to denitrify could catalyse *N*-nitrosation reactions 10-100 times faster than a non-denitrifying *E. coli* strain. It was concluded that this activity was enzymic as the *N*-nitrosation reaction was found to be sensitive to heat and cell disruption (O'Donnell *et al.*, 1988).

From these studies some general themes emerge. The presence of nitrite and *N*-nitrosating species appear to be required for the formation of carcinogenic *N*-nitrosamine compounds. Even though nitrosation can occur in a normal (pH 2) stomach elevated levels are found in achlorhydric stomachs which suggests the involvement of colonising bacteria. The susceptibility of *N*-nitrosation catalytic activity to heat inactivation and cell disruption in the achlorhydric stomach would suggest a biological origin. To determine the true involvement of the bacteria in the production of carcinogenic *N*-nitroso compounds at neutral pH some knowledge of the chemistry of the *N*-nitrosation reaction is required.

1.9.5 *N*-nitrosamine formation

N-nitrosation can be described as the replacement of a hydrogen ion, attached to a nitrogen atom of an amine, by an *N*-nitrosating agent resulting in the formation of the corresponding *N*-nitrosamine (Figure 1.25). This can occur both chemically via an acid-catalysed reaction and biologically. Both mechanisms are discussed below.

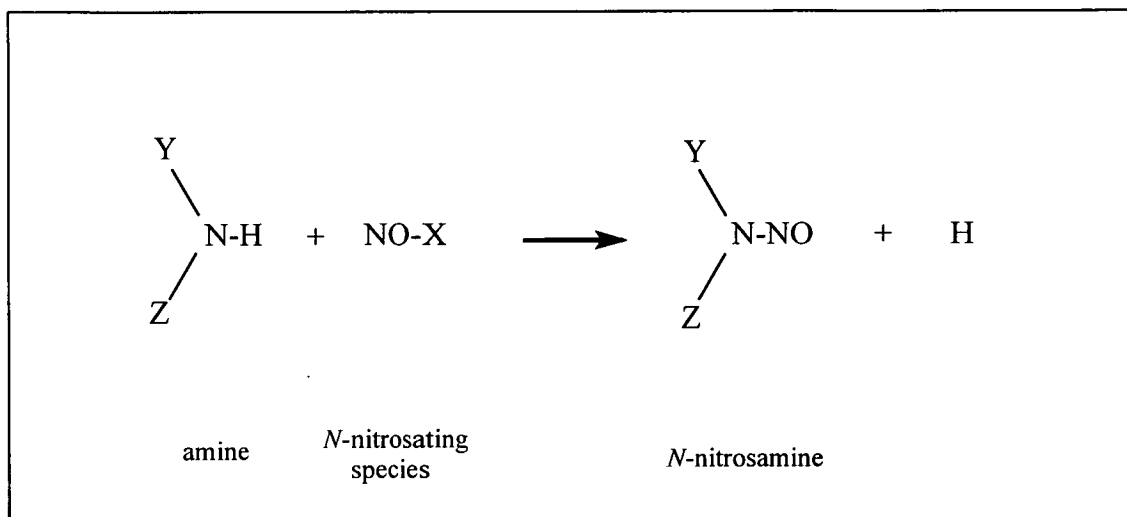


Figure 1.25. Representation of the *N*-nitrosation reaction showing the involved products.

1.9.5.1 Acid catalysed *N*-nitrosation

Under the acidic conditions present in the 'normal' stomach nitrite becomes protonated to form nitrous acid. Depending on the pH this can react to produce a number of intermediates which are potent *N*-nitrosating agents (Figure 1.26). The pH also affects the amount of unprotonated amine and the concentration of the active form of the *N*-nitrosating species. e.g. at pH 2 the nitrous acidium ion is the most prevalent but at pH 3 dinitrogen trioxide is the primary agent (Shuker, 1988).

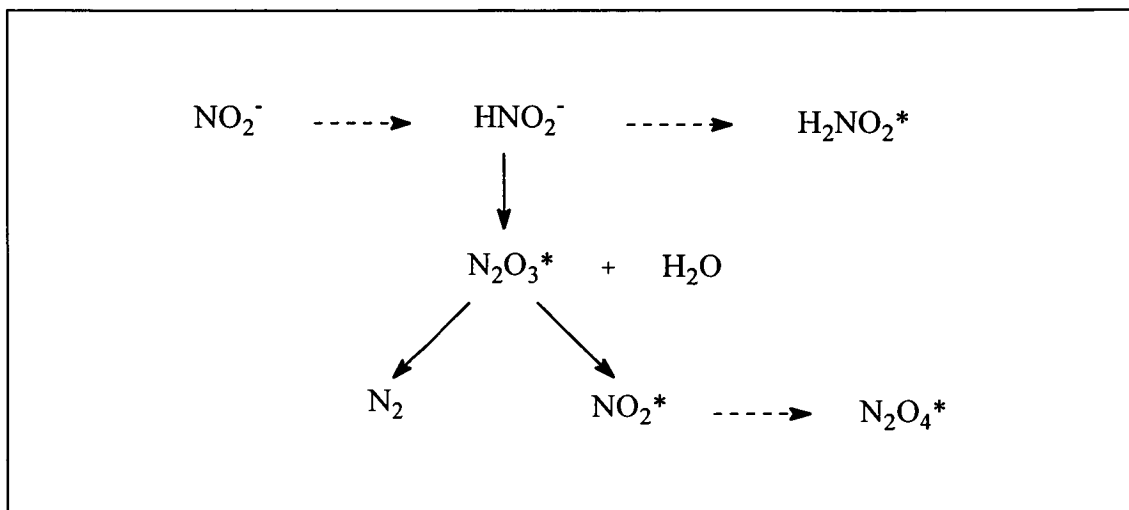


Figure 1.26. Acid catalysed formation of *N*-nitrosating agents. * :*N*-nitrosating species, H_2NO_2 nitrous acidium ion, N_2O_3 dinitrogen trioxide, N_2O_4 dinitrogen tetroxide.

N-nitroso compounds are divided into nitrosamines and nitrosamides. Nitrosamines are more stable than nitrosamides but are still volatile compounds (Mirvish, 1975; Mirvish, 1995). This has caused many analytical problems when trying to study them. *N*-nitroso compounds require metabolic activation by cytochrome P-450. This results in degradation of the nitrosamine compound coupled to alkylation of a cellular component, usually DNA. The target of nitrosamine alkylation is dependent on the specific nitrosamine species but generally leads to tissue destruction. The alkylating action of nitrosamine decay is thought to be related to their carcinogenic potential. Some species specifically alkylate DNA bases, especially N^7 and O^6 of guanine and O^4 of thymine. O^6 -alkylguanines pair with thymine rather than cytosine and this produces a $\text{G}:\text{C} \rightarrow \text{A}:\text{T}$ mutation that is believed to initiate carcinogenesis. Nitrosamides are also converted to similar alkylating species but they have a physiological half life of 1-10s and decay before they can cause localised damage to DNA. Hence it is most likely that nitrosamines are activated at the site of tumour development (Mirvish, 1995).

1.9.5.2 Bacterial *N*-nitrosation

It has been proposed from studies on *N. subflava* strain B19, isolated from an achlorhydric stomach, that denitrification pathway intermediates are involved in the bacterially catalysed *N*-nitrosation reaction at neutral pH (Brew, 1992; Figure 1.27). A major problem with this hypothesis is the absence of an acidic environment. In the acid catalysed nitrosation reaction outlined above it is the protonation of nitrite that is needed for the reaction to proceed. However it is believed that after nitrite is reduced to nitric oxide there are two possible avenues which may result in bacterially catalysed *N*-nitrosation. The first is that there is a specific enzyme which directly converts nitric oxide to an *N*-nitrosating species (although it could be argued that enzymatic conversion of nitrite could also occur). The second is that an accumulation of nitric oxide occurs, as a result of the interacting bacterial milieu in the gastric cavity, which is then chemically altered to produce an *N*-nitrosating species. Experiments with *E. coli* demonstrated that when air was admitted to anaerobically denitrifying cells nitrosating agents such as N_2O_3 and N_2O_4 were produced (Ji and Hollocher, 1988). This was supported when the nitrosation activity of *N. subflava* was investigated (Brew, 1992). She found that when nitrosation activity was assayed for under totally anaerobic conditions the *N. subflava* cells had no nitrosation activity. If a requirement for oxygen is essential for non-enzymically catalysed nitrosation then a route of entry for oxygen into the stomach has to exist. At present it has been postulated that oxygen enters the stomach by being swallowed with food or from the bloodstream (Brew, 1992).

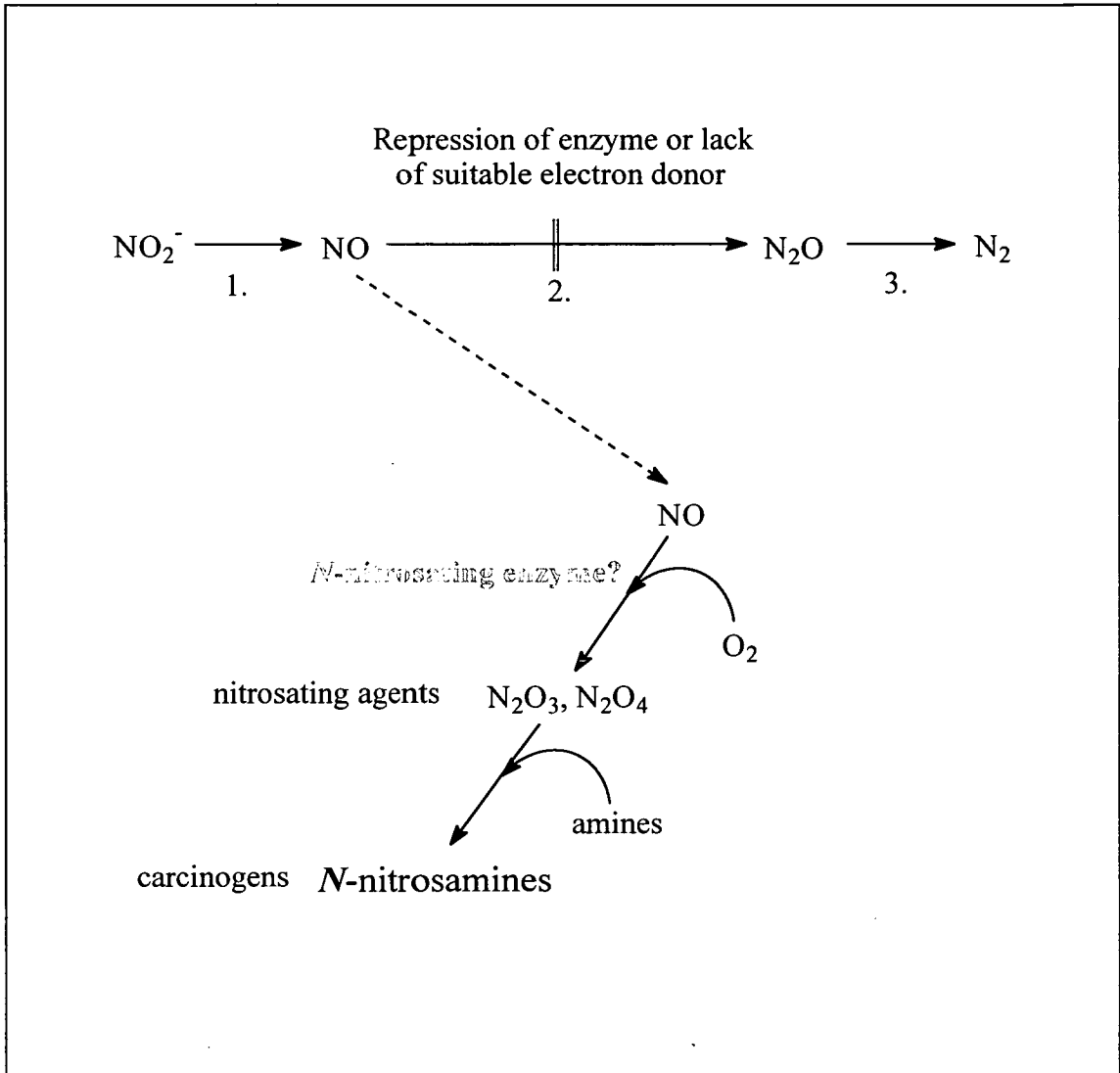


Figure 1.27. Diagram showing the connection between bacterial *N*-nitrosation and denitrification. A possible site for nitric oxide accumulation is included as is the position of the postulated *N*-nitrosating enzyme. Key to restriction enzymes 1. nitrite reductase, 2. nitric oxide reductase, 3. nitrous oxide reductase.

Arguments for enzymic catalysis of *N*-nitrosation include a proposal for a reactive enzyme-nitrogen oxide intermediate, which reacts directly with secondary amines (Leach *et al.*, 1987). This hypothesis was developed further by Smith (1991) who identified nitrite reductase as the enzyme responsible for N-N bond formation to produce N_2O_3 as an intermediate when nitrite was reduced to nitrous oxide (Figure 1.28). In this instance nitric oxide is converted to dinitrogen trioxide whilst still associated with the nitrite reductase enzyme.

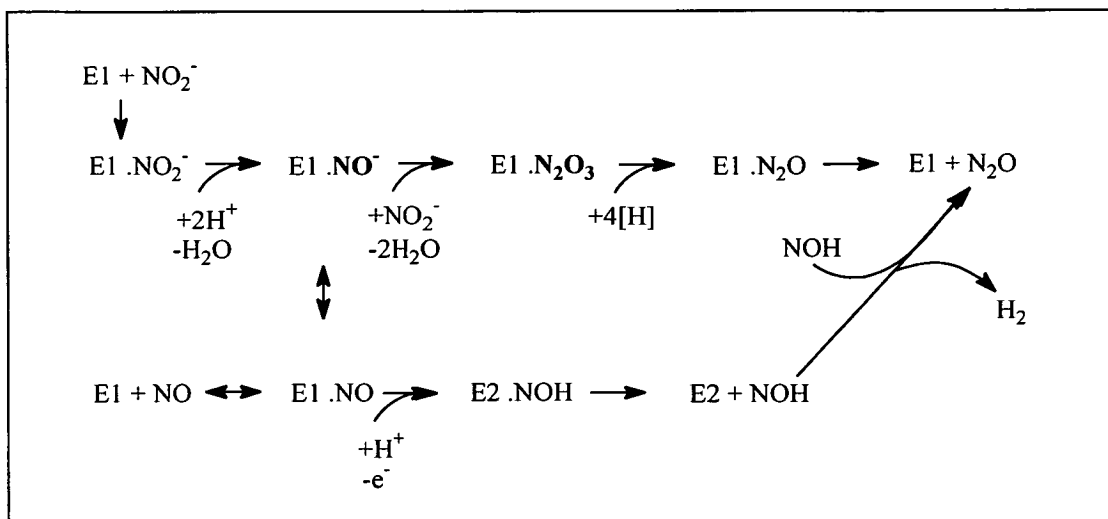


Figure 1.28. Reaction evolving nitrous oxide via N-N bond formation by nitrite and nitric oxide reductase enzymes. Key: E1 nitrite reductase, E2 nitric oxide reductase. *N*-nitrosating agents are highlighted in bold.

Further evidence for the direct catalysis of secondary amines via a denitrification enzyme was provided by Calmels *et al.* (1996). Biochemical and immunological studies were used to identify the cytochrome cd_1 nitrite reductase of *Ps. aeruginosa* as the enzyme responsible for the catalysis of nitrosation through the production of a nitric oxide or NO^+ -like species. It was found that the nitrosating activity of the enzyme was inhibited in the presence of antibodies raised against cd_1 -nitrite reductase and that the N-terminals of both the nitrosating and cd_1 -nitrite reductase enzymes were the same (Calmels *et al.*, 1996). However the experiments in this paper only showed that reduction of nitrite was necessary for nitrosation to occur. Purified cytochrome cd_1 nitrite reductase apparently displayed nitrosation activity. However the same result could easily have been obtained due to oxygen dependent chemical nitrosation of the reduced nitric oxide product as illustrated in Figure 1.27.

A number of studies question the direct involvement of nitrite reductase in catalysis of *N*-nitrosamines. Assays using *E. coli* found that *N*-nitrosation occurred regardless of whether bacterial cells were present in the assay reaction mix or not. It was also discovered that lack of nitric oxide synthesis affected the reaction. It was

concluded that although *N*-nitrosation *per se* is chemical, bacteria are required for the accumulation of nitric oxide (Ji and Hollocher, 1988).

To investigate the conclusions of Ji and Hollocher further a number of studies using various inhibitors to the denitrification pathway of *N. subflava* were carried out by Brew (1992). These studies enabled Brew to determine which of the denitrification enzymes were essential for *N*-nitrosation to occur. Acetylene, a well known inhibitor of nitrous oxide reductase, was able to inhibit this enzyme in *N. subflava* too. Acetylene did not inhibit nitrosation even at increased concentrations. This excluded nitrous oxide reductase and its product dinitrogen from an involvement in bacterial nitrosation. Ascorbic acid was found to inhibit nitrosation but not nitrite reductase. This fitted with the hypothesis put forward by Ji and Hollocher (1988) that nitric oxide accumulation is necessary for nitrosation to occur. Ascorbic acid inhibits nitrosation by reacting with nitrosating agents faster than they react with amines in the stomach. However, reaction of ascorbic acid with the nitrosating agent results in the formation of nitric oxide (section 1.9.6). This liberated nitric oxide is then able to react with oxygen to produce more nitrosating agents. For nitrosation inhibition to be observed in the presence of ascorbic acid a great excess of ascorbic acid is required. As ascorbic acid was seen to inhibit nitrosation but not nitrite reductase, it was concluded that neither nitrite reductase nor its product could be directly involved in bacterial nitrosation. Finally tests were done using chemicals that inhibit more than one step in the denitrification pathway. *N*-nitrosation activity was inhibited by these chemicals indicating that nitrite must be reduced for nitrosation to occur. To summarise Brew (1992) deduced that the only denitrification intermediates that were likely to be involved in bacterial nitrosation were nitric oxide and nitric oxide reductase. Nitrite reductase was determined to be important as it produced nitric oxide from its reduction reaction.

The above studies by Brew, although carried out in batch cultures with one inhibitor at a time, provided information on which chemicals could affect denitrification if present in the achlorhydric stomach. Sources of such inhibitors include the diet, drugs and metabolic by-products of other colonising organisms. It was found that when ethanol was used as electron donor for denitrification in *N.*

subflava very high nitrosation rates were observed. It was proposed that this was due the inability of ethanol to acts as electron donor to nitric oxide reductase resulting in accumulated nitric oxide. Ethanol may be present in the achlorhydric stomach from the diet or as a fermentative metabolic by-product of colonising bacteria such as Streptococci and *E. coli*.

A number of *N. subflava* denitrification deficient mutants using Tn5 mutagenesis were isolated by Brew (1992). One of these mutants (163) looked particularly interesting as it lacked both nitrite reductase and nitrosation activity. A role for nitrite reductase as the actual nitrosating enzyme was dismissed due to evidence from the inhibition studies outlined above. It was also determined that the entire denitrification pathway was unaffected as the nitrous oxide rate of the mutant was greater than the parent strain. A more likely interpretation was that as nitric oxide could not be formed via nitrite reductase it could not accumulate to high enough levels to form nitrosating agents such as N_2O_3 and N_2O_4 on reaction with oxygen. The nitric oxide accumulation hypothesis of Ji and Hollocher (1988) was again supported by the work of Brew (1992).

Despite evidence from other organisms, it seems most likely that a specific bacterial nitrosating enzyme corresponding to a denitrification oxido-reductase does not exist in *N. subflava*. Accumulation of nitric oxide and its subsequent reaction with oxygen to produce nitrosating agents is a more plausible alternative. The proposal by Calmels *et al.*, (1996) that the cytochrome cd_1 nitrite reductase enzyme of *Ps. aeruginosa* also nitrosates can be questioned as the same results would be observed if nitric oxide, produced by nitrite reductase, reacted with oxygen present in the assay system. *N*-nitroso compounds would be detected in both instances. This however does not diminish the importance of nitrite reductase in the formation of carcinogenic *N*-nitrosamines. Understanding the reductive mechanisms of the nitrite reductase enzyme, particularly in organisms isolated from achlorhydric stomachs such as *N. subflava*, may be a means to control bacterially 'mediated' *N*-nitrosation by preventing nitric oxide formation.

1.9.6. Inhibition of *N*-nitrosation

A number of inhibitors of *N*-nitrosation have been well characterised. These compounds are all found naturally in foodstuffs and so another link between diet and cancer can be established. Particularly well characterised are antioxidants such as ascorbic acid and α -tocopherol and their mode of inhibition will be outlined.

Ascorbic acid inhibits nitrosation as the ascorbate anion reacts with nitrosating agents such as dinitrogen trioxide (N_2O_3) and the nitrous acidium ion ($H_2NO_2^+$), at a much greater rate than they are able to react with amines in the stomach (Tannenbaum *et al.*, 1991). Ascorbic acid is converted to the ascorbate anion at around pH 4.3 and so will be the major source of ascorbic acid in the achlorhydric stomach. Ascorbate anion is 230 times more rapidly nitrosated than ascorbic acid as it has a greater nucleophilic activity. Hence the structure of the ascorbate anion makes it particularly suitable for reducing *N*-nitroso compounds (Mirvish *et al.*, 1972; Mirvish, 1986). Vitamin C is therefore a powerful reducing agent and the chemical reaction for the reduction of nitrous acid to nitric oxide by ascorbic acid is shown in Figure 1.29.

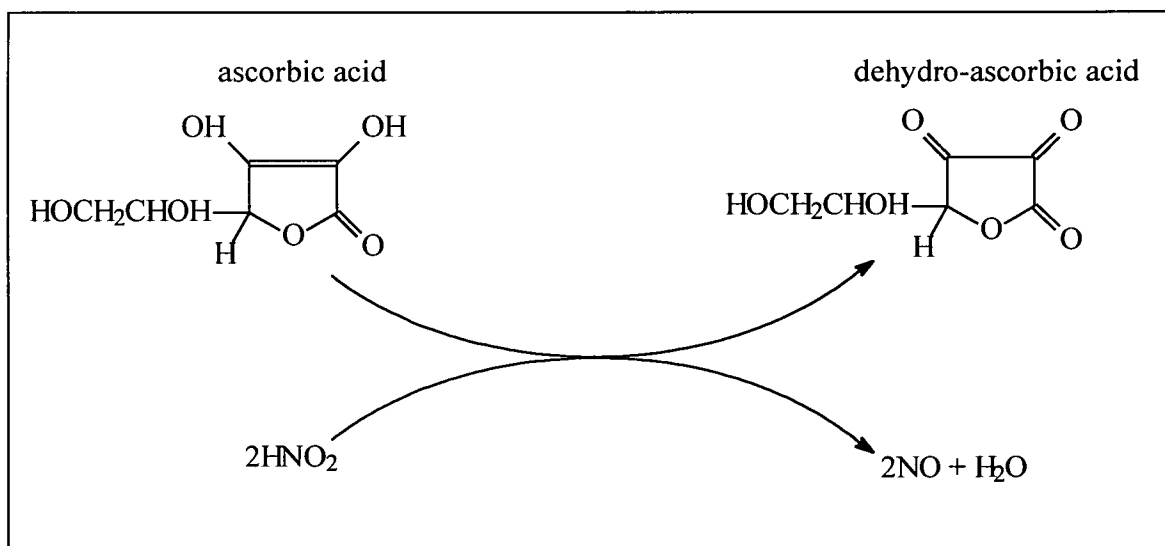


Figure 1.29. Reduction of nitrous acid to nitric oxide by ascorbic acid. Taken from Mirvish (1986).

The ability of ascorbic acid to inhibit nitrosation would appear contradictory as a product of the 'blocking' reaction is nitric oxide. Nitric oxide is proposed to act as a potent nitrosating agent itself by reacting with oxygen to produce dinitrogen trioxide (N_2O_3). However it has been demonstrated that the presence of excess ascorbate in nitrosation assays minimises the effect of this reconversion of nitric oxide to N_2O_3 , and so *N*-nitrosation is still inhibited (Mirvish *et al.*, 1972; Brew, 1992). Nevertheless ascorbate concentration in such studies should be monitored carefully as low concentrations will cause enhancement of *N*-nitrosation due to the production of nitric oxide. This may support work which demonstrated that ascorbic acid was mutagenic and could amplify *in-vitro* carcinogenesis (Stich *et al.*, 1976; Fukushima *et al.*, 1987).

A number of studies have investigated the inhibition of bacterially mediated *N*-nitrosation by ascorbic acid. Mirvish (1986) discussed the effect of ascorbic acid on *N*-nitroso compound formation, carcinogenesis and cancer. The report concluded that ascorbic acid inhibited *N*-nitroso compound formation from nitrite and amines in aqueous solutions. This was confirmed by Tannenbaum *et al.*, (1991) who demonstrated that ascorbic acid inhibited *N*-nitroso compound formation both *in vitro* and *in vivo*. Similarly ascorbic acid was demonstrated to be a potent inhibitor of *N*-nitrosation by the denitrifying organism *Ps. aeruginosa* (Mackerness *et al.*, 1989). The results from each of these studies suggest that increasing the ascorbic acid intake of patients at risk of achlorhydria may be therapeutic.

α -tocopherol (vitamin E) is a phenolic compound and functions as a lipid antioxidant in cells by scavenging free radicals. Nitrite in organic solvents, lipids and emulsions is reduced by α -tocopherol to nitric oxide (Mirvish, 1986). Inhibition of *N*-nitrosation is only possible with free α -tocopherol and not the acetate salt which is the commercially available form (Brew, 1992). The mode of inhibition of α -tocopherol is very similar to that of ascorbic acid but the reconversion reaction that produces further carcinogens from the nitric oxide reductive product does not occur (Mirvish, 1986). Since vitamin E inhibits nitrosation in lipids and vitamin C inhibits

nitrosation in the aqueous phase, a combination of the two vitamins would be especially useful for inhibiting *N*-nitroso compound formation in lipid-water mixtures.

Other important *N*-nitrosation inhibitors include catechins found in tea. A protective effect observed was when tea was taken simultaneously with any food rich in *N*-nitrosable compounds. The protective effect correlated well to the concentration of these compounds in the tea (Tanaka *et al.*, 1998). Again *N*-nitrosation is believed to be blocked as catechins react at a much faster rate with *N*-nitrosating agents than with amines.

It is worth mentioning that work on *N. subflava* by Brew (1992) demonstrated that ascorbic acid has the ability to inhibit *N*-nitrosation but not nitrite reductase. This was taken as evidence that the *N. subflava* nitrite reductase enzyme does not catalyse *N*-nitrosation. Inhibitory studies on nitrite reductase activity using DDC demonstrated that both nitrite reductase and *N*-nitrosation activities were inhibited (Brew, 1992). This seemed to suggest that the nitrite reductase enzyme had the ability to *N*-nitrosate - a contradictory conclusion to that derived from inhibitory studies using ascorbic acid. However the conflicting DDC results can be easily explained. In the presence of DDC, the copper active site of nitrite reductase becomes blocked and nitrite cannot be reduced to nitric oxide. Therefore *N*-nitrosation cannot occur as its nitric oxide substrate is not present. With ascorbic acid, *N*-nitrosation is inhibited as it reacts with the nitrosating species (nitric oxide) at a much quicker rate than amines present in the stomach (Tannenbaum *et al.*, 1991). The nitrite reductase enzyme itself is **not** affected by ascorbic acid and still catalyses the reduction of nitrite to nitric oxide. The fact that DDC inhibits both nitrite reductase and *N*-nitrosation activities in *N. subflava* does not prove that both catalytic activities can be ascribed to the nitrite reductase enzyme. However nitrite reductase is important as it forms the proposed nitric oxide precursor for *N*-nitroso compound formation.

1.9.7 *Helicobacter pylori* and gastric cancer

H. pylori is commonly associated with chronic gastritis. In these cases increased proliferation of the gastric epithelial cells is observed which leads to peptide ulcer formation, and in some cases carcinoma. *H. pylori* is able to survive the acidic conditions found in the stomach which normally act as a barrier to microbial infection. Extensive epidemiological studies have correlated *H. pylori* infection to an increased risk for gastric cancer development thus implicating the bacterium in the pathogenesis of the disease. The hypotheses on how *H. pylori* infection contributes to gastric cancer development are numerous (Banjeree *et al.*, 1994; Correa, 1995; Houben and Stockbrügger, 1995; O'Connor *et al.*, 1995; Crespi and Citarda, 1996; Kuipers, *et al.*, 1996; Jonkers, *et al.*, 1997).

A correlation was observed between the presence of *H. pylori* infection in type B chronic gastritis and reduced ascorbic acid concentration (Sobala *et al.*, 1989). It was postulated that the presence of *H. pylori* somehow affected the secretion of ascorbic acid into the stomach. It has since been shown that *H. pylori* infection causes a reversible lowering of gastric juice ascorbic acid concentrations which may predispose to gastric carcinoma and peptic ulceration (Banerjee *et al.*, 1994). Cytopathic toxins released by the bacterium were proposed to impair mucosal ascorbic acid secretory mechanisms.

H. pylori inflammation has also been associated with excessive production of mutagenic active oxygen species which are known to damage DNA causing strand breaks, translocations and deletions. After successful eradication of *H. pylori* infection the activity of the reactive oxygen species were found to be significantly reduced (Drake *et al.*, 1995). Vitamin C has been shown to scavenge reactive oxygen metabolites (Banjeree *et al.*, 1994). The ability of *H. pylori* to reduce ascorbic acid secretion into the gut appears to accentuate the carcinogenic effects of the active oxygen species.

A number of review articles have surveyed the vast amounts of literature relating to *H. pylori* infection and gastric cancer risk (Correa, 1995; Houben and Stockbrügger, 1995; Crespi and Citarda, 1996; Kuipers *et al.*, 1996). From the

conclusions derived therein it would appear that *H. pylori* is not the main causative factor in gastric cancer development. *H. pylori* infection in the acidic stomach leads to changes in the gastric mucosa. Ascorbic acid secretion becomes reduced as a consequence and acid catalysed formation of *N*-nitroso compounds occurs. Some groups have also suggested that *H. pylori* infection may be a predisposing factor in gastric cancer development in the achlorhydric stomach (O'Connor *et al.*, 1995; Crespi and Citarda, 1996). It is postulated that the gastric mucosa changes in the presence of *H. pylori*, replacing the normal gastric epithelium with the intestinal type, where *H. pylori* cannot grow. Glands involved in the secretion of gastric acid are therefore lost from the stomach. The resulting alkalisation of the gastric pH favours bacterial colonisation and nitrosamine formation via the mechanisms outlined in section 1.9.5.2 (O'Connor *et al.*, 1995; Crespi and Citarda, 1996). Therefore, it would appear that *H. pylori* infection may play a role in creating a favourable gastric environment for the onset of risk conditions associated with achlorhydria.

1.10 Summary

Most of the published data regarding bacterially mediated *N*-nitrosation has come from *E. coli* and *Ps. aeruginosa*. However these organisms are isolated from achlorhydric stomachs with a much lower degree of frequency than *Neisseria* spp. (Forsythe *et al.*, 1988). To gain an understanding of bacterial catalysis of *N*-nitrosation and how this could occur in an achlorhydric stomach, the denitrification pathway of *Neisseria subflava* was thoroughly investigated (Brew, 1992). This organism was chosen as it was frequently isolated from the achlorhydric stomach, has a high nitrite reductase activity and can reduce nitrite produced by other organisms (Forsythe and Cole, 1987; Forsythe *et al.*, 1988). It was deduced by Brew (1992), after studies on each of the denitrification oxidoreductase enzymes, that *N. subflava* did not possess a specific nitrosating enzyme. Instead she proposed that under certain conditions nitric oxide would accumulate in the achlorhydric stomach

for chemical conversion to potent nitrosating agents on reaction with oxygen. As the enzyme responsible for the production of nitric oxide in *N. subflava* is nitrite reductase, characterisation of this enzyme and the corresponding gene became the focus of this study.

A number of Tn5 mutants deficient in nitrite reductase activity were available for analysis. One of these, mutant 163, looked of particular interest as it had zero nitrite reductase and *N*-nitrosation activities when assayed (Brew, 1992). Although Brew concluded otherwise it was decided to investigate the nitrite reductase of *N. subflava* to determine whether or not it could catalyse *N*-nitrosation reactions. However, as little structural information about the entire denitrification pathway of *N. subflava* was available, preliminary characterisation of the nitrite reductase protein was also undertaken.

1.11 Aims of this study

The main aim of this study was to purify the nitrite reductase enzyme from *N. subflava* for *in vitro* analysis to determine if it directly catalyses *N*-nitrosation. The following techniques were devised to enable a thorough investigation of the *N. subflava* nitrite reductase to be undertaken.

- Sequence analysis of the Tn5 insertion mutant 163 to identify and clone the nitrite reductase gene.
- Examination of the mutant 163 sequence to determine whether the nitrite reductase enzyme contains haem cd₁ or copper in its active site.
- Clone the nitrite reductase gene into an appropriate vector to overexpress the nitrite reductase protein in *E. coli* for purification.
- Activity stain *N. subflava* B19 and mutant 163 cell lysates on native polyacrylamide gels to compare the nitrite reductase activity of wild type and mutant 163 strains.

- *In vitro* nitrite reductase and *N*-nitrosation activity assays on the purified protein to determine if the nitrite reductase enzyme also has the ability to *N*-nitrosate.

Chapter Two

Materials and Methods

2.1 Bacterial Strains and Growth Conditions, Plasmids and General Materials.

2.1.1 Laboratory Suppliers

2.1.1.1 General laboratory chemicals

Most chemicals were of analytical reagent or molecular grade and purchased from the following suppliers:

Aldrich Chemical Company Ltd., Gillingham, Dorset.

Amersham International plc, Amersham, Buckingham.

BBL Microbiology Systems, Cockeysville, USA.

BDH Ltd., Poole, Dorset.

Difco Laboratories Ltd., West Molesey, Surrey.

Fisher Scientific International, Loughborough, Leicestershire.

Oxoid Ltd., Basingstoke, Hampshire.

Protogel., National Diagnostics, Atlanta, Georgia.

Sigma Chemical Company, Poole, Dorset.

2.1.1.2 Enzymes

Restriction endonucleases and shrimp alkaline phosphatase were obtained from Boehringer Mannheim, Lewes, East Sussex and Promega Corporation, Madison. T₄ DNA ligase, Taq polymerase and Vent_R® DNA polymerase were bought from New England Biolabs (NEB), Hitchin, Hertfordshire. T7 DNA polymerase was supplied by Pharmacia Biotech, St. Albans, Hertfordshire.

2.1.1.3 Isotopes

Amersham International plc supplied the radioisotopes (³²P and ³⁵S) and the nylon membrane (Hybond-N).

2.1.1.4 Oligonucleotides

Synthetic oligonucleotides were purchased from The OSWEL DNA Service, Southampton or Perkin-Elmer Applied Biosystems, Warrington, Cheshire.

2.1.2 Growth Media and Buffers

Growth media are listed in section 2.1.2.1. Phage, bacterial and other commonly used buffers are listed in section 2.1.2.2. L-broth and L-agar were the media of choice for manipulations involving *E. coli* and Brain Heart Infusion (BHI; Difco) broth and agar were used for growth of *N. subflava*. Other denitrifying strains were used during the course of this study; *Ps. stutzeri* and *Al. xylooxidans* were grown on nutrient broth and half strength Tryptic Soy broth (TSB; BBL Microbiology Systems.) respectively. Where bacteriophage λ was used the media was supplemented with 0.1M MgSO₄.

2.1.2.1 Growth media

Luria broth (L-broth)	Difco Bacto tryptone	10g
	Difco Bacto yeast extract	5g
	NaCl	5g
	Distilled water to 1 litre	
	pH to 7.2 using NaOH	
L-agar	L-broth + 15g Difco agar per litre	
Nutrient broth	Oxoid No.2 nutrient broth	25g
	Distilled water to 1 litre	
Nutrient agar	Nutrient broth + 12.5 g Davis NZ agar	

BBL agar	BBL trypticase	10g
	NaCl	5g
	Agarose	10g
	Distilled water to 1 litre	
BBL top agar	BBL trypticase	10g
	NaCl	5g
	Agarose	6.5g
	Distilled water to 1 litre	
BHI broth	Difco BHI broth	37g
	Distilled water to 1 litre	
BHI agar	BHI broth + 15g Difco agar No3	
TSB broth (half strength)	BBL TSB broth	15g
	Distilled water to 1 litre	
SOC broth	Bactotryptone	4g
	Bacto yeast extract	1g
	5M NaCl	0.4ml
	1M MgCl ₂	2ml
	1M KCl	0.5ml
	1M MgSO ₄	2ml
	glucose	0.72g
	Distilled water to 200ml	

2.1.2.2 Commonly used buffers

TE buffer	10mM Tris-acetate (pH 8.0) 1mM EDTA (pH 8.0)	
TAE buffer (working solution)	40mM Tris-acetate 2mM EDTA	
10× stock TAE buffer	Tris base Glacial acetic acid 0.5M EDTA Distilled water to 1 litre	48.4g 11.4ml 20ml
Phage buffer	Na ₂ HPO ₄ KH ₂ PO ₄ NaCl 1M Mg SO ₄ 0.1M CaCl ₂ 1% (w/v) gelatin solution Distilled water to 1 litre	7g 3g 5g 1ml 10ml 1ml

Where appropriate the solutions in sections 2.1.3 and 2.1.4 were sterilised by autoclaving at 120°C, 15 psi for 15 minutes.

2.1.3 Selection For Antibiotic Resistance

The routine concentration of antibiotics used in this study are shown in Table 2.1. Those antibiotics dissolved in water were filter sterilised using a 0.45 μ m filter (Millipore).

Antibiotic	Abbreviation	Solvent	conc. of stock solution (mg ml ⁻¹)	final conc. in media (μ g ml ⁻¹)
Ampicillin	Amp	H ₂ O	100	50
Chloramphenicol	Chl	ethanol	20	25
Kanamycin	Kan	H ₂ O	25	25 or 50
Nalidixic acid	Nal	H ₂ O (pH 11 with NaOH)	25	40
Streptomycin sulphate	Strep	H ₂ O	100	200
Tetracycline hydrochloride	Tet	50% ethanol	10	10

Table 2.1 Antibiotic solutions used in this study.

2.1.4 Plasmids

Plasmids used and constructed during this study are listed in Table 2.2.

Plasmid	Description	Reference or Source
pUC18/19	lacZ cloning vectors with polycloning sites in opposite orientations. Amp ^R	Yanisch-Perron <i>et al.</i> , 1985
pBluescript II KS ⁻	lacZ cloning vector derived from pUC19. Amp ^R	Stratagene
pBR325	pBR322 derivative. Amp ^R , Tet ^R , Chl ^R	NBL Gene Sciences
pACYC177	Low copy number cloning vector compatible with pUC19 and pBR322. Amp ^R , Kan ^R	Chang and Cohen, 1978
pSL1180/90	Superlinker phagemid derived from pUC118/119. Amp ^R	Brosius, 1989
pASHOK	'Promoterless' cloning vector derived from pBR322. Amp ^R	Kumar and Hayward, pers. comm.
pKT231	Broad host range, high copy number vector. Kan ^R , Strep ^R	Bagdasarian <i>et al.</i> , 1981
pZS55	11kb <i>Bam</i> HI fragment from	Sowerby, 1997

	<i>N. subflava</i> strain 55 cloned into pUC19. Amp ^R , Kan ^R	
pZS163	11kb <i>Cla</i> I fragment from <i>N. subflava</i> strain 163 cloned into <i>Acc</i> I site of pUC19. Amp ^R , Kan ^R	Sowerby, 1997
pAniA350	350bp PCR product cloned into <i>Bam</i> HI and <i>Eco</i> RI sites of pKS ⁻	This work
pAniA10	2.0kb <i>Hind</i> III fragment from <i>N. subflava</i> strain B19 cloned into pBR325	This work

Table 2.2 Plasmids used and constructed during this study.

2.1.5 Bacterial Strains

The genotypes of bacterial strains used in this work are shown in Table 2.2. References are cited where appropriate.

Name	Genotype	Reference or Source
<i>E. coli</i> DH5 α TM	F ⁻ , <i>recA1</i> , <i>supE44</i> , <i>endA1</i> , <i>deoR</i> , <i>phoA</i> , <i>hsdR17</i> (<i>r</i> _K ⁻ , <i>m</i> _K ⁺), <i>gyrA96</i> , <i>relA1</i> , <i>thi-1</i> , (<i>argF-lacZYA</i>)U169, ϕ 80 <i>lacZM15</i> .	Life technologies
<i>E. coli</i> DH5 α F'IQ TM	F ⁻ , <i>recA1</i> , <i>supE44</i> , <i>endA1</i> , <i>deoR</i> , <i>phoA</i> , <i>hsdR17</i> (<i>r</i> _K ⁻ , <i>m</i> _K ⁺), <i>gyrA96</i> , <i>relA1</i> , <i>thi-1</i> , (<i>argF-lacZYA</i>)U169, ϕ 80 <i>lacZM15/F'</i> , <i>proAB</i> ⁺ , <i>lacI</i> ^q Δ M15, <i>zzf::Tn5</i> [Kan ^R]	Life technologies
<i>E. coli</i> NM767	Δ (<i>hsdRMS</i> , <i>mcrB</i> , <i>mrr</i>), <i>e14</i> ^o <i>mcrA</i> , <i>sbcC201</i> , (<i>P2cox3</i>)	NBL Gene Sciences
<i>E. coli</i> NM772	Δ (<i>hsdRMS</i> , <i>mcrB</i> , <i>mrr</i>), <i>e14</i> ^o <i>mcrA</i> , <i>sbcC201</i> , <i>recD1009</i> , <i>supE44</i>	NBL Gene Sciences
<i>E. coli</i> XL1-Blue	[<i>F'</i> : <i>Tn10</i> (Tet ^R), <i>proA</i> ⁺ , <i>proB</i> ⁺ , <i>lacI</i> ^q , <i>lacZ</i> Δ M15]	NBL Gene Sciences

<i>E. coli</i> DL795	<i>recA1, endA1,</i> <i>gyrA96(Nal^R), thi,</i> <i>hsdR17(r_k⁻m_k⁺), supE44,</i> <i>relA1, lac</i>	NBL Gene Sciences
<i>N. subflava</i> B19	Δ (<i>hsdRMS, mcrB, mrr</i>), <i>e14^omcrA, sbcC201,</i> <i>recD1009, supE44,</i> <i>recA::Cm^R</i>	Forsythe <i>et al.</i> , 1988
<i>N. subflava</i> 163	Kan ^R	Brew, 1992
<i>N. subflava</i> 55	Kan ^R	Brew, 1992

Table 2.3 Bacterial strains used in this study.

2.1.6 Growth of Bacterial Strains

Liquid cultures of bacteria were grown in the appropriate broths by inoculating a given volume with a single colony. A 10% overnight culture was used to inoculate large volumes of culture. For the maintenance of plasmids and the selection of specific strain characteristics antibiotics were included in the media in the concentrations shown in Table 2.1. Liquid cultures of *E. coli* were typically grown overnight at 37°C in an orbital shaker with a rotation speed of 150 rpm.

2.1.6.1 Growth conditions of *N. subflava* B19

The wild type strain of *N. subflava* B19 was subcultured every other day onto fresh BHI plates and incubated at 37°C in a candle jar.

When broth cultures were required a loopful of growth was removed from the plate and used to inoculate 20ml BHI broth and grown aerobically at 37°C in an orbital shaker (rotation rate approximately 150 rpm). Larger volumes were obtained by using a 5% inoculum of an overnight broth culture.

N. subflava B19 was also grown anaerobically, (Brew, 1992). A loopful of growth from an overnight plate was used to inoculate 10-15ml BHI broth supplemented with 2mM sodium nitrite in a Universal bottle. This was incubated overnight at 37°C without agitation. This 10ml culture was used to inoculate 100ml BHI broth supplemented with 5mM sodium nitrite in 150ml medical flasks and again incubated overnight at 37°C without agitation. After this incubation small dinitrogen bubbles could be seen at the surface of the turbid culture. Finally, 10ml of this culture was used to inoculate 100ml BHI broth supplemented with 10mM sodium nitrite, again in 150ml medical flasks and again incubated overnight at 37°C without agitation. This method was also employed when anaerobic growth of other denitrifying strains was required. The growth media of *Ps. stutzeri* and *Al. xylooxidans* were mentioned in section 2.1.2. *Ps. stutzeri* was grown statically at 37°C whereas *Al. xylooxidans* was grown at 30°C.

N. subflava will also grow aerobically in L-broth, however growth is sub-optimal and BHI broth should be the media of choice - particularly when growing *N. subflava* anaerobically (pers. obs).

2.1.6.2 Maintenance and growth of *N. subflava* strain 163 carrying a Tn5 insertion

N. subflava Tn5 carrying mutant strain 163 was grown on BHI plates supplemented with Nal (40µg ml⁻¹) and Kan (50µg ml⁻¹) and incubated in a candle jar. Broth cultures of these strains were produced in the same way as for aerobic cultures of the wild type except that the broths were always supplemented with Nal and Kan at the same concentrations as the BHI plates.

2.1.6.3 Long term storage of bacterial cultures

Bacteria were grown overnight as a thick lawn of cells on appropriate plates. A 2ml aliquot of suitable broth supplemented with glycerol 15% (v/v) was poured over the plates and the cells were scraped from the agar surface using a sterile Pasteur pipette. The cell cultures were stored at -80°C in sterile glass vials and were viable for three years.

Cells were resuscitated by rapidly thawing the cultures at 37°C and streaking them out on suitable agar for incubation overnight. *N. subflava* cells needed to be incubated at 37°C in a candle jar for good growth to be observed after an overnight incubation as this organism resuscitates best under microaerophilic conditions, (pers. obs).

Glycerol cell suspensions were freeze thawed no more than three times before being discarded to reduce the risk of contamination.

2.2 DNA Techniques

2.2.1 Large Scale Preparation of Chromosomal DNA

A single colony was used to inoculate 5ml of growth media which was incubated at a suitable temperature with shaking overnight, refer to section 2.1.6. A 0.5ml aliquot of this overnight was used to inoculate 100ml of appropriately supplemented media and the culture incubated at a suitable temperature overnight with vigorous shaking. The culture was chilled on ice for 15 minutes and transferred to two 250ml centrifuge bottles. The cells were pelleted by centrifugation at 5,000 rpm in a pre-cooled Sorvall GSA rotor for 15 minutes at 4°C. Care was taken to remove all the supernatant and any excess was removed with a Pasteur pipette. The cells were resuspended in 20ml STE buffer and 1ml Sigma proteinase K (4mg ml⁻¹) was added. The mixture was split into two 10.5 ml volumes and poured into sterile Universals. The solution was mixed by gentle inversion. A 0.5ml aliquot of 10% SDS solution was added to each of the Universals which were then incubated for 6 hours at 50°C in a waterbath without shaking. An equal volume of phenol/chloroform/isoamyl alcohol (25:24:1 v/v) was added to the lysed cells and stored at 4°C overnight.

Cellular debris was pelleted by centrifuging the lysed solutions at 10,000 rpm at room temperature for 15 minutes in a HB-4 swinging bucket rotor using sterile corex tubes. The upper aqueous layer was removed using a Gilson P1000 and transferred to a sterile 25ml glass beaker. Care was taken not to remove any of the protein interface. The aqueous layer was extracted with an equal volume of water-saturated chloroform to remove any phenol which may still be present. After centrifugation at 5,000 rpm at room temperature in a Sorvall GSA rotor for 5 minutes the upper aqueous layer was again transferred to a sterile 25ml glass beaker. A 1ml aliquot of 3M sodium acetate (pH 5.2) and 2 volumes of 100% (v/v) ethanol pre-chilled to -20°C were added to the solution and mixed by swirling. A clean sterile glass rod was used to spool the DNA from the mixture. The spooled DNA was drained of ethanol and transferred to a Universal bottle containing 70% (v/v) ethanol.

This solution was spun in a MSE Centaur 2 benchtop centrifuge for 10 minutes, the ethanol poured off and the pelleted DNA allowed to air dry for 10 minutes. The DNA was dissolved in 250-500 μ l TE buffer depending on pellet size. This method yields approximately 100mg of chromosomal DNA.

Solutions used:

STE: TE buffer, 10mM NaCl

2.2.2 Small Scale Preparation of Chromosomal DNA

Growth media (5ml) containing appropriate selective antibiotics was inoculated with a single bacterial colony overnight at the permissive temperature. A 1.5ml aliquot of the culture was transferred to a microcentrifuge tube and centrifuged in an MSE microcentrifuge for 2 minutes at 14,000 rpm. The supernatant was discarded. The pellet was resuspended in 567 μ l of TE buffer, 3 μ l proteinase K (20mg ml⁻¹) and 30 μ l 10% SDS. The mixture was vortexed thoroughly and incubated at 37°C for 1 hour. A 100 μ l aliquot of 5M NaCl was added and mixed thoroughly. Hexadecyltrimethyl ammonium bromide (CTAB) / NaCl solution (80 μ l) was added, mixed thoroughly and incubated for 10 minutes at 60°C. An equal volume of phenol/chloroform/isoamyl alcohol (25:24:1 v/v) was added, mixed thoroughly and the tubes were centrifuged at 14,000 rpm for 5 minutes in an MSE microcentrifuge. The aqueous layer was transferred to a fresh microcentrifuge tube and an equal volume of chloroform/isoamyl alcohol (1:1 v/v) added, mixed thoroughly and again centrifuged for 5 minutes at 14,000 rpm in an MSE microcentrifuge. The supernatant was transferred to a fresh microcentrifuge tube and 0.6 volume of isopropanol was added. The contents were mixed and then centrifuged for 5 minutes at 14,000 rpm in an MSE microcentrifuge. The isopropanol was removed and the pellet washed in 1ml of ice-cold 70% (v/v) ethanol then centrifuged for 5 minutes at 14,000 rpm in an MSE microcentrifuge. The 70% (v/v) ethanol was

removed and the pellet dried in a Savant Speed-Vac. The DNA was dissolved in 20-100µl TE buffer depending on pellet size.

Solutions used:

CTAB / NaCl solution: 4.1g NaCl was dissolved in 80ml H₂O and 10g CTAB (hexadecyltrimethyl ammonium bromide) was added slowly while heating and stirring. The final volume was adjusted to 100ml with distilled water.

2.2.3 Large Scale Preparation of Plasmid DNA from *E. coli*

A single colony was used to inoculate 5ml of L-broth (with appropriate antibiotic supplements) which was incubated overnight as described in section 2.1.6. A 0.5ml aliquot of the overnight was used to inoculate 2 × 250ml volumes of L-broth containing appropriate antibiotic supplements and the cultures were incubated at a suitable temperature overnight with shaking. The cells were pelleted by centrifugation at 7,000 rpm in a pre-cooled Sorvall GSA rotor for 5 minutes at 4°C. The supernatants were discarded and the cells drained for 2 minutes by standing the centrifuge pots upside down on tissue paper. (All subsequent instructions are for a single 250ml culture which was carried out in duplicate.)

The cell pellet was resuspended in 9ml ice-cold GTE buffer and then had 20ml of freshly prepared lysis solution added. The centrifuge pot was incubated on ice for 5 minutes and then had 10ml of ice-cold solution III added. The pot was gently shaken several times after this addition and then left to stand on ice for a further 15 minutes. The concentrated cell solution was centrifuged at 8,000 rpm in a pre-cooled Sorvall GSA rotor for 5 minutes at 4°C. If a concentrated cell pellet was not formed then the cells were recentrifuged under the same conditions. The supernatant was poured into a fresh 250ml centrifuge pot through some sterilised cotton wool to remove any lumps which were present. A 0.6 volume of isopropanol was added and the solution mixed. The mixture was left to stand at room

temperature for 2 minutes and was centrifuged at room temperature in a Sorvall GSA rotor for 5 minutes at 8,000 rpm. The supernatant was discarded and the remaining pellet washed with 70% (v/v) ethanol and left to drain well as before. The pellet was dried under vacuum for 2-5 minutes and was resuspended in 9ml TE buffer and kept on ice.

The resulting DNA solution was transferred to a sterile Universal bottle and 9g CsCl was added. The Universal was mixed gently by inversion until the CsCl dissolved. (If necessary the Universal was placed in a waterbath at 30°C to help the salt dissolve.) A 720 μ l aliquot of ethidium bromide (10mg ml⁻¹) was added to the solution which was then spun in a MSE Centaur 2 benchtop centrifuge for 5 minutes at room temperature. A “furry” scum formed at the surface of the CsCl solution. A Pasteur pipette was used to transfer the pink liquid underneath this precipitate to a Beckman Ti50 Sorval crimp seal tube. As the above plasmid preparation was routinely done in duplicate there were two Ti50 crimp seal tubes at this stage and the tubes, stoppers and caps from each prep were balanced to within 0.01g.

The tubes were placed in a Beckman Ti50 fixed angle rotor and centrifuged at 45,000 rpm for 24 hours at 18°C. The tubes were removed from the rotor avoiding unnecessary handling. Under UV illumination two ethidium bromide stained bands could be seen, the lower band contained the supercoiled plasmid DNA. This band was extracted by the insertion of a 0.9 × 40mm needle into the top of the tube which acted as a vent and another needle, attached to a 5ml syringe, inserted just below the band ensuring that the bevel of the needle pointed up. Approximately 1-2ml was withdrawn to ensure that the entire plasmid band was drawn into the syringe. The plasmid/CsCl solution was transferred to a small 5ml glass tube. To extract the ethidium bromide an equal volume of n-butanol was added to the glass tube. This was shaken gently to mix the two phases and allowed to settle. The n-butanol/ethidium layer (uppermost) was expelled and care was taken not to lose any of the plasmid containing (bottom) layer. This extraction procedure was repeated four times and then the plasmid/CsCl solution transferred to 8/32 inch dialysis tubing. (Dialysis tubing was prepared by boiling in 5mM EDTA for 10 minutes.) The ends of the tubing were sealed with clips and the plasmid/CsCl solution was

dialysed against 4 litres of TE at 4°C for 1 hour. The TE was replaced with fresh, chilled TE buffer and dialysis repeated for a further 4 hours. The TE was changed once more and the dialysis allowed to continue overnight at 4°C.

The plasmid solution was aliquoted into 0.5ml volumes in microcentrifuge tubes and had 50µl 3M sodium acetate (pH5.0) and 1ml ice cold ethanol added. These solutions were mixed gently and placed on ice for 30 minutes. The plasmid DNA was precipitated by centrifugation at 14,000 rpm for 30 minutes at 4°C in an MSE microcentrifuge. The ethanol was removed and the pellets washed with 1ml of ice cold 70% (v/v) ethanol. The tubes were vortexed briefly and centrifuged for a further 10 minutes at 14,000 rpm at 4°C in an MSE microcentrifuge. The 70% (v/v) ethanol was removed and the pellets dried in a Savant Speed-Vac. The pellets were resuspended in 300-500µl TE depending on the size of the pellet. The DNA concentration was determined as described in section 2.2.7.

Solutions used:

GTE buffer	50mM glucose 25mM Tris-HCl (pH8.0) 10mM EDTA
Lysis solution	0.2N NaOH 1% SDS
Solution III	3M potassium acetate 5M glacial acetic acid (11.5 ml in 100ml total volume)

2.2.4 Plasmid Miniprep by Alkaline Lysis

This routine plasmid ‘miniprep’ procedure is a slight variation on that first described by Birnboim and Doly (1979). A 5ml aliquot of growth media containing the appropriate selective antibiotics was inoculated with a single colony. The culture

was incubated at a suitable temperature overnight with shaking. A 1.5ml aliquot of the culture was transferred to a microcentrifuge tube and the cells pelleted by centrifuging at 14,000 rpm for 1 minute in an MSE microcentrifuge. The supernatant was removed and discarded and the pellet resuspended in 100µl GTE buffer. The cell suspension had 200µl lysis solution added and was mixed by inverting the tube 5 times. The tube was left to stand on ice for 3 minutes. A 150µl aliquot of ice cold 3M sodium acetate (pH 5.2) was added and the tube was again inverted 5 times before being placed on ice for 5 minutes. The cell debris was pelleted by centrifugation at 14,000 rpm for 5 minutes in an MSE microcentrifuge. The supernatant was decanted into a fresh microcentrifuge tube and 400µl of phenol/chloroform/isoamyl alcohol (25:24:1 v/v) was added. The tube was vortexed for 1 minute and then centrifuged for 1 minute at 14,000 rpm in an MSE microcentrifuge. The upper aqueous layer was transferred to a fresh microcentrifuge tube, had 800µl ice cold ethanol added and was vortexed briefly. The ethanol solution was allowed to stand at room temperature for 2 minutes and the DNA was pelleted by centrifuging in an MSE microcentrifuge at 14,000 rpm for 5 minutes at 4°C. The ethanol was removed and the pellet washed in 400µl 70% (v/v) ethanol. The tube was centrifuged for 2 minutes at 14,000 rpm in an MSE microcentrifuge, had the 70% (v/v) ethanol removed and the pellet was dried in a Savant Speed-Vac. The pellet was dissolved in 10-20µl TE containing RNase A (20µg ml⁻¹) and incubated at 37°C for 15 minutes. A yield of about 1-2µg plasmid DNA was expected.

At this point the DNA could be used for transformation or analysed by restriction digestion. For sequence analysis the preparation was further processed to remove RNA breakdown products. This was achieved by precipitation with polyethylene glycol. A 20µl aliquot of the resulting plasmid prep had 8µl PEG/NaCl solution added. This mixture was vortexed thoroughly and placed on ice for 60 minutes. The precipitate was centrifuged at 14,000 rpm for 10 minutes at 4°C in an MSE microcentrifuge. The supernatant was carefully removed leaving a small transparent DNA pellet behind. The pellet was successively rinsed with 0.5ml 70% (v/v) and 100% (v/v) ethanol and dried in a Savant Speed-Vac as above. The DNA

was finally resuspended in 10-15 μ l TE. The plasmid was then suitable for alkaline denaturation and double stranded sequencing.

Solutions used:

GTE buffer	50mM glucose 25mM Tris-HCl (pH8.0) 10mM EDTA
Lysis solution	0.2N NaOH 1% SDS
PEG/NaCl solution	30% PEG 8000 1.5M NaCl (Prepared from autoclaved stocks of 50% PEG and 5M NaCl to avoid DNase contamination.)

2.2.4.1 Chloramphenicol amplification of pACYC177 plasmids in *E. coli*

Many of the currently used plasmid vectors (e.g., the pUC series) replicate to such a high copy number that they can be purified in large yield from cultures that have been grown to late log phase in standard media, see sections 2.2.3 and 2.2.4. However vectors such as pACYC177 do not replicate so freely and need to be amplified by incubating the partially grown bacterial culture in chloramphenicol (Chl) for several hours. Chl inhibits host protein synthesis and therefore prevents replication of the bacterial chromosome (Sambrook *et al.*, 1989), but replication of the vector continues. Consequently the copy number of the vector increases for several hours. The method used was a variation on that described by Sambrook *et al.*, 1989.

A 25ml volume of L-broth containing appropriate antibiotic supplements was inoculated with 1.5ml of an overnight culture. This was incubated for exactly 2.5

hours at 37°C on an orbital shaker with 250-300rpm rotation. The OD₆₀₀ of the resulting culture was 0.4. A 125µl aliquot of Chl (34mg ml⁻¹) was added to give a final concentration of 170µg ml⁻¹. The culture was incubated overnight for a further 12-16 hours at 37°C with vigorous shaking, 250-300 rpm. The culture was then taken through the plasmid 'miniprep' method as described in section 2.2.4.

2.2.5 Large Scale Preparation of Bacteriophage λ DNA

A 5ml volume of L-broth was inoculated with a single colony of *E. coli* NM772 and incubated overnight at 37°C with shaking. A pre-warmed 200ml of L-broth supplemented with 10mM MgSO₄ was inoculated with 0.5ml of the overnight NM772 culture and incubated at 37°C with vigorous shaking, 250 rpm. When the OD₆₀₀ reached 0.5 the λ EMBL3 phage in lysate form (see section 2.4.4) was added to give a multiplicity of infection (m.o.i.) of 0.1. The OD₆₀₀ was monitored. The OD₆₀₀ increased as the cells continued to grow and divide and then fell as the cells lysed and released the phage. This took up to 8 hours. When lysis was well established and the OD₆₀₀ had dropped to a constant value, 0.4ml of chloroform was added and the culture incubated for a further 10 minutes at 37°C with shaking. The phage solution was centrifuged in a Sorvall GSA rotor at room temperature for 10 minutes at 4,000 rpm. The supernatant was decanted into a fresh centrifuge pot and 8g solid NaCl was added which was dissolved by gentle swirling. RNase A and DNase were added to a concentration of 1mg ml⁻¹ each and the mixture incubated at room temperature for 1 hour. PEG 8000 (20g) was added, dissolved by swirling and placed on ice for at least 1 hour but preferably overnight. The lysate/PEG 8000 solution was centrifuged in a Sorvall GSA rotor at 10,000 rpm for 10 minutes at 4°C. The supernatant was removed and discarded and the PEG/phage pellet was resuspended in 8ml of phage buffer and transferred to a Universal bottle. An equal volume of chloroform was added and vortexed briefly to wash the PEG 8000 from the phage. The chloroform/phage/PEG 8000 mixture was spun in a MSE Centuar 2 benchtop centrifuge at 4,500 rpm for 15 minutes to layer the PEG 8000 at the

chloroform (lower) : phage buffer (upper) interface. The phage buffer layer which contained the phage was carefully removed.

CsCl in phage buffer solutions was prepared to densities of 1.3, 1.5 and 1.7g ml⁻¹. A step gradient was set up by placing 1.5ml of the 1.3g ml⁻¹ in a 35ml ultracentrifuge tube and then successively underlaying the 1.5g ml⁻¹ and 1.7g ml⁻¹ solutions. The bacteriophage solution was carefully placed on top of the step gradient and balanced to within 0.01g with another tube. The step gradient was centrifuged at 35,000 rpm in a MSE 16×4 swinging bucket rotor for 1 hour at 18°C. The tubes were removed from the rotor and clamped firmly. A piece of black card was placed behind the tube to aid the visualisation of the opaque grey/blue band at the top of the 1.5g ml⁻¹ step. The band was extracted using a syringe with a 0.9 × 40mm needle. The phage buffer/CsCl solution was transferred to 8/32 inch dialysis tubing and dialysed against 4 litres of TE overnight at 4°C. (Dialysis tubing was prepared by boiling in 5mM EDTA for 10 minutes.) Aliquots (0.5ml) were transferred to microcentrifuge tubes and 0.5ml phenol was added. The tubes were inverted several times to mix the two phases and then centrifuged for 5 minutes at 14,000 rpm in an MSE microcentrifuge. The aqueous layer was transferred to fresh microcentrifuge tubes and an equal volume of phenol/chloroform/isoamyl alcohol (25:24:1 v/v) added. The tubes were inverted several times to mix the two phases and then centrifuged for 5 minutes at 14,000 rpm in an MSE microcentrifuge. The aqueous layer was removed and an equal volume of chloroform added to it. The tubes were inverted several times and then centrifuged for 5 minutes at 14,000 rpm. The aqueous layer was transferred to a fresh microcentrifuge tube and 1/10 volume of 3M sodium acetate (pH 5.2) added. 2 volumes of ice cold ethanol were added, the tubes were mixed by inversion and placed on ice for 15 minutes. The phage DNA was precipitated by centrifuging at 14,000 rpm at 4°C for 15 minutes in an MSE microcentrifuge. The ethanol was removed and the pellets washed with 1ml of ice cold 70% (v/v) ethanol and then centrifuged at 14,000 rpm for 5 minutes at 4°C in an MSE microcentrifuge. The pellets were dried in a Savant Speed-Vac. The phage DNA was resuspended in 300-500µl TE depending on pellet size. The DNA concentration was determined as described in section 2.2.7.

2.2.6 Precipitation of DNA

A 1/10 volume of 3M sodium acetate (pH 5.0) was added to the DNA solution and mixed by vortexing. Ice cold ethanol, 2 volumes, were added and the tubes placed on ice for 10 minutes. The mixture was centrifuged at 14,000 rpm in an MSE microcentrifuge for 10 minutes. The ethanol was removed and 1ml of ice cold 70% (v/v) ethanol added. The tubes were vortexed for 10 seconds and centrifuged at 14,000 rpm for 5 minutes in an MSE microcentrifuge. The 70% (v/v) ethanol was removed and the pellet dried in a Savant Speed-Vac. The pellet was dissolved in a suitable volume of TE or dH₂O.

2.2.7 Determination of DNA Concentration

DNA solution (10 μ l) was added to 990 μ l of TE buffer in a quartz cuvette. The OD₂₆₀ and the OD₂₈₀ were measured. An OD₂₆₀ of 1.0 corresponds to 50mg ml⁻¹ for double stranded DNA, (Sambrook *et al.*, 1989). An OD₂₆₀/OD₂₈₀ ratio of 1.8 indicates relatively pure DNA. Contaminants such as proteins and carbohydrates increase or decrease this ratio.

2.2.8 Restriction of DNA

The digestion of DNA using restriction endonucleases was performed in 10-20 μ l volumes containing 0.1-1 μ g DNA, 1x appropriate restriction enzyme buffer and restriction enzyme in 2-5 fold excess. The final volume was made up using distilled water. Some restriction endonucleases require the presence of BSA in the reaction mixture so, when required, BSA was added according to manufacturers instructions. The digests were incubated at the permissive temperature for the particular restriction endonuclease for 2 hours.

2.2.8.1 Digestion of DNA using two restriction enzymes

For digestion of DNA using two restriction enzymes one of two approaches was taken. If the enzymes had a compatible buffer then both enzymes were added in equal concentration to the reaction mixture. Alternatively, if the buffers of the two restriction enzymes were totally incompatible, the DNA was purified from the reaction by ethanol precipitation after digestion with the first enzyme. The resuspended DNA was then digested with the second restriction enzyme.

It is important that the two restriction sites in a double digest are not too close to each other. If they were, they were checked to ensure they had the required number of bases (different for each restriction endonuclease) at each end of the cleavage site for efficient digestion to occur (NEB catalogue, 1997).

2.2.9 Dephosphorylation of DNA

Vector DNA digested with a single restriction endonuclease was dephosphorylated after digestion to minimise the recovery of parental clones. Shrimp alkaline phosphatase (SAP) from Boehringer Mannheim was used as this enzyme is completely and irreversibly inactivated by heat treatment. The phosphatase enzyme works by removing the terminal 5' phosphate from restricted DNA preventing it religating to form intact vector molecules.

DNA was digested as described in section 2.2.8 except that a total volume of 8 μ l was used. SAP was directly added to the restriction reaction thereby removing an unnecessary ethanol precipitation step. 1 unit of SAP and 1 μ l of the supplied 1 \times dephosphorylation buffer were added to the digests and incubated for 20 minutes at 37°C. For phosphorylation of blunt ended fragments the DNA was left incubating at 37°C for 1 hour. SAP was inactivated by incubating at 65°C for 15 minutes. The DNA was now considered ready for ligation.

2.2.10 Agarose Gel Electrophoresis of DNA

Agarose gel electrophoresis was used to separate DNA fragments after digestion with restriction enzymes and to identify PCR products. The concentration of agarose used depended on the sizes of DNA fragments being separated. For fragments of 300bp to 1.5kb 1.5-2.0% agarose was used, between 1.5kb to 4kb 1% agarose and above 4kb 0.8% agarose. The agarose was dissolved in TAE buffer by brief boiling, cooled to 55°C and ethidium bromide was added to a final concentration of $1\mu\text{g ml}^{-1}$. The agarose solution was then poured into the gel tray, the comb(s) inserted and left to solidify for 30 minutes. Two types of gel electrophoresis equipment were used. The minigel (5cm x 7.5cm) was used for rapid (1-2 hours) separation of DNA fragments usually for ligation reactions or preparing probes for hybridisation. The midigel (13cm x 15cm) was used to analyse potential clones and run chromosomal digests prior to Southern blotting onto nylon filters. Once the gel was set the comb was removed and it was placed into the electrophoresis tank fully filled with TAE. The wells of the gel were loaded by pipetting the samples beneath the TAE buffer surface. The minigel was run at 50-100mA and midigels were typically run overnight at 20mA. Once the gel had run sufficiently (this could be gauged by observing the position of migration of the marker dye) the power supply was switched off and the DNA visualised by exposing the gel to UV illumination.

2.2.11 Extraction of DNA from Agarose Gels

Two approaches were used to extract DNA fragments from agarose gels after electrophoresis. A modification to the GeneClean kit method manufactured by BIO 101 was used to isolate smaller fragments of 4kb or less. The principle behind the system is a silica matrix which binds to DNA in high salt solution but allows DNA to be eluted in low salt concentrations. Under UV illumination the desired DNA bands were excised using a clean scalpel blade and placed in sterile microcentrifuge tubes. The gel fragments were weighed and 3 volumes of 6M NaI were added to each. These were incubated at 50°C for 5 minutes or until the gel slices dissolved. The

microcentrifuge tubes containing the dissolved gel slices were placed on ice and 15 μ l silica matrix was added. These were inverted 2-3 times and placed back on ice for 5 minutes with inversion every minute. The tubes were centrifuged in an MSE microcentrifuge at 14,000 rpm for 20 seconds to pellet the silica matrix and the supernatant discarded. The pellet was gently resuspended in 0.5ml of 'New' wash (an ethanol based buffer to remove the NaI) and centrifuged as above. This process was repeated a further two times and then the pellet resuspended in 10 μ l dH₂O. This was incubated at 50°C for 10 minutes and then centrifuged at 14,000 rpm for 1 minute in an MSE microcentrifuge to pellet the silica matrix. The aqueous solution contained the DNA previously bound to the silica matrix. This was transferred to a fresh microcentrifuge tube and centrifuged once more to remove residual silica matrix. The DNA fragment in solution was then available for further manipulation.

When larger DNA fragments of 4kb or over were required the Qiagen QIAEX[®] II Gel Extraction Kit was used according to the manufacturers instructions. The reason for employing two different systems is that the silica matrix method has a tendency to shear larger DNA molecules when two or more silica particles bind to the DNA fragment. Repeated pelleting and resuspension of the silica matrix with bound DNA can exert forces on the DNA that lead to degradation. The Qiagen system is optimised so as to overcome these shearing forces.

Solutions used:

Silica matrix-	3M NaI 10% silica
'New' wash	50mM NaCl 10mM Tris-HCl (pH7.5) 2.5mM EDTA 50% (v/v) ethanol

2.2.12 Ligation of DNA Fragments

Ligation reactions were carried out in 10-20 μ l volumes. The total amount of DNA used per reaction was 0.1-0.5mg with 1 \times ligation buffer (NEB), T4 DNA ligase and dH₂O to make up the total volume where necessary. For sticky ended ligations a threefold molar excess of fragment to vector was used, whilst for blunt ended ligations a six to one molar ratio was used. Ligase concentration was 1 Unit per reaction for blunt ended ligations and 0.2 Units per reaction for sticky ended ligations. Sticky ended ligations were incubated at 16°C for 3 hours and blunt ended ligations incubated overnight also at 16°C.

2.2.13 Preparation and Transformation of Competent Cells (CaCl₂ method)

For transformation of ligation mixtures the following procedure was followed. Medium (5ml) containing the appropriate selective antibiotics was inoculated with a single colony and incubated with shaking at the appropriate temperature overnight. A 200 μ l aliquot of the overnight culture was used to inoculate 25 ml of L-broth, with appropriate selection, and incubated at a suitable temperature until the OD₆₀₀ reached 0.3. The culture was transferred to a sterile 30ml corex tube and placed on ice for 10 minutes. The chilled culture was centrifuged in a Sorvall SS-34 rotor at 4,000 rpm for 10 minutes. The supernatant was discarded and the corex tube was inverted to drain off excess media. The cells were resuspended in 5ml ice cold 0.1M CaCl₂. The cells were stored on ice for 30 minutes and centrifuged again as above. The supernatant was discarded and the pellets resuspended in 1ml ice cold 0.1M CaCl₂. The cells were now competent and ready to use (although the competence of the cells has been shown to increase after overnight storage on ice). A 5 μ l aliquot of the ligation mix was added to 200 μ l of competent cells, mixed gently and placed on ice for 30 minutes. The mixture was transferred to a 42°C waterbath for 5 minutes and then placed on ice for 2 minutes, after which 0.8 ml L-broth supplemented with 0.2mM glucose was added. The

culture was then incubated for 1 hour at a temperature to allow to expression of the antibiotic selection marker. Aliquots (200 μ l) of transformed cells were plated on selective media.

[note: If the selection was for tetracycline resistance alone the 1 hour expression step was omitted.]

2.2.13.1 Blue/white colony selection for transformant colonies

Many of the vectors in current use (e.g., the pUC series) carry a short segment of *E. coli* DNA that contains a truncated β -galactosidase gene (*lacZ*). Embedded in this coding region is a polycloning site that does not disrupt the reading frame so that a small number of amino acids are added to the N-terminal fragment of β -galactosidase. Vectors of this type are used in host cells that code for the C-terminal portion of the β -galactosidase. In the host cell the N-terminal and C-terminal fragments associate to form an enzymatically active enzyme - a process known as α -complementation. These bacteria are easily recognised as they form blue colonies in the presence of the chromogenic substrate X-gal. However, insertion of a fragment of foreign DNA into the polycloning site of the plasmid results in the production of an N-terminal fragment that is not capable of α -complementation. Bacteria carrying vectors with insert fragments therefore form white colonies.

To use this selection method X-gal and IPTG are added as supplements to the appropriate selective agar plates. A 1ml aliquot of X-gal (20mg ml⁻¹) and a 0.2ml aliquot of IPTG (20mg ml⁻¹) are added to 500ml molten agar. IPTG is required in the agar as it stimulates the promoter of the *lac* operon.

2.2.14 Preparation of Cells for High Efficiency Electro-Transformation

L-broth, 200ml in a 2 litre conical flask containing selective antibiotics if required, was inoculated with 0.5ml of a fresh overnight culture and incubated with vigorous shaking (200 rpm) at a suitable temperature until the OD₆₀₀ reached 0.4-0.7. The culture was transferred to a 250ml GSA centrifuge pot and placed on ice for 1

hour. The culture was centrifuged in a chilled Sorvall GSA rotor at 4,000 rpm for 10 minutes at 4°C. The supernatant was discarded without disturbing the pellet. The pellet was resuspended in 100ml ice cold sterile dH₂O and pelleted as above. This was repeated a further two times and the cell pellet resuspended in 0.5ml chilled 10% (v/v) sterile glycerol after the final centrifugation. Aliquots of 150µl were placed in sterile microcentrifuge tubes and placed on ice. The cells were snap frozen in a dry ice/ethanol bath and stored at -80°C until needed. Cells could be stored in this way for up to six months.

2.2.15 Preparation of DNA for Electroporation

DNA ligation mixtures used for transforming cells by electroporation have to be in salt free solution to prevent arcing as the DNA solution/cell suspension is exposed to a large electrical charge. The presence of salts result in a premature release of the charge and a greatly reduced transformation efficiency.

The ligation mixture was briefly centrifuged in an MSE microcentrifuge and dH₂O added to increase the total volume to 100µl. An equal volume of phenol/chloroform (1:1 v/v) was added, the mixture vortexed for 30 seconds and centrifuged in an MSE centrifuge for 1 minute at 14,000 rpm at room temperature. The upper aqueous layer was transferred to another sterile microcentrifuge tube and an equal volume of chloroform was added. The mixture was vortexed and centrifuged as above. The upper aqueous layer was transferred to a sterile microcentrifuge tube and a 1/10 volume of 3M sodium acetate (pH 5.2) and 2 volumes of chilled ethanol were added. The mixture was vortexed briefly and placed on ice for 30 minutes. The ethanol mixture was centrifuged in an MSE microcentrifuge at 14,000 rpm for 20 minutes at 4°C. The supernatant was removed and the pellet had 0.5ml of 70% (v/v) ethanol added. The tube was inverted several times to wash the DNA pellet and was centrifuged at 14,000 rpm for 5 minutes at room temperature in an MSE microcentrifuge. The supernatant was removed, the pellet dried in a Savant Speed-Vac and resuspended in 5µl dH₂O. This 5µl aliquot was used to transform a 150µl volume of cells.

2.2.16 Electro-Transformation of Ligation Mixtures

The electro-transformation competent cells were thawed slowly at room temperature and placed on ice. The equipment used was a Biorad Genepulser and Pulse Controller. The Genepulser was set at 25 mF and 2.5 kV and the Pulse Controller at 200 Ohms. The pulse at these settings has a time constant of 4.5-5.0 milliseconds giving a field strength of 12.5 kV/cm. Competent cells (150 μ l) were mixed with 5 μ l of the ligated DNA. The mixture of cells and DNA was transferred to a chilled electroporation cuvette (1mm electrode width, Biorad) and the side of the cuvette gently tapped to ensure that the mixture was distributed evenly on the bottom. The cuvette was placed in the safety chamber slide and inserted into the chamber. The cells were pulsed and immediately resuspended in 1 ml of SOC broth (see section 2.1.2) and transferred to a microcentrifuge tube. The tubes containing the transformed cells were gently agitated (100 rpm rotation on an orbital shaker) to allow the transformants to express for antibiotic selection at a suitable incubation temperature for 1 hour. Aliquots (100 μ l) of the cell suspension were spread on appropriate selective plates and incubated overnight at a suitable temperature.

2.2.17 DNA Sequencing

2.2.17.1 Introduction

DNA sequencing was performed using the Pharmacia T7 Sequencing Kit. The annealing buffer, labelling mix, T7 DNA polymerase and stop solution were supplied with this kit and details of the composition of these solutions were found in the manufacturer's instructions. The kit is based upon the chain-terminating dideoxynucleotide sequencing method developed by Sanger *et al.* (1977). In the original procedure, primer extension was catalysed by the Klenow fragment of DNA polymerase I. The kit replaces the Klenow enzyme with the T7 DNA polymerase, which has the advantage of creating longer chain terminated fragments with a more

even distribution of label between fragments. The major practical difference in using T7 polymerase over Klenow is that primer extension reactions are performed in two stages, a labelling reaction and a termination reaction. The two stages are necessary because the enzyme uses dideoxynucleotides very readily, and therefore in order to allow the synthesis of long chain-terminated fragments, dideoxynucleotides are excluded from the first stage of the reaction, being added for the second. Even so, the time required for the reactions using the T7 enzyme is considerably less than those using the Klenow enzyme.

2.2.17.2 Annealing of primer to double stranded template

The DNA templates used in the sequencing reactions were double stranded plasmid DNAs purified either by CsCl density centrifugation or by the 'miniprep'/PEG precipitation method in section 2.2.4. The oligonucleotide primers used were obtained from the OSWEL DNA service or Perkin-Elmer and tended to be between 17-24 bases in length.

The template was denatured by adding 1.5-2 μ g DNA in a total volume of 8 μ l dH₂O to 2 μ l 1M NaOH. This mixture was left at room temperature for ten minutes whereupon 7 μ l of 3M sodium acetate (pH 5.2) was added followed by 120 μ l of ethanol and 4 μ l dH₂O. The tube was placed on ice for 15 minutes then centrifuged at 14,000 rpm at 4°C for 15 minutes in an MSE microcentrifuge. The ethanol was removed and the almost invisible pellet allowed to air dry briefly before being dissolved in 10 μ l dH₂O.

The following was added to a microcentrifuge tube on ice:

Template DNA (2 μ g)	10 μ l
Primer (30ng μ l ⁻¹)	2 μ l
Annealing buffer	2 μ l
Total	14 μ l

The contents of the tube were mixed thoroughly and incubated at 60°C for 5 minutes, 37°C for 10 minutes and room temperature for 10 minutes. If the sequencing reaction was to be completed at a later time then the tube was stored at -20°C until required.

2.2.17.3 Sequencing reaction

For each template to be sequenced four sterile microcentrifuge tubes were labelled 'A', 'C', 'G' and 'T' respectively and 2.5µl of the corresponding dideoxynucleotide mix was added to each well. To the tube containing the annealed template and primer the labelling mix, (1.375µM each dCTP, dATP, dTTP and dGTP in solution), T7 DNA polymerase and α -[³⁵S] dATP were added as follows:

Annealed template and primer	14µl
Labelling mix	3µl
α -[³⁵ S] dATP	1µl (10µCi)
T7 DNA polymerase (1.5U µl ⁻¹)	2µl
Total	20µl

This labelling reaction was incubated at room temperature for 5 minutes. While this was proceeding the previously dispensed sequencing mixes were incubated at 37°C for 2 minutes in a water bath. After the 5 minute incubation of the labelling reaction, 4.5µl was added to each of the prewarmed sequencing mixes and returned to the water bath for a further 5 minutes to allow chain termination to occur. Finally, 5µl of stop solution was added to each reaction, these could then be stored at -20°C until required for electrophoresis. When the samples were needed for loading onto the sequencing gel they were heated to 80°C for 2 minutes to denature the DNA. Immediately after this incubation 3.5µl of each sample was loaded onto the gel.

2.2.17.4 DNA sequencing gel electrophoresis

DNA sequencing was performed using a 30 x 40cm BRL sequencing apparatus. The glass sequencing plates were thoroughly cleaned with detergent and ethanol. The shorter of the two plates was siliconised using dimethylsilane to ease separation of the plate from the sequencing gel after running the samples. The plates were assembled using 0.2 mm spacers and taped together to prevent leakage.

The 6% acrylamide gel was prepared by adding together the following:

Protogel (30% (w/v) acrylamide/bisacrylamide)	12ml
Urea	25.2g
d.H ₂ O	22ml
10x TBE	6ml

(10x TBE stock - 121g Tris base, 7.4g EDTA, 53.4g Boric acid, make up to 1 litre. pH should be 8.3.)

The urea was allowed to dissolve with the aid of magnetic stirring. Once dissolved, 142.5 μ l of freshly prepared 10% ammonium persulphate solution was added followed by 142.5 μ l of TEMED. This was then stirred slowly for a few seconds and slowly poured between the sequencing plates using a 25ml pipette. The flat edge of a shark-tooth comb was pushed between the plates to layer the top of the gel. Saran wrap was wrapped around the exposed areas of the plate and the top and each side of the gel was clamped with bulldog clips. The gel was then set aside for 1 hour to let the acrylamide polymerise. Once set, the bulldog clips, Saran wrap, tape and comb were removed and distilled water was squirted along the top of the gel. The shark-toothed comb was then replaced with the teeth pointing downwards until just touching the top of the gel. The gel was then clamped into the sequencing apparatus and 1x TBE buffer poured into the top and bottom reservoirs. The gel was then pre-run at 65V for 1 hour. After this the gel was ready to be loaded with the sequencing reactions. The samples were loaded in the order T, C, G and A

immediately after denaturing the DNA (see above). The gel was then electrophoresed at 65V until the blue dye in the stop solution ran off the end of the gel. Once electrophoresis was complete the glass plates were removed from the apparatus, the spacers and combs removed and the two glass plates carefully separated. The plate with the gel attached had a sheet of water dampened blotting paper laid over the gel. A dry sheet of blotting paper was then laid over this and gently pressed down to displace air and flatten out wrinkles in the gel. The sheets of blotting paper were then carefully peeled from the glass plate with the gel now adhered to the paper. The paper and gel sandwich was covered in Saran wrap and then dried in a vacuum gel-drier for 1 hour at 80°C. When dry the gel was placed in an autoradiography cassette and allowed to develop at room temperature. The length of time left to develop was determined by checking the cps of the gel with a Geiger counter. In most instances a good signal was achieved after 24-48 hours.

2.2.18 Automated DNA Sequencing

DNA was initially sequenced manually as in section 2.2.17. A departmental automated sequencer became available part way through this study whereupon this became the preferred method to prepare template DNA for sending to the sequencing facility.

The Applied Biosystems 377A sequencer also uses the dideoxy chain termination method of Sanger *et al.* (1977) but the DNA bands are detected by fluorescent dyes which are incorporated into the dideoxy nucleotides. The Perkin-Elmer Prism™ Ready reaction DyeDeoxy™ Terminator system was used. Double stranded templates were used in the reaction which consisted of 8µl terminator pre-mix, 1µl primer (30ng ml⁻¹) and 600-1000ng template DNA in a total volume of 20µl. Cycle sequencing was performed in a Hybaid Omn-E Thermal Cycler using the following conditions:

96°C	30 seconds
50°C	15 seconds
60°C	4 minutes

25 cycles.

Unincorporated dye-terminators were removed by ethanol precipitation. A 2.0µl aliquot of 3M sodium acetate (pH 5.2) and 50µl 95% (v/v) ethanol were added to the reaction mix. This was vortexed and incubated on ice for 10 minutes. The reaction/ethanol mix was centrifuged at 14,000 rpm for 30 minutes in an MSE microcentrifuge. The ethanol solution was removed and the tiny pellet rinsed with 250µl 70% (v/v) ethanol. The 70% (v/v) ethanol was removed and the pellet dried in a Savant Speed-Vac for 5 minutes. The dried pellet was then sent to the sequencer operator.

2.2.18.1 Sequence analysis

Sequence analysis was carried out using University of Wisconsin Genetics Computer Group (GCG) software on a Unix operating system. Sequence editing was done using the SEQED programme and sequence alignment using the BESTFIT, LINEUP, PILEUP and PRETTY set of programmes. (BESTFIT parameters were always Gap Weight - 12 and Length Weight - 4. PILEUP parameters were always Gap Weight - 3 and Length Weight - 0.1.) Manual sequences were input by hand while sequences obtained from the automated sequencer were edited with GeneJockey II (BioSoft) or Factura (Applied Biosystems Inc) software before being transferred to GCG readable files.

2.2.19 Southern Blotting of DNA onto Nylon Filters

Genomic and plasmid DNAs at appropriate concentrations were digested with fitting restriction enzymes to produce fragments of calculated size. The digests were

run on a midigel at 20 mA for at least 12 hours and then photographed under UV illumination. The gel was then washed in 200 ml of 0.2M HCl for 20 minutes to depurinate the DNA. The gel was washed in 200 ml of 0.5M NaOH/1.5M NaCl solution for 15 minutes to denature the DNA. This step was repeated and the gel rinsed in dH₂O. The gel was then washed in 1M Tris-HCl (pH 8.0)/1.5M NaCl solution for 20 minutes and again rinsed in dH₂O.

Two sheets of blotting paper cut to overhang a large square petri dish by 5cm, were soaked in 20x SSC buffer and laid upon a glass plate in the dish. The glass plate was supported on two smaller circular petri dishes so the blotting paper effectively formed a bridge over this with the ends hanging into the larger petri dish. The agarose gel was then laid upon this blotting paper with the same surface uppermost as in the electrophoresis tank. A sheet of positively charged Hybond-N (AmershamTM-N; nylon membrane), cut to the size of the gel, was soaked in 2x SSC and laid upon the exposed surface of the gel. Two sheets of blotting paper cut to the size of the gel were soaked in 2x SSC and laid on top of the nylon membrane. This was followed by a further eight sheets of blotting paper and a pile of tissue paper approximately 5cm in height. Finally, a glass plate was placed on top of this followed by a 1 kilogram weight. 20x SSC buffer was then poured into the large petri dish until the ends of the overhanging blotting paper were submerged. The DNA was left to transfer via capillary blot from the gel to the nylon membrane overnight. After this time the nylon filter was removed and a corner cut as a marker for orientation of the blot. The DNA was then fixed onto the filter by exposing to UV using a UV crosslinker on 'autocrosslink' setting (1800 UV Stratalinker, Stratgene). The blot was used for hybridisation with the prepared labelled DNA probe.

Solutions used:

20x SSC buffer	NaCl	175.2g
	Tri-sodium citrate	88.2g
	Adjust to pH 7.2	
	Make up to 1 litre with distilled water	

2x SSC

100ml 20x SSC

Make up to 1 litre with distilled water

2.2.20 Preparation of Labelled DNA Probe

The required probe DNAs were always cloned in plasmids. 1 µg of the plasmid DNA was cut with the appropriate restriction enzymes and then subjected to agarose gel electrophoresis. The gel was observed on a long wave UV transilluminator and the desired band excised cleanly. The DNA was then purified from the gel using the modified GeneClean method described in section 2.2.11. The DNA was labelled using the 'Ready To Go™, DNA Labelling Kit (-dCTP) from Pharmacia Biotech. A 50ng quantity of the DNA probe fragment to be labelled was added to the reaction mix according to the manufacturer's instructions. The reaction mixture was incubated at 37°C for 15-30 minutes depending on the length of the fragment to be labelled.

2.2.21 Probing Nylon Membranes

The hybridisation oven used in all probing experiments was the midi-dual from Hybaid. Approximately 1 hour before use the oven was switched on to the appropriate temperature (usually 55°C) and allowed to equilibrate. Two hybridisation glass tubes had 10ml 2x SSC added and were placed in the rotisserie of the oven to allow equilibration to the correct temperature. One tube was used in the probing procedure whilst the second acted as a balance in the rotisserie. During this time the Prehyb/Hyb buffer was heated to the appropriate temperature. The nylon membrane from the Southern blot, colony blot or plaque lifts (see sections 2.2.19, 2.2.22 and 2.4.2 respectively) was soaked with 2x SSC, placed upon a separating mesh also soaked in 2x SSC and rolled up into a tube. This was then placed inside one of the glass hybridisation tubes which was rotated to allow the nylon membrane to lay flat against the tube interior. This ensured maximum and even exposure of the membrane to the probe. The 2x SSC solution in the glass tube was discarded and 15ml of the

temperature equilibrated Prehyb/Hyb buffer added. The glass tube was placed back in the oven and left to prehybridise for 1 hour with the rotisserie speed set at 7. After this prehybridisation period the Prehyb/Hyb buffer was discarded and replaced with a fresh 15ml aliquot of the same temperature equilibrated solution. A 15 μ l aliquot of labelled DNA probe, as described in section 2.2.20, was added to this fresh Prehyb/Hyb solution. The glass tube containing the nylon membrane and the probe was then placed back in the oven and left to hybridise overnight with the same rotisserie speed setting.

After an overnight hybridisation a lot of the probe was non-specifically bound to the membrane which affected the validity of the result obtained if not removed. To remove the unwanted probe from the membrane repeated washes were done at the same temperature as the probing had been carried out with solutions containing decreasing salt concentrations. The hybridisation solution was removed from the glass tube and safely discarded. Temperature equilibrated 6x SSC/0.1% SDS solution (50ml) was added and the tube placed in the hybridisation oven for 10 minutes with the rotisserie speed setting at 7. After 10 minutes the solution was replaced with fresh 6x SSC/0.1% SDS and the incubation repeated. This duplicated wash procedure was repeated with the same volumes of 2x SSC/0.1% SDS solution and 0.1xSSC/0.1% SDS solution. After the final wash the nylon membrane was removed from the glass tube and sealed inside a plastic bag. The cps over the surface of the membrane was determined with a Geiger counter to enable the length of time the membrane needed to develop properly to be calculated. The membrane was then placed in an autoradiography cassette and allowed to develop at -80°C according to the following exposure times:

500cps	2 hours
50cps	10 hours
25cps	20 hours
12.5cps	30 hours

Solutions used:

20x SSC buffer	NaCl	175.2g
	Tri-sodium citrate	88.2g
	Adjust to pH 7.2	
	Make up to 1 litre with distilled water	
2x SSC buffer	100ml 20x SSC	
	Make up to 1 litre with distilled water	
6x SSC/0.1% SDS	300ml 20x SSC	
	10ml 10% SDS	
	Make up to 1 litre with distilled water	
2x SSC/0.1% SDS	100ml 20x SSC	
	10ml 10% SDS	
	Make up to 1 litre with distilled water	
0.1x SSC/0.1% SDS	2.5ml 20x SSC	
	10ml 10% SDS	
	Make up to 1 litre with distilled water	
Prehyb/Hyb buffer	1ml 0.5M EDTA	
	250ml 1M Na ₂ HPO ₄ (pH 7.2)	
	35g solid SDS	
	Make up to 500ml with distilled water and heat to 65°C to dissolve the SDS.	

2.2.22 Colony Blotting Plasmid Mini-Libraries

This method was employed when large numbers of transformant colonies were produced upon transformation that needed further screening. This often occurred when cloning to produce plasmid mini-libraries. Genomic DNA was appropriately digested, agarose gel electrophoresed, Southern blotted and probed to determine which fragments were hybridising to the probe. As genomic DNA runs as a smear through agarose gels it is difficult to pin-point which exact fragment of DNA is hybridising. To ensure that the right fragment was cloned into the appropriate vector a region of DNA spanning the fragment size giving the hybridisation signal was excised from the gel under UV transillumination and extracted from the agarose. The resulting DNA solution contained a number of different sized fragments including the fragment of interest. This 'mixed' DNA solution was used in ligation and transformation reactions as outlined in sections 2.2.12 and 2.2.13. Of the resulting transformants it was impossible to know which contained the correct fragment of genomic DNA without another selection procedure.

The transformant colonies were patched onto duplicate numbered grid plates and incubated overnight at the appropriate temperature with antibiotic selection. A sheet of positively charged Hybond-N (AmershamTM-N; nylon membrane), cut to the same size as the mini-library agar plates, was placed on top of one of the plates and left for 1 minute to allow the membrane to soak through. The plate and the membrane were asymmetrically marked to allow correct alignment of any positive colonies. The membrane was removed from the plate and placed onto a pad of blotting paper soaked in 0.5M NaOH/1.5M NaCl solution for five minutes to denature the DNA. The membrane was placed onto a second pad of blotting paper soaked in 1M Tris HCl (pH 8.0)/1.5M NaCl solution for five minutes. This second five minute treatment was repeated on a fresh pad of appropriately soaked blotting paper. The membrane was then placed in a tray containing 50ml 2x SSC solution with the bacterial surface uppermost for 5 minutes. Any remaining bacterial residue was removed by squirting chloroform over the membrane surface. This was necessary to ensure a sharp signal was obtained upon probing. DNA was then fixed onto the membrane as mentioned in

section 2.2.19. and probed as described in section 2.2.21. Any resulting positives were identified by aligning the signal on the autoradiograph to the colonies on the plates.

Solutions used:

20x SSC buffer	NaCl	175.2g
	Tri-sodium citrate	88.2g
	Adjust to pH 7.2	
	Make up to 1 litre with distilled water	

2x SSC	100ml 20x SSC
	Make up to 1 litre with distilled water

2.2.23 Stripping Probes from Nylon Membranes

Once the Southern blot, colony blot or plaque lift had been probed, it was sometimes necessary to analyse the blot with a second, different probe. In these cases the initial labelled probe was removed. A solution of 0.1% (w/v) SDS was boiled and poured over the membrane. This was allowed to cool to room temperature keeping the membrane completely submerged. The signal from the blot was then negligible and the membrane ready to be hybridised with the next labelled probe.

2.2.24 The Polymerase Chain Reaction (PCR)

PCR was used to produce probe fragments, confirm clonings and to create engineered molecules for cloning. Primers were usually between 17-24 bases in length and were obtained from the OSWEL DNA service or Perkin-Elmer. All PCR primers were designed adhering to the following requirements:

- not GC rich (problems with high annealing temperatures)
- must not form primer dimers (no possibility of more than three consecutive bases on primers complementing and pairing with each other)

- annealing temperatures of primers must be as close to each other as possible
- must not fold into hairpin loops with a fold energy less than 0, and have a free 3' tail.

The Wisconsin GCG 9 package FOLDRNA and PRIME programmes were used when designing primers.

For PCR reactions to confirm clonings *Taq* DNA polymerase (NEB) was used. For reactions where the PCR product would be cloned Vent_R® DNA polymerase (NEB) was used because this enzyme has a 3' → 5' proof-reading activity. A typical reaction mixture is represented below:

<i>Taq</i> (or Vent _R ®) DNA polymerase	0.5µl (1 Unit)
10x <i>Taq</i> (or Vent _R ®) buffer	5µl
Primer 1	1µl (30ng µl ⁻¹)
Primer 2	1µl (30ng µl ⁻¹)
dNTP's	1µl (12.5mM mixed stock)
MgCl ₂	2µl (25mM stock)
Template	1-10ng plasmid DNA 100ng chromosomal DNA
Distilled water to 50µl	

The melting temperature used was always 94°C for 1 minute. Annealing temperature varied depending on which primers were being used. The annealing temperature (T_m) was judged by the following formula

$$2(nA+nT) + 4(nG+nC) = T_m$$

where nA, nT, nG and nC are the number of adenine, thymine, guanine and cytosine residues in the primer.

The extension temperature used was always 72°C. As a general rule, 1 minute per kb of extension was allowed.

2.3 Protein Techniques

2.3.1 Production of Whole Cell Lysates

A single colony was used to inoculate 5ml of suitable growth media (with appropriate antibiotics) which was incubated at a permissive temperature with shaking overnight. A 0.5ml aliquot of this overnight was used to inoculate 100ml of appropriately supplemented media and the culture incubated overnight with shaking. The media of choice was dependent on the strain of bacteria to be grown - see section 2.1.2 for details. If *N. subflava* B19 was to be grown anaerobically then the culture was incubated as described in section 2.1.9. The resulting 100ml culture was split into two 50ml volumes and placed into two sterile pre-chilled 250ml centrifuge pots. The cells were centrifuged in a Sorvall GSA rotor at 10,000 rpm for 10 minutes at 4°C. The supernatant was discarded. One of the pellets was resuspended in 5ml 10mM Tris-HCl (pH 8) whilst the second was resuspended in 4.5ml 10mM Tris-HCl (pH 8) and 0.5ml 10% (v/v) Triton X-100 was added. The cell suspensions were placed on ice. The reason for the different treatment of the cell pellets was to observe the effects that the detergent Triton X-100 had upon the protein profiles of the cells when activity stained as described in section 2.3.6. The cell suspensions were placed into 20ml polypropylene tubes and subjected to sonication. The sonicator used in all manipulations was the Ultrasonic Liquid Processor from Heat Systems Incorporated. Each of the cell suspensions were sonicated for four bursts of 30 seconds at power 8 with 30 second gaps between, cooled by an ice bath. *N. subflava* strains B19 and 163 were more difficult to disrupt and were sonicated for ten bursts of 30 seconds at power 8 with 30 second gaps between, cooled by an ice bath. The cell lysates were stored in 50µl aliquots in 10% sterile glycerol at -20°C. Samples prepared in this way were viable for up to 18 months providing they were only thawed once.

2.3.2 Preparation of Non-Denaturing Polyacrylamide Gels

Techniques under denaturing conditions such as SDS-PAGE are useful for characterising proteins in terms of their physiochemical properties such as size, charge and hydrophobicity. However these procedures generally result in the loss of biological and biochemical activity of the proteins being separated. It is often useful to characterise proteins in terms of their activity and it is then beneficial to use native or non-denaturing electrophoresis.

The Bio-Rad Mini-Protean II Dual Slab Cell was used to run mini-gels (7cm x 8cm) for non-denaturing PAGE. Gel containing 10% (w/v) acrylamide were generally used as these gave good resolution for protein bands between 16 - 68 kDa. Reagents and gel preparation were based on the Laemmli buffer system (Laemmli, 1970). The gel plates were laid together separated by 0.75mm spacers, placed in the gel pouring stand and clamped together according to the manufacturer's instructions. The resolving gel was poured first. All the ingredients were mixed together in a 10ml glass beaker, the TEMED and 10% (w/v) ammonium persulphate were added last. The 10% ammonium persulphate solution was always freshly prepared. The solution was quickly mixed and then poured between the gel plates using a Pasteur pipette. The resolving mix was poured into the gap until ~2cm from the top of the smaller plate. This was then layered with dH₂O and allowed to polymerise at room temperature for 45 minutes to 1 hour. The dH₂O was poured off and the gel-air interface was thoroughly rinsed. Excess water was removed from the gel space using a strip of blotting paper. The comb was inserted into position at the top of the glass plates and the 4% stacking gel poured into the remaining gel space. The gel apparatus was then left at room temperature for 15 minutes for the stacking gel to polymerise. The comb was removed and the wells washed thoroughly with dH₂O to remove any unpolymerised acrylamide. The gel was then ready for running protein samples.

Solutions used:*Resolving gel (10% (w/v))*

Distilled water	4.1ml
1.5M Tris-HCl pH 8.8	2.5ml
Protogel 30% (w/v) acrylamide/bisacrylamide stock	3.33ml
10% (w/v) ammonium persulphate	50 μ l
TEMED	5 μ l

Total volume of 10ml, sufficient for pouring 2 mini resolving gels.

Stacking gel (4% (w/v))

Distilled water	3.1ml
0.5M Tris-HCl pH 6.8	1.25ml
Protogel 30% (w/v) acrylamide/bisacrylamide stock	0.65ml
10% (w/v) ammonium persulphate	31.25 μ l
TEMED	6.25 μ l

Total volume of 5ml, sufficient for pouring 2 mini stacking gels.

On occasion it was necessary to run denaturing gels containing SDS or Triton X-100. In these instances 100 μ l of the dH₂O in the resolving gel solution was replaced with 100 μ l of 10% (w/v) SDS stock or 100 μ l of 10% (v/v) Triton X-100. In the stacking gel 50 μ l of dH₂O was replaced with 50 μ l 10% (w/v) SDS stock or 50 μ l 10% (v/v) Triton X-100.

2.3.3 Running Non-Denaturing Polyacrylamide Gels

Once set the clamp assemblies containing the gel sandwiches were removed from the casting stand. The clamp assemblies were fitted together to form an upper buffer chamber and placed into the gel tank, according to the manufacturer's instructions. Running buffer (1x) was poured into the upper buffer chamber until the loading wells were submerged. Bubbles were removed from the wells using a

Pasteur pipette and from within the upper buffer chamber with a 10ml pipette. The remaining 1x running buffer was poured into the bottom of the tank to cover the electrode. The gel was now ready for loading. The samples were first thawed, if frozen, and diluted 1:1 with sample buffer. SDS samples were also boiled for 5 minutes before loading on the gel. 30 μ l of each sample and 10 μ l of the appropriate marker proteins were loaded into separate wells. The lid of the tank was attached and the gel run at 100V either overnight at 4°C or until the marker dye in the sample buffer reached the bottom of the well. After electrophoresis the upper buffer chamber was removed from the tank and the 1x running buffer discarded. The clamp assemblies were taken apart and the glass plates with the gels sandwiched between removed. The glass plates were eased apart by twisting the spacers and the gels placed in the appropriate staining solution.

Solutions used:

Native/SDS/Triton X-100 sample buffer

Distilled water	4.0ml
0.5M Tris-HCl pH 6.8	1.0ml
Glycerol	0.8ml
10% (w/v) SDS or 10% (v/v) Triton X-100 or just distilled water	1.6ml
0.05% (w/v) bromophenol blue	0.2ml

When running SDS gels 0.4ml of 2- β -mercaptoethanol was also added.

5x Running buffer pH 8.3

Tris base	9g
Glycine	43.2g
SDS or Triton X-100 (omitted if running a native gel)	3g or 3ml

Made up to 600ml with dH₂O and store at 4°C (sufficient for eight runs).

2.3.4 Silver Staining Polyacrylamide Gels

Many different silver stain protocols are available. This method was taken from Tan (1998). The gels were silver stained in a small plastic tub by the addition of the following stain solutions:

<i>Solution</i>	<i>Volume (ml)</i>	<i>Incubation time</i>
Fixative A	200	30 minutes/overnight
Fixative B	200	15 minutes
Fixative B	200	15 minutes
Oxidiser	100	5 minutes
Distilled water	200	5 minutes
Distilled water	200	5 minutes
Distilled water	200	5 minutes
Silver reagent	100	20 minutes
Distilled water	200	5 minutes
Developer	100	30 seconds
Developer	100	30 seconds
Developer	100	until developed
Stop	200	for storage

After each incubation period the stain solution was discarded before the addition of the next.

It is easy when silver staining to obtain a high degree of background on the gel which can interfere with the visualisation of stained protein bands. It is crucial that the final incubation with developer is watched carefully so that the stop solution is added to prevent the development of the gel proceeding too far. The speed with which protein bands are identified at this stage is dependent on the amount of protein loaded on the gel and the degree of separation upon electrophoresis, consequently the time needed to develop the gels may vary.

Solutions used:

Fixative A -	40% (v/v) methanol, 10% (v/v) acetic acid in distilled water.
Fixative B -	10% (v/v) ethanol, 5% acetic acid in distilled water.
Oxidiser -	potassium dichromate, 0.1g in 100ml distilled water containing 0.02ml concentrated nitric acid.
Silver reagent -	silver nitrate, 0.2g in 100ml distilled water.
Developer -	sodium carbonate, 9g in 300ml distilled water containing 0.15ml formaldehyde.
Stop -	0.5% (v/v) acetic acid in distilled water.

All of the solutions were freshly prepared using 'Analar' quality chemicals.

2.2.5 Coomassie Brilliant Blue Staining Polyacrylamide Gels

Polyacrylamide gels were placed in 50ml of Coomassie stain in a small plastic tub and incubated with gentle shaking at room temperature for 30 minutes. The stain was poured off and retained and 100ml destaining solution added. Foam bungs were placed in the tub to absorb the Coomassie stain that leached from the gel. The destaining gel was incubated at room temperature with gentle shaking until the marker bands were clearly visible and the background of the gel destained thoroughly - usually 1-3 hours.

Solutions used:

Coomassie stain -	0.1% (w/v) Coomassie brilliant blue R-250
	40% (v/v) methanol
	10% (v/v) acetic acid

Once prepared solutions were filtered through a Whatman No. 1 filter to

remove any solid particles. The solution could be used to stain gels on a number of occasions.

Destain solution - 40% (v/v) methanol
 10% (v/v) acetic acid

2.3.6 Detection of Nitrite Reductase Activity in Non-Denaturing Polyacrylamide Gels

Sites of nitrite reducing activity were located by the method of Zumft *et al.*, 1987. Gels were placed in a small plastic tub containing 50ml methyl viologen buffer and incubated for 5 minutes at 4°C. The gels were removed from this buffer and quickly placed into 50ml sodium nitrite buffer. This was incubated at 4°C until bleaching of the gels was observed. The areas of white patching on the dark blue background corresponded to nitrite reductase activity. After the appearance of the white bands the gels were negatively stained by the addition of 10ml triphenyl tetrazolium chloride (TTC) solution to the nitrite buffer with gentle shaking to ensure good mixing. The gels were incubated at 4°C in the dark until the gel background became red. This took about 10-15 minutes. The stain solution was poured from the plastic tub and 100ml distilled water was poured over the gels to wash them. The water was removed and the gels fixed in 100ml 50% (v/v) ethanol overnight. The gels were now ready to be photographed.

It must be stressed that nitrite reductase enzymes are particularly oxygen sensitive and prolonged exposure to air will result in the loss of enzymic activity on the gels. Although anaerobic hoods are not required for the activity stain protocol all changes of solution must be quick and the gels kept submerged in the presence of the reducing agent sodium dithionite to prevent loss of activity. Similarly, as whole cell lysates were used in the activity stains the running of the gels and the staining procedure must be carried out at 4°C to prevent protein degradation by cellular proteases.

Solutions used:

Methyl viologen buffer -	10mM methyl viologen 50mM HEPES pH 7.3 Sodium dithionite 2mg ml ⁻¹
Sodium nitrite buffer -	1M sodium nitrite 50mM HEPES pH 7.3
TTC solution -	2.5% (w/v) triphenyl tetrazolium chloride in distilled water

To observe inhibition of copper containing nitrite reductases 10mM diethyldithiocarbamate (DDC) was added to the nitrite buffer.

2.3.7 Whole Cell Nitrite Reductase Assay

The procedure for obtaining the anaerobic conditions needed for the assay was as follows. The phosphate buffer was autoclaved (15 psi for 10 minutes) and then whilst still hot was sparged with oxygen-free nitrogen (White spot nitrogen/BOC). Sparging continued until the buffer reached room temperature at which point it was assumed to be oxygen free and ready for use.

Cells were harvested and resuspended in the anaerobic buffer to achieve a protein concentration of between 4.6 and 9.2mg ml⁻¹ (see section 2.3.11 for protein determination). This suspension was then kept on ice for no more than 1 hour before use.

The nitrite reductase assay mix consisted of 0.5ml cell suspension and 0.1ml 60mM sodium nitrite made up to 5ml with anaerobic 50mM phosphate buffer pH7.5. The electron donors for the assay was 1M glucose; 0.2ml aliquots were added to the reaction mix. Endogenous nitrite reductase activity was measured by omitting the electron donor. The initial reaction mix, consisting of the buffer and the electron

donor, was incubated in a narrow glass tube (1cm diameter by 10cm long) at 37°C in a waterbath for 2 minutes to allow temperature equilibration. The cell suspension was gently added and the mixture left for a further 1-2 minutes. Finally sodium nitrite was added to start the reaction and mixed by gentle inversion. At time intervals, 50µl of the above mix was pipetted into 3.7ml of nitrite solution I to prevent further nitrite reduction. To develop the colour, 300µl of nitrite solution II was added and incubated at room temperature for 30 minutes. The absorbance was read in a spectrophotometer at 540nm. Results can be expressed as nmole nitrite reduced/min/mg protein although on occasion this assay was used qualitatively, simply to detect the presence of an activity rate for nitrite reduction in wild type cells and the absence of such a rate in mutant 163.

A standard curve for nitrite determination was achieved by adding 50µl samples of 12, 25, 37, and 50µM solutions of nitrite to nitrite reagent I and treating as above.

Solutions used:

Sodium nitrite -	60mM
Glucose -	1M
Sodium phosphate buffer, pH7.5 -	50mM (80ml sodium dihydrogen orthophosphate 0.2M, 420ml disodium hydrogen orthophosphate 0.2M, made up to 1 litre with distilled water)
Nitrite reagent I -	Sulphanilic acid (20g sulphanilamide dissolved in 160ml 12M hydrochloric acid, made up to 1 litre with distilled water)
Nitrite reagent II -	0.25g N-1 naphthyl ethylenediamine dihydrochloride in 250ml of distilled water

2.3.8 Nitrite Reductase Assay with Methyl Viologen

This assay measures the activity of the terminal enzyme nitrite reductase independently of other components of the electron transfer chain. Methyl viologen acts as an artificial electron donor that is purple when reduced and colourless when oxidised. The principle of the assay is that a limited amount of dithionite is added to a methyl viologen buffer, made anaerobic by boiling and sparging with nitrogen. The nitrite-dependent oxidation of this reduced methyl viologen can then be measured quantitatively using a spectrophotometer. The rate should be linear and dependent on the volume of cell extract added. For this assay cells have to be broken open and a crude extract used. Neisserial cells are difficult to disrupt using sonication (pers. obs.). For this experiment it was better to use a French press (section 2.3.8.1).

The reaction mixture contained enzyme source (10-100 μ l lysed *N. subflava* cells) and methyl viologen buffer to a total volume of 4ml, and was assayed in a Hellma 21N stoppered cuvette. The enzyme source and anaerobic methyl viologen buffer were used to fill the cuvette and a few anti-bumping granules were added. The teflon stopper (drilled to take a 10-100 μ l syringe needle) was carefully inserted to exclude all air and sodium dithionite (a fresh solution of 25mM in 10mM NaOH) added by syringe to give an A_{600} reading of 1.0 after mixing by inversion. The endogenous enzyme activity was measured for 2 minutes before the reaction started by the addition of 100 μ l of nitrite buffer. The enzyme activity was determined from the rate of decolourisation at 600nm assuming an extinction coefficient of 13 μ mol $\text{cm}^{-1} \text{ml}^{-1}$ for methyl viologen.

Solutions used:

Nitrite buffer	1M sodium nitrite
Methyl viologen buffer	100mM Tris pH 7.8
	100mM K_2HPO_4
	7.5mM KHCO_3

0.3mM methyl viologen

2.3.8.1 Instructions for using the French press

Cell disruption was achieved by high pressure forcing the *N. subflava* cells through a small orifice at high speed in a precise, controlled and reproducible cycle. The machine used in these applications was the 'Z-plus' 1.1KW benchtop cell disrupter from Constant Systems Ltd.

A 200ml overnight culture of aerobically grown *N. subflava* B19 was centrifuged at 4,000 rpm for 10 minutes at 4°C in a Sorvall GSA rotor. The resulting cell pellet was resuspended in 20ml of 50mM Tris (pH 8.0). The 20ml concentrated cell suspension was passed through the 'Z-plus' cell disrupter at a pressure of 40,000 psi, according to the manufacturer's instructions. The resulting lysate was stored on ice and subsequently used in methyl viologen nitrite reductase assays or in the preparation of *N. subflava* membranes.

2.3.9 Preparation of *N. subflava* Membrane

A 200ml culture of aerobically grown *N. subflava* B19 was centrifuged for 10 minutes at 4,000 rpm in a Sorvall GSA rotor at 4°C. The supernatant was discarded and the pellet was resuspended in 20ml of 50mM Tris buffer (pH 8.0). The concentrated cell solution was passed through the French press as described above and a 10ml aliquot was centrifuged for a second time at 10,000rpm for 10 minutes in a Sorvall SS-34 rotor at 4°C. The supernatant was transferred to a Beckman T865-1 screw capped tube and filled completely with 50mM Tris (pH 8.0). The tube was sealed ensuring there were no air bubbles trapped within. This procedure was done in duplicate to ensure the tubes would balance in the centrifuge rotor. The two T865-1 screw capped tubes, seals and screws were balanced to within 0.01g.

The tubes were placed in a Beckman T-865-1 rotor and centrifuged at 4°C for 1.5 hours at 39,000 rpm. The tubes were removed from the centrifuge and the supernatant stored at 4°C. This corresponded to the cytoplasmic cell fraction and

was used in methyl viologen nitrite reductase assays (section 2.3.8). The membrane pellet was resuspended in 1ml 50mM Tris (pH 8.0). The resulting gelatinous membrane fraction was also used in methyl viologen nitrite reductase assays (section 2.3.8).

2.3.10 Sarkosyl Extraction of *N. subflava* Outer Membrane

The detergent *N*-lauryl sarcosinate (sarkosyl) solubilises most cytoplasmic membrane proteins at a concentration of $\geq 0.5\%$ (w/v). Consequently this detergent is a useful tool in the extraction of intact outer membranes from Gram negative organisms (Gould, 1994).

A crude membrane fraction of *N. subflava* B19 was obtained as described in section 2.3.9. A 0.5ml aliquot of the membrane prep was added to 0.5ml 1% (w/v) sarkosyl and incubated at room temperature for 30 minutes. The resulting solution was transferred to a 1.4ml Beckman tube (11 × 34mm). A second tube was also prepared and the two tubes were balanced to within 0.01g. The tubes were placed in the Beckman TL-100.2 rotor and centrifuged at 50,000 rpm for 1 hour at 4°C in the Beckman TL-100 centrifuge. The supernatant was decanted and stored on ice. This corresponded to the inner membrane fraction and was used in subsequent methyl viologen nitrite reductase assays (section 2.3.8). The resulting outer membrane pellet was resuspended in 0.5ml 50mM Tris (pH 8.0) and was also used in methyl viologen nitrite reductase assays (section 2.3.8).

2.3.11 Protein Determination

Protein determination was done using a modified Lowry method (Peterson, 1977). Samples to be assayed were diluted in distilled water to give a protein concentration of approximately 50-200 $\mu\text{g ml}^{-1}$ in a final concentration of 200 μl . Samples were mixed with 50 μl of 0.15% (w/v) Deoxycholate and incubated at room temperature for 10 minutes. A 50 μl aliquot of 72% (w/v) trichloroacetic acid was added before the samples were mixed and centrifuged for 15 minutes at 14,000 rpm

in an MSE microcentrifuge. The supernatant was removed and the pellet resuspended in 200 μ l of distilled water. Samples containing 0, 50, 100, 150 and 200 μ g ml⁻¹ of BSA in a final volume of 200 μ l, were also prepared to establish a standard curve. Next, 600 μ l of a freshly prepared solution containing 2% (w/v) Na₂CO₃, 1% (w/v) SDS, 0.16% (w/v) sodium tartrate, 0.4% (w/v) NaOH and 0.04% (w/v) CuSO₄ was added to each sample and mixed thoroughly. Samples were incubated at room temperature for 10 minutes. A 100 μ l aliquot of Folin and Ciocalteu's reagent (1:1 dilution with distilled water) was then added, and the samples incubated at room temperature for a further 45 minutes. The A₆₆₀ of the samples were measured and the protein concentrations determined from the BSA standard curve plot of A₆₆₀ vs μ g ml⁻¹ protein. All samples were done in duplicate and an average taken.

2.4 Bacteriophage λ Techniques

2.4.1 Construction of *N. subflava* B19 and 163 λ Libraries

The bacteriophage vector chosen for the construction of both the mutant (163) and wild type (B19) *N. subflava* λ libraries was EMBL 3 from the EMBL series of replacement vectors. The EMBL vectors are useful for cloning large (up to 20kb) fragments of genomic DNA as the central stuffer fragment of the wild type vector contains non-essential phage genes and can be replaced with the fragment of interest without loss of phage viability. Viability of bacteriophages can decrease greatly when the lengths of their genomes are greater than 105% or less than 78% of that of a wild type bacteriophage so, when digesting genomic DNA for insertion into these replacement vectors, care was taken to ensure suitably sized fragments were produced for cloning, (approx 10-15kb). The EMBL vectors are particularly useful for cloning *Sau3AI* partial digests, as the *Bam*HI sites in the vector polylinker are flanked by *Eco*RI and *Sal*I sites. In theory cloned fragments can therefore be excised from the recombinants by digestion with *Eco*RI or *Sal*I.

So, taking these points into consideration, *Sau3AI* digested Neisserial genomic DNA was cloned into the *Bam*HI site of EMBL 3.

2.4.1.1 Partial digestion of genomic DNA

Genomic DNA, 1mg in 200 μ l total volume, was added to 160 μ l dH₂O in a sterile eppendorf tube. A 10 μ l aliquot of this undigested DNA was removed to a separate eppendorf labelled 'C'. This acted as a control to which the degree of subsequent digestion was compared. To the original tube 40 μ l of 10x restriction buffer and 4 μ l (0.5U μ l⁻¹) of *Sau3AI* was added on ice. Aliquots, 8 x 45 μ l, were removed from the eppendorf and placed into 8 fresh tubes labelled thus: 2, 4, 8, 12, 15, 20, 30, 50. These numbers corresponded to the incubation time (minutes) that the *Sau3AI* digests were allowed to proceed at 37°C. Immediately after the appropriate incubation period the digests were placed in a 70°C waterbath to inactivate the

enzyme for 5 minutes before being placed on ice. When all of the digests were complete 10 μ l was removed from each of the tubes and electrophoresed on a 0.8% agarose gel for 5 hours at 50V. (See section 2.2.10 for details.) The gel was viewed on a UV transilluminator and the digest that gave maximal production of bands in the 10-15kb region was ethanol precipitated as described in section 2.2.6.

2.4.1.2 Ligation of EMBL 3 vector and insert DNA

The EMBL 3 vector arms were supplied pre-cut by Promega. This eliminated the need to digest the arms from wild type bacteriophage which can be tricky. Ligations were set up using ratios of 1:1 and 1:0.5 vector to insert DNA. To obtain a good library it is usual to have 500ng of vector DNA μ l⁻¹ and this is the concentration that the pre-cut arms were supplied at. The volume of insert DNA was adjusted accordingly to give the same concentration as the vector. A typical ligation reaction mixture is represented below:

Pre-cut arms	500ng (1 μ l)
Insert	500ng (or 250ng depending on ratio)
10x ligation buffer	1 μ l
T4 DNA ligase	0.2 Units
Distilled water to make a final volume of 10 μ l.	

The ligations were incubated overnight at 16°C.

2.4.1.3 *In-vitro* packaging of the ligated DNA

The ligation mixtures had 10 μ l of extract A and 16 μ l of extract B added to them. (Extracts A and B contain the EMBL 3 phage heads and tails and were supplied as part of the Packagene® Lambda DNA Packaging System from Promega.) The solutions were mixed together in eppendorfs by flicking the tubes and centrifuged briefly in an MSE microcentrifuge. They were left at room temperature

for 2 hours to allow the ligated DNA to become packaged into the phage particles. A 500µl aliquot of phage buffer (see section 2.1.3) and 1 drop of chloroform were added to the packaged phage and mixed gently. The tube now contained the EMBL 3 λ library.

2.4.1.4 Estimating the titre of the λ library

The plating cells used to titre phage were *E. coli* NM767. These cells are P2 lysogens and cannot be infected by λ phage carrying the *red* and *gam* genes. These genes are found on the stuffer fragment of EMBL 3 and are therefore replaced by insert DNA upon library construction. NM767 are only infected by recombinant phage and therefore prevent the recovery of parentals (Frischauf *et al.*, 1983).

Aliquots, 2 x 100µl, of a fresh overnight of the plating cells had 2.5ml of BBL top agar supplemented with 10mM MgSO₄ added to them and were poured over BBL bottom agar plates and allowed to set. During this time serial dilutions of the λ library were made in 100µl total volumes of phage buffer. A 10µl aliquot of the 'neat' library solution was added to 90µl of phage buffer to give a 10⁻¹ dilution. A 10µl aliquot of this was removed and added to 90µl phage buffer to give a 10⁻² dilution and so on until a 10⁻⁴ dilution was reached. Aliquots (10µl) of each of these dilutions were spotted onto the BBL plates containing the top agar and the plating cells. These were then left to dry and incubated overnight at 37°C. The titre of the λ library was determined by counting the number of plaques in the 10⁻⁴ dilution spot and, taking the dilution factor into account, calculating back to derive the total number of phage in the 'neat' library solution.

In order to have complete representation of the Neisserial genome in the λ library it was necessary to know how many plaque forming units (pfu's) were needed to fulfil this. The following equation was used to determine this value:

$$N = \ln(1-P) / \ln(1-f)$$

where

P = the specified probability that a given gene is contained within the library

(usually 0.99).

f = the size of the desired fragment as a fraction of the genome size. (λ EMBL 3 can accept inserts of up to 20kb but it is usually much smaller than this. i.e. ~ 4 kb.

N. subflava genome size (assumed to be the same as *E. coli*). i.e. $\sim 4,700$ kb.)

Substituting these figures into the equation resulted in a requirement of 5,400 pfu's to represent the entire Neisserial genome. If the titre of the newly constructed library was found to be less than this value it was not representative of the entire genome and was discarded.

2.4.2 Screening *N. subflava* B19 and 163 λ Libraries

As 5,400 pfu's are required to represent the *N. subflava* genome (see section 2.4.1) it was decided to plate out the λ library over 5 plates with $\sim 1,100$ pfu's per plate. The titre value of the λ library calculated using the method described in section 2.4.1 was used to determine the volume of the library needed to contain 1,100 pfu's. This calculated volume of λ library was added to 100 μ l of a fresh overnight culture of NM772 plating cells. (NM767 cells were used initially to select for recombinant phage whereas NM772 cells were used in all subsequent manipulations involving phage propagation. The reason for this was that NM772 cells are Rec⁺ despite having a *recD*⁻ mutation. Exonuclease V is encoded by the *recB*, *C* and *D* genes. It has two roles: one as a nuclease which degrades lytic phage undergoing rolling circle replication and a second involved in recombination between host and foreign λ DNA. Mutations in the *recD* gene inactive the nuclease whilst leaving the host bacteria recombination proficient (Kaiser *et al.*, 1993, unpublished). This effectively enhances bacterial vigour and consequently increases phage yield from cultures of NM772 Rec⁺ cells.)

The phage/NM772 cell suspension was left at room temperature for 20 minutes to allow the phage to adsorb to the bacterial cell surfaces. A 2.5ml volume of molten BBL top agar supplemented with 10mM MgSO₄ was added, the mixture poured over a fresh BBL agar plate and allowed to set. As five plates were needed to

represent the entire bacterial genome this procedure was repeated a further four times. The plates were incubated overnight at 37°C.

Five pieces of positively charged Hybond-N (Amersham™-N; nylon membrane) were cut to the same size as the agar plates. A single piece of the membrane was placed over the lawn of bacteria and plaques on one of the plates and left there for 2 minutes to soak. The membrane and the plate were asymmetrically marked so that correct alignment of any positive plaques was possible. Care was taken not to move the membrane once it was laid upon the plaques to ensure sharp signals were obtained upon hybridisation. The membrane was carefully removed from the surface of the agar using clean forceps ensuring the top layer of cells, plaques and top agar remained intact on the bottom agar. The membrane was then placed in 50ml 0.5M NaOH/1.5M NaCl for 2 minutes and then transferred to 50ml 1M Tris-HCl (pH8.0)/1.5M NaCl for 2 minutes. Finally the membrane was placed in 50ml 2x SSC for 2 minutes before being placed upon 2 sheets of blotting paper soaked in 2x SSC. This process was repeated for each of the remaining plates resulting with 5 treated membranes ready for hybridisation. The λ DNA from the plaques was fixed onto the membranes as described in section 2.2.19 and the entire library was probed as described in section 2.2.21.

Solutions used:

2x SSC

see section 2.2.19

2.4.3 Picking Bacteriophage λ Plaques

Phage buffer (0.5ml) was placed into a 1.5ml eppendorf tube and 1 drop of chloroform was added. The narrow end of a sterile Pasteur pipette was stabbed through the chosen plaque into the hard agar beneath. The Pasteur pipette was carefully removed from the plate bringing the plaque with it as a plug of agar contained in the end of the pipette. It was important to always choose a well isolated plaque as bacteriophage λ can diffuse considerable distances through the top agar.

The agar plug was placed in the phage buffer/chloroform mixture and incubated at room temperature for 2 hours to let the phage particles diffuse out of the agar. An average plaque yielded 10^5 - 10^7 phage particles which could be stored indefinitely at 4°C in the phage buffer/chloroform solution without loss of viability.

Sometimes it was difficult to identify a single plaque for picking due to a poor signal obtained after hybridisation or the presence of too many plaques on the plate. In these instances the fat end of a sterile Pasteur pipette was used to pick over a large area of agar corresponding to the positive hybridisation signal. The resulting phage buffer/chloroform solution contained a number of mixed bacteriophage that were plated out and probed a second time to identify the plaque of interest.

When screening λ libraries positive plaques were picked and reprobated a number of times until all of the plaques present on the plate were positive to the probe. This ensured that the resulting bacteriophage solution contained a single purified phage ready for further analysis.

2.4.4 Preparation of Plate Lysates from a Single Plaque

A single purified plaque containing 10^5 - 10^7 phage particles was picked and placed into 1ml phage buffer. This was left at room temperature for a minimum of 30 minutes during which time a fresh thick BBL plate was poured and left to set. A 100 μ l aliquot of this phage buffer solution was added to 100 μ l of a fresh overnight culture of NM772 plating cells which was left to adsorb at room temperature for 20 minutes. This gave 10^4 - 10^6 phage plate⁻¹ which was adequate for confluent lysis. Molten BBL top agar (2.5ml) supplemented with 10mM MgSO₄ was added. This was poured over the freshly set BBL plate and also allowed to solidify. A control plate was set up in exactly the same way but with the omission of the phage particles. The plates were incubated for 8 hours at 37°C. Confluent lysis could be judged by comparing the plate containing the phage to the control plate. On the control plate a thick lawn of bacteria could be seen whilst on the phage plate the bacterial growth was weak and the top agar clear due to bacterial cell lysis by the phage. When lysis

was confluent 2ml of L-broth was added to the phage plate. The layer of top agar, cells and phage were scraped off into a Universal. A 20 μ l aliquot of chloroform was added and the Universal shaken on an orbital shaker at 150 rpm for 10 minutes at 37°C. The Universal was then centrifuged at 14,000 rpm for 15 minutes in a MSE Centaur 2 benchtop centrifuge at room temperature. No brake was employed to halt the centrifuge as this disrupted the agar pellet. A sterile Pasteur pipette was used to remove the supernatant to a fresh sterile bottle which had 2-3 drops of chloroform added. The phage lysate was stored at 4°C. The titre of the lysate was calculated as described in section 2.4.1 but the serial dilutions were modified to accommodate the greatly increased titre values of between 10⁹-10¹¹ pfu ml⁻¹ expected from plate lysates. The titred lysates were then used to prepare bacteriophage λ DNA as described in section 2.2.5.

Chapter Three
Analysis of *N. subflava* Mutant 163

3.1 Background Information

The purpose of this section is to inform the reader of the background surrounding this project in more detail than is presented in Chapter One.

3.1.1 Production of *N. subflava* Tn5 mutants

A Tn5 library was produced in wild type *N. subflava* B19 which provided several mutants with different growth phenotypes compared to wild type strains, when grown anaerobically in the presence of nitrite (Brew, 1992). Plasmid pSUP2021 (Simon *et al.*, 1983) was used as the genetic tool to insert Tn5 into the Neisserial chromosome. pSUP2021 possesses the Tn5 transposon, containing a kanamycin resistance gene, and the mobilisation genes to transfer the plasmid DNA from host to recipient strains. Once in the recipient *N. subflava* strain the plasmid could no longer replicate and this caused the transposon to integrate into the host chromosome, causing a mutation. A number of mutants were isolated which presented a reduced growth phenotype compared to wild type; however only one mutant (163) was isolated which displayed complete inability to grow under these test conditions (Brew, 1992). When assayed the nitrosation activity of this mutant was also found to be zero (Brew, 1992). This reinforced the hypothesis presented in section 1.9.5.2 that the reduction of nitrite is necessary for nitrosation to occur.

The mutation in strain 163 suggested that its inability to grow anaerobically in the presence of nitrite was due to Tn5 insertion in the structural nitrite reductase gene or a related regulatory gene. This theory was based on the assumption that Tn5 had only inserted once into the *N. subflava* genome and that *N. subflava* only contained one nitrite reductase. If *N. subflava* contained more than one nitrite reductase gene then expression of each of the genes would need to be interrupted to abolish anaerobic growth with nitrite. This would require either multiple insertions of Tn5 into the chromosome or insertion of Tn5 into a regulatory component governing all nitrite reductase genes. Cointegration of two Tn5 transposons from dimeric donors into

chromosomal DNA is rare but does occur (Berg, 1989). However in these instances the Tn5 molecules integrate directly adjacent to each other and would therefore interrupt the same gene. A single Tn5 insertion into a single structural nitrite reductase or regulatory gene seems the most likely supposition.

3.1.2 Preliminary subcloning from *N. subflava* mutant 163

Subcloning from the mutant 163 chromosome was necessary to allow the DNA flanking the Tn5 insertion to be sequenced. A mini-genomic DNA library from mutant 163 was constructed using the restriction enzyme *Cla*I (Sowerby, 1997). *Cla*I was chosen as this enzyme does not cut within Tn5 and the resulting clone would contain the entire transposon and flanking chromosomal DNA. After appropriate screening the resulting plasmid was found to have a 12.5kb *Cla*I insert, cloned into the *Hinc*II site of pUC19. A 5.8kb length of the insert was estimated to be derived from transposon Tn5 conferring Kan^R. The recombinant plasmid was termed pZS163 (Figure 3.1).

A similar approach was used to subclone from a second Tn5 mutant (Sowerby, 1997). Mutant 55 was found to have a reduced nitrite reductase activity when compared to the wild type (Brew, 1992). Although this mutant strain and plasmid are not analysed further during the course of this study it is worth mentioning the construction of the plasmid at this point as it was used as a source of the kanamycin cassette for probing a mutant 163 λ library and genomic DNA. A unique *Bam*HI site exists in Tn5 approximately half way along its length. (Appendix A1 shows the restriction map of transposon Tn5.) This site was used to construct a second plasmid mini-library in pUC19. As kanamycin was used to select for recombinant plasmids the resulting clone contained only the IS50_L end of Tn5 due to the position of *Bam*HI in the transposon. The plasmid obtained from the mini-library was found to have an insert of ~11kb with 3.1kb of this corresponding to Tn5. The recombinant plasmid was termed pZS55 and the kanamycin cassette used for probing was digested from this construct using *Bam*HI and *Hind*III to liberate a 1.86kb DNA fragment (Figure 3.2).

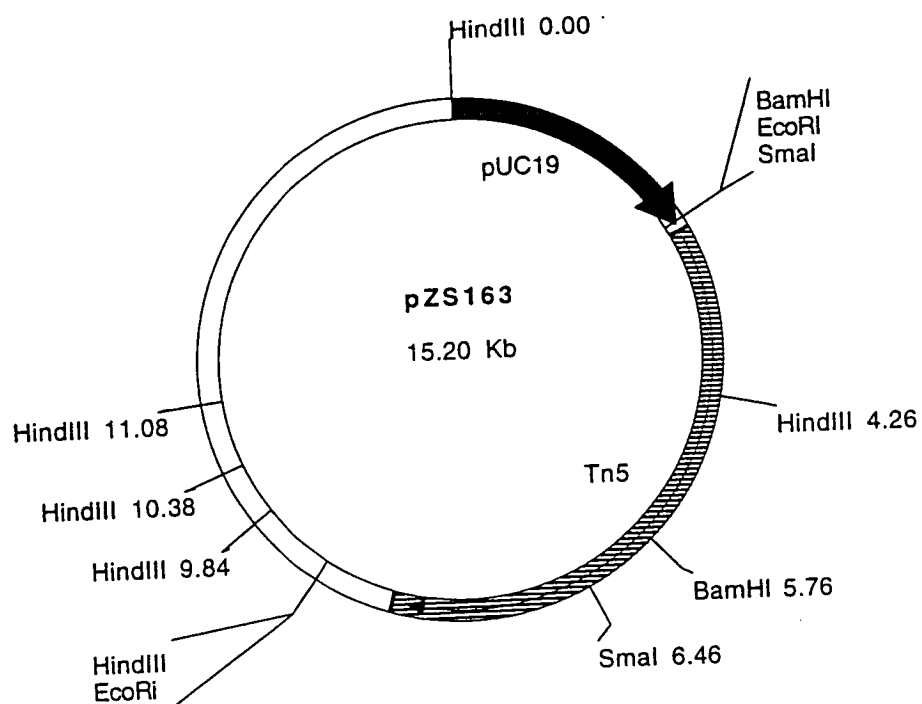


Figure 3.1. Plasmid map of pZS163 (Sowerby, 1997).

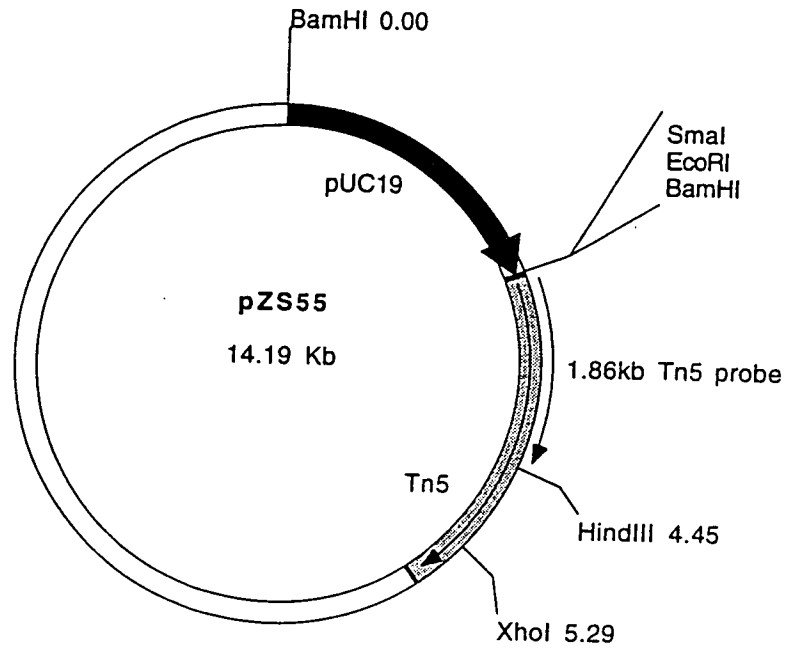


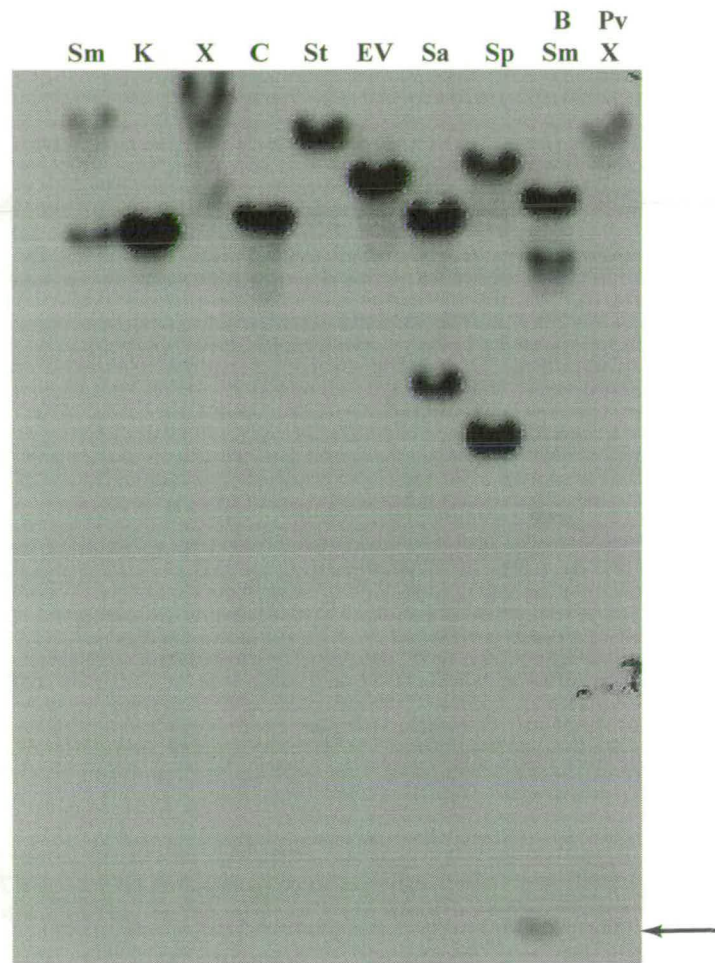
Figure 3.2. Plasmid map of pZS55 (Sowerby, 1997).

3.2 Initial Characterisation of *N. subflava* B19 and Mutant 163 Strains

The previous work described in this chapter was done before I joined the project. The Tn5 mutant strains, and plasmids pZS55 and pZS163, were available for study. All work subsequently described is a result of my efforts unless specific reference is made otherwise.

3.2.1 Confirmation of a single Tn5 insertion in *N. subflava* mutant 163

The work in section 3.1.2 describing the cloning of pZS163 assumed a single Tn5 insertion was causing the Nir⁻ phenotype in mutant 163. To support the validity of sequencing pZS163 it had to be established that there was indeed only one Tn5 insertion in this mutant. Chromosomal DNA from mutant 163 was digested with a variety of enzymes and probed with the 1.86kb *Bam*HI/*Hind*III kanamycin cassette from pZS55 (Figure 3.2). Enzymes were chosen that did not cut within the Tn5 molecule so that any hybridisation to the kanamycin cassette arose from a single Tn5 insertion. To remove the possibility that two or more Tn5 molecules were found on fragments of the same size in the genomic DNA giving rise to a single hybridisation, a number of digests were included in the experiment that cut within the kanamycin cassette. In these lanes two fragments were expected to show hybridisation if there was a single Tn5 insertion. If more fragments were detected then this would be indicative of more than one Tn5 molecule. The results of the probing experiment are shown in Figure 3.3.



Fragment size (kb) showing hybridisation to 1.86kb Kan cassette from pZS55:

Sm = 10.1, 6.4

K = 6.2

X = Poorly defined band

C = 6.6

St = 9.8

EV = 7.8

Sa = 6.6, 3.3

Sp = 8.4, 2.6

B/Sm = 7.2, 5.8, 0.4

Pv/X = 10.0

Figure 3.3. Southern hybridisation of *N. subflava* mutant 163 genomic DNA to the 1.86kb Kan cassette of pZS55. Key to restriction enzymes B = *Bam*HI, C = *Cla*I, EV = *Eco*RV, K = *Kpn*I, Pv = *Pvu*II, Sa = *Sal*I, Sm = *Sma*I, Sp = *Sph*I, St = *Stu*I, X = *Xba*I.

The restriction enzymes in Figure 3.3 that do not cut within Tn5 are *ClaI*, *KpnI*, *StuI* and *XbaI*. (See Appendix 1 for map of Tn5.) By referring to the corresponding lanes on the Southern in Figure 3.3 it can be seen that there is only one band of hybridisation per restriction enzyme. This suggests the presence of a single Tn5 insertion in mutant 163. This deduction is corroborated by the probing evidence from digests using restriction enzymes that are known to cut within the Kan cassette; *SalI*, *SmaI* and *SphI*. By cutting within the Kan cassette two different sized fragments of DNA on the Southern should hybridise to the 1.86kb probe. This is observed in Figure 3.3. A control digest was included on the gel to check that the 1.86kb probe was authentic. The *BamHI/SmaI* digest cuts a 0.5kb fragment from within the Kan cassette. For the probe to be genuine this small fragment had to be present on the resulting Southern. Figure 3.3 shows the presence of a ~0.4kb band at the bottom of the *BamHI/SmaI* lane on the Southern. Although faint, this band was assumed to be due to hybridisation to the expected 0.5kb Tn5 fragment and the 1.86kb probe was presumed to be authentic. Further checks to test probe authenticity were made by hybridising the probe to pZS55 DNA digested with *BamHI* and *HindIII*. Hybridisation to the expected 1.86kb fragment was observed (data not shown).

To summarise, the above probing experiment showed that only one Tn5 molecule had inserted into *N. subflava* B19 genomic DNA upon transposition. Therefore, when sequenced, it is believed that pZS163 should contain DNA flanking the Tn5 insertion, providing information on the gene that was disrupted resulting in mutant 163.

3.2.2 Probing chromosomal DNA with copper and cd_1 probes

Inhibition studies with DDC on the nitrite reductase enzyme of *N. subflava* B19 indicated the presence of a copper containing enzyme (Brew, 1992). However this is a tentative assumption as possible electron donors to nitrite reductase include the copper containing azurin or pseudoazurin proteins which would also be inhibited by DDC. The same Nir^- phenotype would therefore be observed. Consequently further characterisation was needed at a genetic level to clarify which nitrite reductase *N.*

subflava has. A number of probes specific for either copper or cd_1 nitrite reductases have been developed (Coyne *et al.*, 1989; Smith and Teidje 1992; Ward *et al.*, 1993 and Ye *et al.*, 1993). The high degree of identity that exists between the copper nitrite reductases and also, but to a lesser degree, the cd_1 nitrite reductases (Figures 1.8 and 1.11) means that these probes can be used diagnostically to determine the type of nitrite reductase present in a given organism.

Chromosomal DNA from *N. subflava* B19 was digested and screened with a cd_1 probe from *Ps. stutzeri* and copper nitrite reductase gene probes from *Al. faecalis*. The cd_1 probe was made from *Ps. stutzeri* DNA by PCR amplification (Ward *et al.*, 1993). A 717bp region of the structural gene was amplified using primers designed from the published sequence of the *Ps. stutzeri* nitrite reductase gene (Jungst *et al.*, 1991). The fragment represented a section between 628bp and 1345bp from the 5' end of the gene. This included the central region of the gene, with a high degree of similarity to the nitrite reductases from *Ps. aeruginosa* (Sylvestrini *et al.*, 1989) and *Ps. stutzeri* JM300 (Smith and Teidje, 1992). The PCR strategy is represented in Figure 3.4.

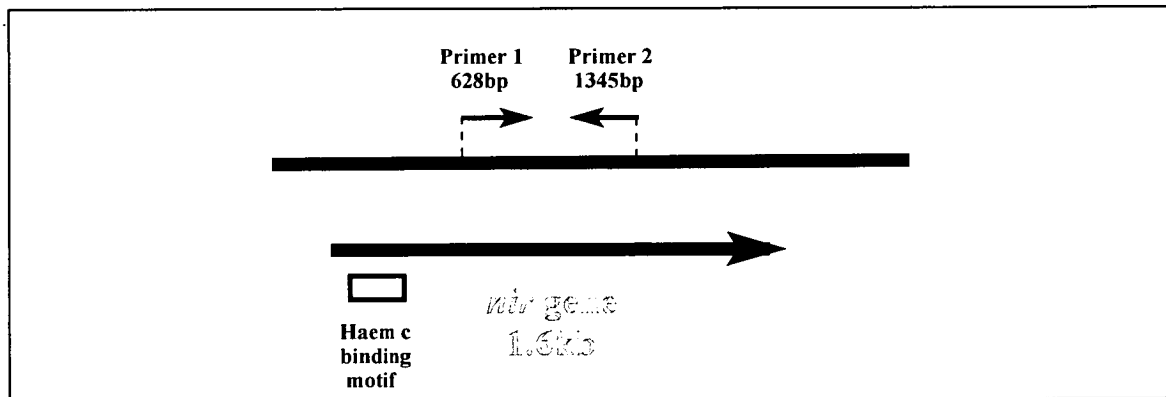


Figure 3.4. PCR strategy, not to scale, to produce the 717bp cd_1 probe from *Ps. stutzeri*. The primer sequences are as follows: Primer 1 5'-d[CGCCAGAGTTCTCCCTGCAG] and Primer 2 5'-d[CAGCTGTGGTTCTGGCCGTT].

Controls were included in the Southern hybridisation consisting of identically digested DNA isolated from organisms known to contain cd_1 nitrite reductases. The organisms chosen as positive controls were *P. denitrificans* (Lam and Nicholas, 1969)

and *T. pantotropha*. (Moir *et al.*, 1993). The results of the probing are shown in Figure 3.5. As you can see from the diagram, the probe hybridised weakly to DNA isolated from the identified cd_1 strains but there was no hybridisation to DNA isolated from *N. subflava* B19. A high degree of background hybridisation was also observed on the resulting autorad. Nevertheless the hybridisation observed to the cytochrome cd_1 nitrite reductase strains was determined to be authentic. Consequently, this result indicates that the nitrite reductase enzyme in *N. subflava* does not contain cytochrome cd_1 in its active site.

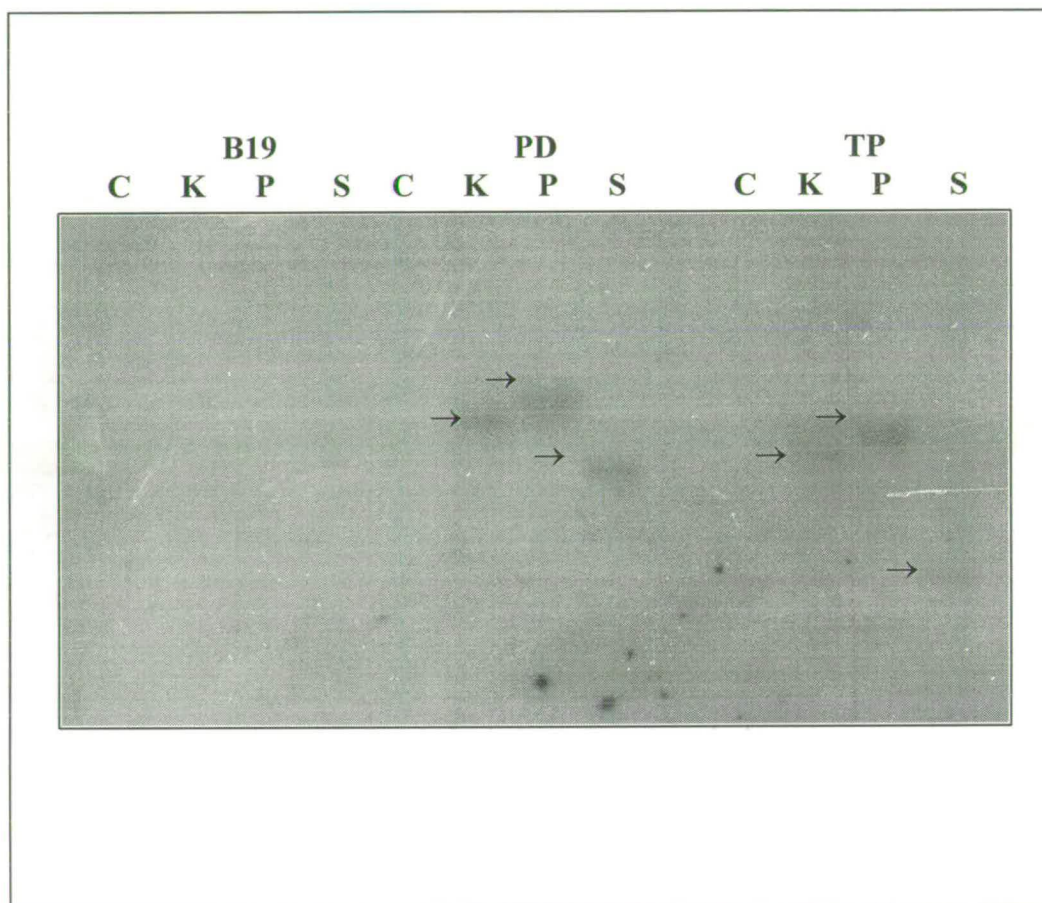


Figure 3.5. Southern hybridisation of denitrifying bacteria to the cd_1 probe of *Ps. stutzeri*. Strains are B19 - *N. subflava* wild type, PD - *P. denitrificans*, TP - *T. pantotropha*. Key to restriction enzymes C = *Cla*I, K = *Kpn*I, P = *Pst*I, S = *Sal*I. As hybridisation to the cd_1 strains is so faint arrows have been included for clarity.

This probing strategy was then repeated using the copper nitrite reductase gene probes from *Al. faecalis*. The copper nitrite reductase gene probes (nir2 and nir3) used in the experiment were digested from pNIR201 (Nishiyama *et al.*, 1993) as shown in Figure 3.6.

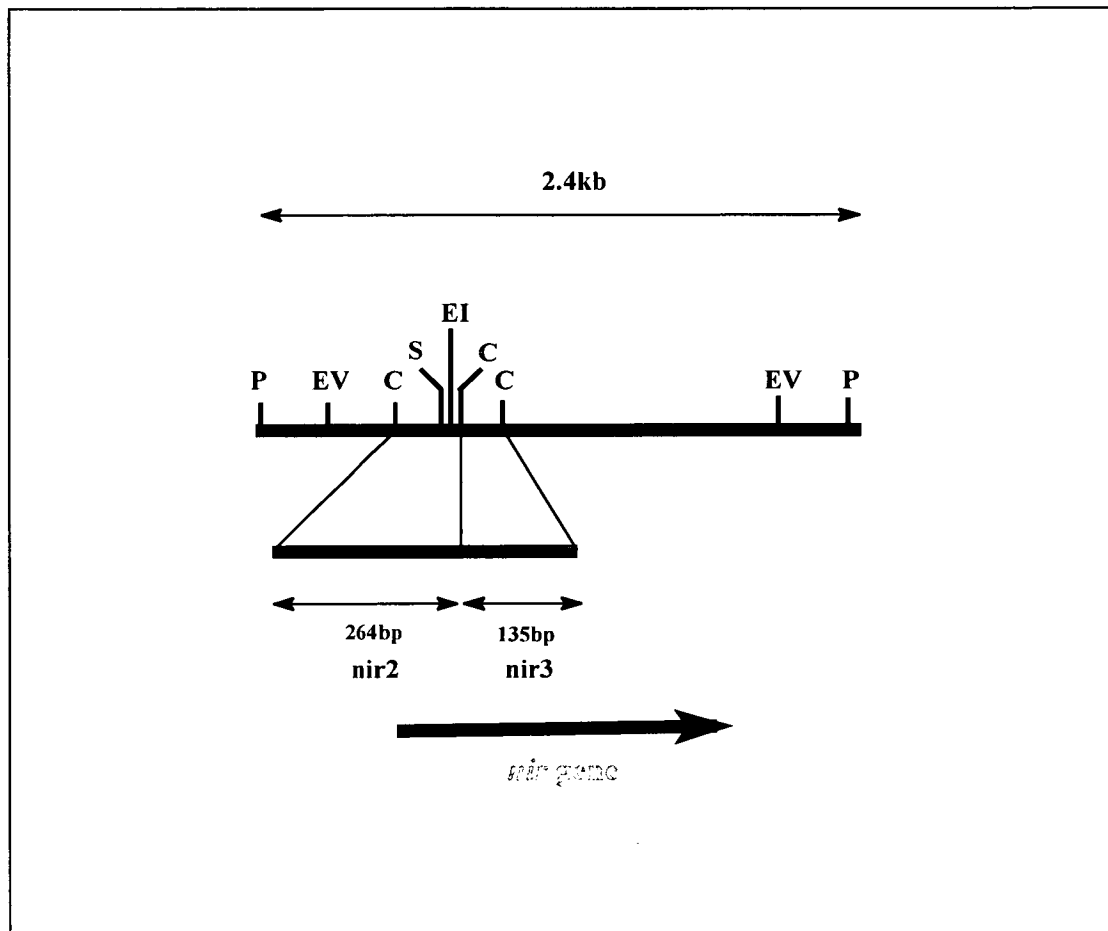


Figure 3.6. Restriction map, not to scale, of pNIR201 containing the *nir* gene from *Al. faecalis*. pNIR201 carries a 2.4kb *Pst*I fragment cloned into the *Pst*I site of pUC19. The positions of the nir2 and nir3 probes are illustrated. Key to restriction sites: C = *Cla*I, EI = *Eco*RI, EV = *Eco*RV, P = *Pst*I, S = *Sph*I. The position of the *nir* gene corresponds to the translated NiR peptide.

Positive controls were again included in the probing experiments. The copper nitrite reductase strains used were *A. cycloclastes* (Iwasaki and Matsubara, 1972) and *Pseudomonas*. sp. G-179 (Ye *et al.*, 1992). DNA was digested as for the *cd*₁ probing experiment and initially probed with nir2. Hybridisation was observed to the two

B19 (data not shown). The same hybridisation pattern was detected when nir3 was used in the probing experiment (Figure 3.7).

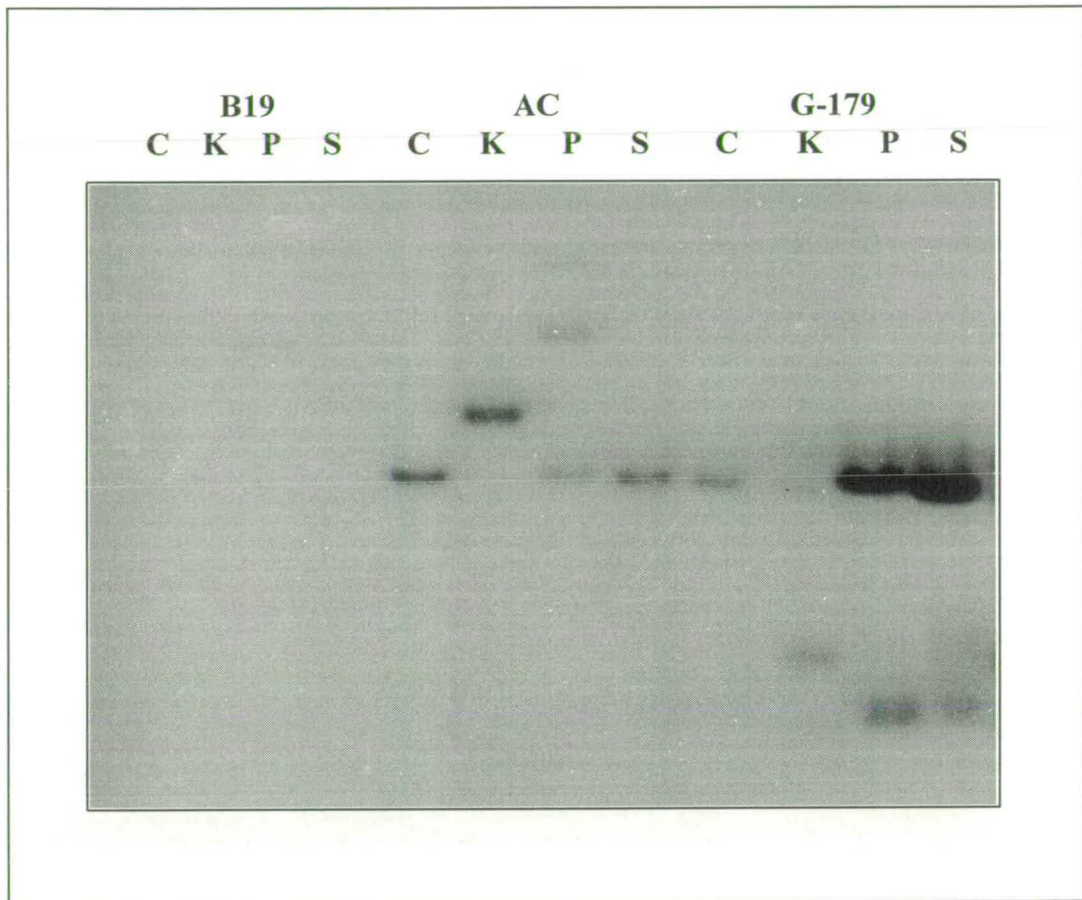


Figure 3.7. Southern hybridisation of denitrifying bacteria to the nir3 copper probe of *Al. faecalis*. Strains are B19 - *N. subflava* wild type, AC - *A. cycloclastes*, G-179 - *Ps. sp. G-179*. Key to restriction enzymes: C = *Clal*, K = *KpnI*, P = *PstI*, S = *Sall*.

These results with the two copper probes might suggest that *N. subflava* B19 did not contain a copper nitrite reductase enzyme, in contradiction to the hypothesis of Brew (1992). Both probing experiments gave negative results indicating that *N. subflava* B19 did not contain either a copper or a cd₁ nitrite reductase. This then raised the question as to which type of nitrite reductase was present.

Section 1.4 gives a comprehensive review of the many different types of nitrite reductase enzymes which have been characterised. However the possibility that *N. subflava* B19 contained one (or more) of these types of enzyme was not investigated due to the recent characterisation of the AniA protein from *N. gonorrhoeae*. The AniA protein, encoded by the *aniA* gene, has been shown to be a novel type of nitrite reductase (Mellies *et al.*, 1997). The enzyme is an outer membrane lipoprotein and contains copper in its active site. Sequence analysis of AniA revealed that all of the copper binding ligands present in the well characterised soluble nitrite reductases were conserved (Mellies *et al.*, 1997). In fact the greatest degree of conservation between the AniA protein and other well characterised copper nitrite reductases occurs over the copper binding domain. However AniA shows a significantly lower degree of similarity over this region when compared to other nitrite reductases, ~36% identity compared to ~80%. Away from this region towards the N- and C-terminals of the AniA protein the degree of similarity decreases even further (refer to figure 1.13). It seemed reasonable to assume, in terms of evolutionary distances, that the *N. subflava* B19 nitrite reductase would be more closely related to the AniA protein of *N. gonorrhoeae* than other more typical copper nitrite reductases (Figure 3.8).

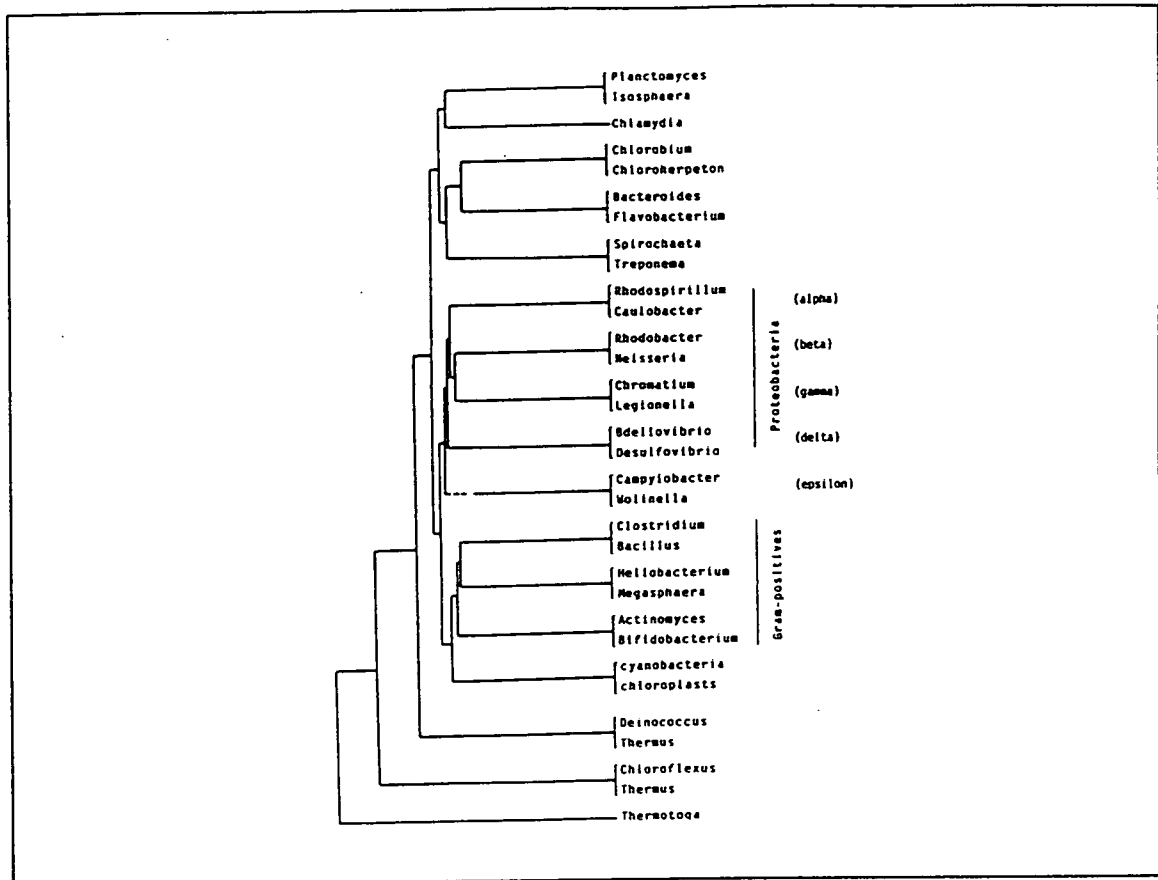


Figure 3.8. Topology tree of the eubacteria based upon phylogenetic relationships. The relative distances separating each of the lines of descent are based on 16S rRNA sequence comparisons.

Species	Oxidase ^a	Glucose ^a	Maltose ^a	Lactose ^a	Sucrose ^a	Reduction of		
						NO ₃ ⁻	NO ₂ ⁻	DNase
<i>Neisseria gonorrhoeae</i>	+	+	-	-	-	-	- ^b	-
<i>Neisseria subflava</i>	+	+	+	-	-	-	+	-
<i>Escherichia coli</i>	-	+	+	+	d	+	d	-

Table 3.1. Characteristics of *Neisseria* spp. *Escherichia coli* is included for comparison. Abbreviations: +, most strains positive; -, most strains negative; d, some strains positive, some strains negative.

^a Indicates the production of acid from these sugars.

^b *N. gonorrhoeae* strains that are negative in 0.1% nitrite can reduce 0.01% potassium nitrite.

A lack of hybridisation of the two copper nitrite reductase gene probes to *N. subflava* B19 genomic DNA may be explained using the above information. The copper nitrite reductase gene probes used in the hybridisation experiments were present at the 5' end of the *Al. faecalis* nitrite reductase gene (Figure 3.6). Over this region the degree of amino acid identity between the nitrite reductase enzymes of *Al. faecalis* and *N. gonorrhoeae* is 26% (Figure 3.9). This degree of identity is likely to be even lower in the corresponding coding DNA in each organism, as a variety of codons can encode a single amino acid and the choice of codon is species specific. The very low DNA similarity between the *Al. faecalis* and *N. gonorrhoeae* nitrite reductase genes would reduce the interaction between the nir2 and nir3 probes, and target sequence DNA in subsequent probing experiments. Assuming the two Neisserial enzymes to be very similar would account for the lack of hybridisation of the two *Al. faecalis* copper nitrite reductase gene probes to *N. subflava* B19 DNA.

Attempts were made to 'engineer' an interaction between the two copper nitrite reductase gene probes and *N. subflava* B19 DNA by reducing the stringency of the probing experiments from 55°C to 40°C but again no hybridisation was observed (data not shown). This suggests that the above suppositions made about the lack of interaction due to low DNA similarity between the copper nitrite reductase gene probes and *N. subflava* B19 target DNA are correct. Even at a much lower stringency differences between the probe and target DNA sequences were too great for an interaction to be manipulated.

3.3 Genetic Analysis of pZS163

3.3.1 Sequence analysis

The restriction map of pZS163 was derived by Sowerby (1997) and is shown in Figure 3.1. This restriction map was confirmed by digesting and probing the plasmid DNA prior to any subcloning and sequencing. Unfortunately it was determined that there is only a tiny region of chromosomal DNA corresponding to 170bp at the IS50_R end of Tn5 before entry into the cloning site of pUC19. Consequently most of the sequence obtained from this clone comes from chromosomal DNA at the IS50_L end of the Tn5 insertion.

It was not possible to sequence directly from pZS163 using the specifically designed Tn5 primer (Sowerby, 1997) as this primer was made from the insertion sequence ends of the Tn5 molecule. The IS50_L and IS50_R ends of Tn5 are inverted repeats characteristic of composite transposons (Berg, 1989). Consequently the Tn5 primer would have had two sites to anneal to in pZS163 and the resulting sequence would have been indecipherable.

Due to the nature of Tn5 insertions it was expected that chromosomal DNA directly flanking the insertion site would provide some information as to the type of gene that had been interrupted with relation to the phenotype of mutant 163. Consequently two fragments extending over the IS50_R end of Tn5 were subcloned into pBluescript KS⁻ for sequencing. These corresponded to a 3.0kb *Bam*HI fragment and a 5.0kb *Xho*I fragment. Figure 3.10 illustrates the fragments subcloned to generate the 170bp sequence data at the IS50_R end of the Tn5 insertion, and Table 3.2 shows the primers used in all subsequent sequencing reactions.

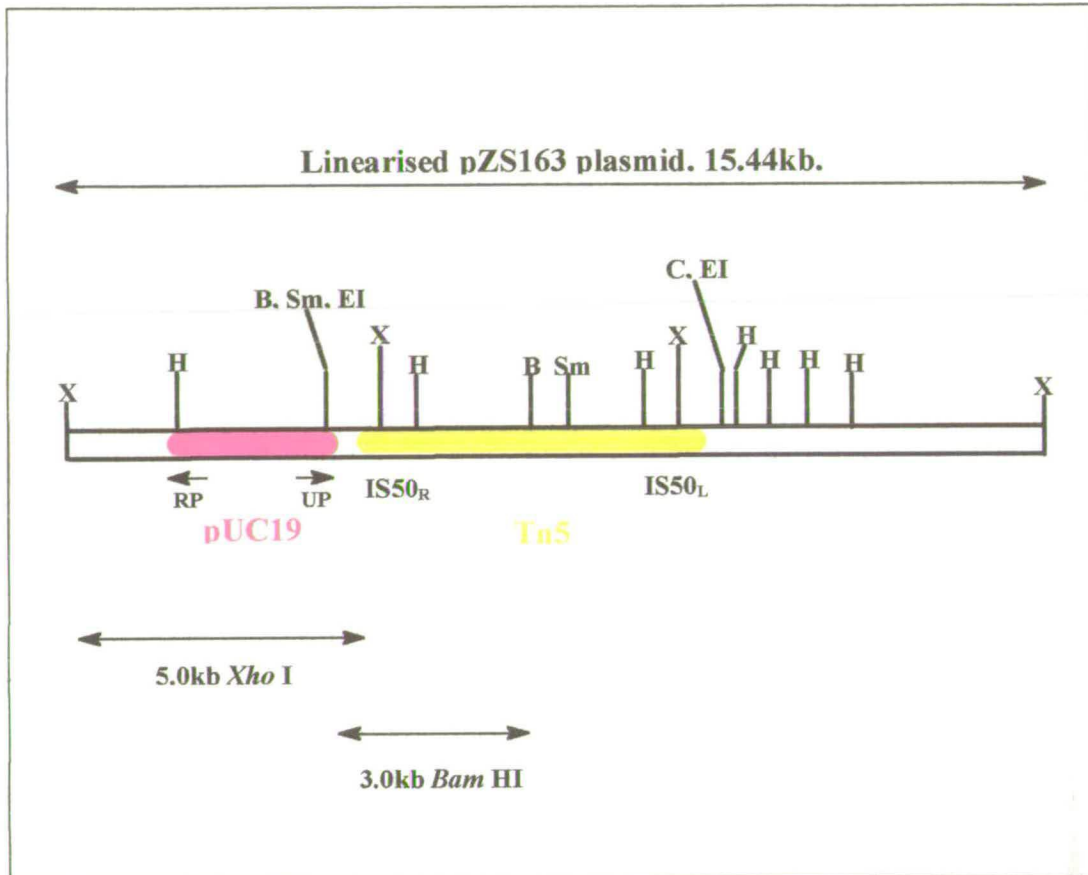


Figure 3.10. A linearised representation, not to scale, of pZS163 to illustrate the positions of the 5.0kb and 3.0kb fragments subcloned into pBluescriptKS⁻ for sequencing the 170bp region of DNA between Tn5 and pUC19. Key to restriction enzymes B = *Bam*HI, C = *Cla*I, EI = *Eco*RI, H = *Hind*III, Sm = *Sma*I, X = *Xho*I. The positions of the Universal primer (UP) and Reverse primer (RP) of pUC19 are illustrated for orientation.

Primer name	Sequence
M13 Universal Sequencing Primer	5'-d[GTAAAACGACGGCCAGT]-3'
M13 Reverse Sequence Primer	5'-d[CAGGAAACAGCTATGAC]-3'
T3 Sequencing Primer	5'-d[ATTAACCCTCACTAAG]-3'
Tn5 Sequencing Primer	5'-d[ACTTGTGTATAAGAGTCAG]-3'

Table 3.2. List of the most common sequencing primers used in this study derived from vector cloning sites. The Tn5 primer is also included.

To obtain sequence from the IS50_L end of the Tn5 insertion in pZS163 a similar approach to subcloning and sequencing was adopted (Figure 3.11). A 6.1kb *Xho*I fragment and a 0.9kb *Xho*I/*Eco*RI fragment extending over this region were subcloned into pBluescript KS⁻ for sequencing. A number of *Hind*III fragments are also present at the IS50_L end of the Tn5 insertion and were subcloned into pBluescript KS⁻ for sequencing. These were a 1.7kb *Hind*III fragment extending from within the Tn5 insertion into mutant 163 chromosomal DNA, a 0.6kb *Hind*III fragment adjacent to this and a 0.8kb *Hind*III fragment directly adjacent to the 0.6kb fragment. The orientation of the *Hind*III fragments was determined by restriction analysis. Table 3.3 summarises the subclones derived from both the IS50_R and IS50_L ends of Tn5 from pZS163.

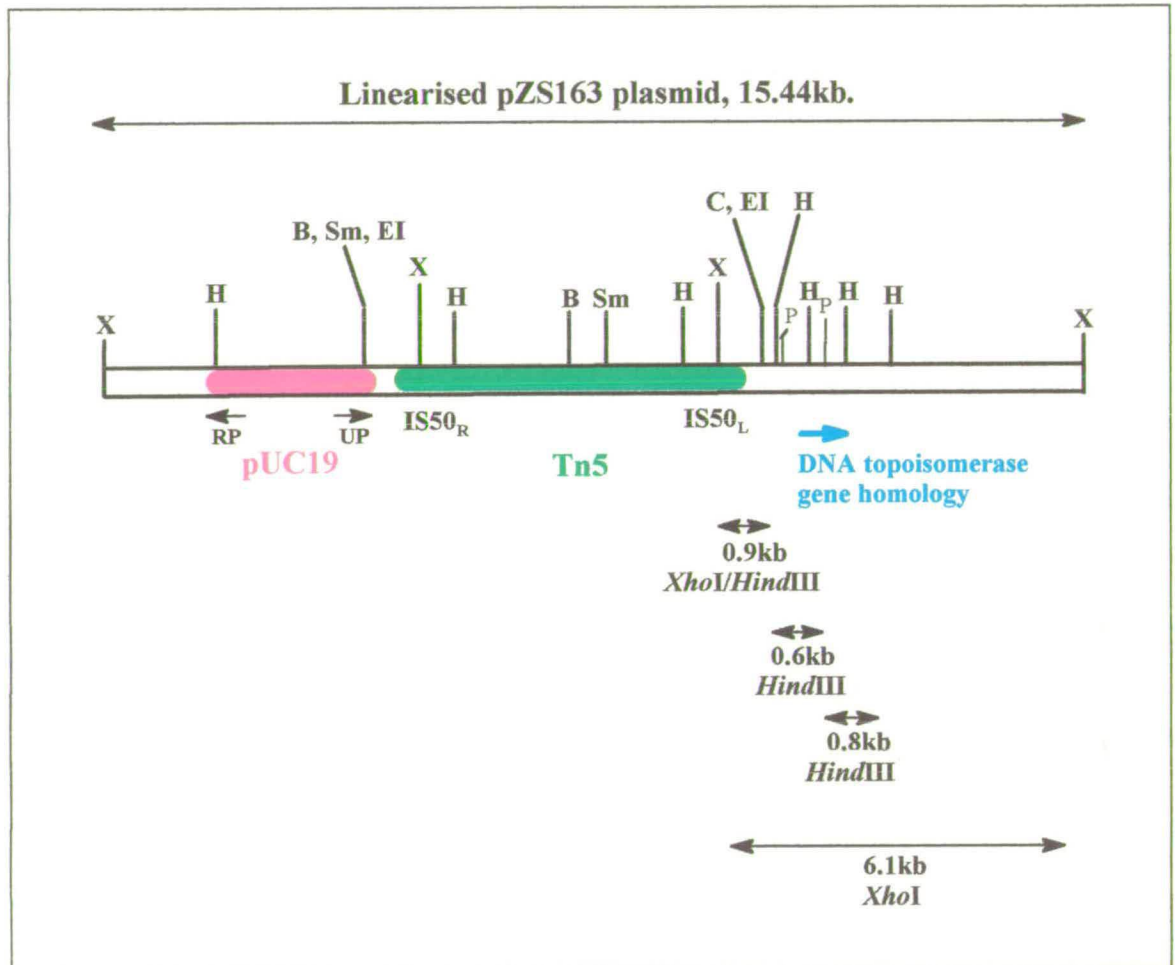


Figure 3.11. A linearised representation, not to scale, of pZS163 to illustrate the positions of the fragments subcloned into pBluescript KS⁻ for sequencing at the IS50_L end of Tn5. Key to restriction enzymes B = *Bam*HI, C = *Cla*I, EI = *Eco*RI, H = *Hind*III, Sm = *Sma*I, P = *Pst*I, X = *Xho*I. The positions of the Universal primer (UP) and Reverse primer (RP) of pUC19 are illustrated for orientation. The region with DNA topoisomerase gene homology is depicted, see text for details.

Fragment cloned	End of Tn5 present	Plasmid name
5.0kb <i>XhoI</i>	IS50 _R	pJT1
3.0kb <i>BamHI</i>	IS50 _R	pJT3
6.1kb <i>XhoI</i>	IS50 _L	pJT4
0.9kb <i>XhoI/EcoRI</i>	IS50 _L	pJT5
1.7kb <i>HindIII</i>	IS50 _L	pJT6
0.6kb <i>HindIII</i>	-	pJT7
0.8kb <i>HindIII</i>	-	pJT8

Table 3.3. Summary of subclones produced from pZS163. See Figures 3.10 and 3.11 for the positions of the fragments in the parent plasmid. Appendix A2 illustrates the plasmid maps for each of these constructs.

The fragments were sequenced in both directions using the Universal and Reverse primers from pBluescript KS⁻ vector DNA and, where appropriate, using the Tn5 primer from the IS50 ends of the Tn5 insertion, if present in the insert fragment. i.e. Tn5 primer was used to sequence pJT1, pJT3, pJT4, pJT5 and pJT6. The sequence data from each of the constructs was aligned and fitted together using the LINEUP and BESTFIT programmes from the GCG9 package to generate a single consensus sequence. This consensus sequence is depicted in Figure 3.12.

```

1   aacgacacat  tgctccttggt  cgcgcaaagc  atctaccgct  tcttgagccg
51  caggcatgtc  tctttacatc  gacagccacc  acggattccc  gtccgatagc
101 aggaaggcgg  ccgatgaagc  tgcgcaaatc  aaaactgaat  cgggccgcag
      ↓
151 gacgcgcacg  tccgagctgg  tcgagggtat  ccgcgaatcg  gtcataccgt
201 cgcgcgcgtg  ccacggcatc  atgacgattt  gaaccataag  ccgcgtaaag
251 caaacccggtg  tggtaattat  caacgcgcac  attcgacaaa  tcgatgaatt
301 ccccggctat  agccttgcac  agttacattc  aatcatcaac  gatgtaaagt
351 tttttggagc  atgagcatgt  atatggattt  ttctacttcc  tacgattatg
401 agactggttt  tggttcctgc  taaaagcatg  tcaaccaatg  acttcatgcg
451 aggcttgggt  gcttcgtgga  aagagccagc  cacatatgtg  cgtcaagttt
501 gctcaagcgg  tcggttctgt  atccgagggg  tatctttaga  gttggccttg
551 gtcgacaaat  gtctgccagg  gcgaattggg  ctaagccttga  ataatgactg
601 ttatttaatg  aagcaggtat  caccgcgaaa  cagtggcgaa  atattcggag
651 tagtcttctg  cagaaagggt  tttactcaat  cggagaactg  tagcaccaac
701 cgaatcccaa  tttactttga  atgatgaact  gtttgaggaa  ttggacgcaa
751 acatagtгаа  tcaaacgatg  tacttgatat  gggtgcgccc  ctatttcgat
801 taataaactt  catctgaaga  cattggccga  cagaggactt  tcttttgtgt
851 ccgtctgtat  tgctcgttctt  caaagtgagg  gctgaatatt  caagatttga
901 gtaatcgtgg  tgactggtcg  ccttggctca  tgcagctgaa  agcatgtttt
951 cattcaacaa  tgttgtctag  gcgacaacag  gaaagagcta  ttgccgaatt
1001 aacctctttt  ggtttaattg  aaagttgtgt  tgatggtatg  ccggcagcgc
1051 gtcgttgtag  atacagtttg  aagatgcttg  ctgatcttac  ctctgaatta
1101 ttttgaacgg  atgtgtgtga  tggttacggc  cacaaaatta  cccccaccga
1151 aggtgttcaa  ttctgaactg  acacaatgct  ggccaagcctt  gtagtccaaa
1201 gggataaaga  gatcgatact  ttcgtgcctt  acaactacta  caccctttca
1251 gtagattttg  agacagcggg  caagtcagtg  ttactacac  tgtggcaggt
1301 gcctgaaaac  tggcgttaata  ctgatggata  ctgtaccaat  cttgaggctg
1351 ttaaggctct  tgtaaacacg  cttgagaaat  ctactggtaa  ggtcattact
1401 ttaacaaaga  gcgtaaaagc  acccgcctcc  gttaccttac  agcctttctg
1451 gctttacaaa  agaagccgga  aaaactggcc  tatcggcttc  caaagtgtct
1501 aaattgcaca  acctcctacg  aaataccaga  taacgtcata  tcgcgcactc
1551 ctgcagatct  gccaaatcgc  agatgagtga  agtgaaagat  gtattgccgc
1601 aatacagact  atcgacaaat  ccatgctcgg  taattgaaaa  agctgatcct
1651 gaacgtcagt  caagagtatg  gaatgataac  caggtaaaca  agcattctca
1701 tcatgcaatt  attccgacca  aggtcagtaa  ttttgattta  acagtccttg
1751 ataagaatga  attaacgggt  tatcgaatga  tacgagaccg  ttatatcgcg
1801 cagttttatc  ctgattttga  atatgactct  actgtgggtg  aggttgaagc
1851 atgttcacat  ttgtttaaag  cctccagcca  atcaccgggt  atttccgggt
1901 ggaaggttct  tttgggtaag  gatgtgttcg  aaggtgatca  aatcgacctg
1951 caggcactta agct

```

Figure 3.12. pZS163 consensus sequence obtained upon analysis of pJT1, pJT3, pJT4, pJT5, pJT6, pJT7 and pJT8 subclones. The position of the Tn5 insertion is highlighted between the 't' and 'g' residues of the 4bp sequence illustrated in bold type at position 168bp. The positions of the *Hind*III sites used to extend the amount of sequence data obtained from the IS50_L end of the Tn5 insertion are underlined. Nucleotide 1 corresponds to the start of mutant 163 chromosomal DNA detected by pUC19 universal primer from pJT1 and pJT3.

The 1964bp consensus sequence produced from the pZS163 subclones was translated into all 6 reading frames with the expectation of identifying the presence of an ORF corresponding to a regulatory or structural gene for nitrite reductase. No ORFs were identified and none of the six reading frames had similarity to a nitrite reductase or regulatory gene of any description when searched through the SwissProt database using the FASTA package on GCG9. Sequence from pZS163 was expected to have similarity to a nitrite reductase gene as a Nir⁻ phenotype was observed when this plasmid was used to transform wild type *N. subflava* (Sowerby, unpublished results). Similarity, albeit it low, was identified in reading frame one to *H. influenzae* DNA topoisomerase III over the 1332-1964bp region of the pZS163 consensus sequence. This similarity is represented in Figure 3.13.

```

450          460          470          480          490          500
DTPVILRLLRSLNLSLRNLLVRSLLXQRAXKHPPPLPYSLSGFTKEAGK-GLSASKVLK
          |: |||||::: |:| |::|
RVLKGLAEKVVKRITNQPAEVTEYKDVREKETAPLPYSLSALQIDAARKFRGMSAQAVLD
          270          280          290          300          310          320

          510          520          530          540          550
LHLLRNTRXRHIAH---SCRS-AKSQMSEVKDVLQPQYRLSTNPCSVIEKAD-PERQSRV
: | :|: | |::: || : ::| :||          : :|: :: |:::|
TCQRLYETH-RLITYPRSDCRYLPEEHFAERHNVLNAISTHCEAYQVLPNVILTEQRNRC
          330          340          350          360          370          380

          560          570          580          590          600          610
WNDNQVNKHHHAI IPTKVSNFDLTVLDKNELTVYRMIRDRYIAQFYPDFEYDSTVVEVE
|||:::|: :||| ||| :| :| :| :| :| :| :| :| :| :| :| :| :| :| :| :|
WNDKKVE--AHHAI IPT-AKNRPVN-LTQEERNIYSLIARQYLMQFCPDAEYRKSKITLN
          390          400          410          420          430

          620          630          640          650
ACSHLFKASSQSPVISGWKVLLGKDVFEQDQIDLQALK
: | |::: :||| ||||:
IAGGTFIAQARNLQTAGWKELLGKEDDTENQEP LLPIVKKGQILHCERGEVMSKKTQPPK
440          450          460          470          480          490

```

Percent Identity: 33.7% over 175 amino acids.

Figure 3.13. Comparison of the translated amino acid sequence obtained from the pZS163 consensus sequence to the amino acid sequence of DNA topoisomerase III from *H. influenzae*. The top amino acid sequence corresponds to translated peptide in reading frame one from the pZS163 consensus sequence and the bottom sequence to the DNA topoisomerase III peptide.

DNA topoisomerase enzymes are able to relax negatively supercoiled DNA and are therefore important in bacterial gene expression (Srivengopal *et al.*, 1984). The exact function of DNA topoisomerase III is unknown but it has been demonstrated to act as potent decatenase capable of segregating DNA replication intermediates (DiGate and Marians, 1988). It is interesting to note that upstream of the encoding gene (*topB*) is the presence of a potential nitrogen starvation promoter indicating an alternative genetic control on *topB* in the absence of nitrogen (DiGate and Marians, 1988). However no relationship between the denitrification genes and DNA topoisomerase genes has been identified. No ORF corresponding to a DNA topoisomerase has been found in any of the well characterised denitrification operons (section 1.2). A number of ORFs in the denitrification supraoperons have yet to be functionally assigned but database searches of these ORFs did not identify any homologies to DNA topoisomerase enzymes (Zumft, 1997).

The position of the DNA topoisomerase III gene in relation to the Tn5 insertion is illustrated in Figure 3.11. The gene lies 1164bp beyond the IS50_L end of the Tn5 insertion position. This suggests that DNA in this region does not correspond to a denitrification gene cluster.

The fact that a nitrite reductase structural or regulatory gene was not identified from pZS163 as expected cast doubt on the validity of sequencing the remainder of the plasmid. It was suspected that a genetic recombination event had occurred at some point resulting in the excision of the anticipated gene. Whether this excision occurred upon Tn5 mutagenesis or the construction of pZS163 at this time was unclear. It was decided to characterise this suspected deletion to determine whether screening a mutant 163 λ library constructed from mutant 163 genomic DNA, or further analysis of pZS163 would be more productive.

3.3.2 Mutant 163/pZS163 deletion characterisation

It seemed reasonable to assume that, if the insertion of Tn5 into *N. subflava* genomic DNA had caused a deletion of some description, then the DNA flanking one (or both) ends of the Tn5 molecule would be the same in the mutant *N. subflava* strain

as in pZS163. However, if it was the construction of pZS163 which caused the deletion to occur then DNA flanking the Tn5 molecule in this plasmid construct would be different to that in the mutant 163 DNA. To determine the point at which the proposed deletion occurred, whether upon Tn5 mutagenesis or pZS163 plasmid formation, a probe was constructed corresponding to the 170bp of mutant 163 chromosomal DNA present in pZS163 between pUC19 and the IS50_R end of Tn5. This was achieved by PCR amplification from pJT3 using the Tn5 primer and the KS sequencing primer; 5'-d[CGAGGTCGACGGTATCG]-3'. The KS sequencing primer of pBluescript KS⁻ was chosen instead of the reverse and T3 primers which also anneal to the pBluescript KS⁻ polylinker as it had a more compatible T_m to the Tn5 primer. The PCR profile was as follows:

	First cycle	Intermediate cycle	Last cycle
Denaturation (94°C)	5 minutes	1 minute	1 minute
Annealing (50°C)	1 minute	1 minute	1 minute
Elongation (72°C)	20 seconds	20 seconds	10 minutes

for a total of 30 cycles.

The purified 170bp PCR product was radiolabelled as described in section 2.2.20 and used to probe chromosomal digests of *N. subflava* B19 and mutant 163 DNA. This 170bp fragment would provide probing evidence relating to the IS50_R end of Tn5. To obtain probing data relating to the IS50_L end of the Tn5 molecule a 280bp *EcoRI/HindIII* fragment was digested from pJT4. This fragment is positioned 104bp away from IS50_L and is therefore not directly adjacent to the Tn5 molecule. This fragment was also purified and used as a radiolabelled probe to screen chromosomal digests of *N. subflava* B19 and mutant 163 DNA. Figure 3.14 shows the positions of the 170bp and 280bp probes in pZS163, and Table 3.4 shows the sizes of the fragments that hybridised to these probes from each of the *N. subflava* genomic DNAs.

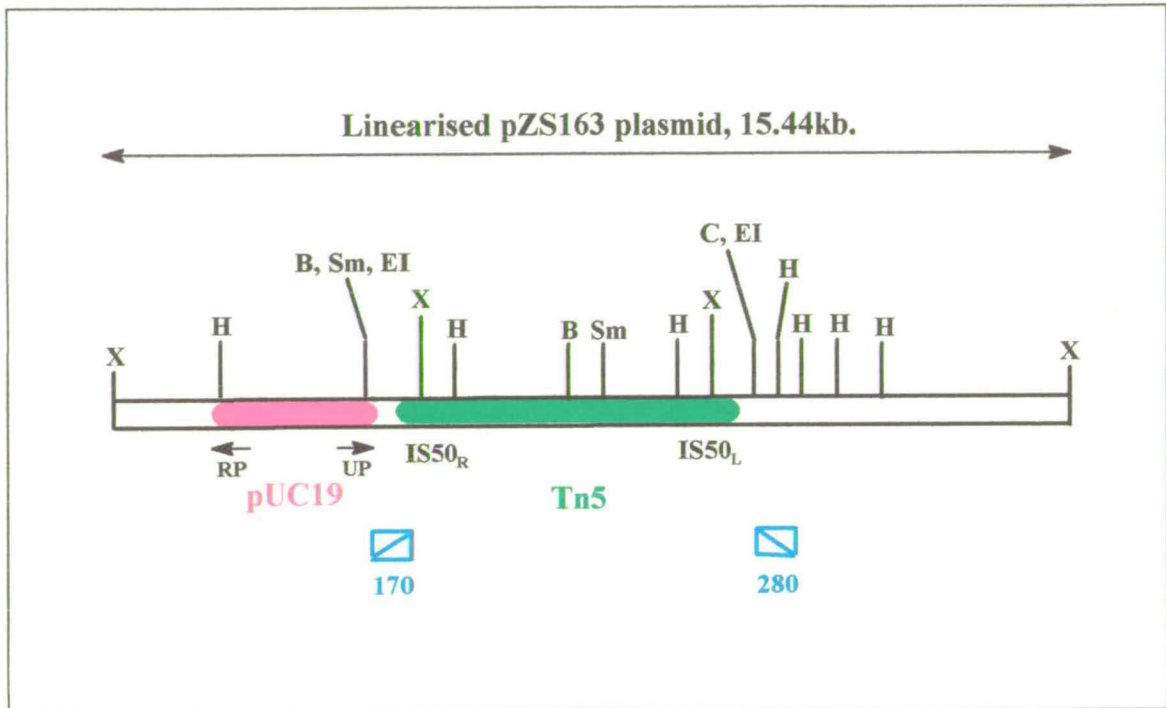


Figure 3.14. Linearised representation, not to scale, of pZS163 showing the positions of the 170bp and 280bp probes. The only restriction site separating the two probes is the *Cla*I site at the IS50_L end of Tn5. Key to restriction enzymes B = *Bam*HI, C = *Cla*I, EI = *Eco*RI, H = *Hind*III, Sm = *Sma*I, X = *Xho*I.

Probe	170	170	280	280
DNA (genomic)	B19	163	B19	163
<i>Cla</i> I	0.7	0.7	8.5	8.5
<i>Kpn</i> I	8.4	8.8	9.4	7.8
<i>Pst</i> I	10.2	13.0	4.4	3.1
<i>Sal</i> I	5.2	5.6	15.0	15.0
<i>Sph</i> I	9.8	11.0	16.0	14.0

Table 3.4. Summary of fragment sizes hybridising to the probes flanking the IS50_R end of Tn5 (probe 170bp) and the IS50_L end of Tn5 (probe 280bp). All fragment sizes are in kb.

According to the pZS163 consensus sequence (Figure 3.12) the two probes used to screen the B19 and mutant 163 genomic DNAs were separated by only 104bp of chromosomal DNA, excluding the Tn5 insertion in mutant 163. Consequently it was expected that in the B19 screening experiments both probes would hybridise to fragments of the same size. The exception being when the DNA was digested with *Clal* as a *Clal* site exists between the two probes. Consequently different hybridisation patterns were expected in this instance. Similarly when mutant 163 DNA was digested different hybridisation profiles were expected from the two probes but the differences obtained would be accounted for using the restriction sites known to be present in Tn5. In the screening experiments on both types of DNA with both probes these points were not observed. To illustrate this, further attention should be directed to the B19 and mutant 163 *KpnI* probing, with both the 170bp and 280bp probes. *KpnI* does not cut either within Tn5 or between the two probes. The difference in fragment sizes showing hybridisation to each of the probes in *KpnI* digested DNA was expected to correspond to a 5.8kb increase in the mutant 163 DNA when compared to B19, due solely to the insertion of the Tn5 molecule. However when comparing the results of the 170bp probe, B19 DNA was found to hybridise to an 8.4kb fragment and mutant 163 DNA to an 8.8kb fragment. With the 280bp probe, a 1.6kb decrease in fragment size was detected with B19 and mutant 163 DNAs hybridising to 9.4kb and 7.8kb fragments respectively. This contrasted with the expected 5.8kb difference between the wild type and mutant DNAs. Similar ambiguities were also found in the other probing results between the B19 and mutant 163 DNAs with a number of different restriction enzymes, as depicted in Table 3.3.

The mutant 163 probing results for the 170bp and 280bp probes were used together with the deduced restriction map of pZS163 to determine the location of the suspected deletion. A *PstI* fragment of 1.6kb present in pZS163 was expected to hybridise to the 280bp probe if DNA flanking the IS50_L end of the Tn5 insertion was the same in both pZS163 and mutant 163 genomic DNA (Figure 3.15).

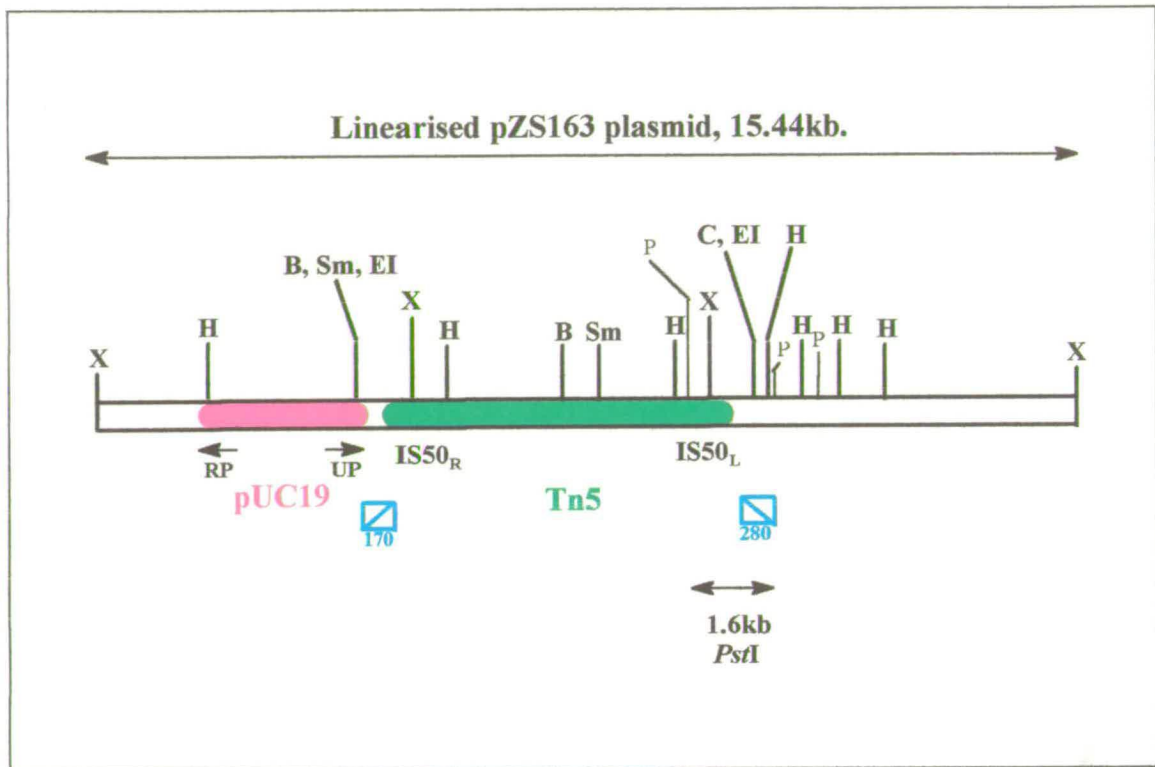


Figure 3.15. Diagram, not to scale, illustrating the 1.6kb *PstI* fragment expected to hybridise to the 280bp probe if the restriction sites present in pZS163 were the same as in mutant 163 DNA. Key to restriction enzymes B = *Bam*HI, C = *Cla*I, EI = *Eco*RI, H = *Hind*III, Sm = *Sma*I, P = *Pst*I, X = *Xho*I.

However a 3.1kb *PstI* fragment was observed to hybridise to mutant 163 DNA with the 280bp probe. This demonstrates that DNA flanking the IS50_L end of Tn5 in pZS163 differs to that found in the mutant 163 genome. However, due to the limited sequence availability over the IS50_R end of Tn5 in pZS163, it was not possible to determine whether the expected and observed hybridisations from pZS163 and mutant 163 genomic DNA to the 170bp probe were the same or not. It was therefore not possible to accurately identify where the deletion occurred.

DNA deletions associated with Tn5 transposition typically occur adjacent to the Tn5 molecule as a result of failed attempts to transpose (Jilk *et al.*, 1993). A number of models exist to explain how these adjacent deletions arise but in all cases the deletion size is < 0.6kb and occurs over the IS50_L end of Tn5 (Jilk *et al.*, 1993).

Hybridisation data obtained from the 280bp probe with 163 genomic DNA was inconsistent with that obtained using plasmid DNA from pZS163. This together with

the reported occurrence of deletions at the IS50_L end of Tn5 suggest that conclusions drawn using data, obtained from the 280bp probe, could be misleading. Hence the 170bp probe was used in subsequent experiments.

3.3.2.1 *N. subflava* B19 library screen with the 170bp probe

The 170bp probe from the IS50_R end of Tn5 in pZS163 (Figure 3.14) was used to screen a newly constructed genomic DNA λ library of the wild type B19 *N. subflava* strain. The reason for using the 170bp probe in this way was to obtain DNA sequence upstream and downstream of the 170bp probe region which was lacking in pZS163. The authenticity of the 280bp probe had already been discounted and consequently the chromosomal DNA surrounding the 170bp probe was believed to contain a structural or regulatory gene for nitrite reductase.

A total of nine positive λ clones were initially identified that consistently hybridised to the probe after a number of purifications. Of these nine potential positives two were identified that looked particularly interesting, λ 170-3 and λ 170-5. The λ DNA was isolated from these positives for further characterisation and digested with a number of different restriction endonucleases. The digests were put to Southern hybridisation and probed with the 170bp probe. This was to detect positively hybridising fragments of a suitable size for subcloning. The digests were also probed with the 280bp probe and the results of both of these sets of probings are shown in Table 3.5.

Probe:	170	280	170	280
DNA:	λ 170-3	λ 170-3	λ 170-5	λ 170-5
<i>Bam</i> HI	14.0	nd	16.0	nd
<i>Bgl</i> II	12.5	nd	14.0	nd
<i>Cla</i> I	nd	nd	1.6, 0.35	nd
<i>Eco</i> RI	11.5	nd	14.5	nd
<i>Eco</i> RV	1.5	nd	1.35	nd
<i>Hind</i> III	5.7	nd	1.65, 0.8	nd
<i>Kpn</i> I	9.2	nd	12.0	nd
<i>Pst</i> I	9.4	nd	5.0	nd
<i>Sal</i> I	6.3	nd	10.0	nd
<i>Sph</i> I	11.0	nd	14.0	nd
<i>Sma</i> I	11.5	nd	8.4	nd

Table 3.5. Summary of fragment sizes hybridising to the 170bp and 280bp probes from the λ 170-3 and λ 170-5 isolates. All fragment sizes are in kb. nd = not detected.

Neither of the λ isolates obtained from the 170bp probe library screen showed any hybridisation to the 280bp probe. This was of significance as it supported the possibility that a deletion had occurred. λ DNA can accept inserts of up to ~20kb and it seemed reasonable to assume that a single λ insert containing genomic DNA from *N. subflava* B19 positive to the 170bp probe would also be positive to the 280bp probe if the suspected deletion was typical of those associated with aberrant Tn5 excisions (Jilk *et al.*, 1993). A deletion size of 0.6kb or smaller would mean that both the 170bp and 280bp probe regions would be present in the λ insert DNA and both would probe positive, unless the position of the insert was such that the 280bp probe was just excluded from the insert fragment - although this seemed unlikely. As the 280bp probe

did not hybridise to DNA isolated from either of the λ 170-3 and 170-5 isolates a much larger deletion than 0.6kb was suspected indicative of the deletion occurring during the construction of pZS163.

A simple way to confirm this deletion hypothesis could be achieved by analysis of a λ library constructed from mutant 163 genomic DNA. The internal Tn5 kanamycin cassette (see section 3.2.1) could be used to screen the mutant 163 λ library. Subcloning and sequencing over the IS50_{L&R} ends of Tn5 from any resulting λ clones would liberate sequence for comparison to sequence from pZS163. If the sequence from the λ library was found to be the same as from pZS163 then it could be assumed that the deletion occurred upon Tn5 transposition. However, if the two sequences were determined to be different, then it could be presumed that the deletion occurred when plasmid pZS163 was made. This sequencing could be used to confirm or contradict the probing results discussed in section 3.3.2.

With this strategy in mind, a mutant 163 λ library was screened with the 1.86kb Tn5 probe liberating two positive clones. However, extensive restriction and probing analyses of the clones showed that they could not be used to identify when the pZS163/mutant 163 deletion occurred as they were found to be false positives. Internal fragments from Tn5, known to be present within the 1.86kb probe region, did not probe positive when appropriately digested λ DNA was screened. Even accounting for the fact that not all of the Tn5 probe region needed to be present in the resulting λ clones for hybridisation to the probe to occur, the calculated restriction maps did not relate to sites present in the λ arms. As these clones were deemed suspect it was decided not to investigate them further by subcloning for sequence examination. It was also decided against screening the 163 λ library for a second time as other experimental avenues were being investigated.

It was decided, after comparing the fragment sizes of λ 170-3 and λ 170-5 DNA to the fragment sizes of genomic B19 DNA positive to the 170bp probe, that the λ 170-3 isolate was most likely to be the true clone containing the gene(s) of interest. This supposition was made as the λ 170-3 isolate hybridised to fragments of a similar size to appropriately digested B19 DNA, when hybridised to the 170bp probe (Table 3.6). The fragment sizes do not match perfectly but the discrepancies can be explained as

fluctuations in DNA migration when separated on different gels, and also to errors when determining fragment sizes from standard curves. The fragment sizes from λ 170-3 matched much better than λ 170-5, although the evidence as to which isolate from the B19 λ library would liberate the most useful information was rather weak. It was therefore decided to subclone and sequence from λ 170-3. The 6.3kb *SaII* fragment from λ 170-3 showing hybridisation to the 170bp probe was subcloned into pBluescript KS⁻. The resulting construct was named pJT170 and is represented in Figure 3.16.

DNA	B19 (genomic)	λ 170-3	λ 170-5
<i>KpnI</i>	8.4	9.2	12.0
<i>PstI</i>	10.2	9.4	5.0
<i>SaII</i>	5.2	6.3	10.0
<i>SphI</i>	9.8	11.0	14.0

Table 3.6. Comparison of fragment sizes hybridising to the 170bp probe in λ and genomic DNA isolates. All sizes are in kb.

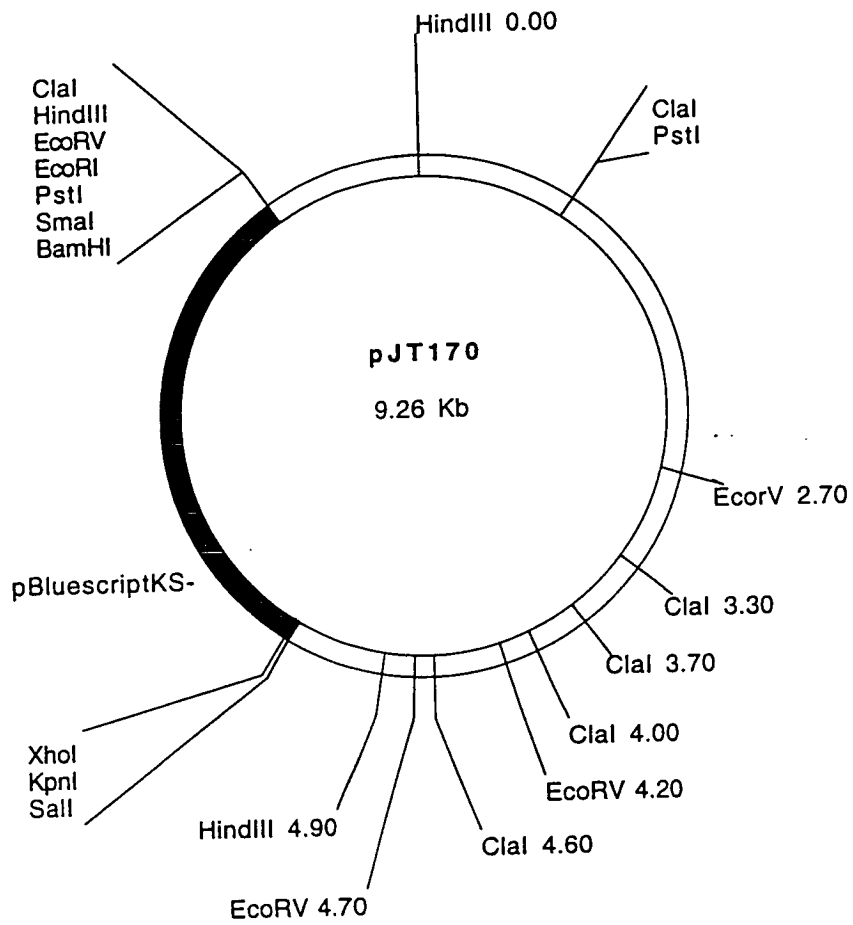


Figure 3.16. Plasmid map of pJT170 constructed from a 6.3kb *SaI* fragment of a B19 λ library, positive to the 170bp probe, cloned into pBluescriptKS⁻.

3.3.2.2 Deletion characterisation using pJT170

A sequencing primer (FP26) was designed within the 170bp probe region of pJT170 to sequence back towards the position where Tn5 inserted into chromosomal DNA to produce mutant 163 (Figure 3.17). The sequence of FP26 is 5'-[TTTACATCGACAGCCACCAC]-3' and shows similarity to the pZS163 consensus sequence between 63bp and 82bp.

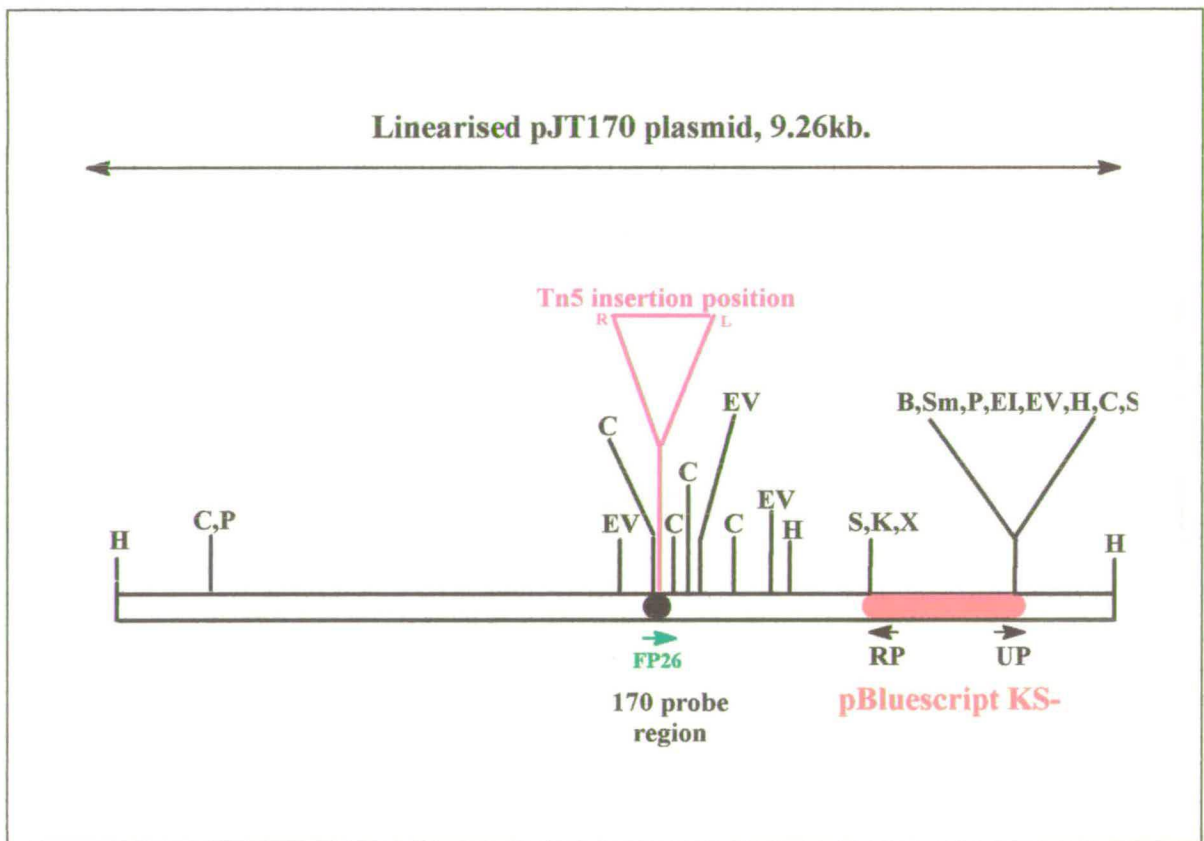


Figure 3.17. Linearised representation, not to scale, of pJT170 showing the position of the FP26 sequencing primer used to determine the deletion site in pZS163. The relative insertion point of the Tn5 molecule deduced from pZS163 is also illustrated. Key to restriction sites B = *Bam*HI, C = *Cla*I, EI = *Eco*RI, EV = *Eco*RV, H = *Hind*III, K = *Kpn*I, S = *Sal*I, Sm = *Sma*I, X = *Xho*I.

Sequencing pJT170 with FP26 enabled the deletion site in pZS163 to be identified. Comparison of the sequence obtained from pZS163 (Figure 3.12) with that from the FP26 sequencing primer determined the deletion site to be 104bp from the

DNA was digested and screened with the 1.86kb probe a fragment size of 6.6kb hybridised. As *Cla*I does not cut within Tn5 it was deduced that the actual *Cla*I fragment of corresponding chromosomal DNA in *N. subflava* B19 was 0.8kb. (6.6kb minus Tn5 length, 5.8kb, to give 0.8kb.) This fragment size was confirmed when B19 DNA was digested and probed with the 170bp probe. In this instance a 0.7kb fragment hybridised conforming to the 0.8kb fragment proposed to exist from the 1.86kb Tn5 probing results. This 0.7kb fragment was also present when mutant 163 DNA was screened with the 170bp probe. Sequence from pZS163 positions the *Cla*I deletion site at nucleotide number 295 (Figure 3.12). A second *Cla*I site also exists in this sequence at position 1213. This second *Cla*I site is therefore present 0.92kb away from the *Cla*I deletion site. If the restriction map of pZS163 was accurate then this 0.92kb *Cla*I fragment would have hybridised to the 280bp probe when mutant 163 DNA was screened. However, an 8.5kb fragment was observed to hybridise instead in both B19 and mutant 163 DNAs. The difference between these two fragment sizes is 7.58kb. (8.5kb minus 0.92kb to give 7.58kb.) This 7.58kb fragment is thought to correspond to the deleted DNA and a possible 'looping out' mechanism by which this DNA was lost during pZS163 formation is represented in Figure 3.19. This method relies on the presence of chromosomal DNA at the 280bp probe end of the deleted fragment having similarity to DNA surrounding the *Cla*I deletion site enabling a crossing over and recombination event to occur.

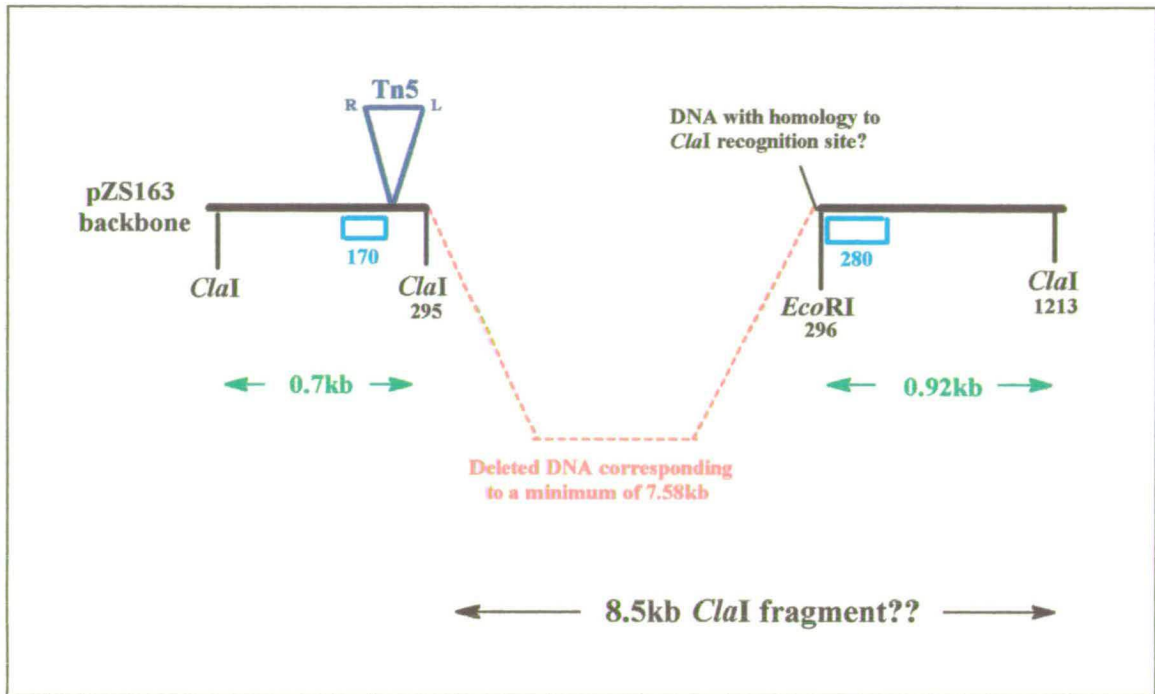


Figure 3.19. Hypothetical looping out mechanism, not to scale, which led to the deletion of DNA in pZS163. The *ClaI* deletion site is at nucleotide position 295 in the pZS163 consensus sequence. The positions of the 170bp and 280bp probes are also illustrated. The 8.5kb *ClaI* fragment highlighted was observed to hybridise to the 280bp probe when both B19 and mutant 163 DNA were screened.

Examination of the other restriction and probing results from Table 3.3 demonstrated that, if the deletion mechanism postulated in Figure 3.19 was correct, then the deletion size needed to be larger than the proposed 7.58kb. For the *PstI* sites detected in both pZS163 and pJT170 to relate to the hybridising 170bp and 280bp genomic fragments the calculated deletion size would need to be at least 11.3kb. Determination of this deletion size was made difficult as partial *PstI* fragments were found to be probing positive to the 170bp and 280bp probes. Also, many of the larger fragments showing hybridisation to the probes were beyond the limits of efficient DNA separation on 0.8% agarose gels. i.e. fragments greater than ~9-10kb were difficult to size accurately. A schematic representation of the relationship between plasmids pZS163 and pJT170, along with the position of the deleted DNA is summarised in Figure 3.20. The previous deletion size of 7.58kb has now been discounted.

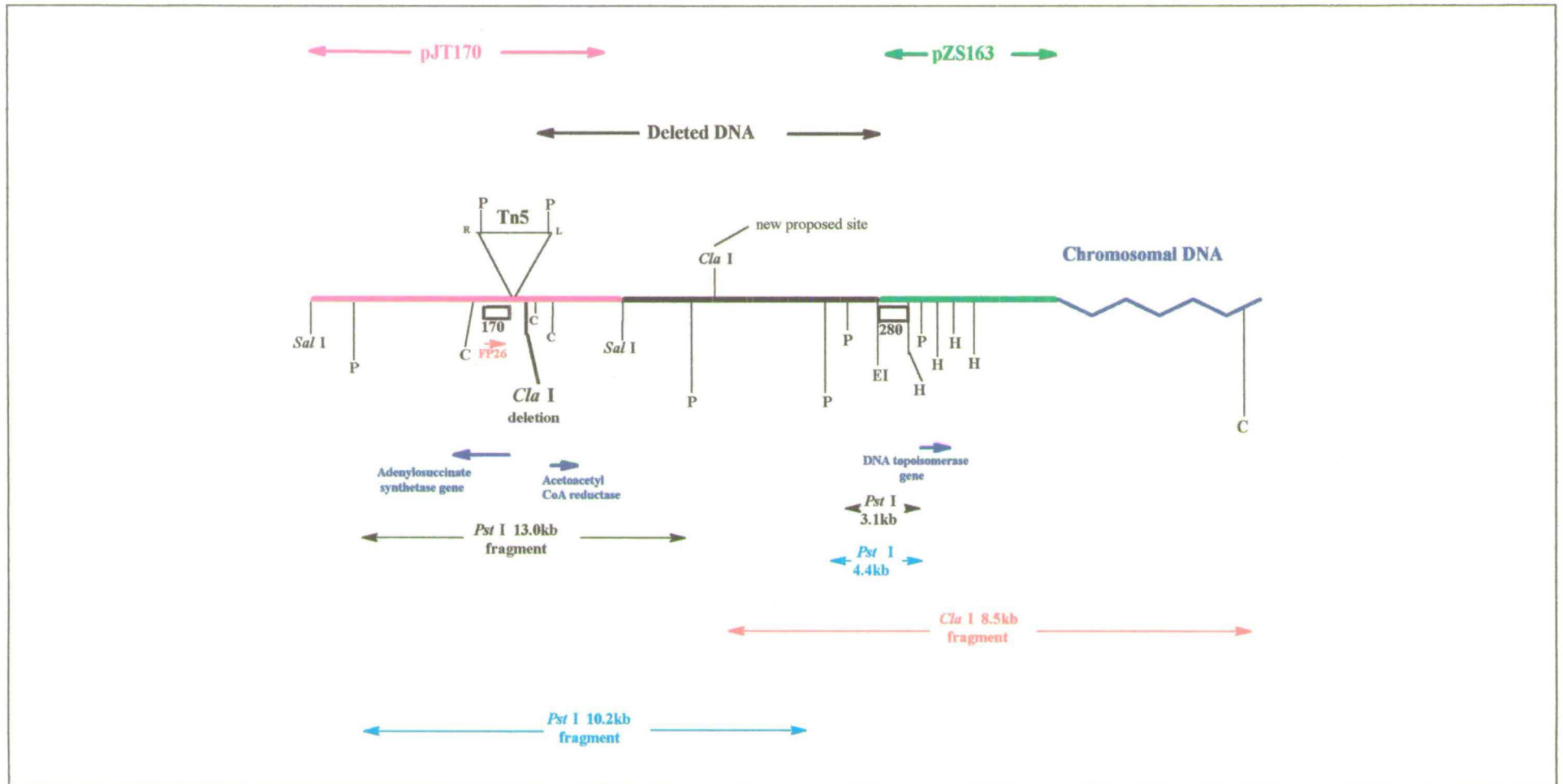


Figure 3.20. Schematic representation, not to scale, of the relationship between plasmids pZS163 and pJT170 along with the identified gene homologies (refer to text). The chromosomal/*Pst*I probing results from Table 3.3 are also illustrated. The probing results relating to the mutant 163 probing are shown in the lighter ink whilst the results relating to B19 are in the darker ink. Key to restriction sites C = *Cla*I, EI = *Eco*RI, H = *Hind*III, P = *Pst*I.

It is interesting to note that the deletion occurred at a *ClaI* restriction site and the construction of pZS163 involved cloning a *ClaI* fragment into pUC19. This was achieved via construction of a mini-genomic library (Sowerby, 1997). It appears that a DNA fragment arising from a partial *ClaI* digest was cloned to produce pZS163. This is supported by the fact that a single insert fragment is not detected when pZS163 is digested with *ClaI* (data not shown). *ClaI* sites, as identified by sequence analysis of pZS163, exist within the plasmid at nucleotide positions 295 and 1213 (Figure 3.12). It therefore seems rational to presuppose that the original size of the *ClaI* DNA insert fragment cloned into pUC19 was too big to be integrated and remain stable in an unaltered form. A number of *ClaI* sites are clustered in pJT170 and the unstable insert appears to have used one of these sites to recombine into a more stable configuration. This resulted in the loss of a large piece of DNA via the looping out mechanism illustrated in Figure 3.19. Another possibility is that two completely random *ClaI* fragments from the pZS163 chromosome cloned to produce pZS163. The two fragments could have arisen from the 0.8kb *ClaI* fragment surrounding the Tn5 insertion position and another undetermined fragment incorporating the 280bp probe. In this case, the real distance between the two fragments would be unknown, but would imply that the λ and genomic DNA fragments hybridising to the 170bp probe would be more likely to liberate the gene affected by the Tn5 insertion in mutant 163 that resulted in the Nir⁻ phenotype than the 280bp probe fragments.

Alternatively it may have been the presence itself of a nitrite reductase structural or regulatory gene that affected the stability of the pUC19 construct, and due to this the region of DNA containing the gene of interest was lost via the recombination mechanism outlined in Figure 3.19.

Whatever the reason for the deletion to have occurred it can be concluded that the Tn5 insertion position in pZS163 is no different to that in mutant 163 and must be responsible for the Nir⁻ phenotype observed in the mutant strain. However, as a deletion took place upon pZS163 formation this plasmid is of little use in the characterisation of the nitrite reductase or related gene(s) from *N. subflava*. Plasmid pJT170 contains DNA immediately surrounding the Tn5 insertion point, including ~2.0kb of the deleted DNA and ~4kb of DNA found upstream of the 170bp probe that is lacking in pZS163.

Sequencing this DNA to identify any significant ORFs related to denitrification became the focus of this study.

3.4 pJT170 Sequence Analysis

The map of pJT170 shown in Figure 3.16 was determined by digestion of the plasmid with a number of different restriction enzymes and probing the resulting gels with the 170bp probe. It was necessary to obtain an accurate map of pJT170 to enable fragments of DNA directly adjacent to the Tn5 insertion position believed to contain the denitrification gene(s) of interest to be subcloned and sequenced. A number of fragments were subcloned into pBluescript KS⁻ for sequence analysis. These were 0.6kb, 0.4kb and 0.3kb *Cla*I fragments and a 1.5kb *Eco*RV fragment. Figure 3.21 illustrates the positions of these fragments within pJT170 and Table 3.7 summarises the nomenclature of the resulting constructs.

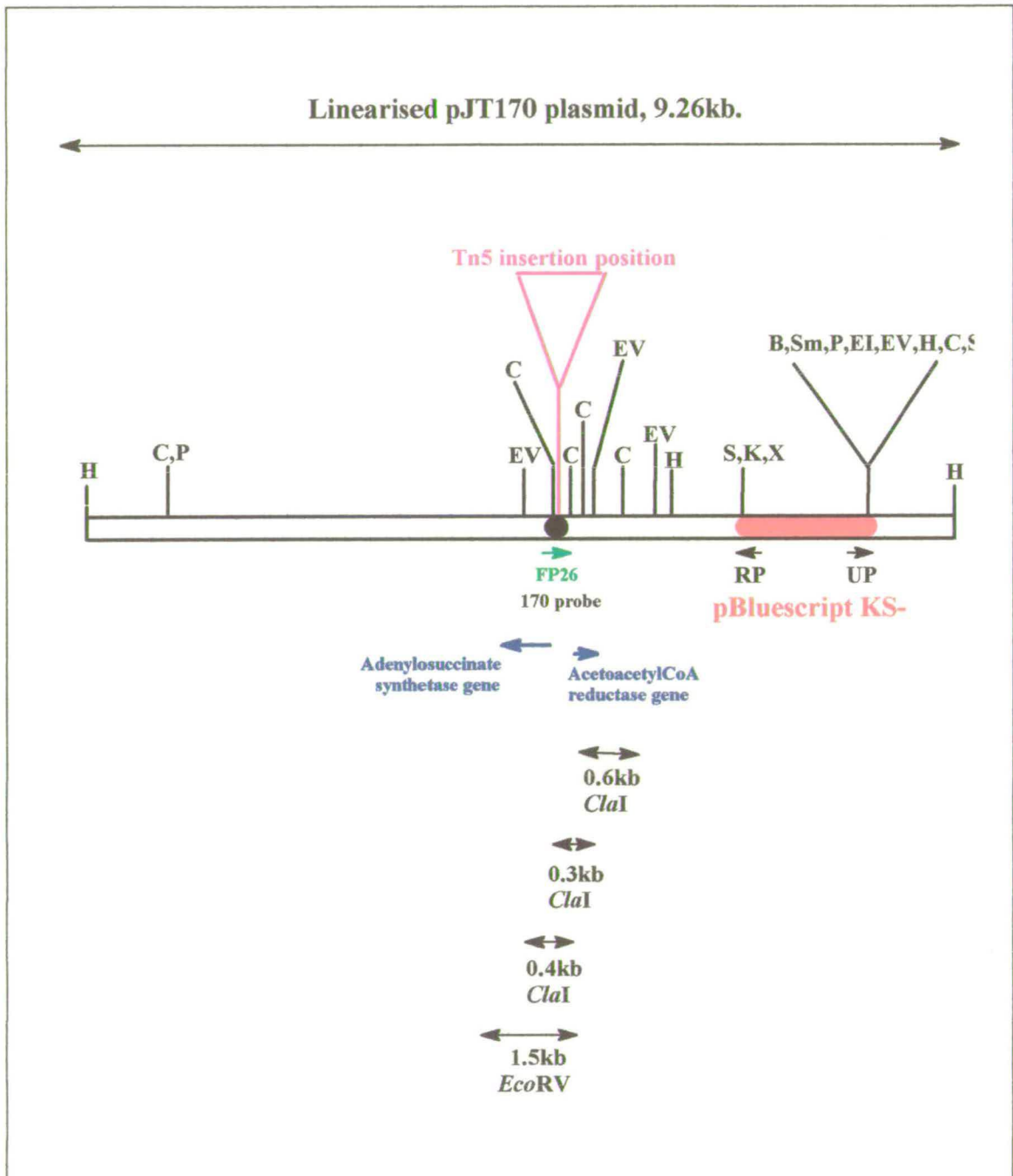


Figure 3.21. A linearised representation, not to scale, of pJT170 to illustrate the positions of the fragments subcloned into pBluescript KS⁻ for sequencing DNA directly adjacent to the 170bp probe region. Key to restriction sites B = *Bam*HI, C = *Cla*I, EI = *Eco*RI, EV = *Eco*RV, H = *Hind*III, K = *Kpn*I, S = *Sal*I, Sm = *Sma*I, X = *Xho* I. The positions of the adenylosuccinate synthetase and acetoacetyl-CoA reductase genes are also illustrated (see text).

Fragment cloned	Plasmid name
0.6kb <i>Cla</i> I	pJT10
0.4kb <i>Cla</i> I	pJT11
0.3kb <i>Cla</i> I	pJT12
1.5kb <i>Eco</i> RV	pJT13

Table 3.7. Summary of the subclones produced from pJT170. See Figure 3.21 for the positions of the fragments within the parent construct. Appendix A3 illustrates the plasmid maps for each of these constructs.

The plasmid inserts were sequenced in both orientations using the M13 Universal and Reverse primers, see Table 3.1 for primer sequences. pJT13 was also sequenced with FP26 from within the 170bp probe region to check the proposed *Cla*I deletion site determined when pJT170 was sequenced with FP26. The sequence data from each of the constructs was aligned and fitted together using the LINEUP and BESTFIT programmes from the GCG9 package to generate a single consensus sequence. This consensus sequence is depicted in Figure 3.23.

```

1   aat t t t c a a a   a a t t a a a a a t   t c a a t t c g t t   t c a a a a g g g g   a t t a n t t t t c
51  c c a a a a c a c c   t t t t a a c c t t   k t t t t c a g m g   g g c c t k t a a c   t t n t t t c c g g
101 a c c g g t t a t t   a g c c g a t a c n   g t a a t n g a t a   a a c g a c a c a t   t g t c c t t g t t
151 c g c g c a a a g c   a t c t a c c g c t   t c t t g a g c c g   c a g g c a t g t c   c t t t t a c a t c
201 g a c a g c c a c c   a c g g a t t c c c   g t c c g a t a g c   a g g a a g g c g g   c c g a t g a a g c
                                     ↓
251 t g c g c a a a t c   a a a a c t g a a t   c c g g c c g c a g   g a c g c g c a c g   t c c g a g c t g g
301 t c g a g a g t a t   c c g c c c a a t c   c g t c a t a c c g   t c c g c c g c g t   g c c a c g g c a t
351 c a t g a c g a t t   t g a a c c a t a a   g c c g c g t a a a   g c a a a c c g g t   g t g g t a a t t a
401 t c a a c g c g c a   a t t c c g a c a a   a t c g a t a t g c   a c t t t t t g a t   t t g g g a a c g c
451 a t c g c a t a c t   g c c t g c a a t t   c a t c c a a g g c   c g c a c t g a c t   g c g g a c a a t t
501 c c g g t a a t t t   c t c t c t a g c c   a c a g t c a g c a   c t t c a c g a c c   g c c a t a c a a t
551 c g g g g c a a c a   a t g a a a a c g c   t t t t g c c c a c   a t a c c g t c a a   g t t t c c a c t c
601 t t t g a c c a a c   t g g c t g a c a g   c t t c g g c a t c   t t t g t c c t g c   a t c g a t g a c a
651 g c a g g a t t g c   c g a t t g c t g c   t c a t c c a a a t   g c g c g g c a t t   t g c t a a a g c a
701 c g g g a a t a c g   c c a a t a t g g c   c c a a t g a a a g   c a a g a c c t c g   c c c a t g t c g g
751 c g a t c t t c a t   g c t t t t c a g c   a t c a a a t c a a   t c a a t t c g a t   a t c c g c t t c a
801 a t g c c t t c c a   a g c c g t a c a t   t t c c g c a c c c   g c c t g c a a a g   g t t c g c g c a t
851 a t t g a g c a a t   c c g t c a g g a c   g c g c a t g a a g   c a c c g a a c c g   g c a t a g c a t a
901 a a c g g t t g a t   g c c t t g g t t g   g c a g a a a g c a   a g t g g g c a t c   a a t a c g c g c c
951 a c c t g c g g c g   t a a t a t c c g c   g c g g a t a c c g   a g c t g a c g g c   c g t a a g c t g
1001 a t c c g c c g c c   g a a a a g c c g g   a c g g a t t g t g   t g c a t g g c g t   c g g t g t c c g g
1051 t t t g a c g g g c   a a c c g c g g t c   a g g t c a a t t a   c a g c g c g t c c   a a g g c g g g g c t
1101 t a a t t g g c g c   g g c a a a a g c c   t t g g c g g t t g   a r t t g g c a a a   a c g t a a a a t t
1151 a c c c g t c a a c   t g c g t g g c

```

Figure 3.22. pJT170 consensus sequence directly surrounding the Tn5 insertion position obtained upon analyses of the pJT10, pJT11, pJT12 and pJT13 subclones. The position of the Tn5 insertion is between the 't' and 'g' residues of the 4bp sequence underlined at position 297bp. The *Clal* deletion site is illustrated in bold type at position 421bp. The last 727bp of this consensus sequence corresponds to new sequence present in the DNA deletion that occurred when pZS163 was constructed.

Due to the 1.5kb size of the *EcoRV* fragment used to construct pJT13 an overlap of Universal and Reverse primed sequence could not be identified. Non-overlapping sequence from the Reverse primed end of pJT13 lies 46bp upstream of the pJT170 consensus sequence and is shown in Figure 3.23. It was decided that separate database searches with these two individual sequences would allow quicker identification of any gene homologies than extending the consensus sequence further via subcloning and sequencing to obtain a single DNA sequence for database searching.

```

1   cagcaacgta ccttgcgcg cttcaaaca caggctttcg cctttgcggt
51  ttttctcgtt caaaacacgg gaaacatcgg taatcatcgg cgtaatgcgc
101 ggtgcaactt tttcaatgac cgccatcacg ttttcaactt ttaccggctc
151 ggcatgtgac aggtggtgca actggacatt gtaataagcc aaaacagctt
201 ccagtttctc aaccagtttt tcaggggtgca acaagtccac cacgcgaatc
251 gcgcgacggg caactttatc ttcataggcc ggaccgatgc cgcgaccggg
301 tgtaccaatt ttgcttttac cgcgggaagc ttcgctgctc tggtaagcgc
351 caatgtggta aggcaaaatc aatgggcagg tcggcgcaat tttcanacgg
401 ccttcgacgt ttttcacacc ggcagcgttc aattcgtcga tttcacccaa
451 caatgcttca ggaanaaacg acaacacctg aagccgatga agcagtccaa
501 agtctcgtgc aaaatgccgc ttggaatcag gcgcaaaatg gtttttttgg
551 ccaccgacga acaaantatg gncsgcattg tggccccctt ggaaacntac
601 tacaccgctg gtttcttccg ccagccaatc aacaatctta acttttgctc
651 ttcatecccc cattgggac cgcattacaaa nacmtttttt aaccataan

```

Figure 3.23. Sequence from pJT13 using the Reverse primer. This sequence lies 46bp upstream of the pJT170 consensus sequence depicted in Figure 3.22.

For each of the two sequences the DNA was translated into all six reading frames. A substantial ORF was identified in reading frame four of pJT13 Reverse primed sequence when this was translated. This protein sequence was searched through the SwissProt database using FASTA from GCG9. Significant homologies to the adenylosuccinate synthetase of a number of different bacteria including *H. influenzae*, *V. parahaemolyticus*, *T. ferroxidans*, *E. coli* and *B. subtilis* were identified, although no denitrification structural or regulatory genes were detected. A typical example of the degree of similarity seen between the pJT13 peptide and adenylosuccinate synthetase is shown in Figure 3.24.

The similarity represented in Figure 3.25 occurs over a small number of amino acids. This does not reduce the validity of the result as this similarity is observed at the very end of the peptide sequence obtained from the pJT170 consensus sequence. It is expected that further downstream sequencing along pJT170 would liberate the rest of the acetoacetyl-CoA reductase peptide homology (refer to Figure 3.21). However this work was not undertaken as it was considered to be outwith the aims of this study.

The acetoacetyl-CoA reductase enzyme is involved in the synthesis of bacterial polymers known as polyhydroxyalkanoic acids or PHAs. These polymers are of interest for their potential commercial exploitation as biodegradable plastics. The acetoacetyl-CoA reductase enzyme is involved in the production of these polymers as it catalyses an intermediate reduction step to produce the immediate precursors needed for polymerisation of PHAs to occur (Schembri *et al.*, 1995). The induction of this enzyme is thought to be linked to phosphate starvation of the cell as high levels of PHAs are found in *Acinetobacter* cells when under nutrient stress. Once cells are shifted to a richer media the production of PHAs is observed to decrease (Peoples and Sinskey, 1989).

No link between the production of PHAs and the denitrification pathway has been established. It has been postulated that the acetoacetyl-CoA reductase genes are under *pho* regulon control (Schembri *et al.*, 1995). In *E. coli* there are more than 20 genes in the *pho* regulon which are expressed co-ordinately when the cells become starved of phosphate as the corresponding peptides are involved in phosphate assimilation and uptake (Wanner, 1987). A consensus sequence is found in the promoter region of all these genes which is known as the phosphate box (Wanner, 1987). It may be that the denitrification genes in *N. subflava* are under a similar control mechanism to the *pho* regulon and this may account for the homology observed in Figure 3.25. However if the homology in Figure 3.25 is studied carefully this assumption would appear to be unlikely as homology to the acetoacetyl-CoA reductase enzyme starts well within the length of the *Acinetobacter* spp. acetoacetyl-CoA reductase peptide at amino acid number 134, a significant distance away from an upstream promoter region of the corresponding DNA. If genes in the *N. subflava* denitrification pathway were under the control of a similar *pho* regulon then it would be

expected that they would become expressed when phosphate was lacking in the cells environment. This would obviously be an alternative control mechanism for denitrification under aerobic conditions unrelated to regulation by anoxia. However *pho* regulon control of the denitrification enzymes is unlikely as most of the genes characterised so far that are subject to regulation by phosphate are concerned with increasing the phosphate concentration of the cell. It has to be conceded that not all of the genes controlled by the *pho* regulon have had a function assigned to them. However, a high degree of similarity is found between corresponding denitrification genes in different organisms, so if any of the unknown *pho* genes were involved in the denitrification process it is likely that they would have demonstrated similarity to these denitrification genes during database searches. Also, no sequence evidence in the upstream promoter regions of any *N. subflava* denitrification genes has been published to allow comparisons to be made to the phosphate box, the *pho* regulon promoter.

It is most likely that there is no relationship between the genes of the denitrification pathway and the PHA biosynthetic pathway. The position of the Tn5 insertion into *N. subflava* genomic DNA has been verified and is thought to be directly responsible for the Nir⁻ phenotype observed in mutant 163 (section 3.3.2.2) and so the similarity identified to the acetoacetyl-CoA reductase gene appears to be purely coincidental. This is supported by the fact that the gene similarity identified between the pJT170 consensus sequence and acetoacetyl-CoA reductase is ~600bp downstream from the Tn5 insertion position.

As no similarity to any structural or regulatory denitrification genes was identified in DNA immediately surrounding the Tn5 insertion site, the Tn5 molecule was deduced to be exerting some downstream effect resulting in the Nir⁻ phenotype observed in mutant 163. Whether this occurs via a global regulatory mechanism, similar to the *pho* regulon, or some other mechanism is unknown at present. (Figure 3.20 illustrates the positions of all the genes identified whilst sequencing pZS163 and pJT170 in relation to the Tn5 insertion position.)

DNA sequence at the very ends of the pJT170 *SalI* insert was also analysed to check for any denitrification gene homologies. Once again each of the sequences obtained was translated into all six reading frames to check for the presence of any

significant ORFs. As none were identified all six reading frames were searched through the SwissProt database using FASTA on GCG9. No significant gene homologies were identified in the searches (data not shown).

Although less than half of pJT170 had been analysed in detail, including the area surrounding the 170bp probe, it was decided that sequencing this plasmid in its entirety would not be productive. Organisms in which the genes of the denitrification pathway have been well characterised have shown the genes to be present in large supraoperon structures over a minimum length of 10kb (Braun and Zumft, 1992; Arai *et al.*, 1995; deBoer *et al.*, 1995). However these are primarily organisms containing cd_1 nitrite reductases and current evidence reports this supraoperon arrangement will not be found in strains containing copper nitrite reductases (Bartnikas *et al.*, 1997; Tosques *et al.*, 1997). However, individual gene clusters of ~3-8kb for each of the denitrification enzymes is expected subject to related regulatory control. From the amount of sequencing carried out on pJT170 one would have expected some nitrite reductase genes to have been identified as this subclone contained DNA immediately next to the genomic insertion position of Tn5. Lack of homologies was taken as evidence that a *N. subflava* nitrite reductase gene cluster was a great distance from the Tn5 insertion point. This suggested that the gene(s) affected by the Tn5 insertion were further within the remainder of the 11.3kb deletion or further upstream of the Tn5 insertion than is present in pJT170.

It was also decided against trying to subclone the next fragments along from the *Sal* I 6.3kb fragment in the λ 170-3 isolate. This could have been achieved as suitably sized DNA fragments existed in λ adjacent to the cloned *Sal* II 6.3kb fragment for use as probes to screen λ 170-3 DNA. This would have provided access to the next sections of DNA along the λ subclone. But if the denitrification gene(s) of interest lay within the deleted DNA they could have been found on any of the remaining 9kb that wasn't cloned into pJT170. To repeatedly subclone, sequence and probe in this way to effectively 'walk' along λ 170-3 DNA until a denitrification gene was found seemed a very long-winded approach with no guarantee that a gene of interest would be located. Also, results presented in section 5.3 suggest that the nitrite reductase gene would not be present in λ 170-3.

Immediately upstream of the Tn5 insertion similarity was identified to the adenylosuccinate synthetase gene. This means that for the Tn5 molecule to be directly causing the Nir⁻ phenotype of mutant 163 chromosomal DNA downstream must be involved. A low degree of similarity ~600bp downstream of the Tn5 insertion was identified to acetoacetyl-CoA genes. A lack of significant homologies in the 600bp of DNA immediately downstream of Tn5 in mutant 163 may be due to the Tn5 molecule inserting into a novel gene, previously uncharacterised and unrelated to denitrification, specific to *N. subflava*. However if this was the case one would have expected to find a good ORF in one of the six reading frames when this sequence was translated. Lack of an ORF indicates that the Tn5 insertion is likely to be within a controlling promoter region, with the ability to distally affect genes for nitrite reductase. This distal affect is a common characteristic of Tn5 insertions (Berg, 1989). Results presented in Chapter Four also support the view that a novel denitrification gene was interrupted by the Tn5 insertion into *N. subflava* chromosomal DNA, resulting in the Nir⁻ phenotype observed in mutant 163.

3.5 Summary

From probing evidence on *N. subflava* wild type and mutant 163 strains it is deduced that an ≥ 11.3 kb deletion occurred when pZS163 was constructed. Initially a large partial *Cla*I fragment cloned into pUC19 which was unstable. The unstable plasmid recombined at one of the *Cla*I sites resulting in the loss of a large (≥ 11.3 kb) DNA fragment. The resulting pZS163 construct contained the Tn5 insertion and chromosomal DNA outwith the deletion site. Sequencing from pZS163 determined the deletion position to be 104bp downstream of the IS50_L end of Tn5. Consequently, further sequencing from this plasmid was not undertaken.

Plasmid pJT170 contained ~4kb of DNA upstream and ~2kb of the deleted DNA immediately downstream of the Tn5 insertion. Sequencing DNA in these two regions did not identify the presence of any denitrification genes. DNA with similarity to the adenylosuccinate synthetase gene was found directly upstream of Tn5. Approximately

600bp downstream from Tn5 an acetoacetyl-CoA reductase gene was located. Although lacking a distinct ORF, the intervening 600bp is proposed to correspond to a specific promoter region, interrupted by Tn5, which distally affects the nitrite reductase gene in mutant 163.

The actual distance of the *nir* gene from the Tn5 insertion position and whether it could have been present on the deleted DNA fragment is unknown. The λ clone, λ 170-3, is believed to contain the Tn5 insertion, the chromosomal DNA deleted during the construction of pZS163 and hence the adenylosuccinate synthetase and acetoacetyl-CoA reductase genes. Although not investigated, it is possible that this λ clone also contains the *nir* gene - although results presented in section 5.3 would suggest otherwise. The significance of the positions of the genes identified upon sequencing pJT170 and pZS163 cannot be established at present. A database of *N. gonorrhoeae* genes exists but these are found on a series of random contigs (http://dna12.chem.ou.edu/cgi-bin/gono_server.pl). Until the contigs become ordered the positions of the DNA topoisomerase, adenylosuccinate synthetase and acetoacetyl-CoA reductase genes in relation to AniA cannot be ascertained. If information such as this had been available at the time of study a more informed decision could have been made when deciding to walk along λ 170-3 to identify the *N. subflava nir* gene.

To summarise, the Tn5 insertion position and **not** a DNA deletion is responsible for the Nir⁻ phenotype observed in *N. subflava* mutant 163. Tn5 achieves this by exerting a distal effect on a downstream nitrite reductase gene - although whether this is a structural or regulatory gene has not been established. Also, probing results with cd₁ and copper nitrite reductase gene probes, and the evidence of the AniA protein in *N. gonorrhoeae*, do not exclude the presence of a divergent membrane bound copper containing nitrite reductase in *N. subflava*.

Chapter Four
Preliminary Nitrite Reductase
Protein Analysis

4.1 Background Information

Work described in this chapter aimed to preliminary characterise the nitrite reductase protein of *N. subflava* to understand the mechanism of reduction and modes of inhibition of the enzyme.

Prior to this study only a limited amount of information on the nitrite reductase protein was available. A number of whole cell assays investigating nitrite reductase electron donors and inhibitory compounds led to the postulation that the enzyme contained copper in its active site (Brew, 1992). This hypothesis has now been investigated further using an activity stain specific for nitrite reductase on native polyacrylamide gels of *N. subflava* whole cell lysates. Previous experiments using this technique have produced contradictory results (Sowerby, 1997; Forsythe, pers. comm.). These conflicting results are discussed in section 4.3 along with staining results obtained during the course of this study. Another reason for the lack of information on the *N. subflava* nitrite reductase protein is that earlier attempts to isolate the protein concentrated on the periplasmic cellular fraction. If the *N. subflava* nitrite reductase is the same as the nitrite reductase (AniA) from *N. gonorrhoeae* then it appears the wrong cellular fractions were being screened for activity. Sequencing results presented in chapter five and results from activity staining on native gels have postulated an outer membrane location for the nitrite reductase protein found in *N. subflava* also.

Due to the lack of nitrite reductase gene sequence produced from mutant 163 and pZS163 (see chapter three) it was decided to check the phenotype of this mutant to confirm it was the same as when first isolated by Brew in 1992. This was necessary to ensure that activity stain and assay results, obtained from cell lysates of mutant 163, were directly resulting from the Tn5 insertion position into the Neisserial chromosome. The results of the growth tests are discussed in section 4.2.

4.2 Growth tests on *N. subflava* B19 and mutant 163

Whole cell nitrite reductase assays were used to check that the *N. subflava* wild type and mutant 163 strains were the same as when originally isolated and characterised by Brew (1992). This was necessary as sequencing DNA immediately adjacent to the Tn5 insertion position in mutant 163 did not liberate the nitrite reductase gene as expected. Although initially developed to assay nitrite reductase activity quantitatively, the assay was used qualitatively to check the phenotypes of *N. subflava* strains B19 and 163. With glucose as electron donor a consistent activity for the reduction of nitrite was demonstrated in *N. subflava* B19, as determined by measuring the degree of colour intensity at 540nm upon the addition of nitrite reagent II. Similarly, zero nitrite reductase activity was detected in mutant 163. This demonstrated that the mutant and wild type strains were the same as when first characterised. It was therefore deduced that the Tn5 insertion was responsible for the Nir⁻ phenotype observed in mutant 163 and that the Tn5 insertion position was the same as when first isolated. The mutant 163 strain was determined to be authentic and was used in further analysis of the nitrite reductase protein of *N. subflava*.

4.3 Native PAGE Analysis of *N. subflava* B19 and Mutant 163

4.3.1 Introduction

Whole cell nitrite reductase assays on mutant 163 showed no activity with a number of different electron donors whereas the endogenous rate of nitrite reductase activity identified in wild type *N. subflava* was determined to be 1130 nmol/min/mg protein (Brew, 1992). Comparison of the nitrite reductase protein(s) in the wild type and mutant 163 strains was achieved using a nitrite reductase specific activity stain for use on native polyacrylamide gels (section 2.3.6). Activity staining *N. subflava* B19 and mutant 163 cell lysates in this way enabled preliminary characterisation of the nitrite reductase enzyme found in this organism to be carried out.

Native proteins separated by PAGE retain their structure and this can be

detected *in situ*. Nitrite reductase enzymes are detected by staining with methyl viologen which becomes colourless when oxidised (Zumft *et al.*, 1987). Under anaerobic conditions it is the nitrite-dependent enzymatic oxidation of methyl viologen that results in decolourisation at the position of the nitrite reductase protein on native gels. This stain fades quickly on the gels and so is difficult to photograph. Counter-staining with triphenyl tetrazolium chloride (TTC) overcomes this problem. The anaerobic conditions required by the activity stain are maintained by keeping the gels submerged in the presence of sodium dithionite. Figure 4.1 outlines the chemistry involved in the nitrite reductase activity stain.

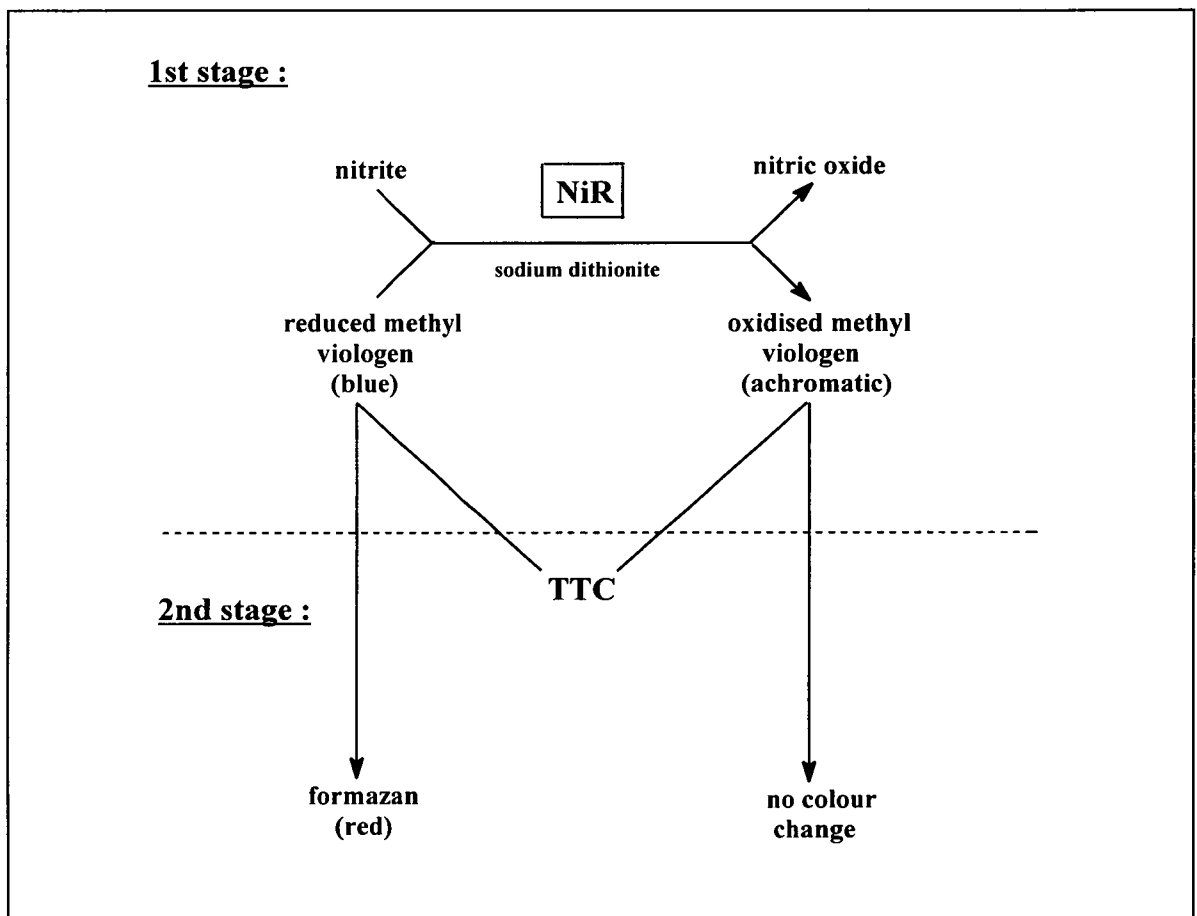
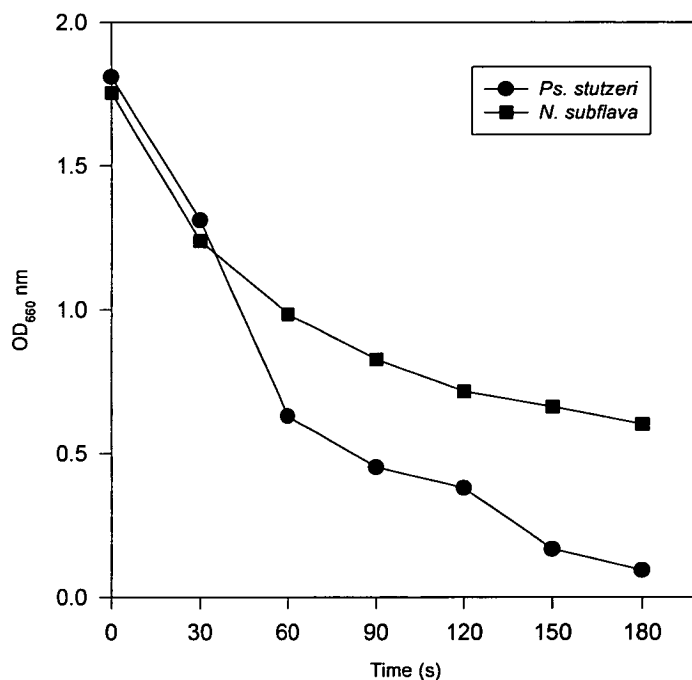


Figure 4.1. Schematic representation of the chemistry involved in the nitrite reductase specific methyl viologen native gel activity stain. Anaerobic conditions are maintained by keeping the gels submerged in the presence sodium dithionite. Key to abbreviations NiR = nitrite reductase, TTC = triphenyl tetrazolium chloride. For experimental protocol see section 2.3.6.

4.3.2 Cell lysis

Initially problems were observed as *N. subflava* cells are very difficult to disrupt. It was doubted whether enough protein would be present in *N. subflava* cell lysates for use in analysis of the nitrite reductase enzyme on native gels. It was previously reported that *N. subflava* could be disrupted upon treatment with lysozyme at a concentration of 50 μ g/ml (Sowerby, 1997). However this could not be repeated in this study. It was found that even after treatment with lysozyme **and** cell sonication for a total of 5 minutes, 30 second bursts with 30 seconds cooling on ice, only ~50% lysis of *N. subflava* was observed (Graph 4.1).



Graph 4.1. Illustration of cell lysis when an overnight anaerobic culture of *N. subflava* B19 was sonicated for 3 minutes, 30 second bursts with 30 seconds cooling on ice. The degree of sonication was monitored by measuring the OD₆₆₀ of the culture after each period of sonication. A similar scale of lysis was observed when aerobically grown *N. subflava* mutant 163 cells were treated in this way. Increasing the sonication time to 5 minutes did not significantly increase the amount of cell lysis (data not shown) however a 5 minute sonication was routinely used to produce cell lysates. For comparison, lysis of a culture of anaerobically grown *Ps. stutzeri* is also included.

Nevertheless, this degree of disruption was found to be sufficient to liberate enough cellular protein for the activity stain to work. Figure 4.2 shows typical protein profiles obtained when whole cell lysates were stained with Coomassie blue after treatment of the cells as described in section 2.3.1. Aliquots of whole cell lysates (15 μ l) were run on the native gels to obtain these protein profiles and this volume was used in subsequent activity staining experiments. As can be seen from Figure 4.2 the protein profiles from the denitrifying strains were significantly fainter than the marker proteins and the quality of the gel photograph is poor because of this. In all lanes faint protein bands were visible throughout the entire length of the gel.

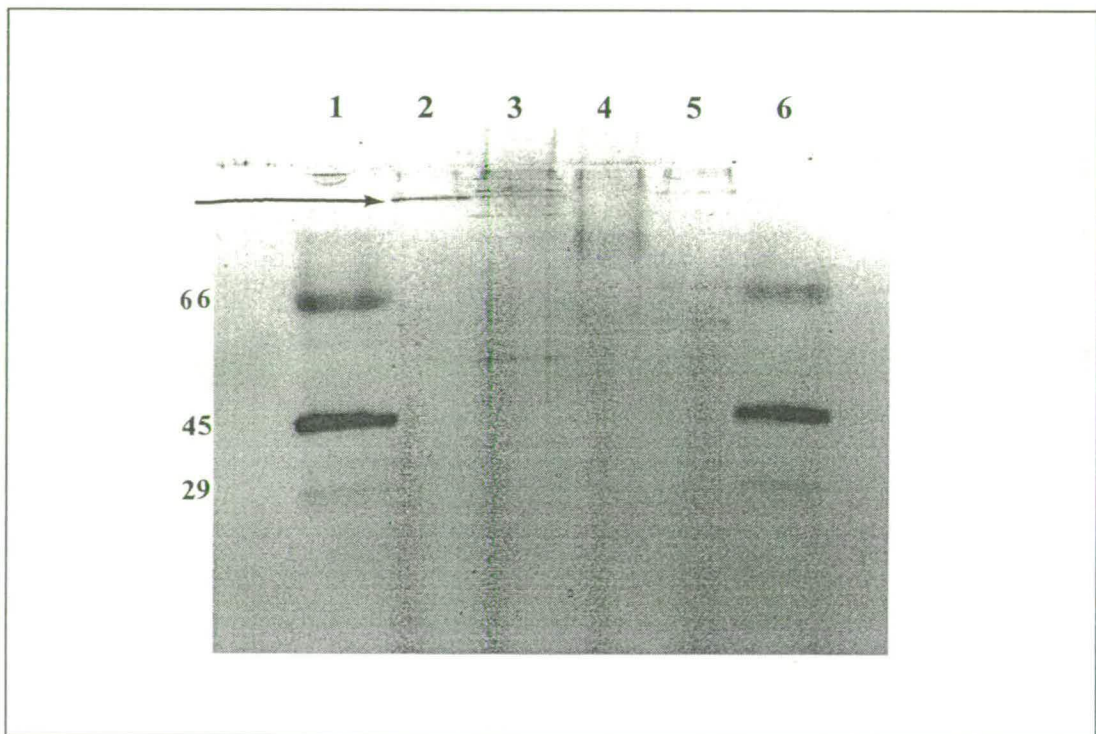


Figure 4.2. Coomassie stained native polyacrylamide gel of whole cell lysates of a number of denitrifying bacteria. Lane 2 - *N. subflava* B19; Lane 3 - *N. subflava* mutant 163; Lane 4 - *Ps.stutzeri*; Lane 5 - *Al. xylooxidans*. Molecular weight markers (kDa) are illustrated on the gel. The arrow points to the protein with apparent nitrite reductase activity as discussed in section 4.3.3.

4.3.3 Nitrite reductase activity stain experiments

4.3.3.1 Comparison of *N. subflava* B19 and mutant 163 strains

To optimise the staining procedure and ensure that any nitrite reductase activity observed was genuine, the denitrifying strains *Ps. stutzeri* and *Al. xylooxidans* were included on some preliminary native gels (data not shown). Once the staining procedure was maximised the nitrite reductase protein of *N. subflava* was investigated. For an initial comparison to be made between the nitrite reductase proteins in both B19 and mutant 163 *N. subflava* strains the B19 cells were grown anaerobically with nitrite whereas mutant 163, which is unable to grow anaerobically, was grown in the presence of oxygen (see section 2.1.9 for details of growth conditions). The cells were disrupted using sonication and the released proteins separated using native PAGE. The gel was activity stained under anaerobic conditions and the results are represented in Figure 4.3.

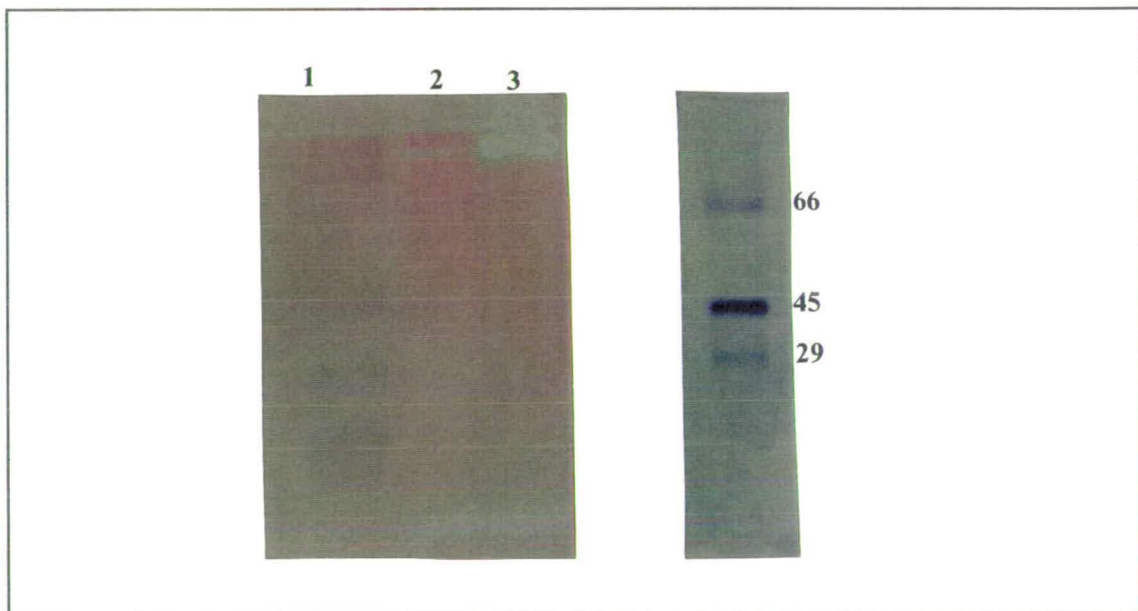


Figure 4.3. Nitrite reductase activity stain of *N. subflava* on a native gel. The areas of decolourisation represent nitrite reductase activity. Lane 1 - Protein markers; Lane 2 - *N. subflava* B19; Lane 3 - *N. subflava* mutant 163. The blue stained gel to the right shows the positions of a second set of molecular markers. The smaller band of clearing in each lane arose due to exposure of the gel to the atmosphere whilst changing some of the stain solutions. It is thought **not** to correspond to nitrite reductase activity.

N. subflava strain B19 showed one faint band with activity at ~200kDa and mutant 163 showed a much thicker band with a greater degree of decolourisation or bleaching at the same molecular size. The very large predicted Mr of the protein with activity in each lane indicated that the nitrite reductase was running as a large protein aggregate on the gels. The Mr of the protein band with activity is 4 × larger than the observed 54kDa molecular weight of the AniA protein monomer from *N. gonorrhoeae* (Hoehn and Clark, 1992). A comparable protein size has been determined for the nitrite reductase enzyme of *N. subflava*. Two dimensional PAGE was used to compare the protein profiles of *N. subflava* B19 and mutant 163 strains. A protein of 45-55 kDa was lacking from the mutant cells but present in the wild type. This protein was postulated to be the nitrite reductase (Sowerby, 1997). Due to an outer membrane location for the AniA protein in *N. gonorrhoeae* it was tentatively assumed that the nitrite reductase protein of *N. subflava* was found associated with the membrane fraction of the cell also. The Mr of the nitrite reductase protein, detected on the native gels, was thought to be so much larger than the Mr predicted from 2D PAGE studies because the proposed association with the outer membrane was not overcome by the sonication step used to obtain cell lysates.

Previous attempts to characterise the nitrite reductase protein on native gels have produced contradictory results. It was reported by Sowerby (1997) that four bands could be identified on native gels which had nitrite reductase activity. Two of these were presumed to be running as large protein aggregates with molecular weights in excess of 150kDa. The two smaller bands did not have a molecular weight assigned to them. Although when these proteins were excised from the native gels and separated via SDS PAGE an apparent molecular weight of 45-55 kDa was reported. This supported work in which Sowerby identified a 45-55 kDa protein as the nitrite reductase enzyme from 2D PAGE. However, these results were contradicted by the work of Forsythe (pers. comm.). He identified a protein band of ~105kDa with nitrite reductase activity plus a megaband of ~250kDa. The nitrite reductase protein was deduced to be running as part of a large protein aggregate in these experiments. A nitrite reductase protein with a different predicted Mr was

identified during this study, but the conclusions drawn are comparable to those deduced by Forsythe. In both cases the nitrite reductase protein is postulated to migrate through native gels as a large membrane/protein aggregate. The only difference between the experiments conducted by Sowerby (1997), Forsythe (pers. comm.) and those reported here, was the method used to obtain cell lysates. Sowerby claimed to disrupt cells using lysozyme alone, but this could not be repeated. (Cell lysis was monitored by measuring the OD of the cell culture at 660nm.) Forsythe sonicated cells for ten minutes. The different results obtained from each of the studies suggest that the nitrite reductase activity profile produced on native gels is dependent on the technique used to obtain cell lysates. From these results it can be inferred that increasing sonication time reduces the degree of association between the outer membrane and the nitrite reductase protein - even though there is no further significant decrease in cell lysis. Results obtained from this study with a sonication time of five minutes demonstrate that nitrite reductase may still be attached to the outer membrane. When the sonication time was increased to ten minutes a degree of disassociation of nitrite reductase appears to have occurred (Forsythe, pers. comm.). The 105kDa molecular mass detected by Forsythe may correspond to a nitrite reductase dimer, as this value is approximately double the 45-55 kDa predicted mass for *N. subflava* nitrite reductase.

The major surprise from the native gel in Figure 4.3 was the greater degree of apparent activity observed in the mutant 163 nitrite reductase enzyme than the B19 strain. It could simply have been argued that much more protein was loaded onto the mutant 163 lane resulting in the observed higher activity. This idea was discounted as Coomassie staining of equivalent native gels showed that in the region where nitrite reductase activity was observed a much thicker protein band was present in the wild type strain than mutant 163 (see Figure 4.2). However, it was unexpected to observe any bleaching at all in the mutant 163 strain, as whole cell nitrite reductase assays on this strain repeatedly showed zero nitrite reductase activity (Brew, 1992; this work). These whole cell assays indicated that an active nitrite reductase enzyme was lacking from the mutant 163 cells. It is possible that the Tn5 insertion into mutant 163 resulted in this strain being unable to allow nitrite to enter into the cell

for reduction as this would give the observed whole cell assay results. Consequently, on native gels, the active nitrite reductase enzyme present in the mutant would be detected when whole cell lysates were separated and screened for activity. Yet this explanation still does not account for the increased nitrite reductase activity observed on native gels in the mutant strain, especially as this strain was grown in the absence of nitrite which is known to induce nitrite reductase activity. It must be mentioned that a degree of nitrite reductase activity detected in mutant 163 on native gels was anticipated, even though it was grown aerobically without the addition of nitrite to the growth medium. Results presented in chapter three suggested that the structural gene for nitrite reductase may not be affected by the Tn5 insertion. This, together with evidence from fermenter studies on nitrite reductase activity which demonstrated a degree of constitutive activity in media lacking nitrite with oxygen tensions as high as 90% (Brew, 1992), implied that a structurally active nitrite reductase enzyme may be detected on native gels in the mutant 163 strain. (Insertion of Tn5 into the structural gene for nitrite reductase would result in a total absence of bleaching on the native gels.) Nitrite reductase activity was observed in mutant 163 but the activity was significantly greater than was detected in the wild type. This suggests the greater nitrite reductase activity detected on the native gels is due to some other gene, which influences nitrite reductase activity, being affected by the Tn5 insertion in mutant 163.

One explanation for the apparent increased nitrite reductase activity in mutant 163 is that the Tn5 insertion has affected a gene for an electron donor in the denitrification pathway. This then blocks a controlled transfer of electrons to the nitrite reductase enzyme. On the native gels this block in the mutant strain is bypassed and the nitrite reductase enzyme is able to reduce nitrite in the activity stain solutions rapidly and without any regulation.

In the denitrification pathway the product of nitrite reduction is nitric oxide. This chemical is highly cyto-toxic and so the enzyme in the denitrification pathway which reduces this to nitrous oxide has a very high reaction rate. Due to the high turnover of the nitric oxide reductase enzyme there would be no regulation on the nitrite reductase protein due to nitric oxide product accumulation. This means that in

wild type *N. subflava* cells the reaction rate of the nitrite reductase enzyme is controlled by the flow of electrons from the cellular UQH₂/UQ pool. In mutant 163 it has been proposed that the flow of electrons from the UQH₂/UQ pool is blocked as a result of the Tn5 insertion accounting for the zero nitrite reductase activity seen in whole cell assays. On native gels this metabolic block in the mutant is by-passed due to an alternative source of electrons to the nitrite reductase enzyme from outwith the denitrification pathway. i.e. from the methyl viologen present in the activity gel solutions which results in the large area of decolourisation observed on the gels. In the wild type strain it is proposed that controlled electron flow to the nitrite reductase enzyme can still occur via the preferred denitrification electron donor.

4.3.3.2 *N. subflava* B19 nitrite reductase activity in the presence of Triton X-100

On native gels nitrite reductase activity was detected at ~200kDa suggesting the protein was running as a large protein aggregate. It was suspected that this is because the nitrite reductase enzyme of *N. subflava* is attached to the outer periplasmic membrane, as is the AniA protein of *N. gonorrhoeae*. It was postulated that the proposed outer membrane interaction had not been overcome during the cell lysis procedure and this was affecting migration through the native gel. With this in mind, the native gel activity stain experiment was repeated with the inclusion of Triton X-100 in the cell sonication procedure and the native gel solutions (see sections 2.3.1 - 2.3.3). The reason for this is that Triton X-100 is a mild detergent which disrupts cell membranes. It was hoped that Triton X-100 would liberate the *N. subflava* nitrite reductase enzyme subunit from its proposed outer membrane attachment position. Consequently a smaller band was expected to show activity than previously observed. However as Figure 4.4 illustrates this was not detected. The same activity pattern was observed as shown in Figure 4.3. Both strains had a single band of activity at ~200kDa with the mutant 163 band having a much greater

degree of bleaching than the band from *N. subflava* B19. It was deduced from this that the Triton X-100 detergent was not strong enough to overcome the interaction between the nitrite reductase enzyme and its proposed outer membrane attachment site. Repeating the experiment with a variety of detergents should eventually enable a different protein profile to be obtained as a consequence of membrane disruption. This would allow identification of the individual nitrite reductase subunit size in *N. subflava* for comparison to the gonococcal AniA enzyme. It could then be determined if the two nitrite reductases from *N. subflava* and *N. gonorrhoeae* are the same. However this work was not pursued within this study due to time limitations. It was not possible to run a whole cell lysate *N. gonorrhoeae* control strain on the native gels as an appropriate strain was not available for this study.

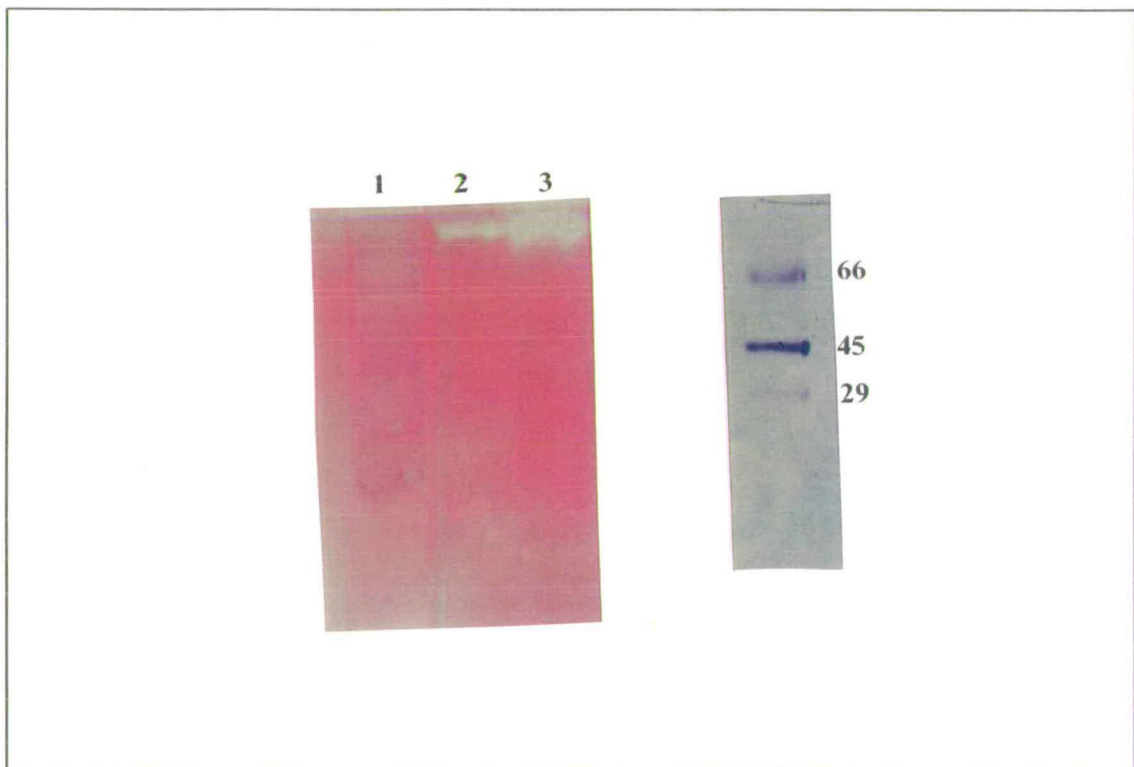


Figure 4.4 Nitrite reductase activity stain of *N. subflava* on a Triton X-100 native gel. The areas of decolourisation represent nitrite reductase activity. Lane 1 - Protein markers; Lane 2 - *N. subflava* B19; Lane 3 - *N. subflava* mutant 163. The blue stained gel to the right shows the positions of a second set of molecular markers.

4.3.3.3 Nitrite reductase activity staining on native gels in the presence of 10mM DDC

Native gel activity staining experiments were repeated with the addition of 10mM DDC in the nitrite buffer. This was to investigate the proposal that the nitrite reductase of *N. subflava* contained copper in its active site (Brew, 1992). *N. subflava* wild type and mutant 163 cell lysates were tested for nitrite reductase activity in the presence of DDC on Triton X-100 native polyacrylamide gels (Figure 4.5). Comparison of Figure 4.4 to Figure 4.5 shows that there is a dramatic decrease in the degree of bleaching observed in mutant 163 in the presence of DDC. Comparison of the Triton X-100 gels also shows that there is reduced nitrite reductase activity in the wild type cell lysates in the presence of DDC. The faint band of nitrite reductase activity detected in both mutant 163 and wild type strains in the presence of DDC was unexpected as total inhibition of nitrite reductase activity was anticipated, with no areas of bleaching on the gel. This anomaly may be explained using evidence from fermenter studies on nitrite reductase activity (Brew, 1992). These studies showed that there is a degree of constitutive nitrite reductase activity whether oxygen is present in the Neisserial growth media or not. The faint bands of activity detected in Figure 4.5 may correspond to this basal level of nitrite reductase activity. Increasing the DDC concentration used in the studies may totally inhibit nitrite reductase activity as detected on native gels, although this was not investigated further as part of this study. The reduced nitrite reductase activity detected in Figure 4.5 is thought not to correspond to a possible second nitrite reductase enzyme, as whole cell nitrite reductase assays consistently show zero nitrite reductase activity in the presence of DDC (Brew, 1992). Despite these observed faint bands with apparent nitrite reductase activity, the nitrite reductase protein from *N. subflava* is proposed to contain copper in its active site. The significant decreases in activity observed on the native gels when DDC was included in the activity stain have been taken as evidence that this is the case.

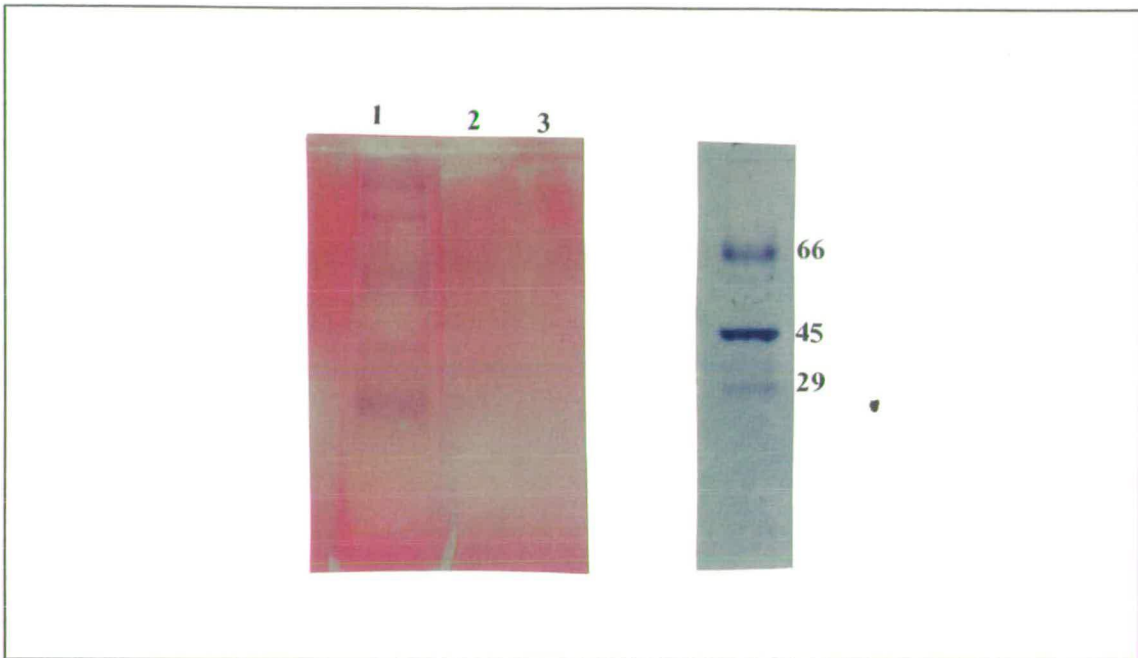


Figure 4.5. Nitrite reductase activity stain of *N. subflava* on a Triton X-100 native gel in the presence of 10mM DDC. The areas of decolourisation represent nitrite reductase activity. Lane 1 - Protein markers; Lane 2 - *N. subflava* B19; Lane 3 - *N. subflava* mutant 163. The blue stained gel to the right shows the positions of a second set of molecular markers.

4.4 Methyl Viologen Nitrite Reductase Assay

This method differs from whole cell assays as nitrite reductase activity is measured independently of the other components of the denitrification electron transfer chain. A French press was used to disrupt the Neisserial cells for this experiment as sonication produced a cell lysate that was too particulate to monitor accurately in the spectrophotometer (data not shown).

Nitrite reductase activity was detected in whole cells of *N. subflava* B19 as 664 nmol/min/mg protein. This value is somewhat lower than the activity detected from the whole cell nitrite reductase assays by Brew (1992): an activity of 1130 nmol/min/mr protein was detected in these assays. This decrease is most likely due to a degree of cellular aeration during the French press procedure which inhibits other reductase enzymes in the anaerobic denitrification pathway. Nevertheless, the methyl viologen nitrite reductase assay was used to investigate which fraction of *N.*

subflava cells had nitrite reductase activity. Unfortunately ambiguous results were obtained.

The membrane fraction of *N. subflava* B19 was extracted as outlined in section 2.3.9. Activity was detected at a rate of 1142 nmol/min/mg protein. Activity was also detected in the cytoplasmic fraction at a rate of 204 nmol/min/mg protein, albeit at a greatly reduced rate. This indicates that most of the nitrite reductase activity has been localised to the membrane fraction. The residual activity detected in the cytoplasm is most likely to result from a small proportion of the enzyme becoming disassociated from its proposed outer membrane attachment position. This suggests that the nitrite reductase enzyme does not exist as an integral outer membrane protein - although the true extent of the association cannot be determined at present. A 50mM Tris buffer (pH 8.0) was used in the preparation of the *N. subflava* membrane fraction. It is possible that the pH and concentration of this buffer disassociated the nitrite reductase enzyme from its outer membrane attachment position. It is anticipated that use of slightly more acidic Tris or phosphate buffers in the membrane extraction procedure will enable nitrite reductase activity to be isolated to the membrane fraction alone. However, due to time constraints this was could not be investigated further.

The detection of a rapid rate for nitrite reduction in the membrane fraction of *N. subflava* cells was seen as an encouraging result. Consequently it was decided to extract and separate the outer and inner membranes using the detergent sarkosyl. Most outer membrane proteins are insoluble in $\geq 0.5\%$ (w/v) sarkosyl, whereas cytoplasmic membranes are completely soluble under these conditions (Gould, 1994). It was hoped that nitrite reductase activity would be detected only in the outer membrane fraction after extraction with sarkosyl. Nitrite reductase activity was found in the outer membrane fraction at a rate of 409 nmol/min/mg protein. However activity was also detected in the inner membrane fraction at a much higher rate of 1441 nmol/min/mg protein. In order for these figures to be directly compared the total activities of each of the cell fractions were calculated. In the membranous fraction of the cell protein was detected at a concentration of 1.42 mg ml^{-1} . This had the capacity to produce 1621nmol nitrite/min. The protein concentrations of the

outer and inner membrane fractions were calculated also. These were determined to be 600 and 266.25 $\mu\text{g ml}^{-1}$ for the inner and outer membrane fractions. The corresponding total enzyme activities were also calculated to be 864 and 110 nmol nitrite/min respectively. These now allowed the total activities of each of the membrane sub-fractions to be calculated as a percentage of the intact membrane. The inner membrane fraction had 53% of the total intact membrane activity, and the outer membrane was found to have 7% of the total activity. This result was disappointing. Ideally, the greater activity should have been observed in the outer membrane fraction. It is postulated that a relatively weak interaction may exist between nitrite reductase and the outer membrane. In the sarkosyl extraction it is proposed that nitrite reductase becomes disassociated from the outer membrane and so does not pellet with the outer membrane fraction in the high spin centrifugation step (section 2.3.10). Consequently the highest nitrite reductase reaction rate is observed in the inner membrane, or supernatant, fraction. As before, it is expected that manipulation of the Tris buffer and sarkosyl concentration used in the extraction procedures will enable outer membrane fractions of *N. subflava* to be isolated which contain all of the cellular nitrite reductase activity. Unfortunately time constraints prevented this work from being conducted as part of this study.

Despite the ambiguous results obtained, detection of a rate of nitrite reductase activity in the outer membrane fraction of *N. subflava* B19 cells was taken as evidence to support an outer membrane location for nitrite reductase in this organism.

A membrane fraction of mutant 163 was also prepared and investigated using the methyl viologen nitrite reductase assay. It was found that both the membrane and cytoplasmic fractions had zero nitrite reductase activity. This seems to directly contradict the findings when mutant 163 was activity stained with methyl viologen on native polyacrylamide gels. It was explained that a proposed block in the electron donor to nitrite reductase was by-passed on the gels accounting for the nitrite reductase activity detected. If this is the case one would expect to observe a rate for nitrite reduction in the mutant 163 membrane fraction, as an active nitrite reductase enzyme would also be present. The lack of nitrite reductase activity observed in the membrane fraction of mutant 163 suggests that the above explanation may not be

true. Therefore an anomaly exists. As methyl viologen donates electrons directly to nitrite reductase it is puzzling why such extremes in nitrite reductase activity are observed from apparently the same enzyme in mutant 163, under the two sets of assay conditions. Obviously further work is needed to understand the true nature of the Tn5 insertion and how it is affecting the phenotype of mutant 163. Time limitations prevented a more detailed characterisation of the nitrite reductase protein from being undertaken during the course of this study.

4.5 Discussion

Based on preliminary protein analysis of *N. subflava* B19 and mutant 163 a possible candidate for the gene disrupted by the Tn5 insertion can be proposed. As discussed in sections 1.4.4 and 1.7 there are a number of different electron transfer proteins involved in the flow of electrons to the terminal reductase enzymes of the denitrification pathway. A primary component of these electron transfer proteins is the cytochrome bc₁ complex which transfers electrons to a number of periplasmic electron carriers and then on to the nitrite, nitric oxide and nitrous oxide reductases respectively (refer to Figures 1.21 and 1.22). In *T. pantotropha* there is evidence to suggest that the first enzyme in the denitrification pathway, nitrate reductase in this case, receives electrons from the quinol pool via a cytochrome bc₁ independent route. In this case UQH₂ is oxidised at the periplasmic face of the cytoplasmic membrane with the release of two protons into the periplasm. Electrons also pass into the periplasm and are used with the two protons to reduce nitrate (Berks *et al.*, 1995). *N. subflava* does not contain a nitrate reductase enzyme so the denitrification pathway in this case starts with the reduction of nitrite. If electron flow in *N. subflava* is comparable to *T. pantotropha* then the route of electron transfer to nitrite reductase may also by-pass the cytochrome bc₁ complex. Interruption of this alternative flow of electrons due to the Tn5 insertion into a structural gene for the proposed electron carrier protein would result in the Nir⁻ phenotype of mutant 163. Only electron flow to the nitrite reductase enzyme is blocked via this mechanism in mutant 163 as work

by Brew (1992) demonstrated that the nitrous oxide reductase enzyme still had activity. It is proposed that electron flow in the denitrification pathway of *N. subflava* occurs as illustrated in Figure 4.6. It can be seen from this diagram that the arrangement of the *N. subflava* denitrification oxido-reductase enzymes is unique as the nitrite reductase and its electron donor protein are proposed to exist in the outer membrane, and not the periplasm as is the case with other denitrifying organisms. Denitrification in *N. subflava* effectively spans the periplasmic space. For electrons to pass from the UQH₂ pool in the cytoplasmic membrane to the outer membrane attached nitrite reductase electron donor, soluble electron transfer protein(s) must be present in the periplasm by-passing the cytochrome bc₁ complex. If the membrane bound nitrite reductase electron donor or the proposed soluble protein(s) transferring electrons to this cannot function, the activity of the nitrite reductase enzyme will be affected. Figure 4.6 shows that the nitrite reductase enzyme receives electrons from its proposed unknown membrane bound electron donor whereas the nitric oxide and nitrous oxide reductases receive electrons from a number of periplasmic electron donors via the cytochrome bc₁ complex. Interruption of the entire denitrification pathway due to a block at this uncharacterised nitrite reductase electron donor would not occur as electrons can still flow to the other terminal nitrogen reductases via cytochrome bc₁ and the periplasmic reductases.

Despite the contradictory results obtained from nitrite reductase activity assays on the mutant 163 membrane fraction, there is substantial evidence to suggest that the alternative electron donor to nitrite reductase is attached to the outer periplasmic membrane in close proximity to nitrite reductase. This may explain why there is no increase in B19 nitrite reductase activity when whole cell lysates of this strain were run on native gels. In *N. subflava* B19, if both functional electron donor and nitrite reductase proteins were running in the same protein aggregate on native gels, the donor protein would be able to transfer electrons directly to the nitrite reductase at a controlled rate due to the close proximity of the two proteins. In the mutant 163 strain cellular donation of electrons to nitrite reductase via this unknown electron donor is obstructed. The observed increase in electron flow seen on the native gels resulting in the larger area of nitrite reductase activity must come from an

external source; the methyl viologen reducing agent in the native gel activity stain solutions fulfils this role. This helps to explain why it is believed that the Tn5 insertion has affected a gene for a membrane bound nitrite reductase electron donor. If one of the transferring periplasmic donor proteins had been affected the activity of both *N. subflava* B19 and mutant 163 nitrite reductases would have appeared the same on the native gels. In this case the affected electron donor would not run as part of the nitrite reductase protein/membrane aggregate as it is soluble. Consequently electron flow to the functional nitrite reductase would come from an alternate source as mentioned previously. The result on the native gels would be that both B19 and mutant 163 strains would have the same nitrite reductase activity. However, the activity of the B19 nitrite reductase on native gels was observed to be significantly less than the mutant 163 strain. In this instance the membrane bound electron donor is still active and electrons are passed to nitrite reductase via this protein at a controlled rate. Insertion of Tn5 into the gene for the membrane bound nitrite reductase electron donor blocks the ability of the membrane bound electron donor to receive and pass on electrons. Consequently, an unregulated flow of electrons reach the nitrite reductase enzyme from an external source as mentioned before.

A membrane bound azurin electron donor to the AniA protein of *N. gonorrhoeae* is proposed to exist (Gotschlich and Seiff, 1987; Berks *et al.*, 1995). However the membrane bound donor protein in *N. subflava* may differ greatly to that in the gonococcal strain as no homologies to azurin proteins were identified upon sequencing and database searching DNA surrounding the Tn5 insertion in both pZS163 and pJT170 (see sections 3.3.1 and 3.4). Also, attempts to prepare a PCR fragment of *N. subflava* DNA containing the azurin gene were unsuccessful (Lambert, 1997). Degenerate primers based on known azurin gene sequences amplified a predicted 260bp fragment from *N. gonorrhoeae* but not *N. subflava*. However, the Tn5 insertion may also be within a controlling promoter region which can distally affect the gene for the proposed membrane bound nitrite reductase electron donor, a characteristic common of Tn5 insertions (Berg 1989). This would account for the lack of ORFs identified in DNA directly adjacent to the Tn5 insertion

in mutant 163 (as discussed in chapter three).

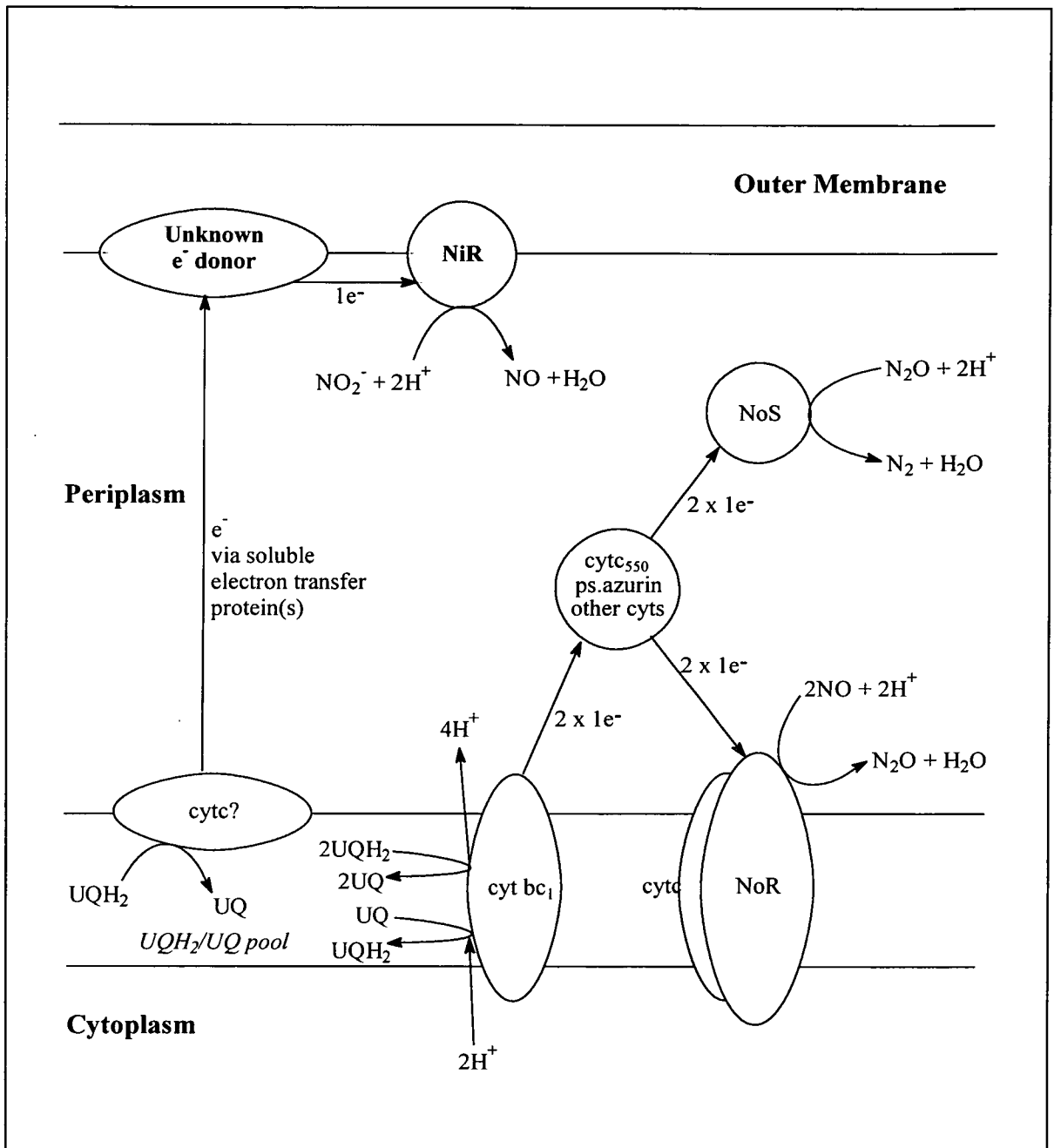


Figure 4.6. Hypothetical organisation of the electron transport system in the denitrification pathway of *N. subflava*. The position of the nitrite reductase and its unknown electron donor are presumed as there is no definitive evidence to place either of them in the outer periplasmic membrane. The interaction between nitrite reductase and the outer membrane is assumed to be relatively weak in nature. If correct this would be a novel denitrification pathway spanning the periplasm. Key to abbreviations NiR = nitrite reductase, NoR = nitric oxide reductase, NoS = nitrous oxide reductase, cyt bc₁ = cytochrome bc₁ complex, cyt c = cytochrome c, cyt c₅₅₀ = cytochrome c₅₅₀, ps.azurin = pseudoazurin.

4.6 Summary

Results from whole cell nitrite reductase assays corroborated the *N. subflava* B19 and mutant 163 phenotypes characterised by Brew (1992). Despite the lack of *nir* gene sequence from pZS163 and mutant 163, the Tn5 insertion into the *N. subflava* chromosome is believed to be responsible for the lack of nitrite reductase activity observed in mutant 163.

Investigations into nitrite reductase activity on native polyacrylamide gels, and evidence of an outer membrane location for the gonococcal nitrite reductase, have enabled an outer membrane location for the nitrite reductase protein of *N. subflava* to be proposed. An outer membrane attachment has also been postulated for the electron donor protein to nitrite reductase (Figure 4.6). The Tn5 insertion that causes the Nir⁻ phenotype in mutant 163 is believed to affect the gene for the electron donor to nitrite reductase resulting in an inactive donor protein and an apparent lack of nitrite reductase activity in mutant 163 cells.

Preliminary investigations into identifying which cellular fraction of *N. subflava* has nitrite reductase activity produced ambiguous results. Activity was identified in the outer membrane fraction, but greater activity was found in the inner membrane fraction too. An explanation has been offered for these unexpected results, see section 4.4, and this is currently being investigated further in the lab. Nevertheless, an outer membrane location for nitrite reductase in *N. subflava* is proposed. Current evidence suggests that the degree of interaction between the outer membrane and nitrite reductase is moderately weak. i.e nitrite reductase is not believed to be found as an integral outer membrane protein.

Activity stain experiments on native gels with the inhibitor DDC have demonstrated that the nitrite reductase protein of *N. subflava* may contain copper in its active site.

Chapter Five
PCR Amplification of the
Nitrite Reductase Gene

5.1 Background Information

Nitrite reductases from various denitrifying organisms fall into two main categories: those which contain cytochrome cd_1 and those which contain copper. Other nitrite reductase enzymes are known to exist and these are briefly summarised in section 1.4. The chemical diethyldithiocarbamate (DDC) is a well known inhibitor of the copper nitrite reductase enzymes (Shapleigh and Payne, 1985). Whole cell nitrite reductase assays of *N. subflava* B19 demonstrated that the enzyme was inhibited in the presence of DDC indicating the presence of a copper containing enzyme (Brew, 1992). The copper nitrite reductases characterised so far are highly homologous, particularly around the active site of the enzyme. Recently a new copper nitrite reductase was discovered from *N. gonorrhoeae* (Mellies *et al.*, 1997). This differs from the other copper enzymes as it has a much lower degree of similarity, ~30% compared to the ~80% observed previously. (Figure 1.13 in the introduction demonstrates this similarity more clearly.) The greatest degree of similarity between the gonococcal enzyme and the other copper nitrite reductases also occurs over the active site of the enzyme where the copper ligands are bound. As *N. subflava* and *N. gonorrhoeae* are found in the same genus it was assumed that the postulated copper nitrite reductase in *N. subflava* would be more homologous to the gonococcal enzyme. It was due to this that the PCR strategy outlined in section 5.2 was devised.

It is worth mentioning at this stage that there was an initial degree of reluctance in using PCR as a genetic tool to identify the *N. subflava* nitrite reductase gene as a previous attempt using a similar PCR approach was unsuccessful in amplifying the gene (Sowerby, 1997).

5.2 PCR Strategy

5.2.1 Primer design

The sequences of a number of copper nitrite reductase peptides were aligned using the PILEUP programme on GCG9. The strains used were *A. cycloclastes*, *Al. faecalis*, *Pseudomonas* sp. G-179, *Ps. aeruginosa*, and *N. gonorrhoeae*. Shorter peptide sequences of ~10 amino acids were searched for along the length of this alignment to identify the regions with the highest degree of conservation. Typically these regions were found surrounding the active sites of the enzymes where the copper ligands were bound. Two regions that looked particularly promising were detected and were used in the design of degenerate PCR primers. The first of these primer positions was located at amino acid number 135 and the second at amino acid number 267 in the nitrite reductase peptide alignment. Figure 5.1 shows this peptide alignment in detail highlighting the positions of the two primers. As these primers were degenerate there was often a choice of bases present at specific points along the primer length due to the 'wobble' nature of the triplet genetic code. To ensure the degeneracy of the primers was as low as possible codon usage of *N. gonorrhoeae* was used to reduce the number of codons present for each amino acid where appropriate. This was based on the assumption that the nitrite reductase in *N. subflava* would be more like the nitrite reductase in *N. gonorrhoeae* than the other more typical copper enzymes as both organisms are in the genus *Neisseria*. To ease cloning of any subsequent PCR products the primers had restriction sites engineered onto their 5' ends. The primer at amino acid 135 (AniA1) had an *EcoRI* site added onto the 5' end and the primer at amino acid 267 (AniA2) had a *BamHI* site added. The concept behind the primer design is outlined in Figures 5.2a and 5.2b and the table of codon usage in *N. gonorrhoeae* is depicted in Figure 5.3.

```

1
nir_achcy .....A AGAAPV.... .....DIS
nir_alcfa .MAEQMQISR RTILAGAALA GALAPVLATT SAWGQGAVRK ...ATAAEIA
nir_psesp .MSEQFRLTR RSMLAGAAVA GALAPVVTSTV AHAEGGGIKT NSAATAANIA
nir_psaer .....MSVF RSVLGACVLL GSCASSL... .....ALAGGAE
panl_ngon MKRQALAAMI ASLFALAACG GEQAAQAPAE TPAASAEAAAS SAAQATAETP

51
nir_achcy TLPRVKVDLV KPPFVHAHDQ VAKTGPRVVE FTMTIEEKKL VIDREGTEIH
nir_alcfa ALPRQKVELV DPPFVHAHSQ VAEGGPKVVE FTMVIEEKKI VIDDAGTEVH
nir_psesp TLERVKVELV KPPFVHAHTQ KAEGEPKVVE FKMTIQEKKI VVDDKGTEVH
nir_psaer GLQRVKVDLV APPLVHPHEQ VVSGPPKVQ FRMSIEEKKM VIDDQGTTLQ
panl_ngon AGELPVIDAV TTHAPEVPPA IDRDPYAKVR VKMETVEKTM KMDD.GVEYR

I II
101
nir_achcy AMTFNGSVPG PLMVVHENDY VELRLINPDT NTLLHNIDFH AA.....T
nir_alcfa AMAFNGTVPG PLMVVHQDDY LELTLINPET NTLMHNIDFH AA.....T
nir_psesp AMTFDGSVPG PMMIVHQDDY VELTLVNPDT NELQHNIDFH SA.....T
nir_psaer AMTFNGSMPG PTLVVHEGDY IELTLVNPAT NSMPHNVD FH AA.....T
panl_ngon YWTFDGDVPG RMIRVREGDT VEVEFSNNPS STVPHNVD FH AA.....T

151
nir_achcy GALGGGALTQ VNPGEETTLR FKATKPGVFV YHCAPEGMVP WHVTSGMNGA
nir_alcfa GALGGGGLTE INPGEKTILR FKATKPGVFV YHCAPPGMVP WHVVSGMNGA
nir_psesp GALGGGALTQ VNPGD TAVLR FKATKAGVFV YHCAPAGMVP WHVTSGMNGA
nir_psaer GALGGAGLTQ VVPGQEVVLR FKADRSCTFV YHCAPQGMVP WHVVSGMNGA
panl_ngon GQGGGAAATF TAPGRTSTFS FKALQPGLYI YHCAVAP.VG MHIANGMYGL

201
nir_achcy IMVLP RDGLK DEKGQPLTYD KIYYVGEQDF YVPKDEAGNY KKYETPGEAY
nir_alcfa IMVLP REGLH DGKGKALTYD KIYYVGEQDF YVPRDENGKY KKYEAPGDAY
nir_psesp IMVLP RDGLK DHKGHELVDY KVVYVGEQDF YVPKDENGKF KKYESAGEAY
nir_psaer LMVLP RDGLR DPQGKLLHYD RVTYIGESDL YIPKDKDGHY KDYPDLASSY
panl_ngon ILVEPKGLP KV.....D KEFYIVQGDF YTKGKKGAQG LQPFDMDKAV

251
nir_achcy EDAVKAMRTL ..TPTHIVFN GAVGALT... ..GDHALT AAVGE..RVL
nir_alcfa EDTVKVMRTL ..TPTHVVFN GAVGALT... ..GDKAMT AAVGE..KVL
nir_psesp PDVLEAMKTL ..TPTHVVFN GAVGALT... ..GDNALQ AKVGD..RVL
nir_psaer QDTRAVMRTL ..TPSHVVFN GRVGALT... ..GANALT SKVGE..SVL
panl_ngon AEQ..... ..PEYVVFN GHVGSIA... ..GDNALK AKAGETVRMY

301
nir_achcy VVHSQANRDT RPHL..... ..IGG HGDYVW.ATG
nir_alcfa IVHSQANRDT RPHL..... ..IGG HGDYVW.ATG
nir_psesp ILHSQANRDT RPHL..... ..IGG HGDYVW.ATG
nir_psaer FIHSQANRDS RPHL..... ..IGG HGDVWV.TTG
panl_ngon VGNGGPNLVS SFHV..... ..IGE IFDKVYVEGG

```

	351			II	400
nir_achcy	KFRNPPDLQ	ETWLIPGGTA	GAIFYTFRQP	GVYAYVNHNL	IEAFELGAAG
nir_alcfa	KFNTPPDVDQ	ETWFIPGGAA	GAIFYTFQQP	GIYAYVNHNL	IEAFELGAAA
nir_psesp	KFANPPELDQ	ETWFIPGGAA	GAAYYTFQQP	GIYAYVNHNL	IEAFELGAAG
nir_psaer	KFANPPQRNM	ETWFIPGGSA	VAALYTFKQP	GTYYVLSHNL	IEAMELGALA
panl_ngon	KLINE...NV	QSTIVPAGGS	AIVEFKVDIP	GSYTLVDHSI	FRAFNGKALG
	401				450
nir_achcy	HFKVTGEWND	DLMTSVVKPA	SM.....
nir_alcfa	HFKVTGEWND	DLMTSVLAPS	GT.....
nir_psesp	HFKVTGDWND	DLMTAVVSPT	SG.....
nir_psaer	QIKVEGQWDD	DLMTQVKAPG	PIVEPKQ...
panl_ngon	QLKVEGAENP	EIMTQKLSDT	AYAGSGAASA	PAASAPAASA	PAASASEKSV
	451				500
nir_achcy
nir_alcfa
nir_psesp
nir_psaer
panl_ngon	Y.....

Figure 5.1. PILEUP of the copper nitrite reductase peptides from a number of different denitrifying organisms. The positions of the two primers used in the nitrite reductase PCR are underlined and the positions of the type I and type II copper binding ligands are shown in bold. Key to organisms nir_achcy = *A. cycloclastes*, nir_alcfa = *Al. faecalis*, nir_psesp = *Pseudomonas* sp. G-179, nir_psaer = *Ps. aeruginosa*, panl_ngon = *N. gonorrhoeae*.

AniA1 primer:							peptide sequence
H	N	V	D	F	H	A	
cac	aac	gtc	gac	ttc	cac	gc	possible codons
t	t	a	t	t	t		
		g					
		t					
2	2	4	2	2	2	1	
							128
							degeneracy
5' - [<u>GGAATTC</u> CAY AAY GTN GAY TTY CAY GC] -3'							AniA1 primer
<i>EcoRI</i>							

Figure 5.2a. Diagram of the design of the AniA1 PCR primer. The degeneracy of this primer was not reduced further when the codon usage table in Figure 5.3 was consulted despite a degeneracy of four from the valine residue. The *EcoRI* restriction site was added to the 5' end of the primer. The choice of restriction enzyme was dependent on its requirement for a small number of nucleotides at the end of the cleavage site to ensure efficient cutting was obtained and that the T_m of the primer wasn't greatly affected. Key to nucleotide abbreviations N= a/c/g/t, Y= c/t.

AniA2 primer:							
V	V	F	N	G	H	V	peptide sequence
gtt	gtt	ttc	aac	ggt	cac	g	possible codons
c	c	t	t	c	t		
a	a			a			
g	g			g			
4	4	2	2	4	2	1	
						512	degeneracy
2	2			2	2	1	
						16	reduced degeneracy (due to codon usage)
c	gtg	acc	gtt	gaa	tac	gac	reverse & complement
a	g				g	c	
5' - [CCGGATCC RTG RCC GTT GAA KAC SAC] - 3'							AniA2 primer
<i>Bam</i> HI							

Figure 5.2b. Diagram of the design of the AniA2 PCR primer. The degeneracy of this primer was reduced from 512 to 16 using the codon usage table in Figure 5.3. This was achieved by reducing the number of codons for valine from 4 to 2 as the 'gta' and 'gtg' valine codons are less frequently used in *N. gonorrhoeae* and so were omitted from AniA2. The number of codons for glycine were also reduced from 4 to 2 after consultation with the codon usage table. As DNA produced from this primer needed to meet DNA extended from AniA1, the primer sequence had to be reversed and complemented prior to the addition of the *Bam*HI restriction site to the 5' end. The choice of restriction enzyme was dependent on its requirement for a small number of nucleotides at the end of the cleavage site to ensure efficient cutting was obtained and that the T_m of the primer wasn't greatly affected. Key to nucleotide abbreviations R = a/g, K = g/t, S = c/g.

P UUU 16.8 (1341)	S UCU 8.5 (682)	Y UAU 14.0 (1121)	C UGU 2.1 (168)
P UUC 23.0 (1840)	S UCC 17.4 (1387)	Y UAC 20.3 (1618)	C UGC 5.6 (451)
L UUA 5.4 (435)	S UCA 5.2 (416)	* UAA 1.6 (128)	* UGA 1.0 (79)
L UUG 27.3 (2178)	S UCG 9.4 (750)	* UAG 0.2 (12)	W UGG 11.0 (881)
L CUU 8.6 (688)	P CCU 7.3 (581)	H CAU 7.6 (609)	R CGU 9.8 (780)
L CUC 10.7 (858)	P CCC 14.1 (1124)	H CAC 13.0 (1040)	R CGC 27.6 (2205)
L CUA 1.4 (115)	P CCA 3.2 (255)	Q CAA 25.7 (2050)	R CGA 3.0 (236)
L CUG 29.3 (2338)	P CCG 15.5 (1241)	Q CAG 15.0 (1195)	R CGG 6.8 (547)
I AUU 18.7 (1495)	T ACU 7.7 (616)	N AAU 17.3 (1385)	S AGU 4.8 (387)
I AUC 28.9 (2305)	T ACC 29.8 (2383)	N AAC 30.6 (2444)	S AGC 18.0 (1438)
I AUA 4.4 (349)	T ACA 7.0 (563)	L AAA 53.4 (4267)	R AGA 3.5 (277)
M AUG 19.8 (1578)	T ACG 12.2 (974)	L AAG 10.9 (874)	R AGG 4.0 (323)
V GUU 18.4 (1468)	A GCU 10.1 (809)	D GAU 22.1 (1763)	G GGU 18.2 (1455)
V GUC 22.8 (1823)	A GCC 44.3 (3536)	D GAC 31.9 (2547)	G GGC 51.5 (4114)
V GUA 11.9 (950)	A GCA 19.1 (1526)	E GAA 46.3 (3701)	G GGA 8.7 (697)
V GUG 15.7 (1252)	A GCG 22.9 (1833)	E GAG 10.6 (846)	G GGG 6.9 (555)

fields: [amino acid] [triplet] [frequency: per thousand] ([number])

Figure 5.3. Codon usage table of *N. gonorrhoeae*. This table was down loaded from CUTG (Codon Usage Tabulated from Genbank). Website: <http://www.dna.affrc.go.jp/~nakamura/CUTG.html>. A total number of 222 coding sequences (79882 codons) were used in the construction of this table.

The annealing temperatures of the two primers were determined to be 62°C (AniA1) and 66°C (AniA2) using the formula described in section 2.2.24. Consequently the PCR thermocycle was designed using these annealing temperatures as a guide for the denaturation temperature. As this PCR method involved use of degenerate primers, the first few thermocycles were executed with a lower annealing temperature (section 2.2.24). A product size of ~350bp was expected from this PCR and this was used to calculate the elongation time of the PCR thermocycle (section 2.2.24). The reaction profile for the degenerate PCR to amplify the nitrite reductase gene of *N. subflava* is represented below:

		First cycle	Intermediate cycle	Last cycle
Denaturation	(94°C)	5 minutes	1 minute	1 minute
Annealing (56°C : 4 cycles)				
	(62°C : 29 cycles)	1 minute	1 minute	1 minute
Elongation	(72°C)	30 seconds	1 minute	10 minutes

for a total of 35 cycles.

5.2.2 PCR results

Chromosomal DNA from *N. subflava* B19 used as the template for the PCR amplification produced a major DNA fragment at the expected 350bp size. A number of other larger bands were also produced indicating that the primers had been able to anneal to a number of different sites in the chromosomal DNA but these were minor products when compared to the bright 350bp band. Figure 5.4 shows the results of the degenerate nitrite reductase PCR when analysed on a 2% agarose gel.

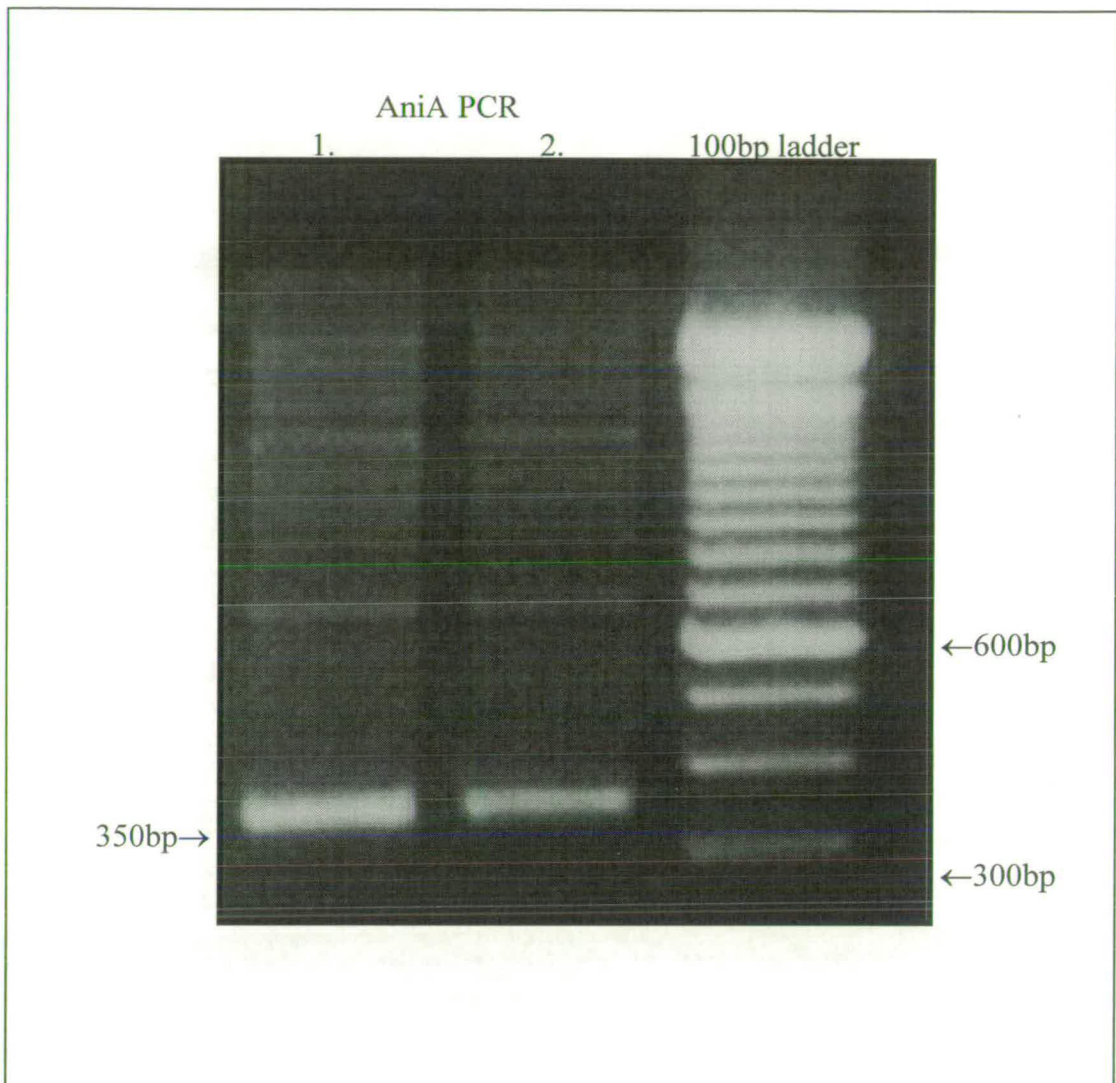


Figure 5.4. Agarose gel electrophoresis of the AniA PCR. A major band of 350bp amplified as expected and this is highlighted. The 100bp ladder shows DNA bands increasing in 100bp increments from the lowest visible 300bp band. The band with the brighter intensity in the ladder corresponds to 600bp. The AniA PCRs in lanes 1 and 2 differ only in the Mg^{2+} concentration. Lane one had $1\mu l$ 25mM $MgSO_4$ added to the reaction mix whereas lane 2 had $2\mu l$ added. As $1\mu l$ was observed to give increased yields of the 350bp product this was used in subsequent PCRs.

The 350bp PCR product purified from the agarose gel as described in section 2.2.11 was cloned into pBluescript KS⁻ after digestion with *Bam*HI and *Eco*RI. The resulting construct was named pANIA350 and is represented in Figure 5.5.

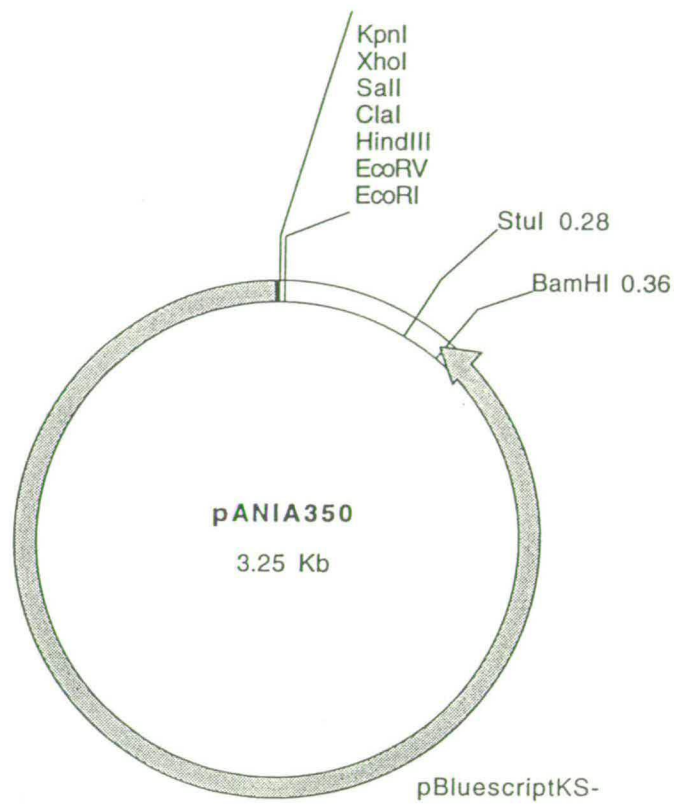


Figure 5.5 Plasmid map of pANIA350.

5.2.3 pANIA350 sequence analysis

The map of pANIA350 shown in Figure 5.5 was determined by sequence analysis of the plasmid. The plasmid contains a 350bp insert and this was sequenced in both orientations using the M13 Universal and Reverse primers as these primers anneal to the pBluescript KS⁺ polylinker. The primer sequences are listed in Table 3.1. When the DNA was translated an ORF was identified in reading frame two that corresponded almost exactly to the AniA nitrite reductase peptide of *N. gonorrhoeae*. Of the 116 amino acids in this ORF only 8 differed to the gonococcal AniA protein and all copper binding ligands present in this region were conserved. After extensive sequence analyses these different amino acids were determined to be genuine and not due to sequencing errors. Figure 5.6 shows the DNA sequence obtained from the pANIA350 insert along with the ORF identified in reading frame two. The positions of the AniA1 and AniA2 sequencing primers are also illustrated as are the amino acid discrepancies and the positions of the conserved copper binding ligands. Figure 5.7 shows an alignment of this ORF to the AniA nitrite reductase from *N. gonorrhoeae*. This was achieved using the BESTFIT programme on GCG9. The ORF identified in pANIA350 was also used to search the SwissProt database using FASTA. Homologies were detected to copper nitrite reductases from a number of different organisms including *Pseudomonas* sp. G-179, *A. cycloclastes*, *Al. faecalis*, *Ps. aureofaciens* and *R. sphaeroides*. The degree of similarity between the pANIA350 ORF and these nitrite reductases was significantly lower than between the pANIA350 ORF and the gonococcal enzyme, although this was expected. Typical homologies observed were between 36.4% and 40% identity over ~ 130 amino acids. Figures 5.8a and 5.8b illustrate examples of these peptide homologies to the *A. cycloclastes* and *Al. faecalis* nitrite reductases. In both examples the type I and type II copper binding ligands are conserved.

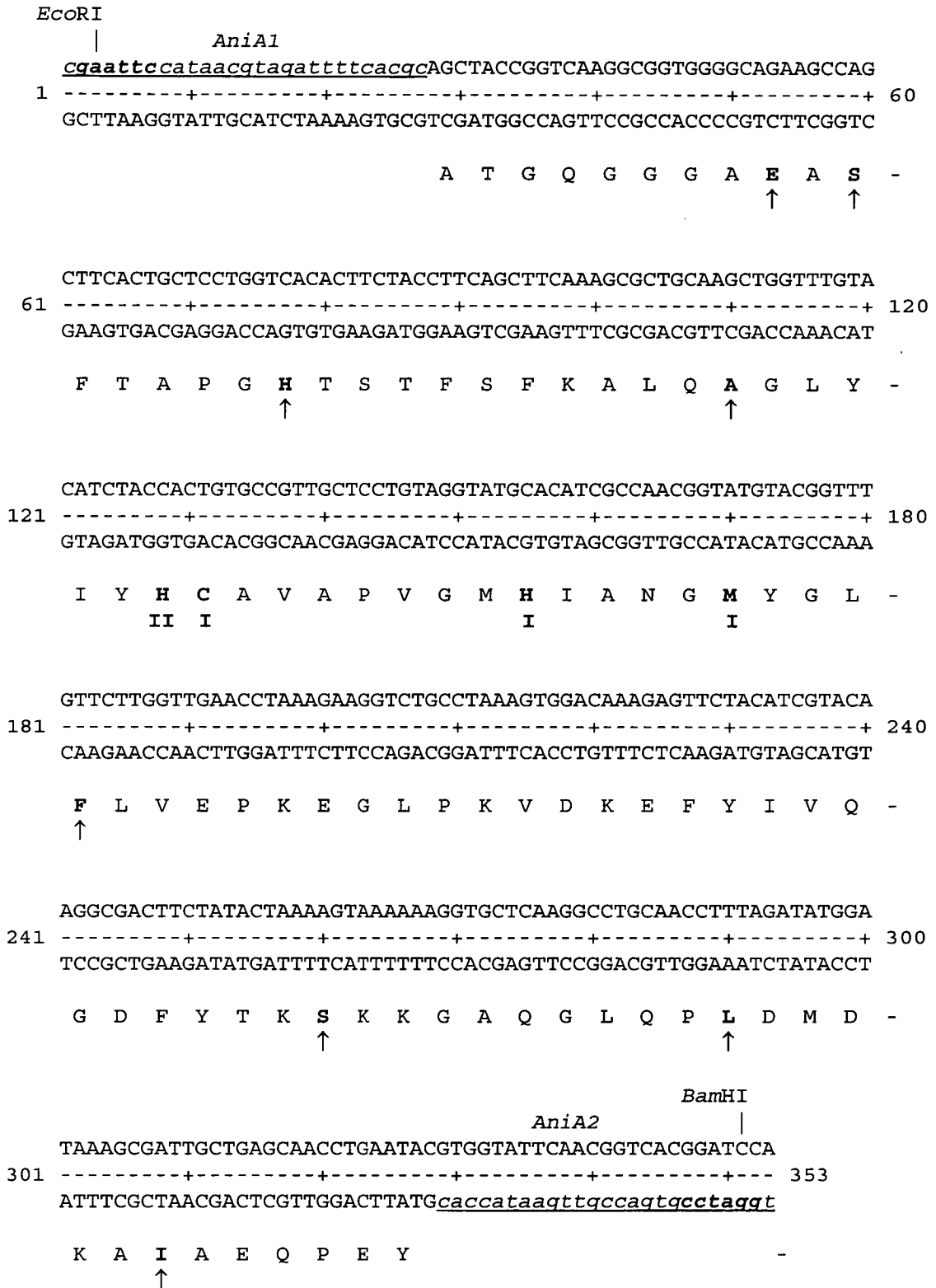


Figure 5.6. DNA sequence from pANIA350 showing the positions of the *EcoRI* and *BamHI* cloning sites. The ORF from reading frame two is also aligned. In this peptide the conserved copper I and II binding ligands are labelled and the amino acids that differ to the AniA gonococcal peptide are depicted by the arrows.

```

          ↓ ↓      ↓      ↓
134  HNVDFAATGQGGGAAATFTAPGRTSTFSFKALQPGLYIYHCAVAPVGMH 183
      ||||||||||||||| |·||| | ||||||| | ||||||| | ||||||| |
3    HNVDFAATGQGGGAEASFTAPGHTSTFSFKALQAGLYIYHCAVAPVGMH 52
      . . . . .
          ↓      .      ↓      ↓
184  IANGMYGLLILVEPK EGLPKVDKEFYIVQGDFYTKGKKGAQGLQPFDMDKA 233
      ||||||| | ||||||| ||||||| ||||||| ||||||| |||||||
53  IANGMYGLFLVEPK EGLPKVDKEFYIVQGDFYTKSKKGAQGLQPLDMDKA 102
      .
          ↓
234  VAEQPEYVVFNGH 246
      : |||||||
103  IAEQPEYVVFNGH 115

```

Percent Identity: 92.9%

Figure 5.7. Peptide alignment of the AniA nitrite reductase from *N. gonorrhoeae* and the ORF obtained from pANIA350. The 8 amino acid differences are highlighted by the arrows. The top peptide corresponds to the gonococcal peptide and the bottom to the pANIA350 ORF.


```

                                I      II10      20      30
                                EFHNVDFAAATGQGGGAEASFTAPGHTSTFSF
                                ||:|||||  ||:  :  ||:  :  :  |
NGTVPGPLMVVHQDDYLELTLINPETNTLMIHIDFAAATGALGGGGLTEINPGEKTILRF
      110      120      130      140      150      160

      40  III      50      I      I 60      70      80
KALQAGLYIYHCAVAPVGM---HIANGMYGLFLVEPKEGLPK-----VDKEFYIVQGD
|| : |:::|||| | || |:::| | :| |:| | | :|: |
KATKPGVFVYHCA--PPGMVPHVVSGMNGAIMVLPREGLHDGKGKALTYDKIYYVGEQD
      170      180      190      200      210

      90      100      110
FYT-----KSKKG-AQGLQPLDMDKAI AE-QPEYVVFNGHGS
||:  | || | | | | :| | :| ||| |
FYVPRDENGKYKKYEAPGDAYEDTVKVMRTLTPHVVFN GAVGALTGDKAMTAAVGEKVL
220      230      240      250      260      270

Percent Identity: 40% over 130 amino acids

```

Figure 5.8b. Peptide alignment of the pANIA350 ORF and the nitrite reductase protein from *Al. faecalis*. The type I and II copper binding ligands are illustrated. The top peptide sequence corresponds to the pANIA350 ORF and the bottom to the *Al. faecalis* nitrite reductase.

These results were taken as strong evidence that the AniA PCR had been successful and a region of DNA corresponding to the *N. subflava* nitrite reductase gene had been amplified. It also demonstrated that assumptions about the higher degree of similarity between the gonococcal and *N. subflava* nitrite reductases made when devising the PCR strategy were correct. Due to the conservation of the type I and type II copper binding ligands in the pANIA350 ORF it was also believed that the nitrite reductase in *N. subflava* contained copper in its active site. Due to the high degree of identity between the pANIA350 ORF and the *N. gonorrhoeae* nitrite reductase peptide sequences it was postulated that the copper containing *N. subflava* nitrite reductase would also be an outer membrane lipoprotein. The *N. gonorrhoeae* nitrite reductase was originally identified as being anaerobically induced and attached to the outer periplasmic membrane (Hoehn and Clark, 1992). The activity of this protein as a nitrite reductase was identified some years later (Mellies *et al.*, 1997).

The identification of the *N. gonorrhoeae* AniA protein as a more divergent copper nitrite reductase helped to explain why the previous PCR attempt to locate the *N. subflava* nitrite reductase gene by Sowerby (1997) was unsuccessful. In this instance the PCR primers were designed from an alignment of the N and C-terminals of the copper nitrite reductases of two organisms, *Al. faecalis* and *Ps. aeruginosa*. The gonococcal AniA nitrite reductase, which is believed to be highly homologous to the *N. subflava* enzyme along its entire length, shows a dramatic decrease in similarity to the N and C-terminals of the nitrite reductases from *Al. faecalis* and *Ps. aeruginosa* than over the more conserved copper binding active site - and here this similarity can be as low as 38.9%. Consequently when the N and C-terminal primers were used in a PCR with *N. subflava* genomic DNA to identify the nitrite reductase gene they were able to anneal to many different regions on the DNA, due to their low sequence similarity, and were able to amplify many DNA fragments. After thorough investigation and sequencing none of the amplified fragments were found to correspond to a nitrite reductase structural or regulatory gene (Sowerby, 1997).

5.3 *N. subflava* B19 Mini-library Construction and Screening

To determine suitably sized DNA fragments of *N. subflava* B19 chromosomal DNA for subcloning the entire nitrite reductase gene, the 350bp insert fragment from pANIA350 was used as a probe to screen genomic digests of *N. subflava* B19 DNA. (The 350bp fragment will be referred to as the 350bp probe from this point forward). The aim of this was to identify hybridising fragments large enough to contain the entire *N. subflava* nitrite reductase gene, ~ 1.2kb based on sequence of the *aniA* gene encoding the AniA nitrite reductase, but small enough to clone easily into conventional cloning vectors such as pUC19 and pBluescript KS⁻. Figure 5.9a shows the results of this probing experiment. Although not detected on this autorad a 0.4kb *Eco*RI fragment should have hybridised to the probe. Extrapolation of a graph used to calculate the DNA fragment sizes indicated the band should have been present at the position of the arrow. It is assumed that there was insufficient chromosomal DNA present on the gel at this point for efficient probing to occur. Subsequent experiments **have** demonstrated the presence of this *Eco*RI fragment in *N. subflava* chromosomal DNA and this is highlighted in Figure 5.9b.

Genomic DNA from the mutant *N. subflava* 163 strain was also screened in this way and Figure 5.10 illustrates that fragments of the same size as B19 DNA were observed to hybridise. These results were taken as further evidence that the deletion size discussed in section 3.3.2.2 was correct and that the *N. subflava* nitrite reductase gene was found a great distance from the Tn5 insertion point.

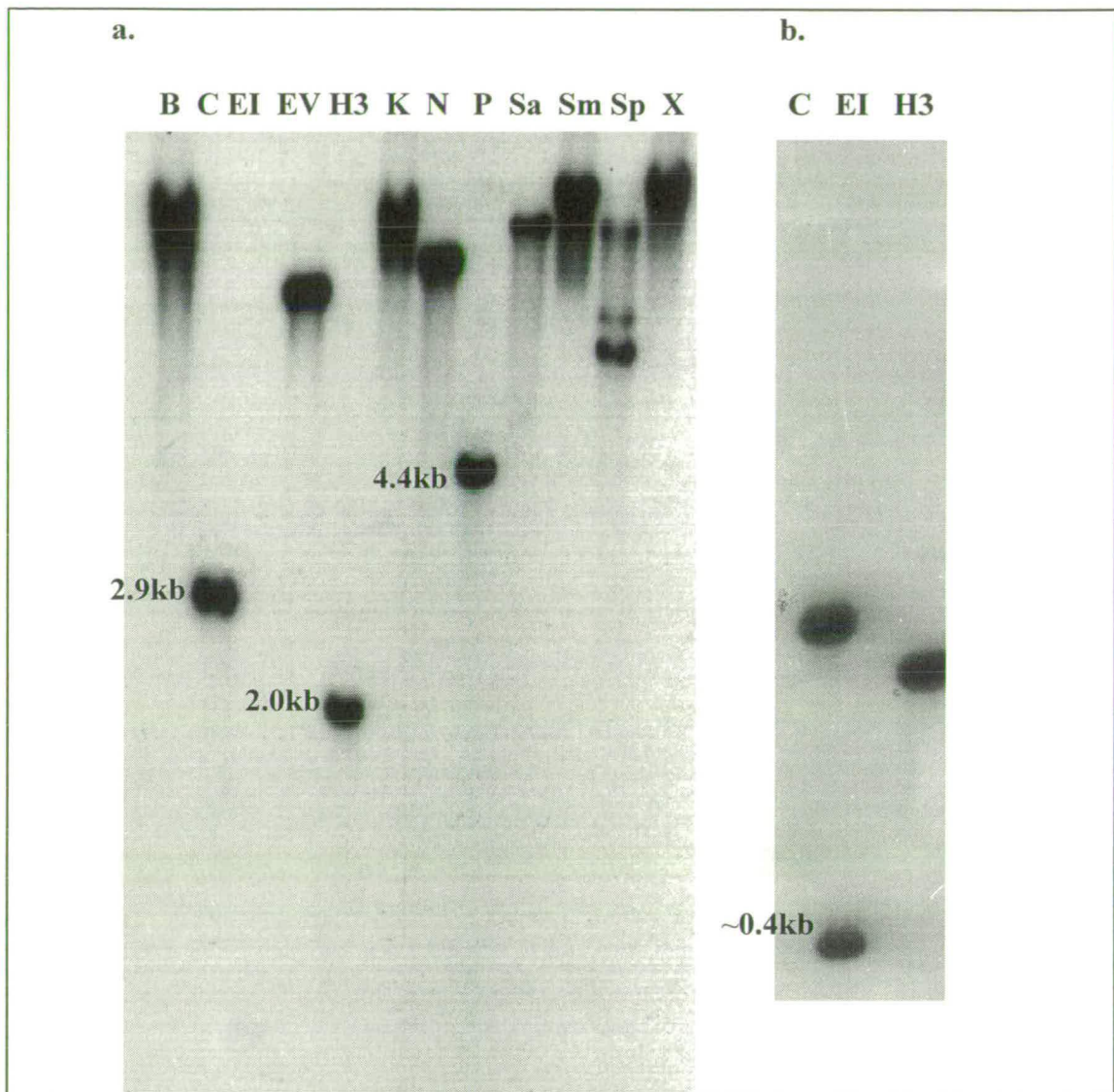


Figure 5.9. a. Southern hybridisation of *N. subflava* B19 chromosomal digests to the 350bp probe. Key to restriction enzymes B - *Bam*HI, C = *Cl*aI, EI = *Eco*RI, EV = *Eco*RV, H3 = *Hind*III, K = *Kpn*I, N = *Nde*I, P = *Pst*I, Sa = *Sal*I, Sm = *Sma*I, Sp = *Sph*I, X = *Xho*I. b. Repeat of *Cl*aI, *Hind*III and *Eco*RI restriction digests on *N. subflava* B19 chromosomal DNA showing the position of the ~0.4kb *Eco*RI fragment with hybridisation to the 350bp probe. The two gels were run independently and the different DNA migration rates account for the differences observed between fragments of the same molecular size.

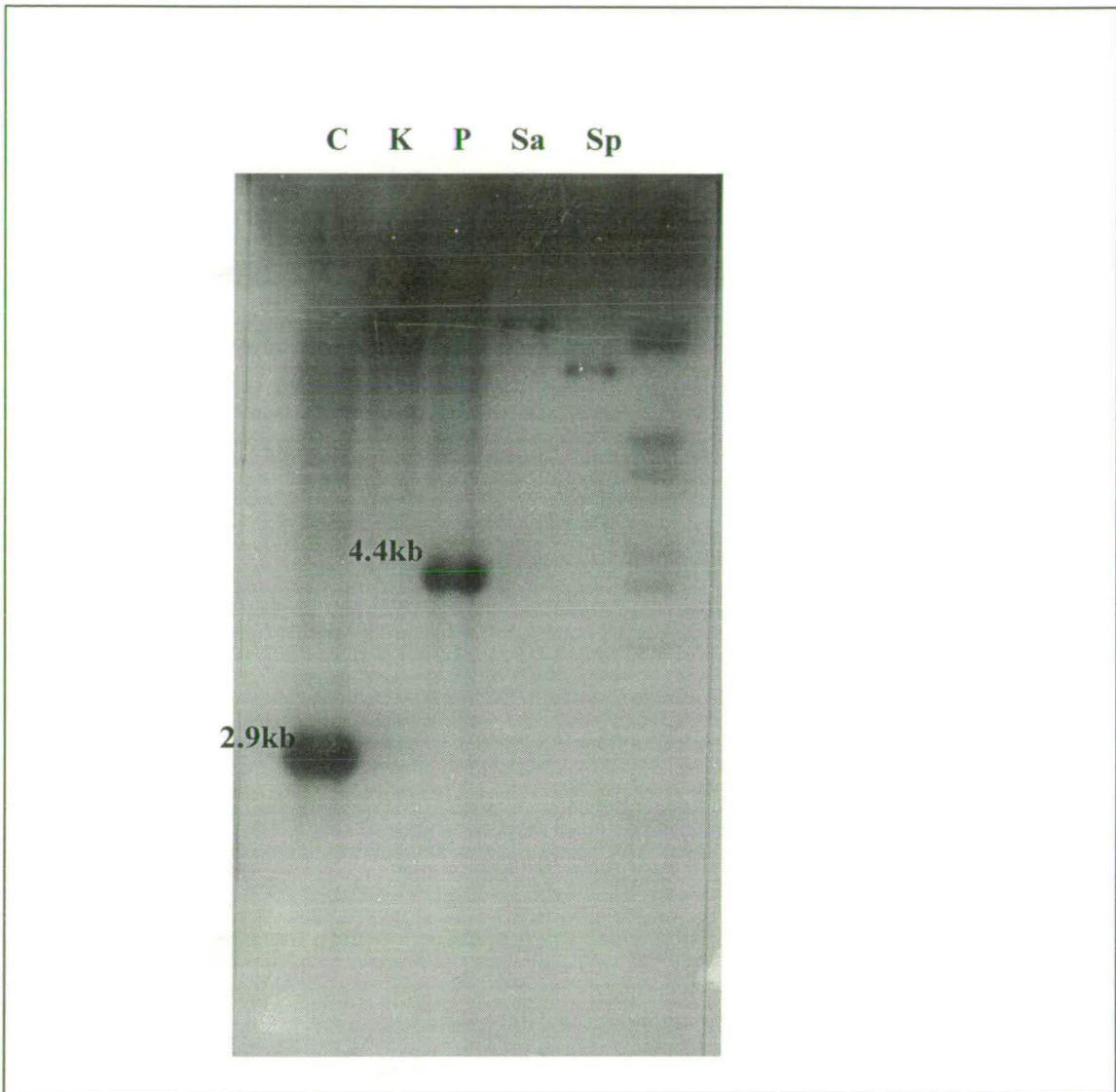


Figure 5.10. Southern hybridisation of *N. subflava* mutant 163 chromosomal digests to the 350bp probe. Key to restriction enzymes C = *Cla*I, K = *Kpn*I, P = *Pst*I, Sa = *Sal*I, Sp = *Sph*I. The 2.9kb *Cla*I and 4.4kb *Pst*I fragments are constant in both wild type and mutant 163 strains. A substantial amount of non-specific hybridisation is apparent as the λ *Bst*EII DNA markers have also hybridised to the probe. However this is not thought to affect the validity of the mutant 163 probing results.

It can be seen that three B19 genomic DNA fragments hybridised to the probe which looked particularly interesting for subcloning. These were a 2.9kb *Clal* fragment, a 2.0kb *HindIII* fragment and a 4.4kb *PstI* fragment. The other fragments that hybridised were deemed too large for subcloning and sequencing. As it is difficult to isolate and purify single DNA bands from genomic digests it was decided that production of a *N. subflava* mini-chromosomal plasmid library in pUC19 would be the simplest way to clone the hybridising DNA fragments of interest. A detailed account of the production and screening of plasmid mini-libraries is given in section 2.2.22.

Initially the 2.9kb *Clal* and 2.0kb *HindIII* fragments were cloned, via production of plasmid mini-libraries, into pUC19 vector and transformed into CaCl₂ DH5 α *E. coli* cells. However even though approximately 40 transformants were obtained upon transformation none of these contained the fragment of interest after colony blotting and probing with the 350bp probe. DNA was found to have inserted into pUC19 in these transformants but probing analysis demonstrated that the 350bp probe region was not present in these inserts (data not shown). Further sequence analysis was therefore determined to be unnecessary. It was believed that the transformant of interest was not recovered due to insertion of the *N. subflava* DNA fragment into the vector DNA in such a way as to allow expression of the nitrite reductase gene. One hypothesis to explain the lack of recombinants containing the 350bp fragment is because the *N. subflava* nitrite reductase is proposed to be bound to the outer membrane. It was thought that levels of the expressed protein were high enough to be affecting *E. coli* cell viability.

In its indigenous host a protein undergoes many post-translational modifications after synthesis of the polypeptide chain is complete. These modifications can include attachment of acyl and formyl groups, phosphate groups, carbohydrates and lipids. For proteins to attach to cell membranes there is usually a signal present within the polypeptide that is recognised by cellular enzymes which cleave the protein at a specific site to allow membrane attachment to take place. With proteins that need to be attached to the outer periplasmic membrane this signal sequence has been identified as [Ala-Leu-Ala-Ala-Cys] near to the N-terminus.

Cleavage of the peptide occurs at the Cys residue of this signal sequence and this then becomes the amino terminus of the mature protein and anchors the protein into the outer membrane (Pugsley *et al.*, 1986). If a protein becomes expressed, in an organism other than its indigenous host, there are many places along the complicated pathway of protein maturation that can be affected by the foreign hosts post-translational modification processes. Expression of the protein may not be completed in the new host, resulting in a truncated peptide which is unable to fold properly; leader sequences for membrane attachment may become buried within the peptide chain and would become inaccessible to the appropriate modifying enzymes. The protein is unable to assume its natural position in the cell and will therefore accumulate in either the cytoplasm or the periplasm. In the case of proteins destined to be positioned in the outer membrane this can be very harmful to the host. It has been demonstrated in *E. coli* that expression of modified LppDK, a major outer membrane lipoprotein, results in cell death (Yakushi, *et al.*, 1997). A single amino acid residue in the N-terminal membrane attachment signal sequence was changed. As the protein was unable to assume its natural position in the outer membrane it was found to accumulate in the inner membrane covalently associated with the peptidoglycan. This was found to prevent separation of the two membranes when the cell divided. Similarly attachment of protein to the outer membrane at the wrong position can seriously reduce membrane viability leading to cell death.

Lack of recovery of the transformant of interest from the plasmid *Cla*I and *Hind*III mini-libraries in pUC19 was thought to be due to similar mechanisms in the *E. coli* host cell affecting the expressed *N. subflava* nitrite reductase outer membrane protein. It was thought that cloning the fragment into the pUC19 vector in the opposite orientation to the *lacZ* promoter would overcome this problem. But the genomic insert fragments were derived from DNA cut with a single restriction enzyme and so would be able to insert into the vector in both orientations with relation to the pUC19 *lacZ* promoter. So there was obviously some other mechanism affecting recovery of the transformant(s) of interest. It was postulated that the promoter of the *N. subflava* nitrite reductase was present on the cloned *Cla*I and *Hind*III fragments and may be activated by *E. coli* sigma (σ) factors. This seemed

unlikely as expression of Neisserial genes in *E. coli* host strains usually involves cloning into specifically designed expression vectors. To reduce the possibility that levels of nitrite reductase protein, produced from either the pUC19 *lacZ* promoter or perhaps an active *N. subflava* promoter, the plasmid mini-library cloning strategy was repeated using a lower copy number vector.

The vector pBR325 was chosen as this has a copy number of ~50 per cell compared to pUC19 which can have >1000. The same cloning procedure was carried out as before for the construction of the pBR325 mini-library. Transformant colonies were initially selected for on Amp plates and then tested for Tet sensitivity. The reason for this was that both the *Cla*I and *Hind*III cloning sites in pBR325 were found in the promoter for the *tet* gene and would interrupt expression of tetracycline resistance in transformant colonies. Appendix A4 illustrates the plasmid map of pBR325. Only 10 transformants were obtained using *Cla*I as the cloning site whereas 70 were obtained using *Hind*III. These numbers were considered low but the colonies were screened with the 350bp probe nevertheless. Only one colony was observed to hybridise to the 350bp probe and the autorad resulting from this colony blot is illustrated in Figure 5.11.

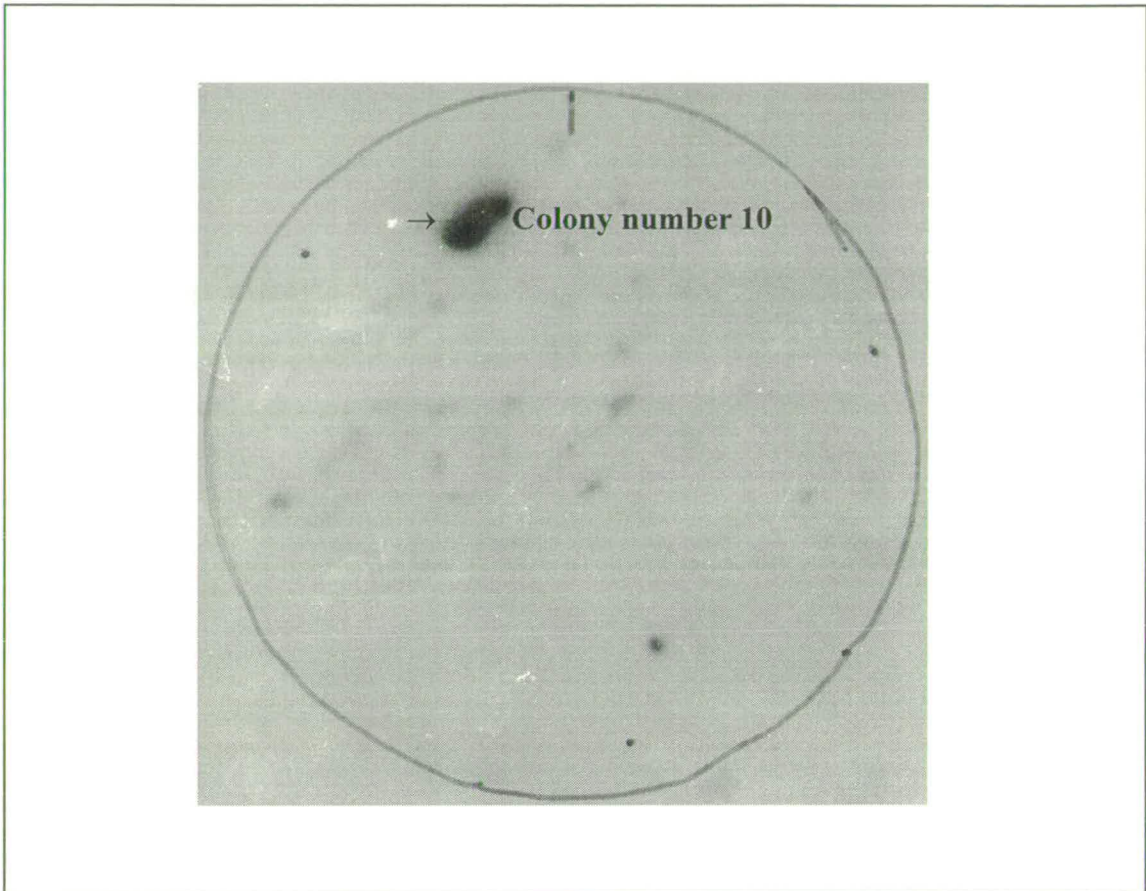


Figure 5.11. Autorad resulting from the pBR325/*N. subflava* B19 *Hind*III mini-library screen with the 350bp probe. Of the 70 colonies that were screened only one showed hybridisation to the probe. This corresponded to the 10th colony on the plate and the resulting construct was named pANIA10.

As a further check that this construct contained the correct fragment of *N. subflava* genomic DNA the *aniA* PCR described in section 5.2.1 was used to amplify the 350bp fragment from crude cell lysates containing the plasmid as described in section 2.2.24. Aliquots (5 μ l and 10 μ l) of the crude cell extract were used in the PCR as well as a positive control from *N. subflava* B19 and the results of this PCR are represented in Figure 5.12.

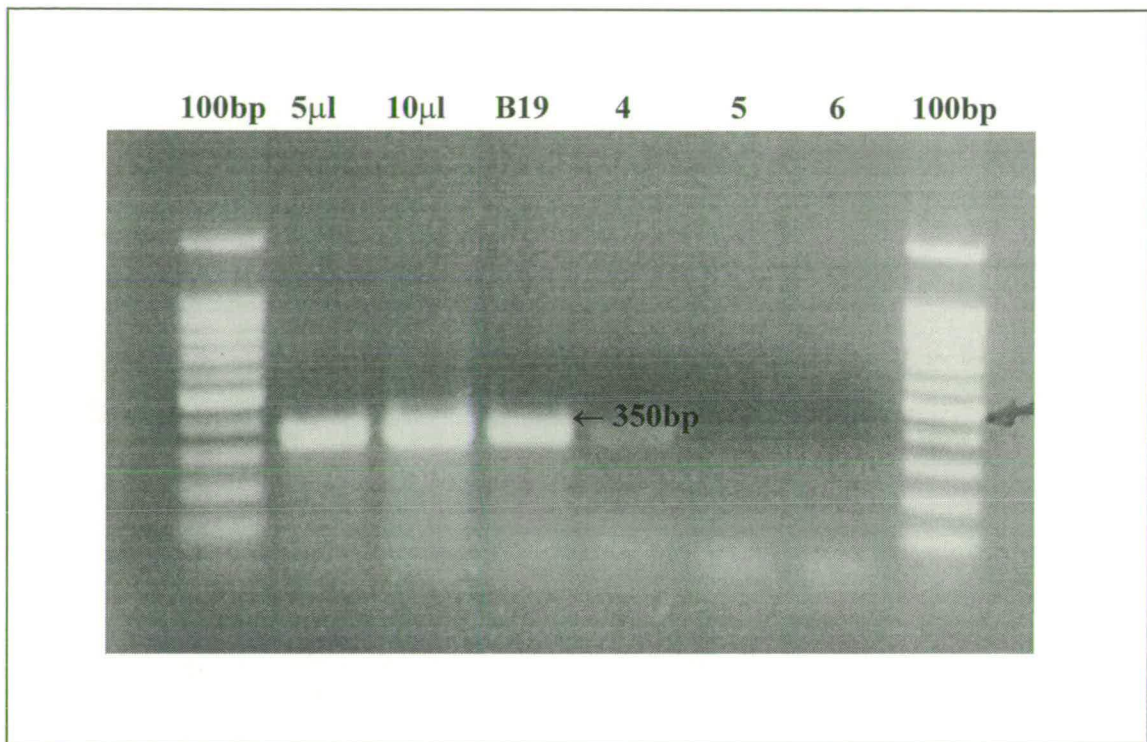


Figure 5.12. Results of *aniA* PCR on pANIA10 from the *N. subflava* B19 *Hind*III 2.0kb mini-library constructed in pBR325. Crude DNA template from whole cell lysates was used in the PCR. Key to lanes: 5µl - 5µl template used; 10µl - 10µl template used; 4, 5 & 6 are the PCR negative controls with no primers, no template and no *Taq* control. The 350bp amplified fragment is illustrated and the brighter band in the 100bp ladder corresponds to 500bp.

5.3.1 Sequence analysis of pANIA10

Sequencing primers specific to pBR325 were designed surrounding the *Hind*III insertion site to sequence in from the ends of the ~2.0kb insert fragment. To increase sequence obtained from pANIA350 two sequencing primers within the 350bp insert fragment were designed to sequence out from the copper active site of the nitrite reductase gene towards the 5' and 3' ends. It was assumed that this sequencing strategy would be successful as pANIA10 was suspected to contain the 350bp probe region within the *Hind*III insert fragment, as it was found to hybridise to this probe when colony blotted. The positions of the two pBR325 primers are illustrated on the plasmid map in Appendix A4. Figure 5.13 depicts the positions of the two internal *N. subflava* nitrite reductase primers, named AniA3 and AniA4. Primer AniA3 was designed to sequence towards the nitrite reductase 3' end of the gene and is positioned between 249bp and 264bp in the 350bp pANIA350 insert fragment, and AniA4 was designed to sequence towards the 5' end of the gene and is positioned between 87bp and 103bp. The sequences of all these primers are listed in Table 5.1.

Primer name	Sequence
pBR325-1	5'-d[GACCAGTGACGAAGGCT]-3'
pBR325-2	5'-d[GCAATTTAACTGTGAT]-3'
AniA3	5'-d[TCTATACTAAAAGTA]-3'
AniA4	5'-d[CGCTTTGAAGCTGAAGG]-3'

Table 5.1. Primers used in the sequence analysis of pANIA10.

```

EcoRI
|
      AniA1 →
cgaaattccataacqtagattttcacgcAGCTACCGGTCAAGGCGGTGGGGCAGAAGCCAG
1  -----+-----+-----+-----+-----+-----+-----+ 60
GCTTAAGGTATTGCATCTAAAAGTGCCTCGATGGCCAGTTCCGCCACCCCGTCTTCGGTC

      A T G Q G G G A E A S -

CTTCACTGCTCCTGGTCACACTTCTACCTTACGCTTCAAAGCGCTGCAAGCTGGTTTGTA
61 -----+-----+-----+-----+-----+-----+-----+ 120
GAAGTGACGAGGACCAGTGTGAAGATggaagtccgaagtttcgcGACGTTTCGACCAAACAT
      ← AniA4
      F T A P G H T S T F S F K A L Q A G L Y -

CATCTACCACTGTGCCGTTGCTCCTGTAGGTATGCACATCGCCAACGGTATGTACGGTTT
121 -----+-----+-----+-----+-----+-----+-----+ 180
GTAGATGGTGACACGGCAACGAGGACATCCATACGTGTAGCGGTTGCCATACATGCCAA

      I Y H C A V A P V G M H I A N G M Y G L -
      II I                               I                               I

GTTCTTGGTTGAACCTAAAGAAGGTCTGCCTAAAGTGGACAAAGAGTTCTACATCGTACA
181 -----+-----+-----+-----+-----+-----+-----+ 240
CAAGAACCAACTTGGATTTCTTCCAGACGGATTTACCTGTTTCTCAAGATGTAGCATGT

      F L V E P K E G L P K V D K E F Y I V Q -

      AniA3 →
AGGCGACttctataactaaaagtaaAAAAGGTGCTCAAGGCCTGCAACCTTTAGATATGGA
241 -----+-----+-----+-----+-----+-----+-----+ 300
TCCGCTGAAGATATGATTTTCATTTTTTCCACGAGTTCGGACGTTGGAAATCTATACCT

      G D F Y T K S K K G A Q G L Q P L D M D -

      BamHI
      |
TAAAGCGATTGCTGAGCAACCTGAATACGTGGTATTCAACGGTCACGGATCCA
301 -----+-----+-----+-----+-----+-----+-----+ 353
ATTTTCGCTAACGACTCGTTGGACTTATGcaccataaagtcccaqtgcctaggt
      ← AniA2
      K A I A E Q P E Y -

```

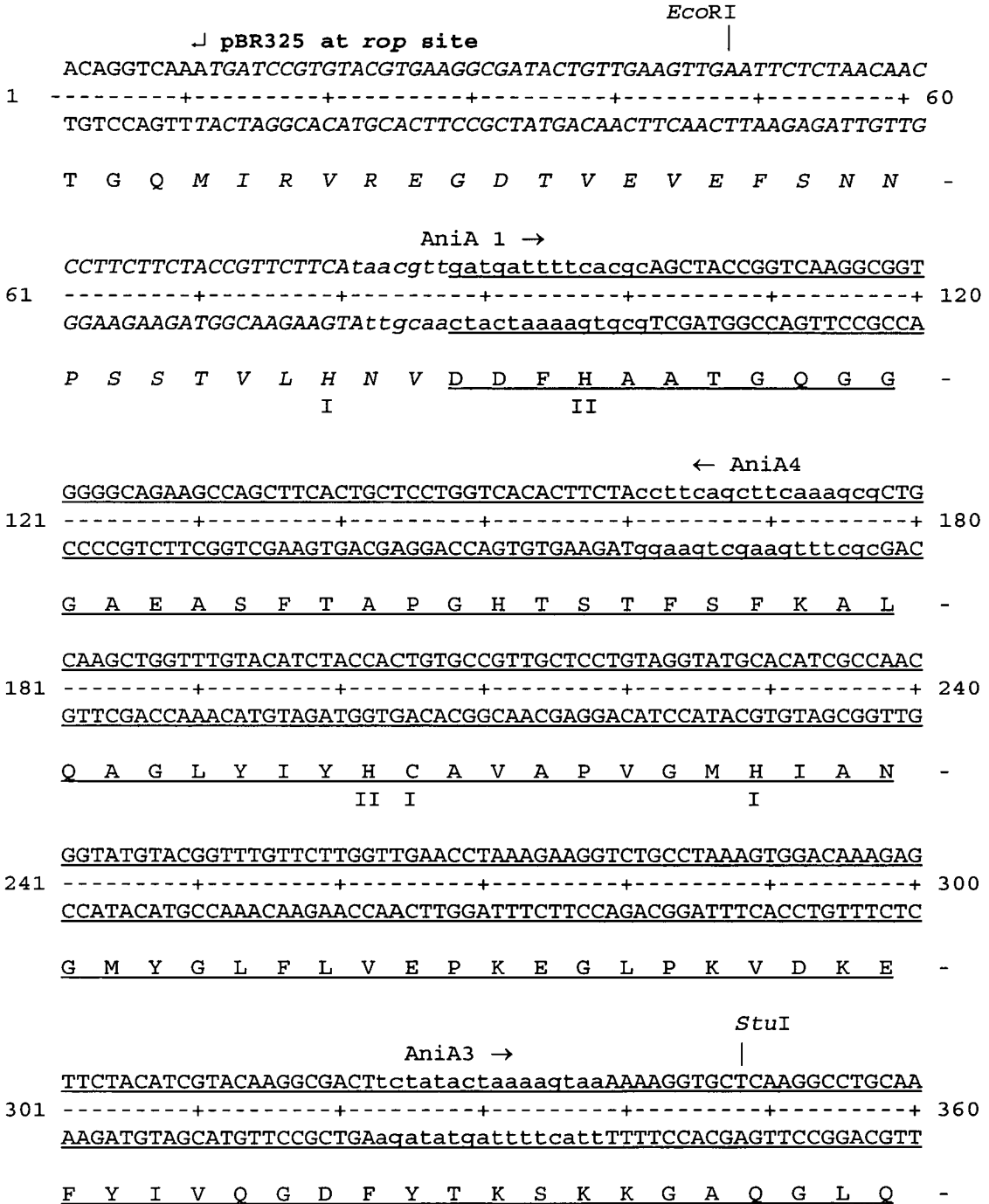
Figure 5.13. DNA sequence from pANIA350 showing the positions of the two internal sequencing primers, AniA3 and AniA4. The positions of the two degenerate PCR primers are also illustrated. I denotes ligands that bind type I copper and II denotes those that bind type II copper.

Sequencing pANIA10 with pBR325-1 and AniA3 extended the sequence obtained from the *Bam*HI end of the pANIA350 sequence to allow identification of the 3' end of the *N. subflava* nitrite reductase gene. However problems were observed when trying to extend sequence at the *Eco*RI end of pANIA350 to identify the 5' end of the gene. Sequence generated from the AniA4 sequencing primer could only extend the nitrite reductase gene by a further 70bp which corresponded to 24 amino acids before the similarity was lost. Additional analysis of sequence from AniA4 demonstrated that after the nitrite reductase gene similarity ended the DNA sequence showed similarity to the pBR325 vector at the position of the *rop* gene. In addition no sequence was produced from the pBR325-2 sequencing primer. At first it was thought that this may have been due to experimental error, but even after a number of repetitions the same result was obtained. It was surmised from this that recombination of the pANIA10 construct had occurred leading to excision of the 5' end of the nitrite reductase gene and this is discussed in section 5.3.2.

Figure 5.14 shows the sequence produced from pANIA10 extending upstream and downstream of the 350bp from pANIA350 and Figure 5.15 illustrates the similarity of the ORF in reading frame 1 from this sequence to the AniA peptide from *N. gonorrhoeae*. It can be seen from this alignment that the further away from the conserved copper binding ligands the more divergent the two peptide sequences become. Consequently the *N. subflava* nitrite reductase protein shows even less homology to the more common soluble nitrite reductases than AniA, see Figures 5.16a and 5.16b. This data further explains the lack of hybridisation of the copper nitrite reductase gene probes from *Al. faecalis* to *N. subflava* genomic DNA as described in section 3.2.2. It is expected that a similar decrease in similarity will be observed at the 5' end too.

These sequence analyses also bring to light another unusual feature of the Neisserial nitrite reductase enzymes. In the soluble nitrite reductases a functionally important histidine residue has been identified; in *A. faecalis* this lies at position 255. This residue is proposed to be involved in proton donation in the active enzyme. In the nitrite reductase enzymes from both *N. gonorrhoeae* and *N. subflava* this His

residue is replaced with tyrosine (Figure 5.16a). This suggests that a different mechanism of catalysis may exist in both the gonococcal and *N. subflava* enzymes.




```

                                     ← pBR325-1 sequencing primer
      TCTGGTGCTTCTGAAGCCGCTAAATAATC
841  -----+-----+----- 869
      AGACCACGAAGACTTCGGCGATTATTAG

      S  G  A  S  E  A  A  K  *
                                     ↑ - C terminal stop codon.

```

Figure 5.14. Sequence obtained from pANIA10 showing the ORF in reading frame 1 corresponding to the *N. subflava* nitrite reductase. Sequence in italics was obtained when sequenced with AniA4, sequence underlined comes from pANIA350 and sequence in bold corresponds to that produced from the AniA3 and pBR325-1 primers. The position at which sequence from pANIA10 displayed similarity to the pBR325 *rop* gene is indicated as are the positions of the type I and type II copper binding ligands. Useful restriction sites detected in the sequence are also illustrated. The tyrosine (Y) residue represented by * highlights the position of the expected histidine residue which acts to donate protons in the more usual periplasmic nitrite reductases. The presence of tyrosine in the Neisserial enzymes is unexpected and not understood at present.


```

          I      II
4  VREGDTVEVEFSNNPSSTVLHNVDFFHAATGQGGGAEASFTAPGHTSTFS 53
   | : | . | . | .. | . : | | : | | | | | | | | | | . | | .
111 VHQDDYLELTLINPETNTLMHNI .DFHAATGALGGGGLTEINPGEKILR 159

          . . . . .
          III      I      I
54 FKALQAGLYIYHCA .VAPVGMHIANGMYGLFLVEPKGLP . . . . .KVD 95
   ||| . | . : : ||| | | | : . | | | : | | : ||| | | |
160 FKATKPGVVFVYHCAPPGMVPHVVSVMNGAIMVLPREGLHDGK GKALTYD 209

          . . . . .

96 KEFYIVQGDFYTKSKKGAQGLQPLMDKAI AEQPEYV .VFKRLKVG FYLA 144
   | : : : | | | . . . . . | : . . . . . | | |
210 KIYYVGEQDFYVPRDENGKYKYEAPGDAYEDTVKVMRTLTPHVVFNGA
259
          . . . . .
          *

145 GNKGF GKAKAGETVWYVTLVNGGPKLGIFFPRL LGEFLDKSICWKGKLD 194
   | | | | | | | | : | | : | | | | | | | | | .
260 VGALTGDKAMTAAVGEKVLIVHSQANRDTRPHLIGGHGD . .YVWATGKFN
307

          . . . . .
          II
195 LRKTVTKYSGFLPGGGSDDRIQSRHFQAGNTVVVDHFI FFPVRFNKGALGQL 244
   | . . | : | | | . . . . . | . | : | | | | |
308 TPPDVDQETWFIPGGAAGAAFYTFQQPGIYAYVNHNLIEA .FELGAAAHF 356

          .

245 KVEGDENPEIMTKKLS 260
   || | : | : : | | | .
357 KVTGEWNDDLMTSVLA 372

```

Percent Identity: 28.9%

Figure 5.16a. Peptide alignment of the *N. subflava* nitrite reductase from pANIA10 (top strand) to the soluble nitrite reductase from *Al. faecalis* (bottom strand). All copper binding ligands are illustrated. The percent identity when the nitrite reductase from *N. gonorrhoeae* is compared to that from *Al. faecalis* is 33.5%. Refer to Figure 5.16b. The position of the functionally significant histidine residue in the *Al. faecalis* sequence is highlighted. In the *N. subflava* peptide this is replaced by a tyrosine residue.

```

12 SLFALAACGGEQAAQAPAETPAASAEAAASSAAQATAETPAGELPVIDAVT 61
   .: | || | | . | . | | | . . .: |
11 TILAGAALAGALAPVLATTSAWGQAVRKATAAEIAALPRQKVELVDPFF 60
   . . . . .

62 THAPEVPPAIDRDYPKVRVKMETVEKTMKMDD.GVEYRYWTFDGDVPGR 110
   || : | | | || . || | | | . | || |
61 VHAHS...QVAEGGPKVVEFTMVIIEKKIVIDDAGTEVHAMAFNGTVPGP 107
   . . . . .

                                I   II
111 MIRVREGDTVEVEFSNNPSSTVPHNVDFHAATGQGGGAAATFTAPGRST 160
   .: | : | . | . | . . | . | | : | | | | | | | | | | | | | | | |
108 LMVVHQDDYLELTLINPETNTLMHNIDFHAATGALGGGGLTEINPGEKTI 157
   . . . . .

                                III   I   I
161 FSFKALQPLGIYIYHCA.VAPVGMHIANGMYGLILVEPKGLP.....K 202
   || | . | | . : : | | | | | | | | : . | | | | : | | : | | | |
158 LRFKATKPGVFVYHCCAPPGMVPHVSVGMNGAIMVLPREGLHDGK GKALT 207
   . . . . .

203 VDKEFYIVQGFYTK.....GKKGAQGLQPFDMDKAVAE.QPEYVVFN 244
   || : | : : | | | | | | | | | | | | | | | | | | | | | | | |
208 YDKIYYVGEQDFYVPRDENGKYYKYEAPGDAYEDTVKVMRTLTPTHVVFN 257
   *

245 GHVGSIAGDNALKAKAGETVRMYVGNGGPNLVSSFHVIGEIFDKVYVEGG 294
   | | | . : | | | : | | | . . : . | . | . | | | | | | | | | |
258 GAVGALTGDKAMTAAVGE..KVLIVHSQANRDTRPHLIGGHGDYVWATGK 305
   . . . . .

                                I
295 KLINENV..QSTIVPAGGSAIVEFKVDIPGSYTLVDHSIFRAFNGKALGQ 342
   . | . . : | | . : | | | | . | . : | | | |
306 FNTPPDVDQETWFI PGGAAGAAFYTFQQPGIYAYVNHNLIEAFELGAAAH 355
   . . . . .

343 LKVEGAENPEIMTQKLS 359
   || | | | : : | | | .
356 FKVTGEWNDDLMTSVLA 37

```

Percent Identity: 33.5%

Figure 5.16b. Peptide alignment of the AniA nitrite reductase from *N. gonorrhoeae* (top strand) and the soluble nitrite reductase from *Al. faecalis* (bottom strand). All copper binding ligands are illustrated. The position of the functionally significant histidine residue in the *Al. faecalis* sequence is highlighted. In the *N. gonorrhoeae* peptide this is replaced by a tyrosine residue.

5.3.2 Recombination in pANIA10

Figure 5.17 illustrates the position of the deletion event which resulted in the loss of the 5' end of the nitrite reductase gene in pANIA10. If the recombination depicted in Figure 5.17 is correct it helps to explain why the colonies from the pBR325 mini-library gave the expected tetracycline sensitive phenotype when screened. In this model the tetracycline resistance gene has been excised and replaced by a 2.0kb fragment of *N. subflava* genomic DNA containing the nitrite reductase gene. Further evidence supporting this deletion hypothesis came from a *Hind*III restriction digest on pANIA10 DNA. Instead of the identification of a 6.0kb intact vector band and a 2.0kb insert band on the resulting agarose gels a vector band of ~5.0kb was always observed with the 2.0kb insert. Figure 5.18 depicts this digest evidence.

The *rop* gene from pBR325 encodes a small (63kDa) peptide that is involved in controlling plasmid copy number. The Rop protein stabilises an interaction between RNA II and its antisense regulator RNA I. RNA II is then unable to form the DNA/RNA primer required for plasmid replication. In the absence of Rop plasmid replication is unregulated and copy number increases. It was initially proposed that nitrite reductase expression was preventing cloning of the structural *nir* gene. However in pBR325 the nitrite reductase gene was cloned in the opposite orientation to the functional *tet* promoter and it was suspected that the protein expression hypothesis was unlikely. The genetic rearrangement depicted in Figure 5.17 shows that the 5' terminus of the cloned nitrite reductase gene is missing and pBR325 vector sequence starts again in the middle of the *rop* gene. The *rop* gene has a total length of ~200bp spanning 2058bp to 2271bp in the vector. Sequence produced from pANIA10 entered the *rop* gene at nucleotide number 2132. This implied a functional Rop protein was lacking leading, to increased pBR325 copy number. It was speculated that increased pBR325 concentration in the *E. coli* strain was influencing plasmid stability and this resulted in the deletion/recombination illustrated in Figure 5.17.

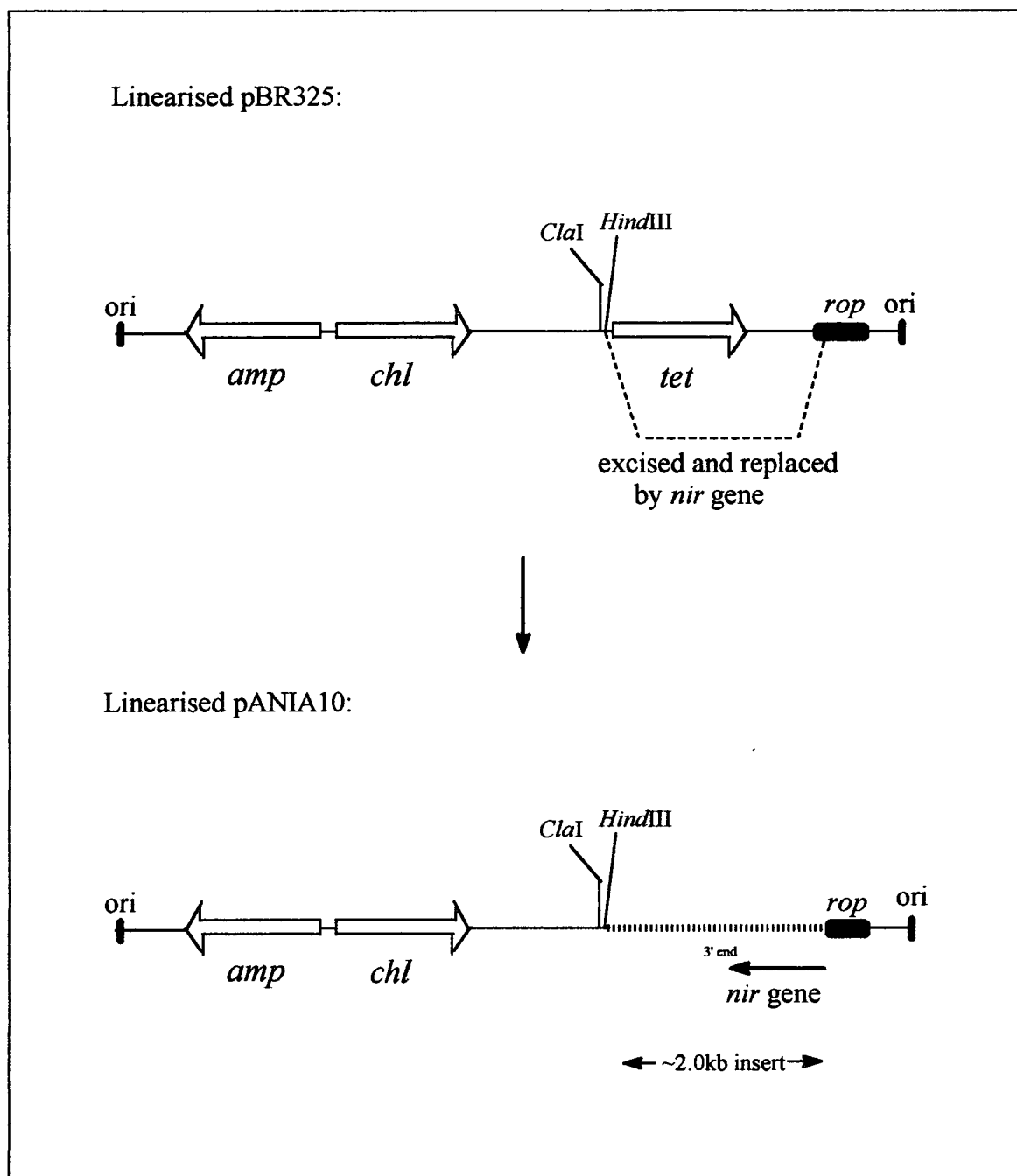


Figure 5.17. Illustration of the proposed deletion that occurred in pANIA10 when *N. subflava* chromosomal DNA was cloned into pBR325. The position of the nitrite reductase structural gene is depicted with the 3' end highlighted for clarity.

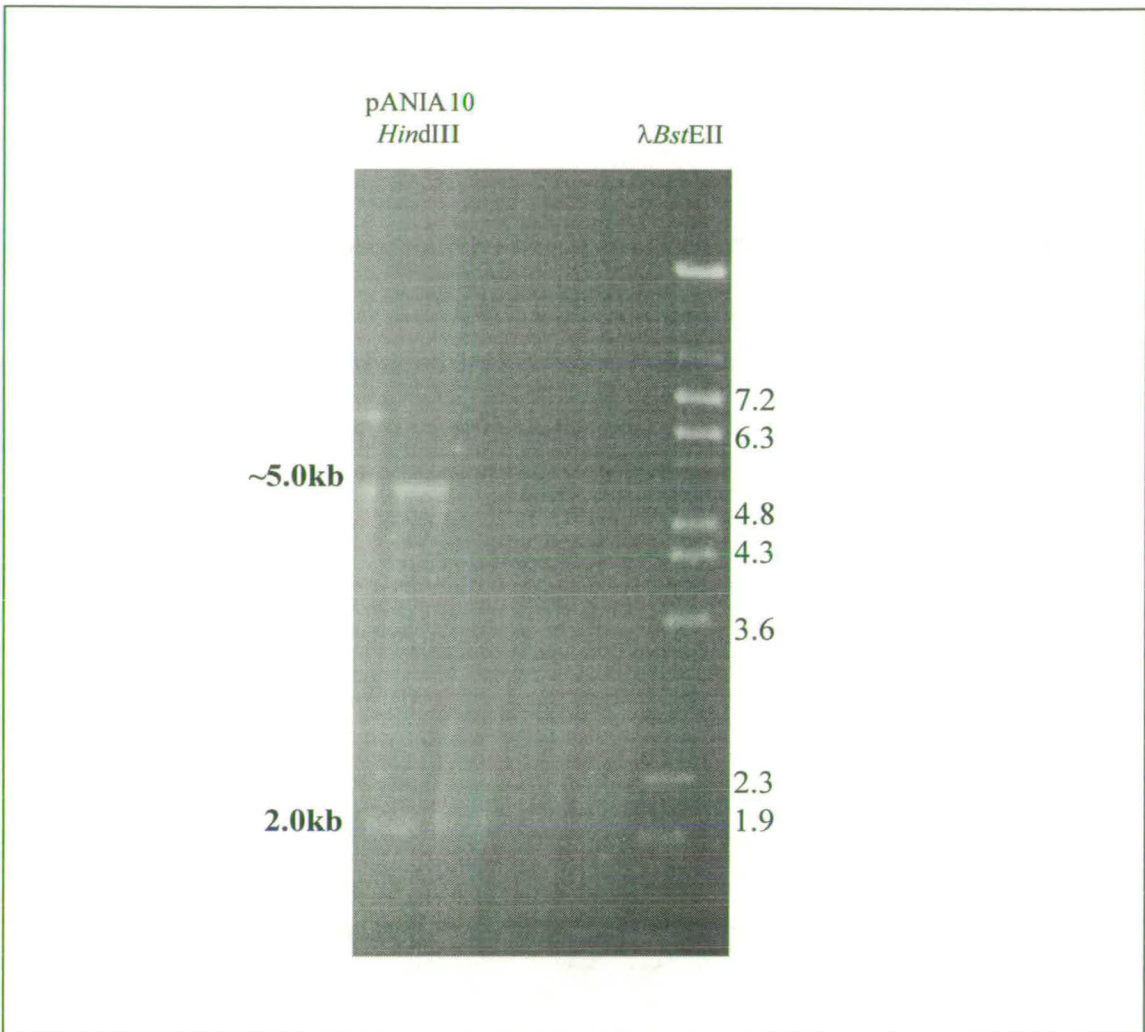


Figure 5.18. pANIA10 *Hind*III digest showing the 2.0kb insert and unexpected ~5.0kb vector fragments. Fragment sizes of λ BstEII are shown in kb. (The lanes between the the *Hind*III digest and the λ markers are from other experiments and are of no importance to the reader.)

It was hypothesised that the excision in pANIA10 was due to the increased copy number of pBR325 resulting in plasmid instability. The excision in pANIA10 resulted in the loss of the 5' terminus of the gene. Consequently no upstream promoter region specific to the nitrite reductase gene was present on the insert fragment therefore any expression of the protein had to result from promoter activity in the pBR325 vector. However this was not possible as the insert fragment was ligated into pBR325 in the opposite orientation to the *tet* promoter.

In an attempt to overcome the cloning problems discussed so far alternative vectors with reduced copy numbers and promoter activities were investigated to produce the *Hind*III and *Cla*I mini-libraries. It was hoped that cloning in this way would allow recovery of at least one clone with the entire nitrite reductase gene present on the insert fragment.

5.4 Alternative Vectors for Mini-library Construction

5.4.1 pACYC177

pACYC177 was chosen as a vector for construction of the *N. subflava* mini-library as it has a very low copy number, ~10-15 copies per cell, and it was thought that this would overcome the plasmid instability problems encountered when using pBR325 to clone the nitrite reductase gene. Although pACYC177 has a very low copy number high yields of the plasmid can be obtained for genetic manipulations as it can be amplified within the cell using chloramphenicol. Section 2.2.4.1 discusses this in detail.

Attempts were made to construct mini-libraries in pACYC177 using the *Cla*I and *Hind*III fragments identified in the B19 genomic DNA screen with the 350bp probe (Figure 4.9). pACYC177 does not contain a polylinker region and so the two restriction sites required for the construction of the plasmid mini-libraries were present at different positions on the pACYC177 map. (Appendix A5 shows the map of pACYC177.) However both *Cla*I and *Hind*III sites were present within the Kan resistance gene. Therefore DH5 α *E. coli* cells were selected for Amp resistance and screened for Kan sensitivity to identify transformant colonies containing genomic DNA inserts.

Once again the transformation frequencies of the transformation experiment were very low. Only 7 transformants using *Cla*I as the cloning site were obtained. The transformation using *Hind*III as the cloning site was marginally better as 63 transformant colonies were obtained that showed the correct antibiotic sensitivity

pattern. Colonies were probed with the 350bp probe to identify possible clones containing the *N. subflava* nitrite reductase gene. The results of the probing were inconclusive. Colonies positive to the probe were identifiable - just - but the areas of hybridisation were very faint and there was a high degree of background hybridisation making the positives difficult to differentiate. Instead of disregarding these weak positive colonies it was decided to investigate them. A total of seven *Hind*III transformant colonies with the strongest hybridisation were picked along with a single *Cl*aI colony. The strains and corresponding constructs were named H25, H29, H30, H39, H50, H66, H68 and C4. Plasmid DNA from each of the positive strains was isolated without the use of *Ch*I amplification as it was thought that this would increase plasmid levels within the cell and therefore increase any levels of expressed protein. Isolated plasmid DNA was used in the *aniA* PCR outlined in section 5.2. This was done as the 350bp fragment was expected to amplify due to the presence of the primer sequences on the genomic DNA insert fragments. It was appreciated that both of the *aniA* PCR primer sequences needed not to be present for the colonies from the pACYC177 mini-libraries to hybridise to the probe and that a negative PCR result may be obtained. But due to the very weak interaction of the 350bp probe to the colonies when they were blotted and screened it was decided that a second check on construct authenticity was required and the *aniA* PCR was the best diagnostic method available. Again, the results of the PCR were ambiguous. A faint 350bp band did amplify during the PCR from some of the constructs but when compared to the positive B19 control this band appeared very weak indeed. Also a number of other contaminating bands amplified, whereas in the positive control only one band at the correct size was observed to amplify. Figure 5.19 illustrates the results of the *aniA* PCR on the seven *Hind*III and single *Cl*aI constructs picked after the mini-library screen with the 350bp probe.

pH25, pH29, pH50 and pH66 were the constructs from which faint 350bp fragments amplified after the *aniA* PCR. *Hind*III digests were done on each of these constructs to check that an insert and vector band were identifiable when the digests were separated by agarose gel electrophoresis. In all cases an insert band of ~2.0kb was present as was the correct sized vector band (data not shown). However the

weak mini-library probing and poor *aniA* PCR evidence would suggest that the insert band, thought to originate from *N. subflava* B19 genomic DNA, did not contain the nitrite reductase gene. However it was decided to investigate one of these clones further using sequence analysis for final confirmation that the insert DNA cloned did not contain a nitrite reductase structural or regulatory gene.

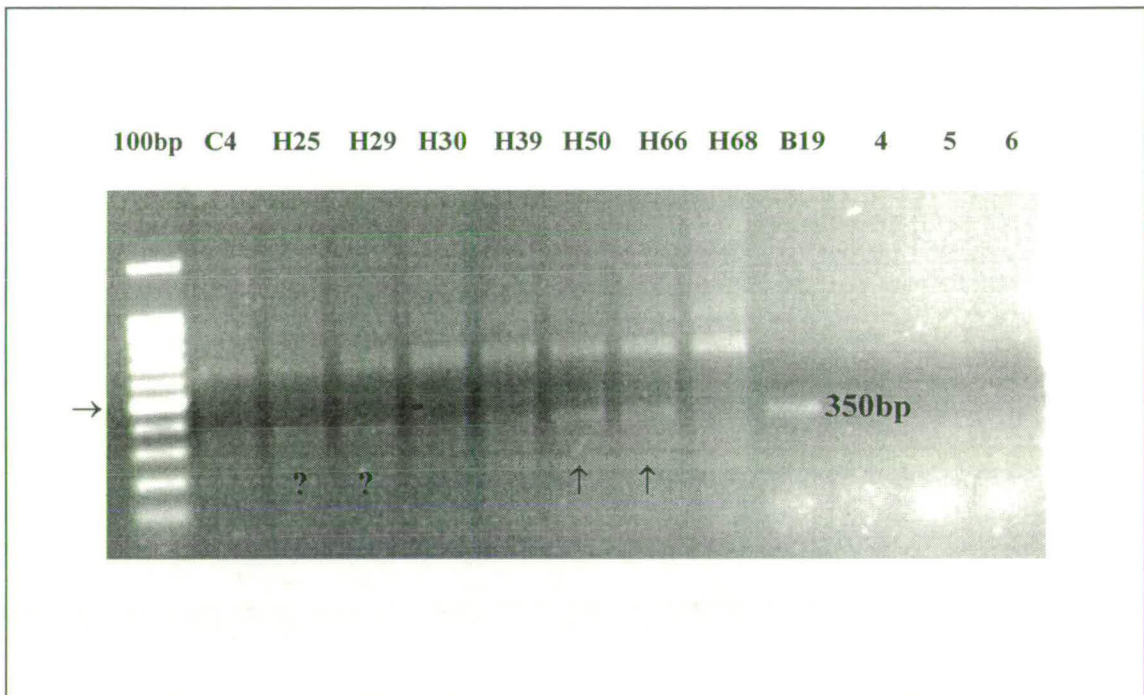


Figure 5.19. *AniA* PCR on pACYC177 transformant plasmids. pH25, pH29, pH50 and pH66 have putatively amplified faint 350bp fragments. Lanes 4, 5 and 6 correspond to the PCR negative controls. The bands on the 100bp ladder increase in 100bp increments with the lowest band corresponding to 100bp. The 500bp band is highlighted for clarity.

Restriction and probing analysis on the pH50 and pH66 constructs indicated that they were the same and that the same region of genomic DNA had inserted into pACYC177 twice during the mini-library construction to produce two separate clones. From equivalent restriction and probing analysis on pH25 and pH29 it was decided to sequence pH25. The reason for this was that the DNA fragments arising from the digests best fitted the known restriction sites present within the nitrite reductase gene as detected in pANIA10 and also the restriction sites present on the

pACYC177 vector. However all probing results were difficult to interpret as hybridisation was weak and in some cases pACYC177 plasmid DNA also hybridised. Nevertheless a putative map of the position of the nitrite reductase gene within the pH25 construct was determined from this restriction and probing analysis and this is represented in Figure 5.20. However it is worth highlighting that although pH25 appeared the best candidate for sequencing based on digest and probing evidence it gave the weakest 350bp fragment when used as a template in the *aniA* PCR (Figure 5.19). Also, all the evidence used to decide which of the *Hind*III mini-library constructs was to be sequenced was rather unsatisfactory. This meant sequencing was the final attempt to gain an unambiguous answer as to whether *N. subflava* chromosomal DNA containing a nitrite reductase structural or regulatory gene had been cloned into pACYC177.

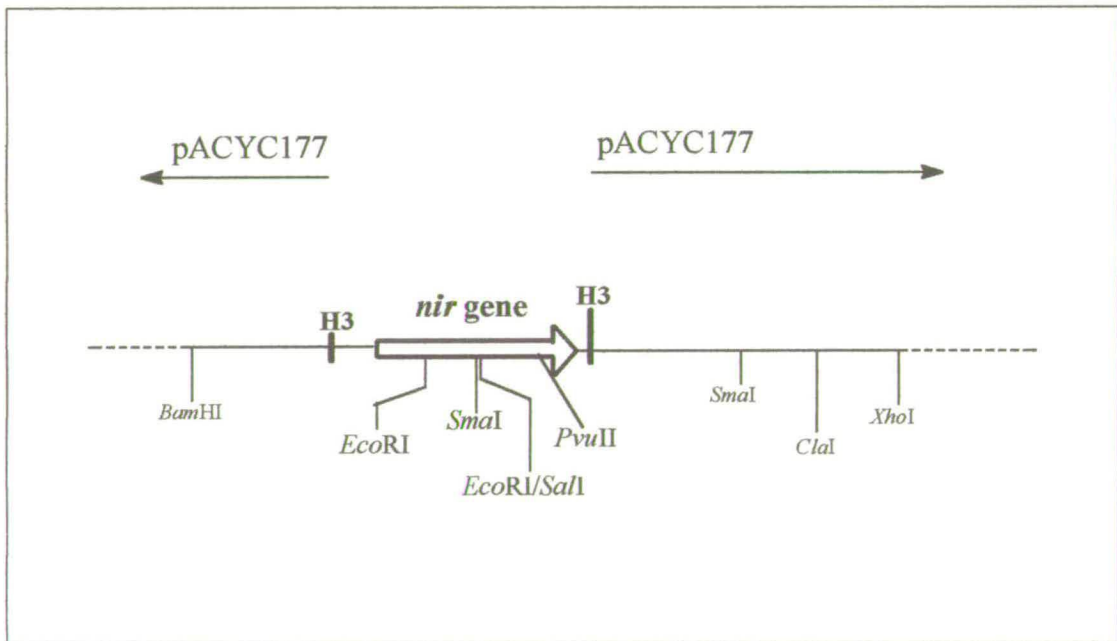


Figure 5.20. Putative map, not to scale, of transformant pH25 from the pACYC177 *Hind*III mini-library as determined by restriction and probing analysis. NB. Probing, restriction and *aniA* PCR results from this construct were ambiguous and this map was speculative until sequencing information became available.

5.4.1.1 pH25 sequence analysis

Sequencing primers surrounding the pACYC177 *Hind*III insert site were designed with the aid of the FOLDRNA package on GCG9. The primers were designed to sequence in from the ends of the ~2.0kb insert fragment in pH25. The positions of the primers are illustrated on the pACYC177 map in Appendix A5; pACYC-1 is positioned from 2429-2444bp and pACYC-2 from 2514-2499bp. Table 5.2 lists the primer sequences.

Primer name	Sequence
pACYC-1	5'-d[GCGTAATGGCTGGCCT]-3'
pACYC-2	5'-d[CACCATGAGTGACGAC]-3'

Table 5.2. Primers designed for the sequence analysis of pH25.

Sequencing the pACYC177 H25 construct was not a straightforward procedure. For automated sequencing a DNA concentration of 1µg/8µl is required. Due to the low copy number of the pACYC177 backbone of pH25 it was impossible to obtain this amount of plasmid DNA using the alkaline lysis 'mini-prep' method described in section 2.2.4. This method is recommended for the production of plasmid DNA using the Applied Biosystems 377A sequencer (Chemistry and Safety Guide, Perkin Elmer). Consequently different techniques were employed to overcome this problem of low plasmid yield.

Multiple aliquots of bacterial cells (1.5ml) were centrifuged to obtain a reasonably sized cell pellet for alkaline lysis. A DNA concentration of 200ng/µl was obtained using this method therefore 5µl of the DNA preparation was used in an automated sequencing reaction. However no sequence at all was obtained from the pACYC177 sequencing primers. This suggested that there was a problem with the

primers as the template DNA had been thoroughly checked prior to the sequencing reactions and was found to have an OD_{260}/OD_{280} of ~ 1.5 . When the pACYC177 sequencing primers had been designed there were a limited number of positions where suitable primers could be found as most of the possible primers had unfavourable fold energies as determined by the FOLDRNA package. Consequently when a pair of suitable primers were located that had favourable fold energies and would not form primer dimers with each other it was decided to use them in sequencing reactions. Further checks on the primers after the poor sequencing result on pH25 showed that they had very low T_m 's. In automated sequencing reactions it is recommended that a T_m of 55-60°C is achieved for both primers. The T_m 's of both pACYC-1 and pACYC-2 were determined to 47 and 45°C respectively. This was obviously much lower than was recommended. In automated sequencing reactions a denaturation temperature of 50°C was used in the sequencing thermocycle (section 2.2.18) therefore the pACYC177 primers would not be able to anneal to the template correctly. Alternative pACYC177 primers were not designed for further sequence analysis as other avenues of investigation were being pursued.

It was discovered whilst trying to increase plasmid yields of pH25 that chloramphenicol could be used to amplify the construct without loss of the 2kb insert fragment. This was unexpected and it was inferred from this that perhaps another mechanism, other than levels of expressed nitrite reductase protein, was affecting the successful cloning of the *nir* gene. (This will be discussed in greater detail in section 5.6.) As accurate sequencing primers were available it was decided to subclone the 2.0kb pH25 insert fragment back into the high copy number vector pUC19. Again as only one restriction enzyme had been used to digest the insert DNA the fragment would be able to insert into the cut vector in both orientations. This was believed to be advantageous as expression of the nitrite reductase protein, if present on the insert fragment, and subsequent toxicity to the host cell would not be a problem as sequence evidence from retrievable clones with the insert fragment in the opposite orientation could be obtained.

A total of 80 transformant colonies were obtained when the 2.0kb insert fragment from pH25 was cloned into pUC19. Fifteen of these transformants were

screened for the presence of the 2.0kb *Hind*III insert fragment in the vector which was found in all cases (Figure 5.21). Theoretically all of the transformants should contain the same insert as a single insert fragment was used in the ligation reaction unlike the construction of *N. subflava* plasmid mini-libraries where a mixture of insert fragments were used. To check that this was the case the *aniA* PCR was used diagnostically to detect the presence of the 350bp amplifiable fragment on a random selection of transformant plasmid constructs. The quality of the gel photograph showing the results of the *aniA* PCR was poor but a faint 350bp fragment was amplified from each of the constructs tested (Figure 5.22). The construct that gave the best *aniA* PCR result was named pH25-6 and this was used for sequence analysis of the 2.0kb insert fragment.

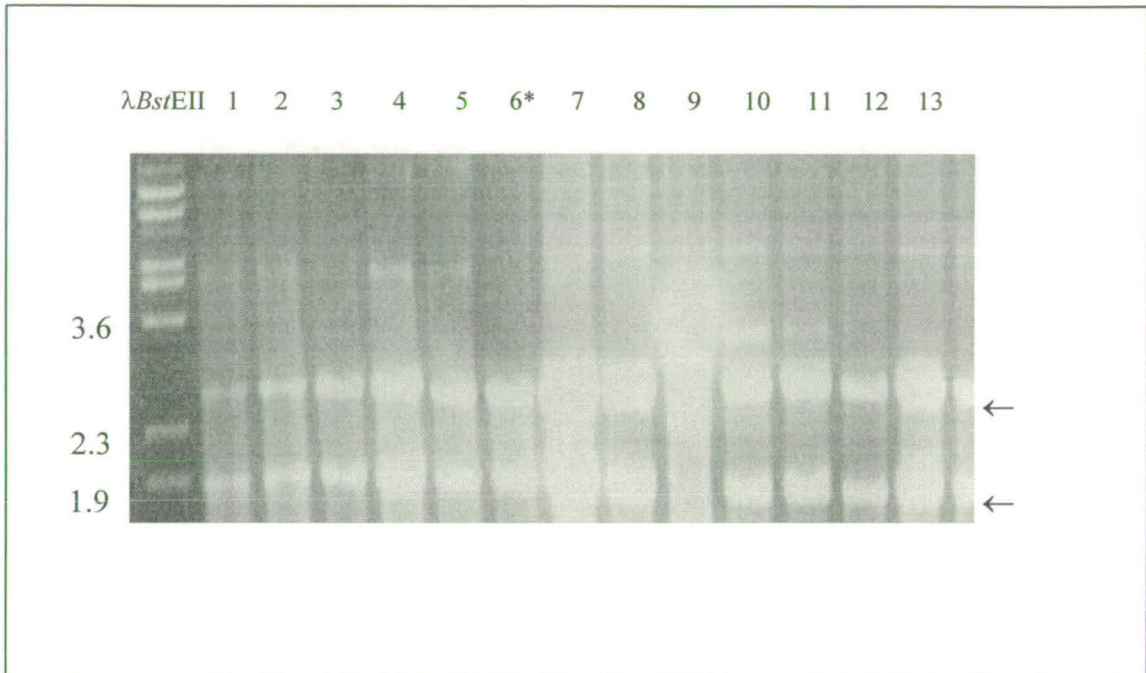


Figure 5.21. Results of the transformation screen when the 2.0kb fragment from pH25 was subcloned into pUC19. pH25 was a positive clone taken for further analysis from a *Hind*III 2.0kb mini-library constructed in pACYC177. The 2.0kb *Hind*III chromosomal DNA insert fragment was positive to a 350bp probe specific for the *N. subflava* nitrite reductase. pACYC177 was the vector of choice due to the cloning problems discussed in section 5.4.1. For further analysis of the 2.0kb insert fragment to be undertaken it had to be further subcloned into pUC19. The 2.7kb vector and 2.0kb insert bands are illustrated from each of the resulting transformants. The sequencing results of pH25-6 are discussed in the text. The sizes of the $\lambda BstEII$ vector are in kb.

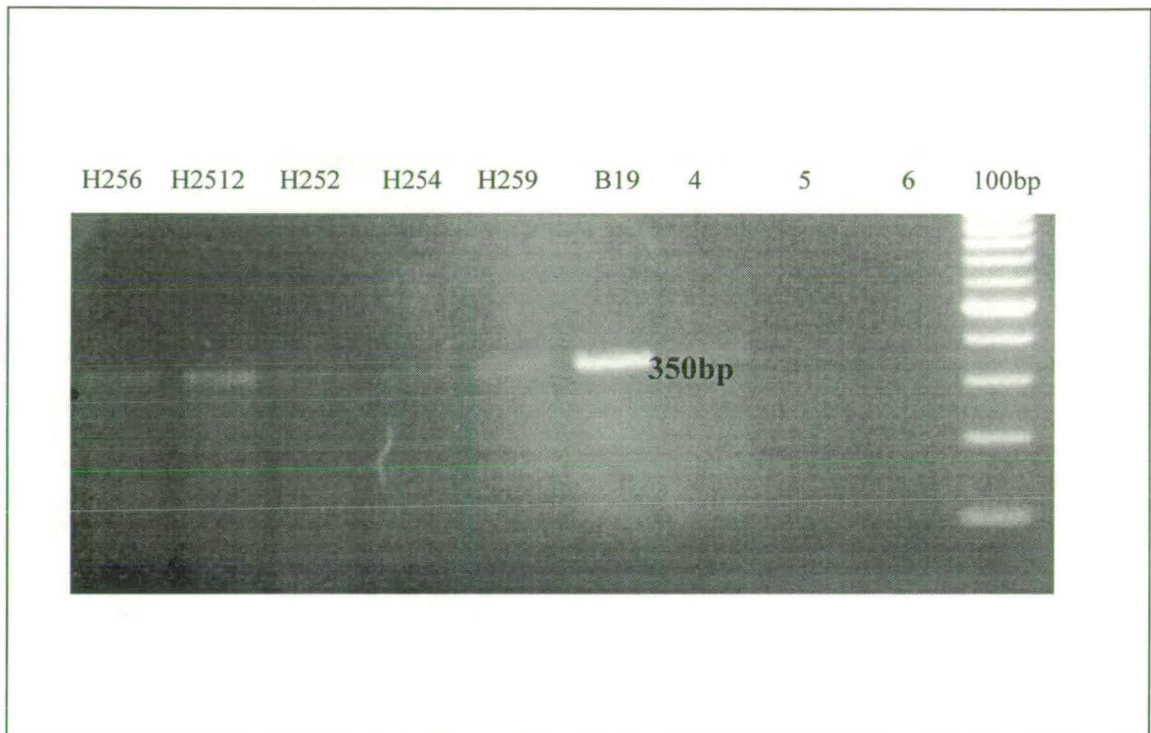


Figure 5.22. Results of the *aniA* PCR on five of the pUC19 transformants screened in Figure 5.21. In all cases a faint 350bp fragment was observed to hybridise. The *N. subflava* B19 positive control is illustrated. The bright band in the 100bp ladder corresponds to 500bp.

5.4.1.2 pH25-6 sequence analysis

pH25-6 was sequenced with the M13 Universal and Reverse primers. Sequencing was also done using the internal AniA3 and AniA4 primers. The sequences for these primers can be found in Tables 3.1 and 5.1 respectively. Good quality sequence was obtained from the Universal and Reverse primers but sequencing with the AniA3 and AniA4 primers was unsuccessful. This suggested that the 2.0kb fragment of chromosomal DNA cloned originally into pACYC177 and then pUC19 was not the fragment of interest containing the *nir* gene. This was despite the fact that a faint 350bp fragment was detected when pH25-6 plasmid DNA was used in the *aniA* PCR.

The insert size of 2.0kb was too large for an overlap to be detected with sequence generated from both Universal and Reverse primers. Consequently the Universally primed and Reverse primed sequences were analysed separately. The sequences from each of these primers are represented in Figures 5.23a and 5.23b. In the forward direction of the Reverse primed sequence and the reverse direction of the Universally primed sequence two ORFs were identified that showed significant similarity to a hypothetical peptide in the *hemM-prs* intergenic region in *E. coli*, *S. typhimurium* and *Ps. aeruginosa*. This similarity was found in reading frame 3 for the Reverse primed sequence and reading frame 1 for the Universally primed sequence. Although peptide similarity was identified in different reading frames from the two sets of sequence data the ORFs do correspond to the same single peptide. An example of the degree of similarity identified between reading frame 1 of the Universally primed sequence and the hypothetical protein from the *hemM-prs* region of the *Ps. aeruginosa* chromosome is depicted in Figure 5.24. The *hemM-prs* similarity identified disproved the map proposed in Figure 5.20 for the arrangement of the *nir* gene in pH25.

a. 1 atntctagag tgcacctgca ggcatgcaag cttcatatga ttgagaaacc
51 tgttggtaaa ttgtatgtgc tttttgatga gatttacttg ctataaacia
101 acaagccccg gaaccagtca ttaatgcatg accatattgg gataactcaa
151 tataagcctt ccaaacttca ggatattcct gaaacacaac cgcctgcata
201 tcattttgaa acggctgtaa cgattggaaa gtcggcatta tgctgggttt
251 ggaatccccg gtcaagcctt catgcgcaaa aatttttagct gttgccacat
301 gaacgggggg cttaacgata acataccatt gtttagggac atctatttca
351 gccagcttct cgcctacgcc tttggcaaaa gcacttcttc caaaaataaa
401 aaaaggaaca tccgcaccaa gacttacacc taaatcaatc agttgctgcc
451 tgctcaaacc gcattgccac cattgggtta aaaccattaa gactgtggct
501 gcatcggagc tgccgcccgc taaacctccg ccggtcggaa tcactttatc
551 caaccagatt tcaacgcegt tcggtacgct tgcatatggt agtaataatt
601 tagccgcccc ataagtcaag tctgttcggg gctcaagtcc ttcgaccggc
651 gtatgcagaa taatttgccc atcggtagcg attttcagat gaacggtatc
701 atataaacgg atnaaacaga aaatacttcc aaattatgat aaccgtcget
751 cctngcggnc ggtaatcctc aaatccaaat tttaatttaa ccggcgcaag
801 aaaaggctgg gattcctnct gaaacangac attgcattct cnatattgct

b. 1 agcttctcct gaagctgctt gccaatgtac tgtatcaacg ttcgatgggt
51 tatgagaagc tgaatcagcc aggcaaggcg attgcccatt tacgccgtgt
101 ggtagagctg tatccggata atccgcacgg ttggaatgct ttgggtata
151 ccttgttgtc aagcggcaag gatttggacg aggcattcaa aatggttcag
201 acggcctatc aaatggagcc ggaaagcgca gccattaatg atagttagg
251 ctgggcttat tatcttaaag gcgatgcaca aacagctttg ccgtatatcc
301 aatatgccta tgaaaaagaa cctgaagccg aagttgccgc gcatttgggc
351 gaagtcctat ggacacttgg cgacccaaaac aaggccaaag aatctggaa
401 tgacggtttg aaacgcggaa gcaatctccg agtattaaaa gagacaatgt
451 ccaaattcgg tataacgccc agcaaaccgc atactcaaaa acacaaataa
501 aactcaaagg ccgtctgaaa agtgtttgat ttcagacggc ctatgaagga
551 atatccatga atttaaaaca aatatcatcg gttgcagcct tattgctttt
601 agccgcttgt gcgcagccaa actttcctca gcaaaacagt tggcaagcag
651 caagagcang tgcaggattt tagtgccgat ggccgattgg ctgtcaaagt
701 ggaaggaaaa ggctcttatg ccaatttcaa ctggacttat cagaacgcgg
751 ttcaaaccat tgatgtgaat acaccgttgg gcaataaccgt aggccaactg
801 tgtcaagaca agcgaaaggc gtattggcan ttagacagta aggataangg

Figure 5.23. Sequence produced from pH25-6. a. Universal primer. b. Reverse primer. An overlap was not detected between the two sets of sequence data. Upon analysis both were found to encode an ORF found in the *hemM-prs* intergenic region in *E. coli*, *S. typhimurium* and *Ps. aeruginosa*.

```

74 NLDLRITXRERLS*FGSIFCXIGLYDTVHLKMRTDGQIILHTPVEGLE 123
   ||| | | | : . : | . | | | : ||| : | .
14 NLFLHILGRRDDGYHELQTLFQFLDHGDELHFEARQDQVRLHTEIAGVP 63

124 PEQDLTYRAAKLLLPHYASVPNGVEIWLDKVIPTGGGLGGGSSDAATVLMV 173
   : . | ||| : | . | || : |||| : | ||| : |||| |||| | :
64 HDSNLIVRAARGLQEASGSPQGVDIWLDKRLPMGGGIGGGSSDAATLLA 113

174 LNQWWQCGLSRQQLIDLGVSLGADVPPFFIFGRSAFAKGVGEKLAEIDVPK 223
   || | | | . : || . |||| | | | . | | | | | : | : | .
114 LNHLWQLGWDEDRIAALGLRLGADVPPVFTGRRAAFAEGVGEKLTVPDIPE 163

224 QWYVIVKPPVHVATAKIFAHEGLTRDSKPSIMPTFQSLQPFQNDMQAVVF 273
   || . : | | | | . |||| | | . | | | | |
164 PWYLVVVPQVLVSTAEIFSDPLLTRDS . PAIKVRTVLEGDSRNDQPVE 212

274 QEYPEVWKA 282
   . |||| |
213 RRYPEVRNA 221

```

Percent Identity: 46.6% over 209 amino acids

Figure 5.24. Peptide alignment of ORF 1 from Universally primed pH25-6 and the Ychb peptide from *Ps. aeruginosa*. The top peptide corresponds to peptide 1 from pH25-6 and the bottom to the *Ps. aeruginosa* Ychb peptide.

In *E. coli* and *S. typhimurium* the *hemM* and *prs* genes are present in an operon structure concerned with the formation of δ -aminolevulinic acid (ALA). The synthesis of ALA is the first step in the biosynthesis of haems, chlorophylls and bile pigments in the C5 pathway (O'Neill and Söll, 1990). The first gene in the operon, *hemA*, is thought to encode a glutamyl-tRNA dehydrogenase and the *prs* gene, the final gene in the operon, encodes a phosphoribosylpyrophosphate synthetase (Hove-Jensen, 1985 and Bower *et al.*, 1988). Figure 5.25 illustrates the C5 pathway for the formation of ALA with the probable catalytic activities of the *hemA* and *prs* gene products highlighted. Between the *hemA* and *prs* genes is a region of ~2kb which until recently had not been well characterised. Two open reading frames were identified in this 2kb region the first of which was named *hemM* and the second *ychb*. The *hemM* gene also encodes a protein that catalyses a reaction in the synthesis of ALA in the C5 pathway although its exact function is undetermined (Ikemi *et al.*,

1992). The *ychb* gene product is functionally unassigned but a role in the formation of ALA is anticipated.

The sequence obtained from pH25-6 displayed similarity to the *hemA-prs* region over the *ychb* gene region. The organisation of the *hemA-prs* operon is shown in Figure 5.26. The position of the sequence similarity from pH25-6 is also represented.

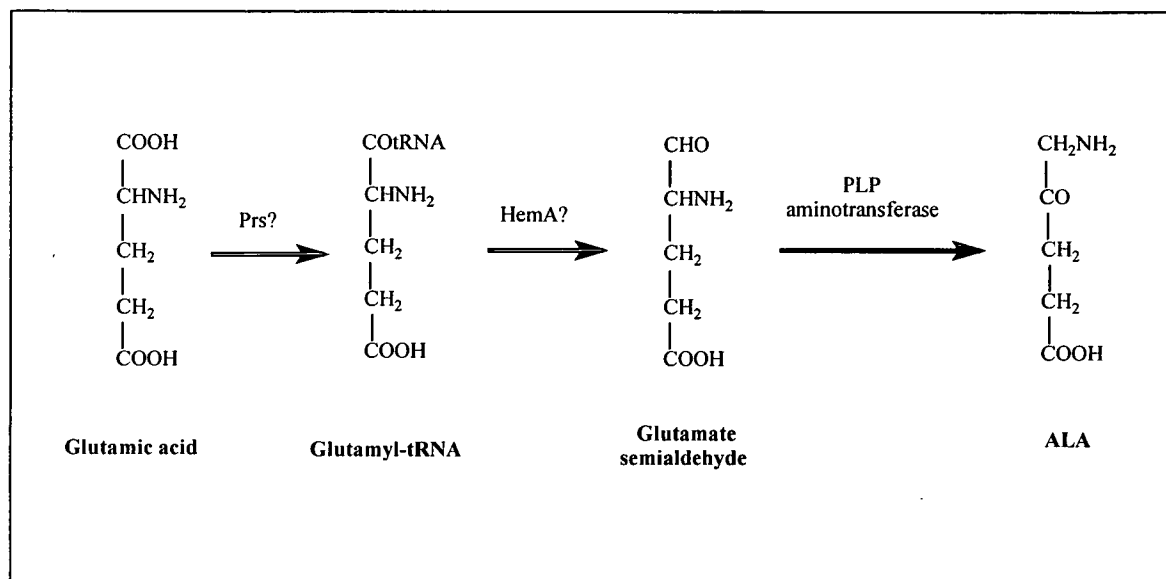


Figure 5.25. The C5 pathway for the formation of ALA. (PLP = pyridoxal phosphate). Putative positions for the *hemA* and *prs* gene products are illustrated.

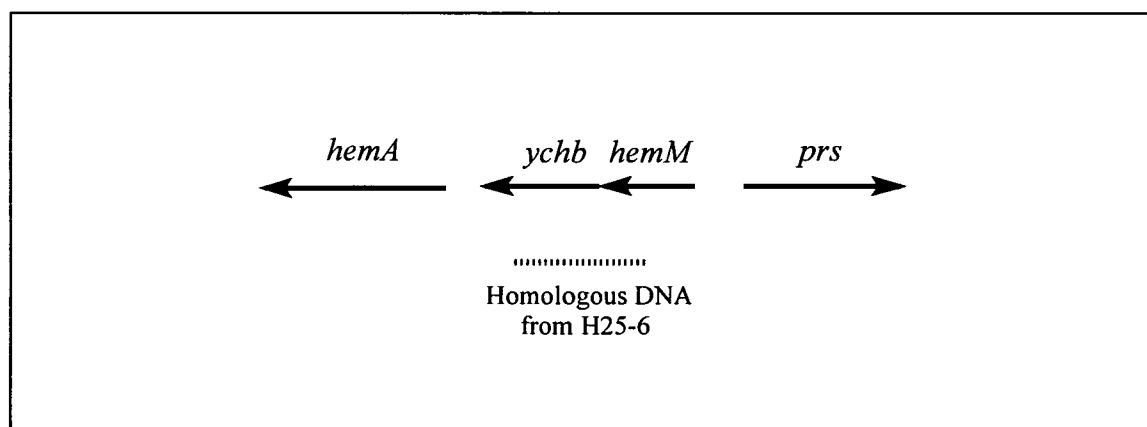


Figure 5.26. Arrangement of the *hemA-prs* operon, not to scale, showing the position of the DNA from pH25-6 with similarity to the undefined *ychb* gene. The *hemM* and *ychb* genes are separated by only 4bp of DNA. Similarity of DNA from pH25-6 to the *ychb* gene starts at nucleotide position 189. This means prior to *ychb* there is 189bp of DNA from pH25-6 which enters the *hemM* gene.

In order to determine that the 2.0kb DNA insert in pH25-6 did originate from *N. subflava* chromosomal DNA, cloned during the construction of the pACYC177 *HindIII* mini-library, sequence from this construct with the Universal primer in the reverse orientation was searched through the *N. gonorrhoeae* sequence database via the Internet (Website - http://dna12.chem.ou.edu/cgi-bin/gono_server.pl). Genomic sequence information from this Website is limited as it is only available in a series of random contigs. However it was possible to establish that the DNA cloned from the pACYC177 mini-library did indeed come from *N. subflava*. When Universally primed sequence from pH25-6 was searched through the database it was found to display substantial similarity to gonococcal DNA in contig 139. Over 466bp, 65% identity was observed (data not shown). This was taken as proof that *N. subflava* DNA was cloned during pACYC177 mini-library construction.

Section 5.3.1 described how *N. subflava* DNA from pANIA10 containing the 3' end of the *nir* gene had homology to DNA in contig 241 from the *N. gonorrhoeae* database. Until the contigs become structured and ordered the significance of these two gene homologies cannot be determined. It is likely that the *nir* gene/denitrification operon and the *hemA-prs* operon are located at different positions on the *N. subflava* chromosome as a role for any of the *hemA-prs* genes in denitrification has not yet been identified.

5.4.2 pASHOK

This plasmid was kindly donated by Dr Richard Hayward of the University of Edinburgh. It is a *lacZ* transcription vector based on pBR322. pASHOK contains a number of transcription terminators surrounding a small polylinker which prevent expression of cloned genes. Despite the presence of the *lacZ* gene blue/white colony selection cannot be used to detect transformants when cloning in pASHOK. (Appendix A6 shows the structure of pASHOK.)

It was decided to construct a *HindIII* mini-library in this vector as for pBR325 and pACYC177. It was believed that the presence of strong transcription terminators would prevent expression of the cloned *nir* gene thereby liberating the 5'

end of the *nir* gene missing from pANIA10. Due to the position of the *Hind*III cloning site in pASHOK an antibiotic sensitivity screen could not be used to detect transformant colonies containing chromosomal insert fragments. Any transformants detected carrying the Amp resistance of pASHOK were screened by colony blots and probing with the 350bp probe. Any positive colonies had their transformant plasmid DNA digested with *Hind*III and the presence of an ~2.0kb insert fragment was looked for on agarose gels. Again transformation frequencies when constructing the *Hind*III mini-library were very low. A total of 100 pASHOK transformant colonies were obtained from two *Hind*III mini-library transformations. When these were screened with the 350bp probe results were inconclusive as probing was weak and there was a high degree of non-specific hybridisation present (Figure 5.28). A total of 8 colonies were picked for further analysis but the expected ~2.0kb insert fragments were not detected in any of these constructs when examined using agarose gel electrophoresis. Ligation and transformation protocols were the same as for construction of the pBR325 mini-library which produced pANIA10 (section 5.3) so it was puzzling why transformants containing 2.0kb chromosomal insert fragments were not obtained when cloning into pASHOK. It was suspected that another factor such as the presence of DNA secondary structure in the 5' end of the *nir* gene was affecting cloning of this gene rather than expression of the proposed membrane bound nitrite reductase. (This is explained further in section 5.6). However it still did not explain why other 2.0kb insert fragments corresponding to *N. subflava* chromosomal DNA did not clone into pASHOK. Due to time constraints this was not investigated further although it was assumed that the large size of pASHOK reduced the efficiency of the ligation reaction.

Obviously cloning into a vector which prevented expression of cloned genes did not overcome the cloning problems associated the *nir* gene. Other cloning strategies therefore had to be developed.

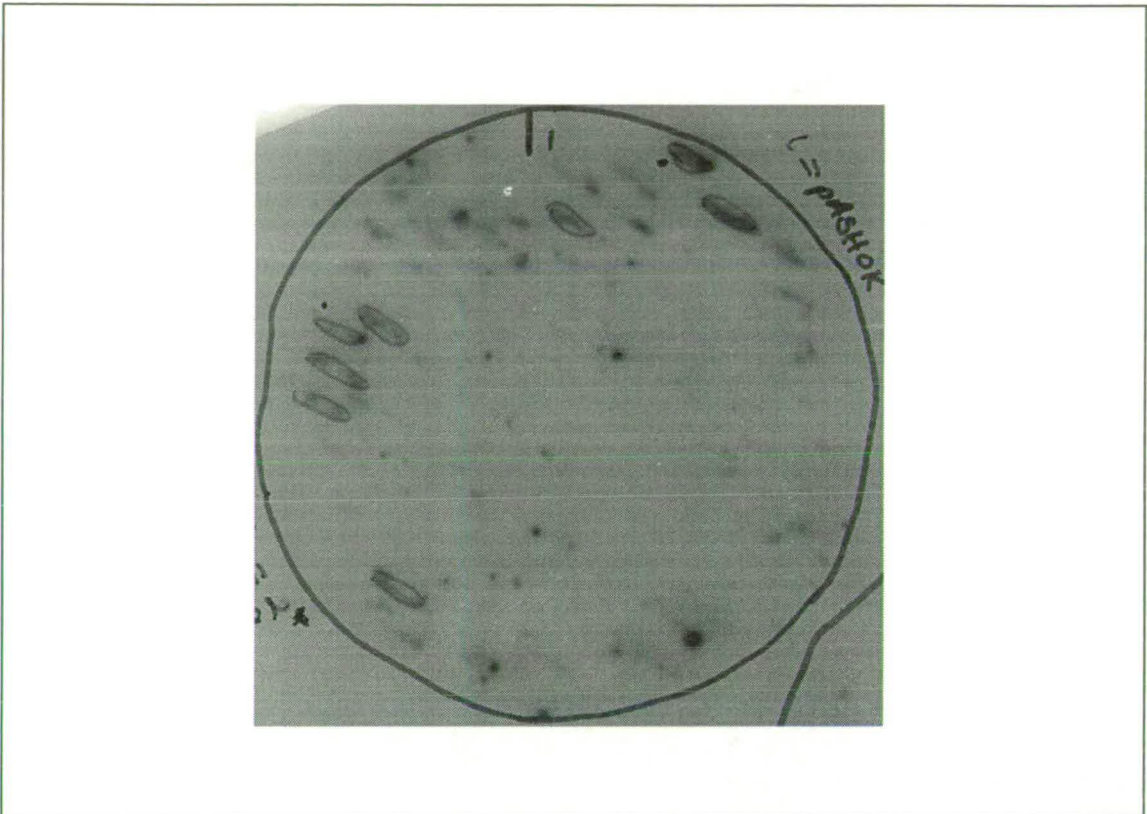


Figure 5.27. Results of pASHOK/*Hind*III mini-library screen. A total of 100 transformant colonies were screened with the 350bp probe. Although the probing results were not consistent a total of 8 colonies were picked for further analysis. These were named pA2, pA9, pA12, pA21, pA22, pA31, pA41 and pA81 and are circled in the above diagram.

5.5 Cloning from λ EMBL 3

The attempts at constructing a *N. subflava* mini-library in pUC19, pBR325, pACYC177 and pASHOK vectors had varying degrees of success but the entire nitrite reductase gene could not be cloned. When constructing a plasmid mini-library a mixture of insert bands of the desired length were used in the ligation reaction. Obviously the chances of cloning the right fragment from this mixture were lower than if the correct fragment only was used in the ligation reaction. Obtaining a single insert fragment containing the *nir* gene for use in ligation reactions was the reason behind subcloning from a complete *N. subflava* B19 genomic library in λ EMBL 3.

A *N. subflava* B19 genomic library in λ EMBL 3 was screened with the 350bp probe as described in section 2.4.2. After a number of purifications two λ clones were isolated that showed strong and consistent hybridisation to the 350bp probe. These were named λ 350-5 and λ 350-9. DNA was purified from the λ clones and used in the *aniA* PCR to determine whether or not the 350bp fragment could be amplified from each of the clones. The results of this PCR are depicted in Figure 5.28. It can be seen from this PCR that a single 350bp fragment was amplified from λ 350-5. When λ 350-9 was used as template for the *aniA* PCR two bands were observed to amplify: one at 350bp and the second at ~330bp. From this it appeared that λ 350-5 was the better candidate for containing the nitrite reductase gene. However subsequent restriction and probing analysis indicated that this was not the case.

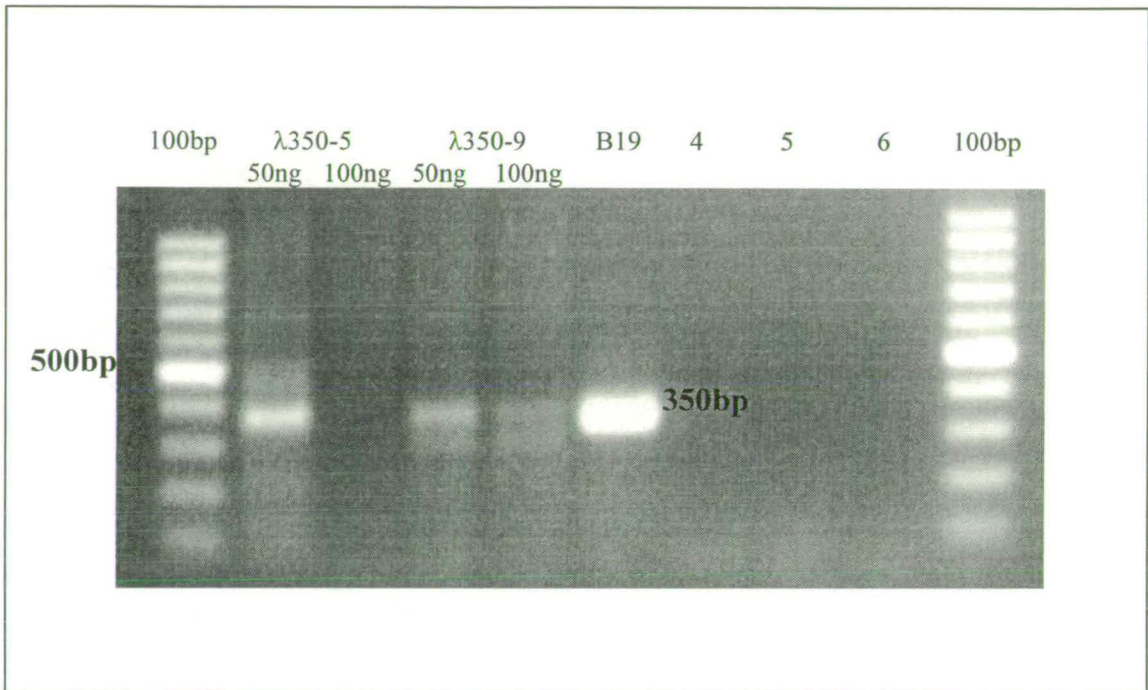


Figure 5.28. Gel photograph of the *aniA* PCR on λ 350-5 and λ 350-9. The positive control with *N. subflava* B19 DNA is highlighted. When λ 350-9 was used as the template for the *aniA* PCR two bands of ~330bp and 350bp were seen to amplify. In the 100bp ladder the brighter band corresponds to 500bp.

λ 350-9 DNA was digested with a number of different restriction enzymes in single and double combinations for Southern hybridisation and probing analysis with the 350bp probe. This was to enable fragments of a suitable size for subcloning to be identified. Comparison of these fragment sizes to appropriately digested wild type *N. subflava* chromosomal DNA did not demonstrate a high degree of similarity (Table 5.3). However the discrepancies were discounted when maps derived for both wild type *N. subflava* and λ 350-9 were compared (Figures 5.29 and 5.30). The position of the *Cla*I site in the λ insert fragment was crucial. In both B19 and λ 350-9 this mapped to 1.8kb upstream of the nitrite reductase gene. All sites predicted to exist downstream in *nir* were replaced by sites in the right arm of λ due to the insert fragment cloning position. From the λ 350-9 map it can be seen that only a portion of the 350bp probe has cloned at the right hand end of the insert fragment. This insert position accounts for differences observed in the probing results listed in Table 5.3

and the unexpected *aniA* PCR result. In λ 350-9 it is predicted that the insert fragment has become cloned with the AniA2 primer spanning the *Bam*HI cloning site. This accounts for the unusual PCR profile obtained when λ 350-9 is used in the *aniA* PCR. The only restriction site which does not map to the same position in both B19 and λ 350-9 is *Hind*III. However this can be explained as partial *Hind*III fragments in λ 350-9 are proposed to be hybridising to the 350bp probe.

DNA from λ 350-5 was also digested in this way and analysed with the 350bp probe (data not shown). It was found that there were no constant fragments in each of the λ clones to suggest they contained overlapping chromosomal insert DNA. The sites detected in λ 350-5 did not confer to the map of the nitrite reductase gene (Figure 5.30) and, despite the encouraging PCR result, no further analysis of λ 350-5 was undertaken

Restriction digest	λ 350-9 fragment size (kb)	B19 fragment size (kb)
<i>Bam</i> HI	0.4	~12
<i>Cla</i> I	2.2	2.9
<i>Hind</i> III	~12	2.0
<i>Pst</i> I	~10	4.4
<i>Sal</i> I	7.4	~12
<i>Sma</i> I	7.0	~14
<i>Bam</i> HI/ <i>Cla</i> I	0.4	nt
<i>Bam</i> HI/ <i>Hind</i> III	0.4	nt
<i>Bam</i> HI/ <i>Pst</i> I	0.4	nt
<i>Bam</i> HI/ <i>Sma</i> I	0.4	nt
<i>Cla</i> I/ <i>Pst</i> I	1.9	nt
<i>Eco</i> RI/ <i>Cla</i> I	nt	0.5
<i>Eco</i> RI/ <i>Hind</i> III	nt	0.5
<i>Hind</i> III/ <i>Pst</i> I	~10	nt
<i>Hind</i> III/ <i>Sma</i> I	6.7	nt
<i>Sal</i> I/ <i>Cla</i> I	nt	3.4
<i>Sal</i> I/ <i>Hind</i> III	nt	1.7
<i>Sma</i> I/ <i>Pst</i> I	7.4	nt

Table 5.3. Fragments from *N. subflava* B19 and λ 350-9 positive to the 350bp probe. Fragment sizes >10kb could not be sized accurately on 0.8% agarose gels. nt - not tested

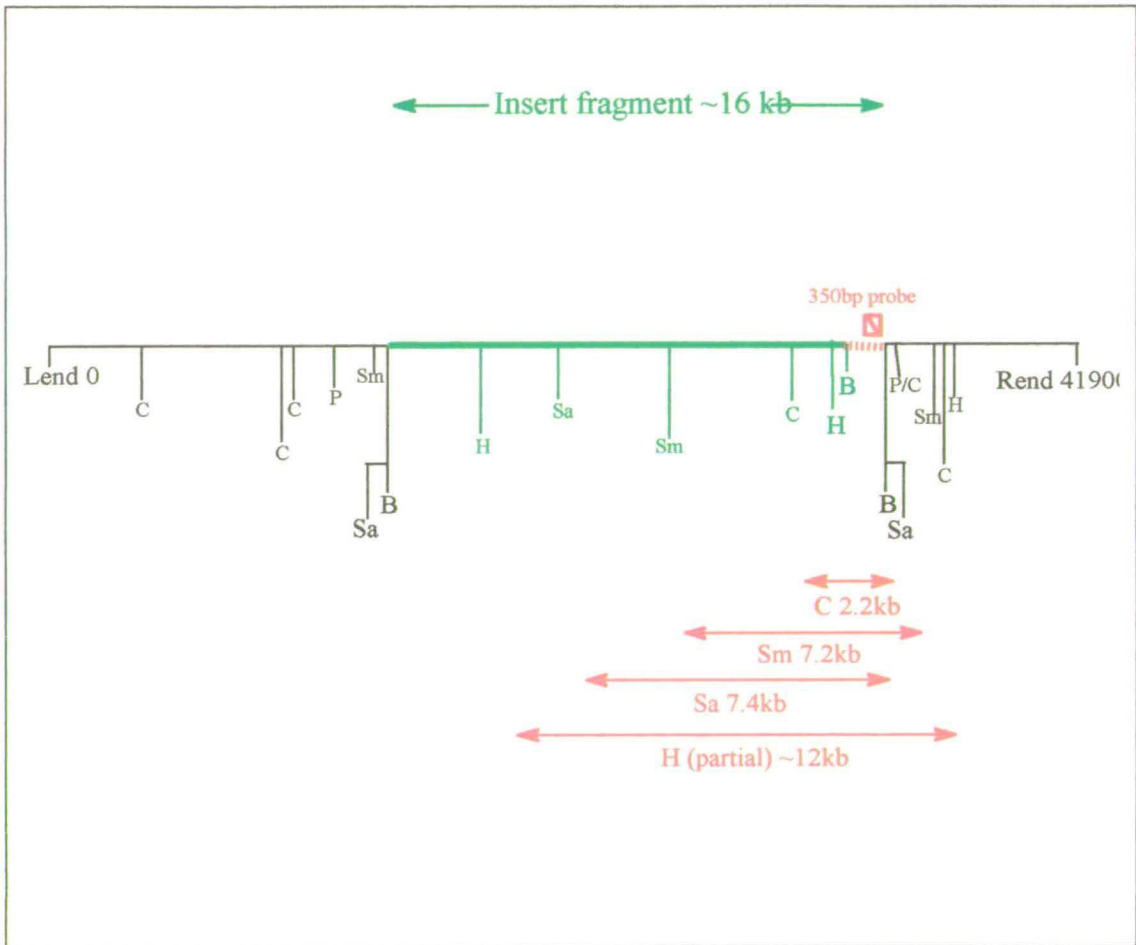


Figure 5.29. Putative map, not to scale, of λ 350-9 as determined by restriction and 350bp probing analysis. Although not all of the probing results given in Table 5.3 fit correctly with this map it was presumed to be a fairly accurate determination of restriction sites. *HindIII* partial fragments were thought to be providing some of the probing results in Table 5.3 thereby affecting map determination. Key to restriction enzymes B - *Bam*HI, C - *Cla*I, H - *Hind*III, P - *Pst*I, Sa - *Sal*I, Sm - *Sma*I.

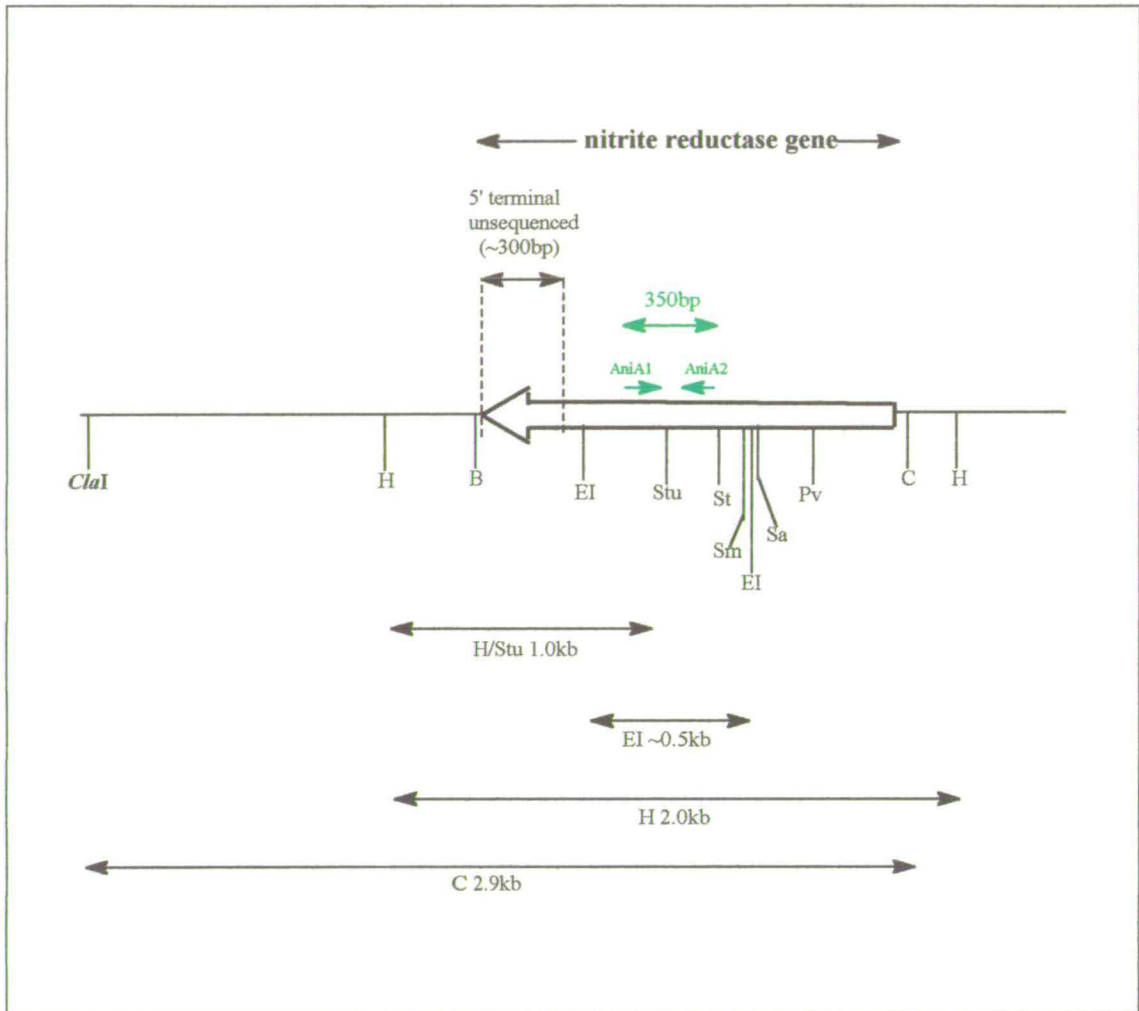


Figure 5.30. Proposed map, not to scale, of the nitrite reductase gene from *N. subflava* B19. Derived from restriction and 350bp probing analysis of *N. subflava* B19 and pANIA10. The *ClaI* site (in bold) upstream of the *nir* gene fits with the predicted position of *ClaI* in λ 350-9 (Figure 5.29). Key to restriction enzymes B - *Bam*HI, C - *Cla*I, EI - *Eco*RI, H - *Hind*III, Pv - *Pvu*II, Sm - *Sma*I, Stu - *Stu*I, St - *Sty*I.

From the 350bp probing on digests of λ 350-9 an obvious fragment for cloning to obtain the 5' end of the *N. subflava nir* gene was the *Cla*I 2.2kb fragment. Numerous attempts were made to clone this fragment into pUC19, pBR325 and pACYC177 in *E. coli* DH5 α . However all efforts were unsuccessful as transformant colonies were not recovered from any of the cloning experiments. Experimental protocols were thoroughly checked to ensure simple practical errors were not at fault. When experimental error was excluded it was hypothesised that another factor, other than expression of the nitrite reductase gene, was affecting cloning. The *Cla*I 2.2kb fragment from λ 350-9 contained only the N-terminal region of the nitrite reductase protein. It was postulated that if expressed, a truncated protein in the *E. coli* host cell would lack the ability to attach to the outer membrane, ensuring cell surface integrity would be maintained. If this was the case another factor had to be affecting the recovery of clones containing the 5' terminal of the *nir* gene. One hypothesis suggested that the lack of recombinant clones containing the 2.2kb *Cla*I fragment was due to DNA, within or upstream of the 5' end of the *nir* gene, containing secondary structure - most likely in the form of a hair-pin loop. It was believed that this was obstructing cloning in conventional *E. coli* strains. Preliminary investigations into this hypothesis are discussed in section 5.6.

In conclusion, cloning the *Cla*I 2.2kb fragment from λ 350-9 was unsuccessful. However this does not reduce the likelihood that λ 350-9 contains the 5' terminal of the nitrite reductase gene as the *aniA* PCR used to check this λ clone produced a 350bp fragment on amplification. Sequence evidence obtained from other unsuccessful attempts to clone the nitrite reductase gene demonstrated that alternative fragments of the Neisserial chromosome can be cloned (sections 3.3; 3.4 and 5.4.1.2). As reducing the copy number of the cloning vector did little to improve cloning the *nir* gene another mechanism, other than nitrite reductase protein expression, was proposed to be affecting the recovery of clones containing *nir*. Strategies designed to overcome the problems associated with cloning DNA containing secondary hair-pin loop structures are discussed in section 5.6.

5.6 Further *nir* Cloning Strategies

This section discusses preliminary investigations into cloning the nitrite reductase gene in systems tolerant to DNA secondary structure. To overcome proposed protein toxicity problems and the possibility that DNA secondary structure was present at the 5' end of the *nir* gene, it was attempted to clone the 5' terminal of *nir* into a modified *E. coli* strain (DL795). This strain is *sbcC*⁻ and *recA*⁻ and lacks the ability to repair DNA. (Strains with the *sbcC* mutation allow stable propagation of plasmids carrying palindromes whilst *recA*⁻ strains have no homologous recombination activity.) DL795 is therefore tolerant to DNA containing secondary structure such as palindromic hair-pin loops.

Cloning directly into wild type *N. subflava* was also investigated as it was thought that the native host would tolerate the proposed DNA secondary structure even if present on an exogenous plasmid. In this case a broad host range cloning vector (pKT231) was used as conventional cloning vectors, such as pUC19 and pBR325, are unable to replicate in strains other than *E. coli*. pUC19 and pBR325 are examples of ColE1 replicons. These plasmids are dependent on the *E. coli* host cell for replication as they utilise cellular DNA and RNA polymerases; they do not encode for these peptides themselves. In other organisms, such as *N. subflava*, the indigenous DNA and RNA polymerases recognise different target sequences for gene expression and ColE1 plasmid replication cannot be initiated. Broad host range cloning vectors, such as pKT231, have been designed specifically from plasmids with the natural ability to replicate in a large number of Gram negative organisms to overcome these problems.

5.6.1 Cloning into *E. coli* DL795

The map of *N. subflava* chromosomal DNA surrounding the nitrite reductase gene (Figure 5.30) identified a 1.0kb *StuI/HindIII* fragment which contained the 5' end of the nitrite reductase gene. At this point the restriction and probing analysis of λ 350-9 was not available so it was decided to construct a *StuI/HindIII* mini-library in

pSL1190. This vector was chosen as it contains a polylinker with both *Hind*III and *Stu*I restriction sites. When cloned into these sites the 5' end of the *nir* gene would be in the opposite orientation to the *lacZ* gene thereby reducing the remote possibility that expression of a truncated nitrite reductase protein may occur. pSL1190 also contains a huge polylinker containing every palindromic hexamer recognition sequence. It was thought that this would increase the choice of restriction enzyme when trying to clone the 5' and 3' ends of the nitrite reductase gene together. (Appendix A7 illustrates the pSL1190 cloning vector.)

Preliminary investigations into cloning with pSL1190 and *E. coli* DL795 were undertaken, unfortunately with little success. A suitable antibiotic selection screen could not be used to detect recombinant clones, so all colonies with Amp resistance were colony blotted and probed with the 350bp probe. A total of 10 colonies from a single transformation experiment probed positive to the 350bp probe (Figure 5.31). However plasmid DNA from these transformants was incorrect. When digested insert fragments of any size were not detected (data not shown). It was postulated that the low yields of insert DNA, obtained upon digestion from the Neisserial chromosome, were affecting the ligation reaction. (A fragment size of 1kb is a tiny proportion of the entire 2Mb *N. subflava* chromosome to digest for genetic manipulations.) At present work is continuing in the laboratory developing this cloning strategy in *E. coli* DL795. Attempts are also being made to clone the 2.2kb *Cla*I fragment from λ 350-9 into pSL1190 to obtain the 5' end of the nitrite reductase gene.

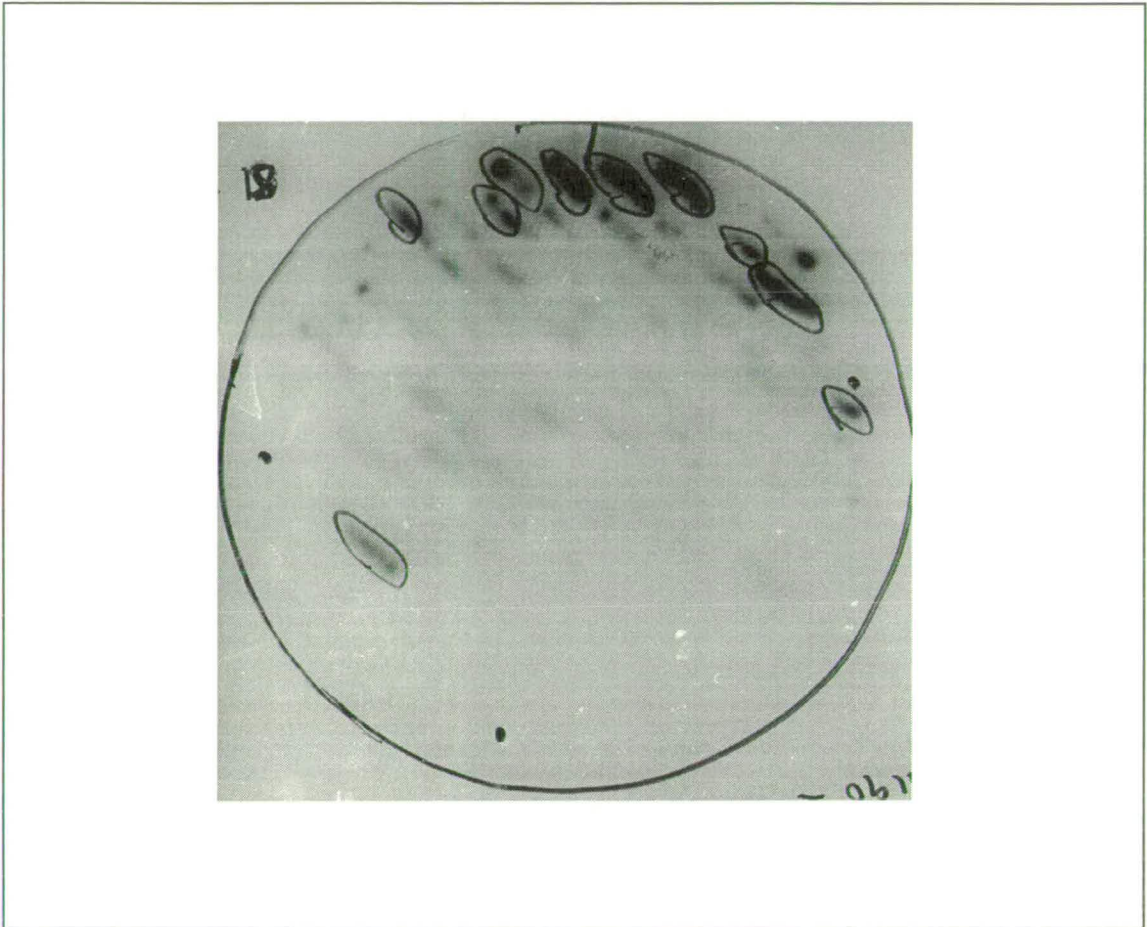


Figure 5.31. Autoradiograph of *Stu*/*Hind*III ~1.0kb mini-library in pSL1190, probed with 350bp probe. A total of 10 transformant colonies were positive to the probe and these were picked for further analysis. The positive colonies are circled.

3.6.2 Cloning into *N. subflava*

Cloning into *N. subflava* B19 was made difficult as the organism is very resistant to transformation. Initial cloning attempts used *N. subflava* cells made competent using CaCl_2 . However the cells never acquired the antibiotic resistance of the donor plasmid. This was also observed when uncut plasmid vector was used as a control. It was summarised from this that the *N. subflava* cells did not acquire competence using CaCl_2 . Consequently electroporation (section 2.2.14) was used to produce competent *N. subflava* for transformation experiments.

The broad host range plasmid pKT231 (Appendix A8) was used for cloning into *N. subflava* B19. This plasmid does not have a multiple cloning site (MCS) so the choice of chromosomal restriction fragments for subcloning was limited. Fortunately it did contain a *Hind*III site and it was decided to construct a plasmid mini-library in pKT231 for propagation in *N. subflava* B19. The *Hind*III site was located within the kanamycin resistance gene of pKT231. This enabled transformant *N. subflava* cells to be efficiently screened. Cells were tested for streptomycin resistance, the other pKT231 antibiotic selectable marker, and these were screened for kanamycin sensitivity. A total of 300 transformant colonies were obtained that were Strep^R, 100 of which were kanamycin sensitive. These Kan^S colonies were blotted and probed with the 350bp probe. A high proportion of background was present on the resulting autorad (data not shown). There were 12 colonies which showed a slightly higher degree of hybridisation and these were picked for further analysis. Unfortunately in each case plasmid DNA could not be isolated from the *N. subflava* parent cells. There are two possible explanations for this unexpected result. *N. subflava* mutants deficient in restriction modification (*hsdR*) are not available. The *hsdR* gene encodes the EcoK restriction system in which the EcoK protein recognises specific DNA sequences and will restrict unmodified DNA. In this case the unmodified DNA would be the pKT231 plasmid backbone. Alternatively cell disruption during the plasmid mini-prep procedure could be at fault. As cell disruption for ligation required electroporation it seems reasonable to suppose that SDS present in the plasmid mini-prep lysis solution would not be sufficient for lysis of *N. subflava* too. Currently work is being undertaken in the laboratory to investigate these two hypotheses. The introduction of a sonication step, or the addition of detergent such as Triton X-100, are being examined to increase the amount of *N. subflava* cell lysis obtained during plasmid minipreparation from recombinant clones. However if it is determined that degradation of recombinant plasmid DNA in *N. subflava* is responsible for the lack of plasmid recovery then alternative vectors would need to be investigated. Recently a versatile shuttle system was developed for transformable and non-transformable strains of *Neisseria* (Kupsch *et al.*, 1996). The 'Hermes' vectors were designed initially for genetic manipulations

in *N. gonorrhoeae* but it is anticipated that using *N. subflava* will not reduce cloning efficiency.

5.7 Summary

The *aniA* PCR amplified a 350bp fragment from *N. subflava* chromosomal DNA as predicted. When sequenced, the fragment was found to correspond to the nitrite reductase gene. From this sequence the nitrite reductase protein was characterised as a copper containing enzyme as the type I and type II copper binding ligands present in the other periplasmic copper enzymes were conserved. Only 8 amino acid discrepancies were identified between gonococcal AniA and the translated peptide from the 350bp fragment. This was taken as evidence that the nitrite reductase peptide of *N. subflava* would also be found in association with the outer membrane.

Use of the 350bp fragment as a probe identified suitably sized fragments of *N. subflava* chromosomal DNA for subcloning and sequencing. Consequently a *HindIII* mini-library in pBR325 was constructed. A single clone (pANIA10) from this mini-library extended sequence at the 3' end of the *nir* gene. The sequence obtained was translated and compared to AniA from *N. gonorrhoeae*. It was found that 71.8% identity existed between the two peptides. This was taken as further evidence that the nitrite reductase peptide in *N. subflava* will also be bound to the outer membrane.

Numerous strategies were developed in an attempt to clone the 5' end of the *nir* gene, all of which were unsuccessful. It was originally postulated that expression of the nitrite reductase gene resulted in the production of an aberrantly folded nitrite reductase peptide. This was proposed to be affecting recovery of the entire *nir* gene by reducing viability of recombinant clones. However this idea was rejected as cloning into the 'promoterless' vector, pASHOK, did not liberate the 5' end of the nitrite reductase gene either. It is also unlikely that *E. coli* cloning strains would be able to express Neisserial genes.

Preliminary investigations into cloning *nir* into systems that permitted DNA secondary structure were undertaken, again without success. However a number of experimental problems were highlighted which were believed to be responsible for the negative results. These are currently being investigated by coworkers in the laboratory.

To summarise, the nitrite reductase gene of *N. subflava* has been identified from sequence analysis, and is proposed to contain copper in its active site. This supports work by Brew (1992) who postulated a copper nitrite reductase after numerous whole cell inhibition studies on the nitrite reductase enzyme. A total of 869bp of the gene has been sequenced and the C-terminal stop codon identified. It is estimated from the length of the gonococcal *aniA* gene that ~300bp of the *N. subflava* gene remains to be sequenced at the 5' terminus.

Chapter Six

Concluding Discussion

It was initially intended to purify the nitrite reductase enzyme from *N. subflava* for *in vitro* analysis to determine if it could directly catalyse *N*-nitrosation reactions. Unfortunately this aim was not fulfilled due to a number of unforeseen problems, however preliminary characterisation of the nitrite reductase has been undertaken. The type of enzyme present in *N. subflava* was identified and a novel arrangement of the denitrification pathway in the periplasm was proposed.

In chapter three, cloning from Tn5 mutant 163 to create plasmid pZS163 did not liberate DNA sequence corresponding to any denitrification genes. This was unexpected as the *N. subflava* mutant strain lacked the ability to reduce nitrite and it was believed that Tn5 had inserted into a structural or regulatory gene for nitrite reductase (Brew, 1992). Extensive genomic DNA probing on *N. subflava* wild type and mutant 163 strains led to the conclusion that an ≥ 11.3 kb deletion occurred when pZS163 was constructed and this accounted for the lack of denitrification gene sequences obtained when pZS163 was sequenced. A 170bp probe positioned directly next to the IS50_R end of the Tn5 molecule in mutant 163 was used to construct pJT170. This construct contained ~ 4 kb genomic DNA upstream and ~ 2 kb of the deleted genomic DNA immediately downstream of the Tn5 insertion. Again sequence obtained from pJT170 did not correspond to any denitrification genes. Directly upstream of the Tn5 insertion position similarity was identified to the adenylosuccinate synthetase gene of a number of different bacteria whilst 600bp downstream from Tn5 an acetoacetyl-CoA reductase gene was located. The intervening 600bp lacked a distinct ORF and was proposed to correspond to a specific promoter region which distally affected the nitrite reductase gene. However there was not enough evidence from the results presented in chapter three to determine whether the gene affected was a structural or regulatory component of the nitrite reductase operon.

Chapter four used nitrite reductase activity assays to investigate nitrite reductase activity in whole cells. It was decided to repeat the whole cell assays on wild type and mutant 163 strains originally done by Brew (1992) to check that the strains were still authentic and unaltered from when first isolated. The reason for this

was the lack of nitrite reductase gene sequence identified directly adjacent to the Tn5 insertion in pZS163. A deletion hypothesis was presented in chapter three to explain the lack of nitrite reductase gene sequence but it was decided that physiological tests on the *N. subflava* strains were necessary to support this. A remote possibility for the absence of nitrite reductase gene sequence was that the Tn5 molecule had moved from its original insertion position in the Neisserial genome. This is a rare phenomenon as Tn5 is a well established genetic tool for use in mutagenesis experiments. However it can occur when the kanamycin resistance carried by the transposon is not selected for in cell cultures. Probing evidence presented in section 3.2.1 demonstrated that only one Tn5 molecule had inserted into the *N. subflava* chromosome but whether the insertion position detected in these experiments was the same as when mutant 163 was first isolated was unknown. Fortunately whole cell nitrite reductase assay results on *N. subflava* B19 and mutant 163 strains correlated well with those recorded by Brew (1992). Brew calculated the nitrite reductase activity of *N. subflava* B19 to be 1130 nmol/min/mg protein, with a value of zero detected for mutant 163. Assays performed as part of this study identified a strong and persistent rate for nitrite reduction in *N. subflava* B19 with zero nitrite reduction detected in mutant 163. These results showed that the phenotype of mutant 163 had not changed from when it was first isolated and it was surmised that the Tn5 insertion position in this strain also remained the same. This supported the conclusion drawn in chapter three, that Tn5 was exerting a distal effect on a downstream nitrite reductase structural or regulatory gene resulting in the Nir⁻ phenotype observed in mutant 163.

Methyl viologen nitrite reductase activity assays on polyacrylamide gels were used to provide evidence as to the type of nitrite reductase enzyme present in *N. subflava*. A possible arrangement for the denitrification pathway was also postulated. A protein with a molecular weight of ~200kDa was detected which had nitrite reductase activity compared to the observed molecular weight of 54kDa for the AniA protein monomer from *N. gonorrhoeae*, hence it was postulated that the nitrite reductase peptide was running as a large protein aggregate on the gels. It was inferred from this that the nitrite reductase protein from *N. subflava* was associated

with the membranous fraction of the cell. This was a constructive result as it appeared to support the idea that the *N. subflava* nitrite reductase would be associated with the outer membrane, as is the case for the AniA nitrite reductase in *N. gonorrhoeae*. However attempts to obtain a different activity profile on native gels by using Triton X-100 in the cell breakage and PAGE steps were unsuccessful. It was thought that the Triton X-100 detergent would disrupt cellular membranes thereby liberating intact nitrite reductase monomers whose activity would be detected on the native gels. However the same nitrite reductase activity profiles were obtained whether Triton X-100 was included in the experiments or not. At this point sequence evidence from pANIA350 became available which also suggested an outer membrane location for the *N. subflava* nitrite reductase. It was therefore deduced that Triton X-100 was not a strong enough detergent to overcome the interaction between the nitrite reductase enzyme and the outer membrane. Time constraints meant that a thorough investigation into which detergents would overcome the hypothesised outer membrane location of the nitrite reductase enzyme could not be undertaken.

Attempts were made using the methyl viologen nitrite reductase assay to determine if the proposed outer membrane location for nitrite reductase was correct. Membranes were extracted from the wild type *N. subflava* cells as described in section 2.3.9. Activity was detected in the membrane fraction at a rate of 1142 nmol/min/mg protein. This result was regarded as encouraging. The low rate of cytoplasmic nitrite reductase activity detected was explained as resulting from a fairly weak interaction between the outer membrane and the reductase protein. The 50mM Tris buffer (pH 8.0) used in the extraction procedure was postulated to have disassociated the nitrite reductase enzyme from the outer membrane. Consequently nitrite reductase activity was observed in the cytoplasm.

Further investigations to try and pinpoint nitrite reductase activity to the outer membrane fraction were undertaken. Sakosyl was used as the detergent in this extraction as it is believed to completely solubilise cytoplasmic proteins at concentrations of 0.5% (w/v). Nitrite reductase activity was indeed identified in the outer membrane fraction but activity was also detected in the inner membrane. (The

rates were 409 nmol/min/mg protein and 1441 nmol/min/mg protein respectively.) It was postulated that the nitrite reductase enzyme becomes disassociated from its outer membrane attachment site and so does not pellet with the membrane fraction upon high speed centrifugation. Hence, a higher activity rate for nitrite reduction is observed in the inner membrane fraction of the cell. It is anticipated that repetition of the outer membrane extraction with Tris buffers over a range of pH values will enable nitrite reductase activity to be localised to the outer membrane fraction of *N. subflava* B19. i.e. there will be no disassociation of nitrite reductase from the outer membrane.

Native gel assays were also used to provide evidence as to the type of nitrite reductase enzyme present in *N. subflava* B19. On native gels the activity of nitrite reductase was severely reduced in the presence of DDC. Total inhibition was not observed but it was believed that this was due to the inclusion of insufficient DDC in the assay conditions. The gel studies were not repeated to observe total inhibition of nitrite reductase activity in the presence of DDC as whole cell assays under these conditions repeatedly recorded zero nitrite reductase activity. It was tentatively assumed from these experiments that the nitrite reductase enzyme in *N. subflava* contained copper in its active site. However it must be conceded that lack of activity could also be a result of inhibition of a copper containing azurin or pseudoazurin electron donor to the nitrite reductase protein. Although work reported by Lambert (1997) indicates that *N. subflava* does not contain an azurin donor protein. Sequence evidence cited in chapter five unambiguously identified the presence of a copper containing nitrite reductase enzyme in *N. subflava*.

The major surprise from the native gel activity assays discussed in chapter four was the greater degree of apparent nitrite reductase activity observed in the mutant 163 strain. It was postulated from this that the Tn5 insertion into mutant 163 had affected a gene for a membrane bound electron donor to nitrite reductase. This subsequently blocked a controlled transfer of electrons to the outer membrane associated nitrite reductase enzyme from the UQH₂/UQ pool. Such an outer membrane location for the nitrite reductase electron donor would account for the zero nitrite reductase activity observed when whole cell assays of mutant 163 were carried

out. On native gels however, the metabolic block in mutant 163 is by-passed due to an alternate source of electrons which are able to flow directly from the sodium dithionite reducing agent in the activity stain solutions. In the wild type strain both the nitrite reductase enzyme and electron donor are thought to run as part of the same protein aggregate and a controlled flow of electrons to nitrite reductase results via the preferred electron donor protein. An outer membrane-bound azurin electron donor to the AniA protein of *N. gonorrhoeae* is proposed to exist (Gotschlich and Seiff, 1987), although the outer membrane associated electron donor to the *N. subflava* nitrite reductase is thought to differ greatly to this. Attempts to PCR DNA containing the azurin gene from *N. subflava* were unsuccessful (Lambert, 1997). Also, DNA in 600bp region of DNA downstream of the Tn5 insertion position in pJT170 did not show any similarity to characterised azurin genes. It was postulated that DNA in this 600bp region distally affected a novel outer membrane-bound electron donor to nitrite reductase.

Results presented in chapter five provided solid evidence as to the type of nitrite reductase present in *N. subflava*. Degenerate PCR primers were designed from sequence alignments of a number of nitrite reductase peptides including AniA from *N. gonorrhoeae*. A 350bp fragment was expected to amplify from this PCR and this was observed. When sequenced the PCR fragment was found to correspond to the nitrite reductase gene from *N. subflava*. The translated ORF had 92.9% identity to the gonococcal AniA protein. Only 8 amino acid differences were identified and after careful analysis these were determined to be true and not due to sequencing errors. All of the conserved copper binding ligands present in copper containing nitrite reductase enzymes were conserved in the ORF from the 350bp PCR product. This was the first time that it could be unequivocally stated that *N. subflava* B19 contained a copper nitrite reductase enzyme. *N. subflava* nitrite reductase gene sequence was lengthened at the 3' end and the C-terminal stop codon was identified in the peptide sequence. The highest degree of similarity between the *N. subflava* and *N. gonorrhoeae* nitrite reductase proteins was observed over the copper binding site. Towards the C-terminal the degree of conservation between the two peptides decreased, although they still had 71.8% identity to each other. Due to

the high degree of similarity between the *N. subflava* and *N. gonorrhoeae* peptides an outer membrane location for the *N. subflava* nitrite reductase was also proposed.

Sequence at the 5' end of the gene could not be produced after numerous attempts using a variety of cloning strategies. Initially recombination between the insert fragment containing the nitrite reductase gene and pBR325 vector was blamed. Recombination in this instance resulted in the insert fragment entering the *rop* gene. It was postulated that the subsequent increased copy number of pBR325 resulted in plasmid instability and the 5' end of the *nir* gene was lost. Another factor considered, which may also have prevented the cloning of the nitrite reductase gene, was due to the proposal that the encoded protein was bound to the outer membrane. It was suggested that expression of the nitrite reductase gene was leading to toxicity problems within the cell thereby affecting recovery of transformant clones. However, an extensive literature search enabled the ability of *E. coli* cloning cells to express Neisserial genes to be discounted. Also, cloning into a specifically designed vector, pASHOK, which did not allow expression of cloned genes, failed to liberate nitrite reductase gene sequence; although it was conceded that experimental problems may have also been to blame in this instance.

It is currently assumed that the inability to clone the 5' end of *nir* is due to DNA secondary structure present either upstream of, or within, the 5' end of the nitrite reductase gene. Preliminary investigations into cloning the nitrite reductase gene into systems tolerant to DNA secondary structure were investigated. However cloning into both *E. coli* DL795 (an *sbcC* and *recA* strain) and wild type *N. subflava* itself also resulted in failure. A number of experimental problems were highlighted in both cases that are currently being investigated in the lab (section 3.6). Time constraints unfortunately meant that I was unable to pursue this work further myself.

Sequence evidence and native gel activity assays from *N. subflava* whole cell lysates suggest an outer membrane location for the nitrite reductase enzyme. This means that a novel arrangement of the denitrification pathway may exist in this organism, different to those previously characterised. In *N. subflava* the denitrification pathway would effectively span the periplasmic space with the nitrite reductase and related electron donor found in association with the outer membrane.

This spatial arrangement is illustrated in Figure 4.6. This arrangement could explain why previous attempts in the lab to purify the nitrite reductase enzyme have been unsuccessful. Efforts were concentrated on identifying activity in the periplasmic cellular fractions as this is the more usual location for nitrite reductase enzymes. It was originally thought that lack of recovery of an active enzyme was due to hypersensitivity to oxygen, although it now appears that the wrong cellular fractions were being screened for activity.

Although the aims of the project outlined in section 1.11 were not fulfilled a number of interesting results were obtained regarding the denitrification pathway of *N. subflava*. Preliminary characterisation of the *N. subflava* nitrite reductase was also achieved. To summarise, the enzyme is proposed to be a copper containing nitrite reductase found in association with the outer membrane. The gene distally affected by the Tn5 insertion in mutant 163 is believed to correspond to a membrane bound donor protein to nitrite reductase, also proposed to be found in association with the outer membrane. The possible outer membrane location of both the nitrite reductase protein and its electron donor mean that a novel arrangement of the denitrification pathway may exist in *N. subflava* which effectively spans the periplasmic space. An outer membrane location for the nitrite reductase and azurin electron donor is also thought to exist in *N. gonorrhoeae*. This spatial arrangement of the denitrification enzymes is proposed to be unique amongst *Neisseria* spp.

Chapter Seven

Future Work

lacking the *hsdR* gene should be investigated as hosts for cloning the 5' end of the nitrite reductase gene. However cloning directly into *N. subflava* severely limits the choice of cloning vector. Conventional vectors such as pUC19 and pBluescript KS⁺ cannot replicate in host strains other than *E. coli*. Broad host range cloning vectors such as pKT231 and pGSS6 would need to be considered, as well as vectors specific for cloning into *Neisseria* such as the 'Hermes' series of shuttle vectors developed for *N. gonorrhoeae* (Kupsch *et al.*, 1996).

2. Further enzyme characterisation. As ambiguous results were obtained from the methyl viologen nitrite reductase assays considerable time must be invested to devise a suitable purification procedure for nitrite reductase. It is anticipated that the enzyme is associated with the outer membrane, however the true nature of membrane association with nitrite reductase is unknown. Attachment to the outer membrane can be transient, via electrostatic interactions, or permanent, with the enzyme existing as an integral membrane protein. Manipulation of the buffers used in the membrane preps and sarkosyl extraction procedure (as discussed in section 4.4) should enable nitrite reductase activity to be detected in one fraction of the cell only. Whether this is the outer membrane fraction or the soluble cell fraction will depend entirely on the degree of association between the outer membrane and the nitrite reductase protein.

3. Expression. If cloning from λ 350-9, as described above, is successful the nitrite reductase gene will be cloned in two halves. Prior to any protein expression experiments the gene would need to be cloned as a single transcript. The choice of expression vector will be dependent on the cloning strategy adopted. Due to the problems encountered when trying to clone the entire gene for sequence analysis in *E. coli* strains it may seem more sensible to consider expressing the protein in its indigenous *Neisseria* host. However it may be easier, in terms of expression vector availability, to simply clone and express the nitrite reductase protein from downstream of the proposed DNA hairpin loop structure, providing this region of secondary structure lies outwith the *nir* structural gene. This would remove the need

to use a specifically modified *E. coli* host strain and conventional protein expression systems such as pET vectors in BL21(DE3)pLysS host strains could be used.

Nitrite reductase activity tests on native polyacrylamide gels could be used to determine which fraction of the host cell accumulates the overexpressed nitrite reductase protein. If a Neisserial expression system is developed it seems reasonable to expect activity to be detected in the outer membrane fraction. However, if an *E. coli* system is employed, the nitrite reductase protein may be present as inclusion bodies in the host cell. The cellular location of the overexpressed nitrite reductase will obviously influence the methods used to purify the protein from intact cells. Information obtained from the methyl viologen nitrite reductase assays on which cellular fractions has nitrite reductase activity will influence the nitrite reductase purification strategy.

Purification of metabolically active nitrite reductase will enable *in vitro* nitrite reductase and *N*-nitrosation assays to be undertaken with a wide variety of electron donors and inhibitors. It could then be determined which conditions (if any) produce the highest *N*-nitrosation rates and comparisons could be made between these assays and the *in vivo* studies by Brew (1992). This information could be used to determine how conditions within the achlorhydric stomach may affect formation of *N*-nitroso compounds.

If the nitrite reductase enzyme was found to have the ability to *N*-nitrosate, site directed mutagenesis could be used to characterise the involvement of the conserved copper ligands in this catalytic reaction. It could be determined whether or not the catalytic mechanisms for nitrite reduction and *N*-nitrosation involve common protein ligands, and the potential of other nitrite reductase enzymes to catalyse *N*-nitrosation could be examined. A role for other amino acid residues in *N*-nitrosation catalysis could also be resolved using site directed mutagenesis.

4. Other alternative *N*-nitrosating enzymes? It is possible that the nitrite reductase enzyme will not be able to catalyse *N*-nitrosation reactions *in vitro*. If this is the case other alternatives from the denitrification pathway would need to be investigated as possible *N*-nitrosating enzymes/agents. The other most likely

denitrification intermediate to have the ability to *N*-nitrosate is nitric oxide reductase. Work by Brew (1992) suggested that nitrite reductase may not have a direct role in catalysing *N*-nitrosation, although its significance in the formation of nitric oxide was highlighted. She proposed that nitric oxide and nitric oxide reductase may also be involved in bacterial *N*-nitrosation. It seems possible that dimerisation and oxidation of nitric oxide on the surface of the nitric oxide reductase enzyme could lead to formation of *N*-nitroso compounds, such as N_2O_3 and N_2O_4 . Mutagenesis using Tn5 could be used to obtain *N. subflava* mutants deficient in nitric oxide reductase activity. A mutant such as this could be used to elucidate the role of nitric oxide in bacterial *N*-nitrosation.

Similarly, if a selective inhibitor for nitric oxide reductase could be found it could be determined whether nitric oxide accumulation is the key for bacterial *N*-nitrosation. Rates of *N*-nitrosation, as measured from whole cell assays, would be high if the accumulation of nitric oxide was significant. Controlling nitrite reductase activity, via site directed mutagenesis of the catalytic copper binding ligands, would obviously help to prevent nitric oxide accumulation. However in the achlorhydric stomach it would be easier to monitor levels of the nitric oxide reductase inhibitor and determine if there is a correlation between increased levels of such an inhibitor and increased gastric cancer susceptibility. Dietary supplements to combat the effects of the nitric oxide reductase inhibitor could then be considered in the treatment of achlorhydric gastric cancer.

5. Other work. Due to the proposed unusual arrangement of the denitrification pathway across the periplasm in *N. subflava* it would be worth genetically characterising other Tn5 mutants, isolated by Brew (1992), to determine a possible location and organisation of the denitrification operon. How well this relates to other reported systems could be investigated.

Mutagenesis experiments could be used to functionally assign nitrite reductase activity to the proposed nitrite reductase gene cloned in pANIA10. A series of versatile suicide vectors have been developed for use in a large range of Gram negative bacteria (Quandt and Hynes, 1993). These vectors contain a lethal

gene that allow for selection of double recombination events and thereby increase the efficiency of gene replacement experiments. Interrupting the intact chromosomal nitrite reductase gene in this way would produce a mutant with reduced nitrite reductase activity and a definitive relationship between the gene sequence cloned in pANIA10 and nitrite reductase activity will have been achieved.

N-nitroso compounds are also implicated in cancers of the bladder and vagina so organisms found at these sites could also be screened for their *N*-nitrosation abilities. Also, the *N*-nitrosation capability of food borne organisms (particularly fungi) could be assessed. If a variety of organisms were found which could *N*-nitrosate then it would increase the intake of preformed *N*-nitroso compounds into the body. These could also be involved in the development of cancer at sites other than the stomach.

This series of experiments would show the connection between nitrite reductase, nitric oxide reductase and *N*-nitrosation very clearly. It would also significantly broaden our knowledge of *N. subflava* denitrification enzyme intermediates in general and lead to a thorough understanding of the mechanisms involved in gastric cancer development in achlorhydric stomachs.

Bibliography

Abraham, Z.H.L., Lowe, D.J. and Smith, B.E. 1993. Purification and characterisation of the dissimilatory nitrite reductase from *Alcaligenes xylosoxidans* subsp. *xylosoxidans* (N.C.I.M.B. 11015): Evidence for the presence of both type I and type II copper centres. *Biochem. J.* **295**: 587-593.

Adman, E.T. 1991. Copper protein structures. *Adv. Prot. Chem.* **42**: 145-197.

Adman, E.T., Godden, J.W. and Turley, S. 1995. The structure of copper nitrite reductase from *Achromobacter cycloclastes* at five pH values, with NO₂⁻ bound and with type II copper deleted. *J. Biol. Chem.* **270**: 27458-27474.

Alefounder, P.R. and Ferguson, S.J. 1980. The location of the dissimilatory nitrite reductase and the control of dissimilatory nitrate reductase by oxygen in *Paracoccus denitrificans*. *Biochem. J.* **192**: 231-240.

Alefounder, P.R., McCarthy, J.E.G. and Ferguson, S.J. 1983. Selection and organisation of denitrifying electron transfer pathways in *Paracoccus denitrificans*. *Biochim. Biophys. Acta.* **724**: 20-39.

Anon., 1991. Cancer Research Campaign. Facts on Cancer. Headquarters, 10 Cambridge Terrace, NW1.

Anon., 1992. MAFF. Nitrate, nitrite and *N*-nitroso compounds in food: Second Report. Food Surveillance Paper No32. Her Majesty's Stationary Office, London.

Arai, H., Igarashi, Y. and Kodama, T. 1991. Nitrite activates the transcription of the *Pseudomonas aeruginosa* nitrite reductase and cytochrome c₅₅₁ operon under anaerobic conditions. *FEBS Letts.* **288**: 227-228.

Arai, H., Igarashi, Y. and Kodama, T. 1995. Expression of the *nir* and *nor* genes for denitrification of *Pseudomonas aeruginosa* requires a novel CRP/FNR-related transcriptional regulator, DNR, in addition to ANR. *FEBS Letts.* **371**: 73-76.

Arai, H., Igarashi, Y. and Kodama, T. 1995. The structural genes for nitric oxide reductase from *Pseudomonas aeruginosa*. *Biochim. Biophys. Acta.* **1261**: 279-284.

Bagdasarian, M., Lurz, R., Rückert, B., Franklin, F.C.H., Bagdasarian, M.M., Frey, J. and Timmis, K.N. 1981. Specific-purpose plasmid cloning vectors. II. Broad host range, high copy number, RSF1010-derived vectors, and a host vector system for gene cloning in *Pseudomonas*. *Gene.* **16**: 237-247.

Ballard, A.L. and Ferguson, S.J. 1988. Respiratory nitrate reductase from *Paracoccus denitrificans*. *Eur. J. Biochem.* **174**: 207-212.

Banjeree, S., Hawksby, C., Miller, S., Dahill, S., Beattie, A.D. and McColl, K.E.L. 1994. Effect of *Helicobacter pylori* and its eradication on gastric juice ascorbic acid. *Gut*. **35**: 317-322.

Bartnikas, T.B., Tosques, I.E., Laratta, W.P., Shi, J.R. and Shapleigh, J.P. 1997. Characterisation of the nitric oxide reductase encoding region in *Rhodobacter sphaeroides* 2.4.3. *J. Bacteriol.* **179**: 3534-3540.

Bell, L.C., Page, M.D., Berks, B.C., Richardson, D.J. and Ferguson, S.J. 1993. Insertion of transposon Tn5 into a structural gene of the membrane-bound nitrate reductase of *Thiosphaera pantotropha* results in anaerobic overexpression of periplasmic nitrate reductase activity. *J. Gen. Microbiol.* **139**: 3205-3214.

Bell, L.C., Richardson, D.J. and Ferguson, S.J. 1990. Periplasmic and membrane bound respiratory nitrate reductases in *Thiosphaera pantotropha*. *FEBS Letts.* **265**: 85-87.

Bennett, B., Berks, B.C., Ferguson, S.J., Thomson, A.J. and Richardson, D.J. 1994. Mo(V) electron paramagnetic resonance signals from the periplasmic nitrate reductase of *Thiosphaera pantotropha*. *Eur. J. Biochem.* **226**: 789-798.

Berg, D.E. 1989. in, 'Mobile DNA.' Eds. Berg, D.E. and Howe, M.M. American Society for Microbiology, Washington, D.C. pp185-210.

Berks, B.C., Baratta, D., Richardson, D.J. and Ferguson, S.J. 1993. Purification and characterisation of a nitrous oxide reductase from *Thiosphaera pantotropha*. Implications for the mechanisms of aerobic nitrous oxide reduction. *Eur. J. Biochem.* **212**: 467-476.

Berks, B.C., Ferguson, S.J., Moir, J.W.B. and Richardson, D.J. 1995a. Enzyme and associated electron transport systems that catalyse the respiratory reduction of nitrogen oxides and oxyanions. *Biochim. Biophys. Acta.* **1232**: 97-173.

Berks, B.C., Page, D.M., Richardson, D.J., Reilly, A., Cavill, A., Outen, F. and Ferguson, S.J. 1995b. Sequence analysis of subunits of the membrane bound nitrate reductase from a denitrifying bacterium: the integral membrane subunit provides a prototype for the dihaem electron-carrying arm of a redox loop. *Mol. Microbiol.* **15**: 319-331.

Berks, B.C., Richardson, D.J., Reilly, A., Willis, A.C. and Ferguson, S.J. 1995c. The *napEDABC* gene cluster encoding the periplasmic nitrate reductase system of *Thiosphaera pantotropha*. *Biochem. J.* **309**: 983-992.

Berks, B.C., Richardson, D.J., Robinson, C., Reilly, A., Aplin, R.T. and Ferguson, S.J. 1994. Purification and characterisation of the periplasmic nitrate reductase from *Thiosphaera pantotropha*. *Eur. J. Biochem.* **220**: 117-124.

Birnboim, H.C. and Doly, J. 1979. A rapid alkaline extraction procedure for screening recombinant plasmid DNA. *Nucleic Acids Res.* **7**: 1513-1520.

Blackburn, N.J., Barr, M.E., Woodruff, W.H., van der Oost, J. and de Vries, S. 1994. Metal-metal bonding in biology: EXAFS evidence for a 2.5Å copper-copper bond in the Cu_A centre of cytochrome oxidase. *Biochemistry.* **33**: 10401-10407.

Blümle, S. and Zumft, W.G. 1991. Respiratory nitrate reductase from denitrifying *Pseudomonas stutzeri*, purification, properties and target of proteolysis. *Biochim. Biophys. Acta.* **1057**:102-108.

Boogerd, F.C., van Verseveld, H.W. and Stouthamer, A.H. 1983. Dissimilatory nitrate uptake in *Paracoccus denitrificans* via a $\Delta\mu_{\text{H}^+}$ -dependent system and nitrate-nitrite antiport system. *Biochim. Biophys. Acta.* **723**: 415-427.

Bower, S.G., Harlow, K.W., Switzer, R.I. and Hove-Jensen, B. 1989. Characterisation of the *Escherichia coli* prsA1-encoded mutant phosphoribosylpyrophosphate synthetase identifies a divalent cation-nucleotide binding site. *J. Biol.Chem.* **264**: 10827-10291.

Braun, C. and Zumft, W.G. 1992. The structural genes of the nitric oxide reductase complex from *Pseudomonas stutzeri* are part of a 30-kilobase gene cluster for denitrification. *J. Bacteriol.* **174**: 2394-2397.

Brew, F.R. 1992. The correlation between nitrite reduction and nitrosation by gastric isolates of *N. subflava*. PhD. Thesis. MTRU, Polytechnic of East London.

Brosius, J. 1989. Superpolylinkers in cloning and expression vectors. *DNA.* **8**: 759-777.

Calam, J., Goodlad, R.A., Lee, C.Y., Ratcliffe, B., Coates, M.E., Stamp, G.W.H. and Wright, N.A. 1991. Achlorhydria induced hypergastrinaemia: the role of bacteria. *Clin. Sci.* **80**: 281-284.

Calmels, S., Béréziat, J.-C., Ohshima, H. and Bartsch, H. 1991. Bacterial formation of *N*-nitroso compounds from administered precursors in the rat stomach after omeprazole-induced achlorhydria. *Carcinogenesis.* **12**: 435-439.

Calmels, S., Cshima, H., Henry, Y. and Bartsch, H. 1996. Characterisation of bacterial cytochrome cd₁ nitrite reductase as one enzyme responsible for catalysis of nitrosation of secondary amines. *Carcinogenesis*. **17**: 533-536.

CanTERS, G.W. and van de Kamp, M. 1992. Protein-mediated electron transfer. *Current Opinion in Struct. Biol.* **2**: 859-869.

Carlson, C.A. and Ingraham, J.L. 1983. Comparison of denitrification by *Pseudomonas stutzeri*, *Pseudomonas aeruginosa* and *Paracoccus denitrificans*. *Appl. Env. Microbiol.* **45**: 1247-1253.

Carlson, C.A., Ferguson, L.P. and Ingraham, J.L. 1982. Properties of dissimilatory nitrate reductase from the denitrifier *Pseudomonas aeruginosa*. *J. Bacteriol.* **151**: 162-171.

Cavicchioli, R., Chiang, R.C., Kalman, L.V. and Gunsalus, R.P. 1996. Role of the periplasmic domain of the *Escherichia coli* NarX sensor-transmitter protein in nitrate-dependent signal-transduction and gene regulation. *Mol. Microbiol.* **21**: 901-911.

Chan, Y-K., McCormick, W.A. and Watson, R.J. 1997. A new *nos* gene downstream from *nosDFY* is essential for dissimilatory reduction of nitrous oxide by *Rhizobium (Sinorhizobium) meliloti*. *Microbiol.* **143**: 2817-2824.

Chang, A.C.Y. and Cohen, S.N. 1978. Construction and characterisation of amplifiable multi-copy DNA cloning vehicles derived from the p15A cryptic megeplasmid. *J. Bacteriol.* **134**: 1141-1156.

Chaudhry, G.R. and MacGregor, C.H. 1983. *Escherichia coli* nitrate reductase subunit A: its role as the catalytic site and evidence for its modification. *J. Bacteriol.* **154**: 387-394.

Chen, J., Chang, W., Chang, T., Chang, W., Liu, M., Payne, W.J. and LeGall, J. 1996. Cloning, characterisation and expression of the nitric oxide-generating nitrite reductase and of the blue copper protein of *Achromobacter cycloclastes*. *Biochem. Biophys. Res. Comm.* **219**: 423-428.

Chen, L., Durley, R., Poliks, B.J., Hamada, K., Chen, Z., Mathews, F.S., Davidson, V.L., Satow, Y., Huizinga, E., Vellieux, F.M.D. and Hol, W.G.J. 1992. Crystal structure of an electron-transfer complex between methylamine dehydrogenase and amicyanin. *Biochemistry.* **31**: 4959-4964.

- Chiang, R.C., Cavicchioli, R. and Gunsalus, R.P.** 1992. Identification and characterisation of *narQ*, a second nitrate sensor for nitrate-dependent gene regulation in *Escherichia coli*. *Mol. Microbiol.* **6**: 1913-1923.
- Chiang, R.C., Cavicchioli, R. and Gunsalus, R.P.** 1997. 'Locked-on' and 'locked-off' signal transduction mutations in the periplasmic domain of the *Escherichia coli* NarQ and NarX sensors affect nitrate- and nitrite-dependent regulation by NarL and NarP. *Mol. Microbiol.* **24**: 1049-1060.
- Chyou, P-H., Nomura, A.M., Hankin, J.H. and Stemmermann, G.N.** 1990. A case cohort study of diet and stomach cancer. *Cancer Res.* **50**: 7501-7504.
- Coggon, D. and Acheson, E.D.** 1984. The geography of cancer of the stomach. *British Med. Bulletin.* **40**: 335-341.
- Compan, I. and Tuoti, D.** 1994. Anaerobic activation of ArcA transcription in *Escherichia coli* - roles of FNR and ArcA. *Mol. Microbiol.* **11**: 955-964.
- Correa, P.** 1988. A human model of gastric carcinogenesis. *Perspectives in Cancer Res.* **48**: 3554-3560.
- Correa, P.** 1995. *Helicobacter pylori* and gastric carcinogenesis. *Am. J. Surg. Pathol.* **19**: S37-S43.
- Correa, P.** 1995. The role of antioxidants in gastric cancer carcinogenesis. *Crit. Rev. Food Sci. and Nut.* **35**: 59-64.
- Coyne, M.S., Arunakumari, A., Averill, B.A. and Teidje, J.M.** 1989. Immunological identification and distribution of dissimilatory haem cd₁ and non-haem copper nitrite reductases in denitrifying bacteria. *Appl. Environ. Microbiol.* **55**: 2924-2931.
- Craske, A. and Ferguson, S.J.** 1986. The respiratory nitrate reductase from *Paracoccus denitrificans*. *Eur. J. Biochem.* **158**: 429-436.
- Crespi, M. and Citarda, F.** *Helicobacter pylori* and gastric cancer: An overrated risk? *Scand. J. Gastroenterol.* **31**: 1041-1046.
- Cutruzzolà, F., Arese, M., Grasso, S., Bellelli, A. and Brunori, M.** 1997. Mutagenesis of nitrite reductase from *Pseudomonas aeruginosa*: tyrosine-10 in the haem c domain is not involved in catalysis. *FEBS Letts.* **412**: 365-369.

- Cuypers, H. and Zumft, W.G.** 1993. Anaerobic control of denitrification in *Pseudomonas stutzeri* escapes mutagenesis of an *fnr*-like gene. *J. Bacteriol.* **175**: 7236-7246.
- Cuypers, H., Berghöfer, J. and Zumft, W.G.** 1995. Multiple *nosZ* promoters and anaerobic expression of *nos* genes necessary for *Pseudomonas stutzeri* nitrous oxide reductase and assembly of its copper centres. *Biochim. Biophys. Acta.* **1264**: 183-190.
- Darwin, A.J., Tyson, K.L., Busby, S.J.W. and Stewart, V.** 1997. Differential regulation by the homologous response regulators NarL and NarP of *Escherichia coli* K-12 depends on DNA binding site arrangement. *Mol. Microbiol.* **25**: 583-595.
- deBoer, A.P.N., Reijnders, W.N.M., Kuenen, J.G., Stouthammer, A.H. and van Spanning, R.J.M.** 1994. Isolation, sequencing and mutational analysis of a gene cluster involved in nitrite reduction in *Paracoccus denitrificans*. *Antonie Leeuwenhoek.* **66**: 111-127.
- deBoer, A.P.N., Van der Oost, J., Reijnders, W.N.M., Westerhoff, H.V., Stouthamer, A.H. and Van Spanning, R.J.M.** 1996. Mutational analysis of the *nor* gene cluster which encodes nitric oxide reductase from *Paracoccus denitrificans*. *Eur. J. Biochem.* **242**: 592-600.
- DeMoss, J.A. and Hsu, P.-Y.** 1991. NarK enhances nitrate uptake and nitrile excretion in *Escherichia coli*. *J. Bacteriol.* **173**: 3303-3310.
- DiGate, R.J. and Marians, K.J.** 1988a. Identification of a potent decatenating enzyme from *Escherichia coli*. *J. Biol. Chem.* **263**: 13366-13373.
- DiGate, R.J. and Marians, K.J.** 1988b. Molecular cloning and DNA sequence analysis of *Escherichia coli topB*, the gene encoding topoisomerase III. *J. Biol. Chem.* **264**: 17924-17930.
- Dodd, F.E., Hasnain, S.S., Hunter, W.N., Abraham, Z.H.L., Debenham, M., Kanzler, H., Eldridge, M., Eady, R.R., Ambler, R.P. and Smith, B.E.** 1995. Evidence for two distinct azurins in *Alcaligenes xylosoxidans* (NCIMB 11015): Potential electron donors to nitrite reductase. *Biochemistry.* **34**: 10180-10186.
- Dolby, J.M., Webster, A.D.B., Borriello, S.P., Barclay, F.E., Bartholomew, B.A. and Hill, M.J.** 1984. Bacterial colonisation and nitrite concentration in the achlorhydric stomachs of patients with primary hypogammaglobulinaemia of classical pernicious anaemia. *Scand. J. Gastroenterol.* **19**: 105-110.

Drake, I.M., Warland, D., Carswell, N., Schorah, C.J., Mapstone, N., Axon, A.T.R., Chalmers, D.M., Dixon, M.F. and White, K.L.M. 1995. Reactive oxygen species (ROS) activity and damage in *Helicobacter pylori* associated gastritis (HPG) - effect of eradication therapy. *Gut*. **37**: S1-A155.

Farrar, J.A., Lappalainen, P., Zumft, W.G., Saraste, M. and Thomson, A.J. 1995. Spectroscopic and mutagenesis studies on the Cu_A centre from the cytochrome-c-oxidase complex of *Paracoccus denitrificans*. *Eur. J. Biochem.* **232**: 294-303.

Ferguson, S.J. 1988. in 'The nitrogen and sulphur cycles', SGM symposium 42. Eds. Cole, J.A. and Ferguson, S.J., Publ. Cambridge University Press. pp1-29.

Forsythe, S.J. and Cole, J.A. 1987. Nitrite accumulation during anaerobic nitrate reduction by binary suspensions of bacteria isolated from the achlorhydric stomach. *J. Gen. Microbiol.* **133**: 1845-1849.

Forsythe, S.J., Dolby, J.M., Webster, A.D.B. and Cole, J.A. 1988. Nitrate and nitrite reducing bacteria in the achlorhydric stomach. *J. Med. Microbiol.* **25**: 253-259.

Fukushima, S., Shibata, M.A., Shirai, T., Kurata, Y., Tamono, S. and Imaida, K. 1987. Promotion by L-ascorbic acid of urinary bladder carcinogenesis in rats under conditions of increased urinary K ion concentration and pH. *Cancer Res.* **47**: 4821-4824.

Fülop, V., Moir, J.W.B., Ferguson, S.J. and Hajdu, J. 1993. Crystallisation and preliminary crystallographic study of cytochrome cd₁ nitrite reductase from *Thiosphaera pantotropha*. *J. Mol. Biol.* **232**: 1211-1212.

Fülop, V., Moir, J.W.B., Ferguson, S.J. and Hajdu, J. 1995. The anatomy of a bifunctional enzyme: Structural basis for reduction of oxygen to water and synthesis of nitric oxide by cytochrome cd₁. *Cell*. **81**: 369-377.

Garland, P.B., Downie, A. and Haddock, B.A. 1975. Proton translocation and the respiratory nitrate reductase of *Escherichia coli*. *Biochem. J.* **152**:547-559.

Gil, R., Casado, J. and Izquierdo, C. 1994. The nitrosation of amino acids. *Int. J. Chem. Kinetics.* **26**: 1167-1178.

Glockner, A.B., Jüngst, A. and Zumft, W.G. 1993. Copper-containing nitrite reductase from *Pseudomonas aureofaciens* is functional in a mutationally cytochrome cd₁-free background (NirS⁻) of *Pseudomonas stutzeri*. *Arch. Microbiol.* **160**: 18-26.

Godden, J.W., Turley, G., Teller, D.C., Adman, E.T., Liu, M.Y., Payne, W.J. and LeGall, J. 1991. The 2.3 Angstrom X-ray structure of nitrite reductase from *Achromobacter cycloclastes*. *Science*. **253**: 438-442.

Gotschlich, E.C. and Seiff, M.E. 1987. Identification and gene structure of an azurin-like protein with a lipoprotein signal peptide in *Neisseria gonorrhoeae*. *FEMS Letts*. **43**: 253-255.

Gould, G.W. 1994. Membrane protein expression systems - a users guide. Publ. Portland Press, London.

Gudat, J.C., Singh, J. and Wharton, D.C. 1973. Cytochrome oxidase from *Pseudomonas aeruginosa*. I. Purification and some properties. *Biochim. Biophys. Acta*. **292**: 376-390.

Guest, J.R. 1992. Oxygen regulated gene expression in *Escherichia coli*. *J. Gen. Microbiol.* **138**: 2253-2263.

Günter Grossman, J., Abraham, Z.H.L., Adman, E.T., Neu, M., Eady, R.R., Smith, B.E. and Hasnain, S.S. 1993. X-ray scattering using synchrotron radiation shows nitrite reductase from *Achromobacter cycloclastes* to be a trimer in solution. *Biochemistry*. **32**: 7360-7366.

Härtig, E. and Zumft, W.G. 1998. The requirement of RpoN (σ^{54}) in denitrification by *Pseudomonas stutzeri* is indirect and restricted to the reduction of nitrite and nitric oxide. *Appl. Env. Microbiol.* **64**: 3092-3095.

Heiss, B., Frunze, K. and Zumft, W.G. 1989. Formation of the N-N bond from nitric oxide by a membrane bound cytochrome bc complex of nitrate-respiring (denitrifying) *Pseudomonas stutzeri*. *J. Bacteriol.* **171**: 3288-3297.

Hill, B.C. 1991. The reaction of electrostatic cytochrome c oxidase complex with oxygen. *J. Biol. Chem.* **266**: 2219-2226.

Hill, B.C. 1993. The sequence of electron carriers in the reaction of cytochrome c oxidase with oxygen. *J. Bioenerg. Biomemb.* **25**: 115-120.

Hilton, J.C. and Rajagopalan, K.V. 1996. Identification of the molybdenum cofactor of dimethyl sulphoxide reductase from *Rhodobacter sphaeroides* f. sp. *denitrificans* as bis(molybdopterin guanine dinucleotide)molybdenum. *Arch. Biochem. Biophys.* **325**: 139-143.

- Hochstein, L.I. and Tomlinson, G.A.** 1988. The enzymes associated with denitrification. *Ann. Rev. Microbiol* **42**: 231-261.
- Hoehn, G.T. and Clark, V.L.** 1990. Distribution of a protein antigenically related to the major anaerobically induced gonococcal outer membrane protein among other *Neisseria* species. *Infect. Immun.* **58**: 3929-3933.
- Hoehn, G.T. and Clark, V.L.** 1992a. Isolation and nucleotide sequence of the gene (*aniA*) encoding the major anaerobically induced outer membrane protein of *Neisseria gonorrhoeae*. *Infect. Immun.* **60**: 4695-4703.
- Hoehn, G.T. and Clark, V.L.** 1992b. The major anaerobically induced outer membrane protein of *Neisseria gonorrhoeae*, Pan1, is a lipoprotein. *Infect. Immun.* **60**: 4704-4708.
- Hoeren, F.U., Berks, B.C., Ferguson, S.J. and McCarthy, J.E.G.** 1993. Sequence and expression of the gene encoding the respiratory nitrous-oxide reductase from *Paracoccus denitrificans*. New and conserved structural and regulatory motifs. *Eur. J. Biochem.* **218**: 49-57.
- Houben, G.M.P. and Stockbrügger, R.W.** 1995. Bacteria in the aetiopathogenesis of gastric cancer: A review. *Scand. J. Gastroenterol.* **30**: No. S212 S12 p13-18.
- Hove-Jensen, B.** 1985. Cloning and characterisation of the *prs* gene encoding phosphoribosylpyrophosphate synthetase of *Escherichia coli*. *Mol. Gen. Genet.* **201**: 269-276.
- Howes, B.D., Abraham, Z.H.L., Lowe, D.J., Brüser, T., Eady, R.R. and Smith, B.E.** 1994. EPR and electron double resonance (ENDOR) studies show nitrite binding to the type II copper centres of the dissimilatory nitrite reductase of *Alcaligenes xylosoxidans* (NCIMB 11015). *Biochemistry.* **33**: 3171-3177.
- Hulse, C.L. and Averill, B.A.** 1990. Isolation of high specific activity pink, monomeric nitrous oxide reductase from *Achromobacter cycloclastes*. *Biochem. Biophys. Res. Comm.* **166**: 729-735.
- Hulse, C.L., Averill, B.A. and Tiedje, J.M.** 1989. Evidence for a copper-nitrosyl intermediate in denitrification by the copper-containing nitrite reductase of *Achromobacter cycloclastes*. *J. Am. Chem. Soc.* **111**: 2322-2323.
- Hussain, M., Ichihara, S. and Mizushima, S.** 1982. Mechanism of signal peptide cleavage in the biosynthesis of the major lipoprotein of the *Escherichia coli* outer membrane. *J. Biol. Chem.* **257**: 5177-5182.

Ikemi, M., Murakami, K., Hashimoto, M. and Murooka, Y. 1992. Cloning and characterisation of genes involved in the biosynthesis of δ -aminolevulinic acid in *Escherichia coli*. *Gene*. **121**: 127-132.

Iwasaki, H. and Matsubara, T. 1972. A nitrite reductase from *Achromobacter cycloclastes*. *J. Biochem.* **71**: 645-652.

Ji, X.-B. and Hollocher, T.C. 1988. Mechanism for nitrosation of 2,3-diaminonaphthalene by *Escherichia coli*: Enzymatic production of NO followed by O₂-dependent chemical nitrosation. *Appl. Environ. Microbiol.* **54**: 1791-1794.

Jilk, R.A., Makris, J.C., Borchardt, L. and Reznikoff, W.S. 1993. Implications of Tn5-associated adjacent deletions. *J. Bacteriol.* **175**: 1264-1271.

Johnson, J.L., Bastian, N.R. and Rajagopalan, K.V. 1990. Molybdopterin guanine dinucleotide: A modified form of molybdopterin identified in the molybdenum cofactor of dimethyl sulphoxide reductase from *Rhodobacter sphaeroides* forma specialis *denitrificans*. *Proc. Natl. Acad. Sci. USA* **87**: 3190-3194.

Johnson, M.K., Bennet, D.E., Morningstar, J.E., Adams, M.W.W. and Mortenson, L.E. 1985. The iron-sulphur cluster composition of *Escherichia coli* nitrate reductase. *J. Biol. Chem.* **260**: 5456-5463.

Jones, A.M. and Hollocher, T.C. 1993. Nitric oxide reductase of *Achromobacter cycloclastes*. *Biochim. Biophys. Acta.* **1144**: 359-366.

Jonkers, D., Houben, G., Arends, J.W., Stobberingh, E. and Stockbrügger, R. 1997. The role of *Helicobacter pylori* and non-*Helicobacter pylori* bacterial flora in gastric carcinogenesis: histological, serological and microbial data from 39 newly diagnosed patients. *Gastroenterol.* **112**: A162.

Jüngst, A. and Zumft, W.G. 1992. Interdependence of respiratory NO reduction and nitrite reduction revealed by mutagenesis of *nirQ*, a novel gene in the denitrification gene cluster of *Pseudomonas stutzeri*. *FEBS Letts.* **314**: 308-314.

Jüngst, A., Braun, C. and Zumft, W.G. 1991. Close linkage in *Pseudomonas stutzeri* of the structural genes for respiratory nitrite reductase and nitrous oxide reductase, and other essential genes for denitrification. *Mol. Gen. Genet.* **225**: 241-248.

Jungst, A., Wakabayashi, S., Matsubara, H. and Zumft, W.G. 1991. The *nirSTBM* region coding for cytochrome cd₁ dependent nitrite respiration of

Pseudomonas stutzeri consists of a cluster of mono-, di- and tetrahaem proteins. *FEBS Letts.* **279**: 205-209.

Kastrau, D.H.W., Heiss, B., Kroneck, P.M.H. and Zumft, W.G. 1994. Nitric oxide reductase from *Pseudomonas stutzeri*, a novel cytochrome bc complex. Phospholipid requirement, electron paramagnetic resonance and redox properties. *Eur. J. Biochem.* **222**: 293-303.

Kawasaki, S., Arai, H., Kodama, T. and Igarashi, Y. 1997. Gene cluster for dissimilatory nitrite reductase (*nir*) from *Pseudomonas aeruginosa*: sequencing and identification of a locus for haem d₁ biosynthesis. *J. Bacteriol.* **179**: 235-242.

Kinlen, L.J., Webster, A.D.B., Bird, A.G., Haile, R., Peto, J., Soothill, J.F. and Thompson, R.A. 1985. Prospective study of cancer in patients with hypogammaglobulinaemia. *Lancet.* February: 263-265.

Kroneck, P.M.H., Antholine, W.A., Riester, J. and Zumft, W.G. 1989. The nature of the cupric site in nitrous oxide reductase and the Cu_A in cytochrome c oxidase. *FEBS Letts.* **248**: 212-213.

Kuipers, E.J. and Meuwissen, S.G.M. 1996. *Helicobacter pylori* and gastric carcinogenesis. *Scand. J. Gastroenterol.* **31**: S218. pp. 103-105.

Kukatani, T., Watanabe, H., Arima, K. and Beppu, T. 1981. Purification and properties of a copper-containing nitrite reductase from a denitrifying bacterium, *Alcaligenes faecalis* S-6. *J. Biochem.* **89**:453-461.

Kukimoto, M., Nishiyama, M., Murphy, E.P., Turley, S., Adman, E.T., Horinouchi, S. and Beppu, T. 1994. X-ray structure and site-directed mutagenesis of a nitrite reductase from *Alcaligenes faecalis* S-6: Roles of two copper atoms in nitrite reduction. *Biochemistry.* **33**: 5246-5252.

Kukimoto, M., Nishiyama, M., Ohnuki, T., Turley, S., Adman, E.T., Horinouchi, S. and Beppu, T. 1995. Identification of the interaction site of pseudoazurin with its redox partner, copper-containing nitrite reductase from *Alcaligenes faecalis* S-6. *Prot. Eng.* **8**: 153-158.

Kukimoto, M., Nishiyama, M., Tanokura, M., Murphy, M.E.P., Adman, E.T. and Horinouchi, S. 1996. Site-directed mutagenesis of an azurin from *Pseudomonas aeruginosa* enhances formation of an electron-transfer complex with a copper-containing nitrite reductase from *Alcaligenes faecalis* S-6. *FEBS Letts.* **394**: 87-90.

- Kupsch, E-V., Aubel, D., Gibbs, C.P., Kahrs, A.F., Rudel, T. and Meyer, T.F.** 1996. Construction of Hermes shuttle vectors: a versatile system useful for genetic complementation of transformable and non-transformable *Neisseria* mutants. *Mol. Gen. Genet.* **250**: 558-569
- Laemelli, U.K.** 1970. Cleavage of structural proteins during the assembly of the head of bacteriophage T4. *Nature.* **227**: 680-685.
- Lam, Y. and Nicholas, D.J.D.** 1969. A nitrite reductase with cytochrome oxidase activity from *Paracoccus denitrificans*. *Biochim. Biophys. Acta.* **180**: 459-472.
- Lambert, C.** 1997. Cloning the denitrification genes of *Neisseria subflava*. Hons. Project. Edinburgh University.
- Lappalainen, P. and Saraste, M.** 1994. The binuclear Cu_A centre of cytochrome oxidase. *Biochim. Biophys. Acta.* **1187**: 222-225.
- Lazizzera, B.A., Bates, D.M. and Kiley, P.J.** 1993. The activity of the transcription factor FNR is regulated by a change in oligomeric state. *Genes Dev.* **7**: 1993-2005.
- Leach, S.A., Thompson, M. and Hill, M.** 1987. Bacterially catalysed *N*-nitrosation reactions and their relative importance in the human stomach. *Carcinogenesis.* **8**: 1907-1912.
- Lechago, J. and Correa, P.** 1993. Prolonged achlorhydria and gastric neoplasia: Is there a causal relationship? *Gastroenterol.* **104**: 1554-1557.
- Lee, H.S., Abdelal, A.H.T., Clark, M.A and Ingraham, J.L.** 1991. Molecular characterisation of *nosA*, a *Pseudomonas stutzeri* gene encoding an outer membrane protein required to make copper containing N₂O reductase. *J. Bacteriol.* **173**: 5406-5413.
- Libby, E. and Averill, B.A.** 1992. Evidence that the type II copper centres are the site of nitrite reduction by *Achromobacter cycloclastes* nitrite reductase. *Biochem. Biophys. Res. Comm.* **187**: 1529-1535.
- Lin, J.T., Goldman, B.S. and Stewart, V.** 1994. The *nasFEDCBA* operon for nitrate and nitrite assimilation in *Klebsiella pneumoniae* M5al. *J. Bacteriol.* **176**: 2551-2559.

- Liu, M-Y., Liu, M-C., Payne, W.J. and LeGall, J.** 1986. Properties and electron transfer, specifically of copper proteins from the denitrifier *Achromobacter cycloclastes*. *J. Bacteriol.* **166**: 604-608.
- Mackerness, C.W., Leach, S.A., Thompson, M.H. and Hill, M.J.** 1989. The inhibition of bacterially mediated *N*-nitrosation by vitamin C: relevance to the inhibition of endogenous *N*-nitrosation in the achlorhydric stomach. *Carcinogenesis*. **10**: 397-399.
- Malkin, R. and Malmström, B.G.** 1970. The state and function of copper in biological systems. *Adv. Enzymol.* **35**: 177-244.
- Mellies, J., Jose, J. and Meyer, T.F.** 1997. The *Neisseria gonorrhoeae* gene *aniA* encodes an inducible nitrite reductase. *Mol. Gen. Genet.* **256**: 525-532.
- Michalski, W.P., Hein, D.H. and Nicholas, D.J.D.** 1986. Purification and characterisation of nitrous oxide reductase from *Rhodopseudomonas sphaeroides* f. sp. *denitrificans*. *Biochim. Biophys. Acta.* **872**: 50-60.
- Mirvish, S.S.** 1975. Formation of *N*-nitroso compounds: Chemistry, kinetics and *in vivo* occurrence. *Toxicol. Appl. Pharmacol.* **31**: 325-351.
- Mirvish, S.S.** 1983. The etiology of gastric cancer. Intra-gastric nitrosamide formation and other theories. *J. Natl. Cancer Inst.* **71**: 629-647.
- Mirvish, S.S.** 1986. Effects of vitamins C and E on *N*-nitroso compound formation, carcinogenesis, and cancer. *Cancer.* **58**: 1842-1850.
- Mirvish, S.S.** 1995. Role of *N*-nitroso compounds (NOC) and *N*-nitrosation in etiology of gastric, esophageal, nasopharyngeal and bladder cancer and contribution to cancer of known exposures to NOC. *Cancer Letts.* **93**: 17-48.
- Mirvish, S.S., Wallcave, L., Eagen, M. and Shubik, P.** 1972. Ascorbate-nitrite reaction: Possible means of blocking the formation of carcinogenic *N*-nitroso compounds. *Science.* **177**: 65-68.
- Moir, J.W.B. and Ferguson, S.J.** 1994. Properties of *Paracoccus denitrificans* mutant deleted in cytochrome *c*₅₅₀ indicate that a copper protein can substitute for this cytochrome in electron transport and to nitrite, nitric oxide and nitrous oxide. *Microbiol.* **140**: 389-397.

- Moir, J.W.B., Baratta, D., Richardson, D.J. and Ferguson, S.J.** 1993. The purification of a cd₁-type nitrite reductase from, and the absence of a copper-type nitrite reductase from, the aerobic denitrifier *Thiosphaera pantrotropha*: the role of pseudooazurin as an electron donor. *Eur. J. Biochem.* **212**: 377-385.
- Møller, H., Landt, J., Pedersen, E., Jensen, P., Autrup, H. and Jensen, O.M.** 1989. Endogenous nitrosation in relation to nitrate exposure from drinking water and diet in a danish rural population. *Cancer Res.* **49**: 3117-3121.
- Nicholls, D.G. and Ferguson, S.J.** 1992. *Bioenergetics 2*. Academic Press, London.
- Nishiyama, M., Suzuki, J., Kukimoto, M., Ohnuki, T., Horinouchi, S. and Beppu, T.** 1993. Cloning and characterisation of a nitrite reductase gene from *Alcaligenes faecalis* and its expression in *Escherichia coli*. *J. Gen. Microbiol.* **139**: 725-733.
- Noji, S., Nohno, T., Saito, T. and Taniguchi, S.** 1989. The *narK* gene product participates in nitrate transport induced in *Escherichia coli* nitrate-respiring cells. *FEBS Letts.* **252**: 139-143.
- Nurizzo, D., Cutruzzolà, F., Arese, M., Bourgeois, D., Brunori, M., Cambillau, C. and Tegoni, M.** 1998. Conformational changes occurring upon reduction and NO binding in nitrite reductase from *Pseudomonas aeruginosa*. *Biochem.* **37**: 13987-13996.
- O'Connor, F., Buckley, M. and O'Morain, C.** 1995. *Helicobacter pylori* and gastric cancer. *Eur. J. Cancer Prevent.* **4**: 139-144.
- O'Donnell, C.M., Edwards, C. and Ware, J.** 1988. Nitrosamine formation by clinical isolates of enteric bacteria. *FEMS Letts.* **51**: 193-197.
- O'Donnell, C.M., Edwards, C., Corconan, G.D., Ware, J. and Edwards, P.R.** 1988. in 'The relevance of *N*-nitroso compounds to human cancer exposure and mechanisms.' Eds. Bartsch, H., O'Neill, I. and Schulte-Hermann, R. IARC Scientific publications No. 84, Lyon. pp400-403.
- O'Neill, G.P. and Söll, D.** 1990. Transfer RNA and the formation of a haem and chlorophyll precursor, 5-aminolevulinic acid. *Biofactors* **2**: 227-234.
- Packer, P.J., Van Acker, B., Reed, P.I., Haines, K., Thompson, M.H., Hill, M.J. and Leach, S.A.** 1990. The effect of gastric achlorhydria on the urinary recovery of nitrate in man: relevance to urinary nitrate as a measure of dietary nitrate exposure. *Carcinogenesis.* **11**: 1373-1376.

- Page, L., Griffiths, L. and Cole, J.A.** 1990. Dependent physiological roles of two independent pathways for nitrite reduction to ammonia by enteric bacteria. *Arch. Microbiol.* **154**: 349-354.
- Park, S.J. and Gunsalas, R.P.** 1995. Oxygen, iron, carbon and superoxide control of the fumarase *fumA* and *fumC* genes of *Escherichia coli* - role of *arcA*, *fnr* and *soxR* gene products. *J. Bacteriol.* **177**: 6255-6262.
- Park, S.J., Tseng, C.P. and Gunsalas, R.P.** 1995. Regulation of succinate dehydrogenase (*sdhCDAB*) operon expression in *Escherichia coli* in response to carbon supply and anaerobiosis - role of ArcA and FNR. *Mol. Microbiol.* **15**: 473-482.
- Parr, S.R., Barber, D., Greenwood, C. and Brunori, M.** 1977. The electron-transfer reaction between azurin and the cytochrome c oxidase from *Pseudomonas aeruginosa*. *Biochem. J.* **167**: 447-455.
- Parsonage, D., Greenfield, A.J. and Ferguson, S.J.** 1985. The high affinity of *Paracoccus denitrificans* cells for nitrate as an electron acceptor. Analysis of possible mechanisms of nitrate and nitrite movement across the plasma membrane and the basis for inhibition by added nitrite of oxidase activity in permeabilised cells. *Biochim. Biophys. Acta.* **807**: 81-95.
- Peakman, T., Crouzet, J., Mayaux, J.F., Busby, S., Mohan, S., Harborne, N., Wootton, J., Nicolson, R. and Cole, J.** 1990. Nucleotide sequence, organisation and structural analysis of the products of the genes in the *nirB-cysG* region of the *Escherichia coli* K-12 chromosome. *Eur. J. Biochem.* **191**: 315-323.
- Peoples, O.P. and Sinskey, A.J.** 1989. Poly- β -hydroxybutyrate biosynthesis in *Alcaligenes eutrohpus* H16. *J. Biol. Chem.* **264**: 15293-15297.
- Peterson, G.L.** 1977. A simplification of the protein assay method of Lowry *et al.* which is more generally applicable. *Analytical Biochem.* **83**: 346-356.
- Philippot, L., Clays-Josserand, A., Lensi, R., Trinsoutreau, I., Normand, P. and Porier, P.** 1997. Purification of the dissimilative nitrate reductase of *Pseudomonas fluorescens* and the cloning and sequencing of its corresponding genes. *Biochim. Biophys. Acta.* **1350**: 272-276.
- Pugsley, A.P., Chapon, C. and Schwartz, M.** 1986. Extracellular pullulanase of *Klebsiella pneumoniae* is a lipoprotein. *J. Bacteriol.* **166**: 1083-1088.
- Quandt, J. and Hynes, M.F.** 1993. Versatile suicide vectors which allow direct selection for gene replacement in Gram negative bacteria. *Gene.* **127**: 15-21.

- Rajagopalan, K.V. and Johnson, J.L.** 1992. The pterin molybdenum cofactors. *J. Biol. Chem.* **267**: 10199-10202.
- Ralt, D., Wishnok, J.S., Fitts, R. and Tannenbaum, S.R.** 1988. Bacterial catalysis of nitrosation: Involvement of the *nar* operon of *Escherichia coli*. *J. Bacteriol.* **170**: 359-364.
- Reed, P.I., Smith, P.L.R., Summer, K., Haines, K., Burgess, B.A., House, F.R. and Walter, C.L.** 1984. The influence of enterogastric reflux on gastric juice bacterial growth, nitrite, and *N*-nitroso compound concentrations following gastric surgery. *Scand. J. Gastroenterol.* **19**: S92. 232-234.
- Rice, P.A., Yang, S.W., Mizuuchi, K. and Nash, H.A.** 1996. Crystal structure of an IHF-DNA complex: A protein-induced DNA u-turn. *Cell.* **87**: 1295-1306.
- Richardson, D.J., Bell, L.C., Moir, J.W.B. and Ferguson, S.J.** 1994. A denitrifying strain of *Rhodobacter capsulatus*. *FEMS Letts.* **120**: 323-328.
- Richardson, D.J., McEwan, A.G., Page, M.D., Jackson, B. and Ferguson, S.J.** 1990. The identification of cytochromes involved in the transfer of electrons to the periplasmic NO₃⁻ reductase of *Rhodobacter capsulatus* and resolution of a soluble NO₃⁻-reductase - cytochrome-c₅₅₂ redox complex. *Eur. J. Biochem.* **194**: 263-270.
- Robertson, L.A. and Kuenen, J.G.** 1984. Aerobic denitrification: a controversy revived. *Arch. Microbiol.* **139**: 351-354.
- Rowe, J.J., Ubbink-Kok, T., Molenaar, D., Konings, W.N. and Driessen, A.J.M.** 1994. NarK is a nitrite-extrusion system involved in anaerobic nitrate respiration by *Escherichia coli*. *Mol. Microbiol.* **12**: 579-586.
- Ruddell, W.S.J., Bone, E.S., Hill, M.J. and Walter, C.L.** 1978. Pathogenesis of gastric cancer in pernicious anaemia. *Lancet.* March: 521-523.
- Sambrook, J., Fritsch, E.F. and Maniatis, T.** 1989. Molecular cloning: a laboratory manual. Second edition, Cold Spring Harbour Laboratory Press, Cold Spring Harbour, New York.
- Sanger, F.S., Nicklen, S. and Coulson, A.R.** 1977. DNA sequencing with chain terminating inhibitors. *Proc. Natl. Acad. Sci. USA.* **74**: 5463-5471.
- Sann, R., Kostka, S. and Friedrich, B.** 1994. A cytochrome cd₁-type nitrite reductase mediates the first step of denitrification in *Alcaligenes eutrophus*. *Arch. Microbiol.* **161**: 453-459.

- Satoh, T.** 1981. Soluble dissimilatory nitrate reductase containing cytochrome c from a photodenitrifier, *Rhodobacter sphaeroides* f. sp. *denitrificans*. *Plant & Cell Physiol.* **22**: 443-452.
- Sawada, E., Satoh, T. and Kitamura, H.** 1978. Purification and properties of a dissimilatory nitrite reductase of a denitrifying phototrophic bacterium. *Plant & Cell Physiol.* **19**: 1339-1351.
- Schembri, M.A., Bayly, R.C. and Davies, J.K.** 1995. Phosphate concentration regulates transcription of the *Acinetobacter* polyhydroxyalkanoic acid biosynthetic genes. *J. Bacteriol.* **177**: 4501-4507.
- Sears, H.J., Bennett, B., Spiro, S., Thomson, A.J. and Richardson, D.J.** 1995. Identification of periplasmic nitrate reductase Mo(V) EPR signals in intact cells of *Paracoccus denitrificans*. *Biochem. J.* **310**: 311-314.
- Sears, H.J., Ferguson, S.J., Richardson, D.J. and Spiro, S.** 1993. The identification of a periplasmic nitrate reductase in *Paracoccus denitrificans*. *FEMS Letts.* **113**: 107-112.
- Seery, J.P.** 1991. Achlorhydria and gastric carcinogenesis. *Lancet.* **338**: 1508-1509.
- Shanmugam, K.T., Stewart, V., Gunsalus, R.P., Boxer, D.H., Cole, J.A., Chippaux, M., DeMoss, J.A., Giordano, G., Lin, E.C.C. and Rajagopalan, K.V.** 1992. Proposed nomenclature for the genes involved in molybdenum metabolism in *Escherichia coli* and *Salmonella typhimurium*. *Mol. Microbiol.* **6**: 3451-3454.
- Shapleigh, J.P. and Payne, W.J.** 1985. Differentiation of cd_1 cytochrome and copper nitrite reductase production in denitrifiers. *FEMS Letts.* **26**: 275-279.
- Shearer, G.S. and Kohl, D.H.** 1988. Nitrogen isotopic fractionation and ^{18}O exchange in relation to the mechanism of denitrification of nitrite by *Pseudomonas stutzeri*. *J. Biol. Chem.* **263**: 13231-13245.
- Shuker, D.E.G.** 1988. in 'Nitrosamines: Toxicology and Microbiology'. Ed. Hill, M.J. Publ. VCH. pp48-67.
- Siddiqui, R.A., Warnecke-Eberz, U., Hengsberger, A., Schneider, B., Kostka, S. and Friedrich, B.** 1993. Structure and function of a periplasmic nitrate reductase in *Alcaligenes eutrophus* H16. *J. Bacteriol.* **175**: 5867-5876.

Silvestrini, M.C., Galeotti, C.L., Gervais, M., Schininà, E., Barra, D., Bossa, F. and Brunori, M. 1989. Nitrite reductase from *Pseudomonas aeruginosa*: sequence of the gene and the protein. *FEBS Letts.* **254**: 33-38.

Simon, R., Priefer, U. and Puhler, A. 1983. A broad host range mobilisation system for *in vivo* genetic engineering - transposon mutagenesis in gram negative bacteria. *Bio-technology.* **1**: 784-791.

Smith, G.B. and Teidje, J.M. 1992. Isolation and characterisation of a nitrite reductase gene and its use as a probe for denitrifying bacteria. *Appl. Environ. Microbiol.* **58**: 376-384.

Smith, N.A. 1994. Nitrate reduction and *N*-nitrosation in brewing. *J. Inst. Brew.* **100**: 347-355.

Snyder, S.W. and Hollocher, T.C. 1987. Purification and some characteristics of nitrous oxide reductase from *Paracoccus denitrificans*. *J. Biol. Chem.* **263**: 2136-2323.

Sobala, G.M., Pignatelli, B., Schorah, C.J., Bartsch, H., Sanderson, M., Dixon, M.F., Shires, S., King, R.H.F. and Axon, A.T.R. 1991. Levels of nitrite, nitrate, *N*-nitroso compounds, ascorbic acid and total bile acids in gastric juice of patients with and without precancerous conditions of the stomach. *Carcinogenesis.* **12**: 193-198.

Sobala, G.M., Schorah, C.J., Sanderson, M., Dixon, M.F., Tompkins, D.S., Godwin, P. and Axon, A.T.R. 1989. Ascorbic acid in the human stomach. *Gastroenterol.* **97**: 357-363.

Solomonson, L.P. and Barber, M.J. 1990. Assimilatory nitrate reductase: Functional properties and regulation. *Ann. Rev. Plant Physiol. Plant Mol. Biol.* **41**: 225-253.

Sowerby, Z. 1997. Bacterial *N*-nitrosation and nitrite reduction in the model organism *Neisseria subflava*. PhD. Thesis. Nottingham Trent University.

Spiro, S. 1992. An FNR-dependent promoter from *Escherichia coli* is active and anaerobically inducible in *Paracoccus denitrificans*. *FEMS Letts.* **98**: 145-148.

Spiro, S. 1994. The FNR family of transcriptional activators. *Antonie Leeuwenhoek.* **66**: 23-36.

- Spiro, S. and Guest, J.R.** 1991. Adaptive responses to oxygen limitation in *Escherichia coli*. *TIBS*. Aug: 310-314.
- Srivenugopal, K.S., Lockshon, D. and Morris, D.R.** 1984. *Escherichia coli* DNA topoisomerase III: purification and characterisation of a new Type I enzyme. *Biochemistry*. **23**: 1899-1906.
- Stewart, V.** 1993. Nitrate regulation of anaerobic respiratory gene expression in *Escherichia coli*. *Mol. Microbiol.* **9**: 425-434.
- Stewart, V.** 1994. Dual interacting two-component regulatory systems mediate nitrate- and nitrite-regulated gene expression in *Escherichia coli*. *Res. Microbiol.* **145**: 450-454.
- Stich, H.F., Karim, J., Koropatnick, J. and Lo, L.** 1976. Mutagenic action of ascorbic acid. *Nature*. **260**: 722-724.
- Stockbrügger, R.W., Cotton, P.B., Eugenides, N., Bartholomew, B.A., Hill, M.J. and Walters, C.L.** 1982. Intra-gastric nitrites, nitrosamines, and bacterial overgrowth during cimetidine treatment. *Gut*. **23**: 1048-1054.
- Stockbrügger, R.W., Cotton, P.B., Menon, G.G., Beilby, J.O.W., Bartholomew, B.A., Hill, M.J. and Walters, C.L.** 1984. Pernicious anaemia, intra-gastric bacterial overgrowth, and possible consequences. *Scand. J. Gastroenterol.* **19**: 355-364.
- Stouthammer, A.H.** 1988. in 'The Biology of Anaerobic Microorganisms'. Ed. Zehader, A.J.B. Publ. J. Wiley and Sons. pp245-293.
- Strange, R.W., Dodd, F.E., Abraham, Z.H.L., Günter Grossman, J., Brüser, T., Eady, R.R., Smith, B.E. and Hasnain, S.S.** 1995. The substrate-binding site in Cu nitrite reductase and its similarity to Zn carbonic anhydrase. *Structural Biol.* **2**: 287-293.
- Suppmann, B. and Sawers, G.** 1994. Isolation and characterisation of hypophosphite-resistant mutants of *Escherichia coli*; identification of the FocA protein, encoded by the *pfl* operon, as a putative formate transporter. *Mol. Microbiol.* **11**: 965-982.
- Suzuki, S., Yoshimura, T., Kohzuma, T., Shidara, S., Masuko, M., Sakurai, T. and Iwasaki, H.** 1989. Spectroscopic evidence for a copper-nitrosyl intermediate in nitrite reduction by blue copper-containing nitrite reductase. *Biochem. Biophys. Res. Comm.* **164**: 1366-1372.

Sylvestrini, M.C., Galeotti, C.L., Gervais, M., Schinina, E., Barra, D., Bossa, F. and Brunori, M. 1989. Nitrite reductase from *Pseudomonas aeruginosa*: sequence of the gene and the protein. *FEBS Letts.* **254**: 33-38.

Tan, K.A.L. 1997. Molecular characterisation of a sodium-dependent NADH-ubiquinone oxidoreductase from *Vibrio alginolyticus*. PhD. Thesis. Edinburgh University.

Tanaka, K., Hayatsu, T., Negishi, T. and Hayatsu, H. 1998. Inhibition of *N*-nitrosation of secondary amines *in vitro* by tea extracts and catechins. *Mutation Res. - Genet. Toxicol. Environ. Mutagenesis.* **412**: 91-98.

Tannenbaum, S.R., Wishnok, J.S. and Leaf, C.D. 1991. Inhibition of nitrosamine formation by ascorbic acid. *Am. J. Clin. Nutr.* **53**: 247S-250S.

Timkovich, R., Dhesi, R., Martinkus, K.J., Robinson, M.K. and Rea, T.M. 1982. Isolation of *Paracoccus denitrificans* cytochrome cd_1 : Comparative kinetics with other nitrite reductases. *Arch. Biochem. Biophys.* **215**: 47-58.

Tyson, K.L., Cole, J.A. and Busby, S.J.W. 1994. Nitrite and nitrate regulation at the promoters of two *Escherichia coli* operons encoding nitrite reductase: identification of common target heptamers for both NarP- and NarL- dependent regulation. *Mol. Microbiol.* **13**: 1045-1055.

Uden, G. and Trageser, M. 1991. Oxygen regulated gene expression in *Escherichia coli* - Control of anaerobic respiration by the FNR protein. *Antonie Leeuwenhoek.* **59**: 65-76.

van Spanning, R.J.M., de Boer, A.P.N., Reijnders, W.N.M., de Geir, J.-W.L., Delorme, C.O., Stouthammer, A. H., Westerhoff, H.V., Harms, N. and van der Oost, J. 1995. Regulation of oxidative phosphorylation: the flexible respiratory network of *Paracoccus denitrificans*. *J. Bioenerg. Biomemb.* **27**: 499-512.

van Spanning, R.J.M., Wansell, C., Harms, N., Oltmann, L.F. and Stouthamer, A.H. 1990. Mutagenesis of the gene encoding cytochrome c_{550} of *Paracoccus denitrificans* and analysis of the resultant physiological effects. *J. Bacteriol.* **172**: 986-996.

Völkl, P., Huber, R., Drobner, E., Rachel, R., Burggrat, S., Trincove, A. and Stetter, K.O. 1993. *Pyrobaculum aerophilum* sp. nov., a novel nitrate reducing hyperthermophilic Archaeum. *Appl. Environ. Microbiol.* **59**: 2918-2926.

- Wanner, B.L.** 1987. In, *E. coli* and *S. typhimurium*; cellular and molecular biology. Vol. 2: pp. 1326-1333. Ed. Frederick C. Neidhardt. American Society for Microbiology, Washington D.C.
- Ward, B.B., Cockcroft, A.R. and Kilpatrick, K.A.** 1993. Antibody and DNA probes for detection of nitrite reductase in seawater. *J. Gen. Microbiol.* **139**: 2285-2293.
- Weeg-Aerssens, E., Wu, W., Ye, R.W., Teidje, J.M. and Chang, C.K.** 1991. Purification of cytochrome cd₁ nitrite reductase from *Pseudomonas stutzeri* JM300 and reconstitution with native synthetic haem d₁. *J. Biol. Chem.* **266**: 7496-7502.
- Wharton, D.C., Gudat, J.C. and Gibson, Q.H.** 1973. Cytochrome oxidase from *Pseudomonas aeruginosa*. II. Reaction with copper protein. *Biochim. Biophys. Acta.* **292**: 611-620.
- Wikström, M., Bogachev, A., Finel, M., Morgan, J.E., Puustinen, A., Raitio, M., Verkhovskaya, M. and Verkhovsky, M.I.** 1994. Mechanism of proton translocation by the respiratory oxidases. The histidine cycle. *Biochim. Biophys. Acta.* **1187**: 106-111.
- Williams, P.A., Fülöp, V., Garman, E.F., Saunders, N.F.W., Ferguson, S.J. and Hajdu, J.** 1997. Haem-ligand switching during catalysis in crystals of a nitrogen cycle enzyme. *Nature.* **389**: 406-412.
- Williams, S.B. and Stewart, V.** 1997. Nitrate- and nitrite-sensing protein NarX of *Escherichia coli* K-12: Mutational analysis of the amino-terminal tail and first transmembrane segment. *J. Bacteriol.* **179**: 721-729.
- Wolf, S.A. and Smith, J.M.** 1988. Nucleotide sequence analysis of the *purA* gene encoding adenylosuccinate synthetase of *Escherichia coli* K12. *J. Biol. Chem.* **263**: 19147-19153.
- Yanisch-Peron, C., Vieira, J. and Messing, J.** 1985. Improved M13 phage cloning vectors and host strains: nucleotide sequences of the M13mp18 and pUC19 vectors. *Gene.* **33**: 103-119.
- Ye, R.W., Averill, B.A. and Teidje, J.M.** 1992. Characterisation of Tn5 mutants deficient in dissimilatory nitrite reduction in *Pseudomonas* sp. strain G-179, which contains a copper nitrite reductase. *J. Bacteriol.* **174**: 6653-6658.
- Ye, R.W., Averill, B.A. and Tiedje, J.M.** 1994. Denitrification - production and consumption of nitric oxide. *Appl. Environ. Microbiol.* **60**: 1053-1058.

Ye, R.W., Fries, M.R., Bezborodnikov, S.G., Averill, B.A. and Teidje, J.M. 1993. Characterisation of the structural gene encoding a copper-containing nitrite reductase and homology of this gene to DNA of other denitrifiers. *Appl. Environ. Microbiol.* **59**: 250-254.

Ye, R.W., Haas, D., Ka, J.O., Krishnapillai, V., Zimmerman, A., Baird, C. and Tiedje, J.M. 1995. Anaerobic activation of the entire denitrification pathway in *Pseudomonas aeruginosa* requires ANR, an analog of FNR. *J. Bacteriol.* **177**: 3606-3609.

Zimmerman, A., Reimann, C., Galimand, M. and Haas, D. 1991. Anaerobic growth and cyanide synthesis of *Pseudomonas aeruginosa* depend on ANR, a regulatory gene homologous with FNR of *Escherichia coli*. *Mol. Microbiol.* **5**: 1483-1490.

Zumft, W.G. 1997. Cell biology and the molecular basis of denitrification. *Microbiol. Mol. Biol. Revs.* **61**: 533-616.

Zumft, W.G., Braun, C. and Cuypers, H. 1994. Nitric oxide reductase from *Pseudomonas stutzeri*. Primary structure and gene organisation of a novel bacterial cytochrome bc complex. *Eur. J. Biochem.* **219**: 481-490.

Zumft, W.G., Döhler, K. and Körner, H. 1985. Isolation and characterisation of transposon Tn5-induced mutants of *Pseudomonas perfectomarina* defective in nitrous oxide respiration. *J. Bacteriol.* **163**: 918-924.

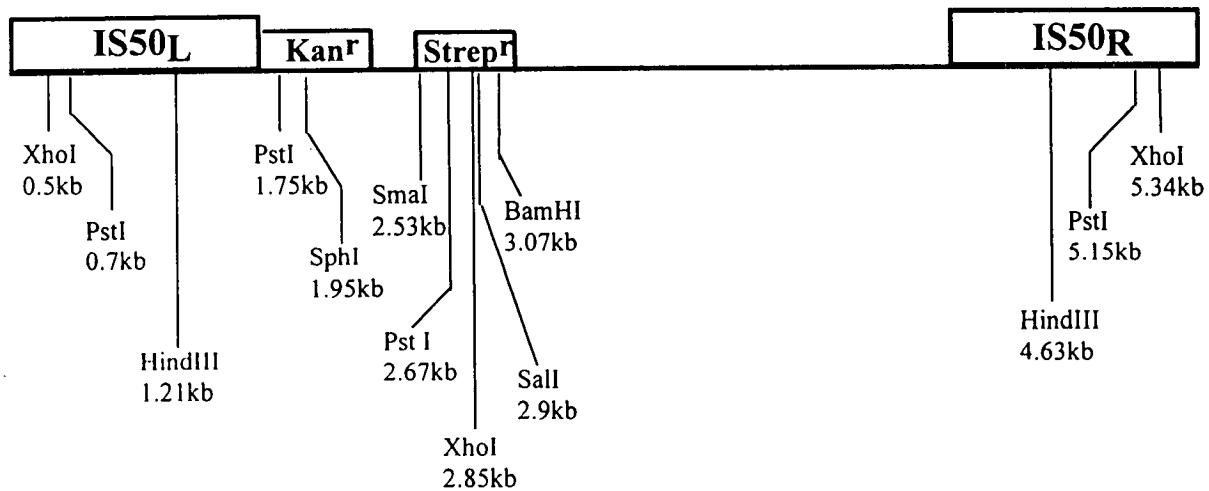
Zumft, W.G., Döhler, K., Körner, S., Löchelt, S., Viebrock, A. and Frunzke, K. 1988. Defects in cytochrome cd_1 -dependent nitrite respiration of transposon Tn5-induced mutants from *Pseudomonas stutzeri*. *Arch. Microbiol.* **149**: 492-498.

Zumft, W.G., Dreusch, A., Löchelt, S., Cuypers, H., Freidrich, B. and Schneider, B. 1992. Derived amino acid sequences of the *nosZ* gene (respiratory N_2O reductase) from *Alcaligenes eutrophus*, *Pseudomonas aeruginosa* and *Pseudomonas stutzeri* reveal potential copper-binding residues. Implications for the Cu_A site of N_2O reductase and cytochrome c oxidase. *Eur. J. Biochem.* **208**: 31-40.

Zumft, W.G., Gotzmann, D.J. and Kroneck, P.M.H. 1987. Type I, blue copper proteins constitute a respiratory nitrite-reducing system in *Pseudomonas aureofaciens*. *Eur. J. Biochem.* **168**: 301-307.

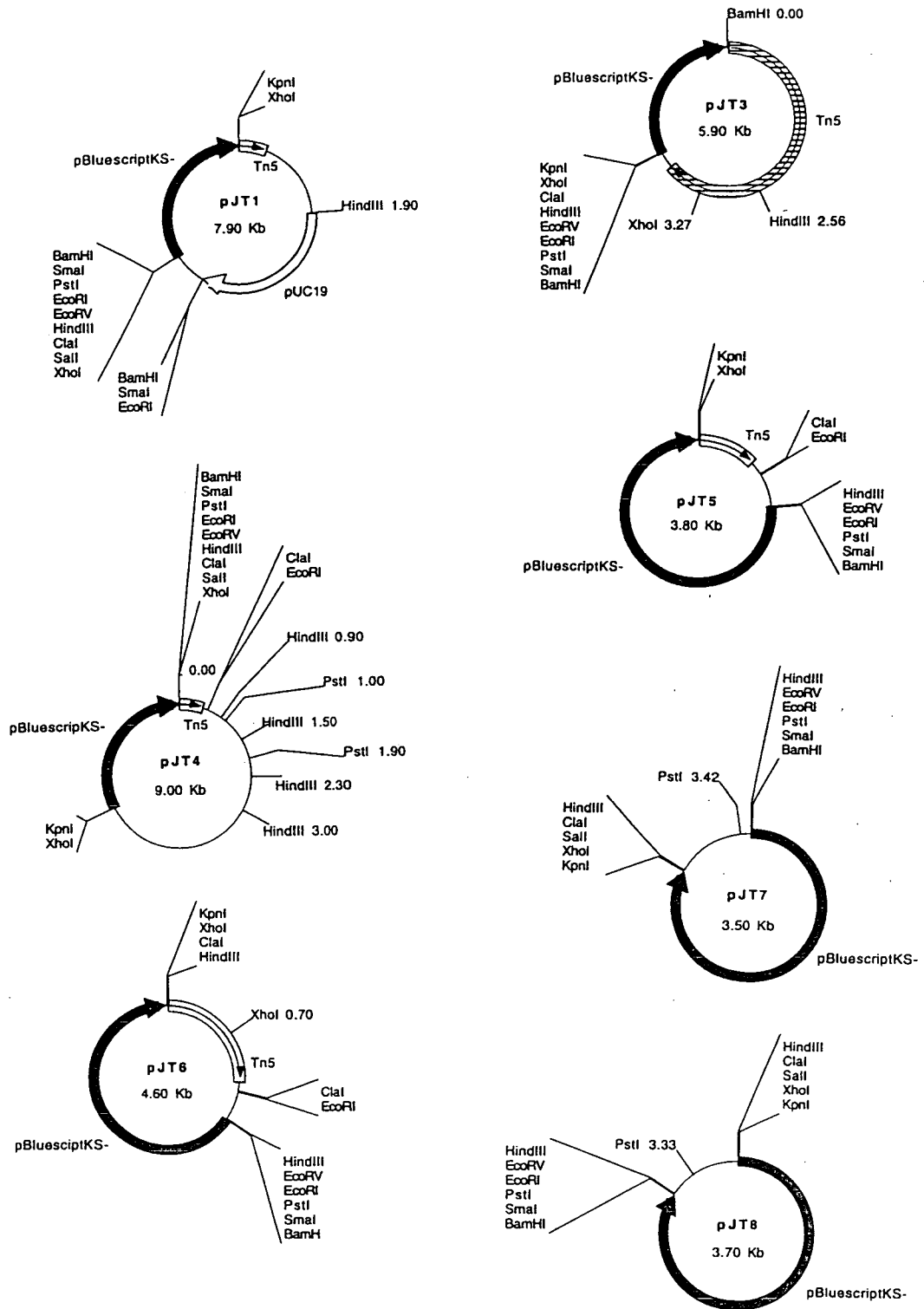
Zumft, W.G., Viebrock, A. and Körner, H. 1988. in 'The nitrogen and sulphur cycles', SGM symposium 42. Eds. Cole, J.A. and Ferguson, S.J., Publ. Cambridge University Press. pp245-279.

Appendix

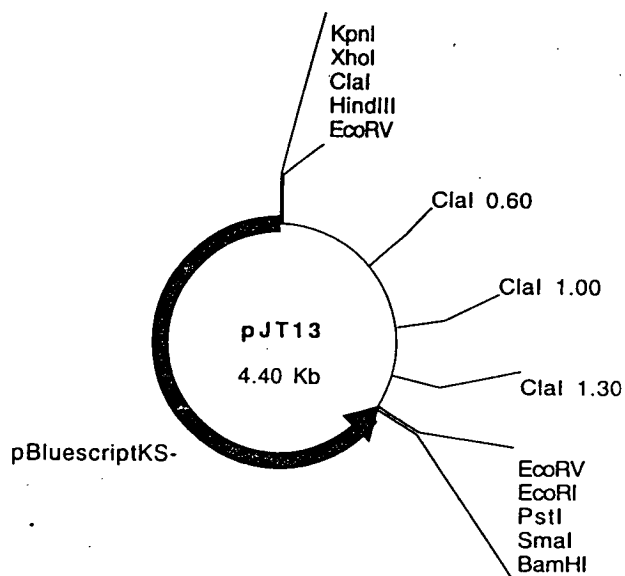
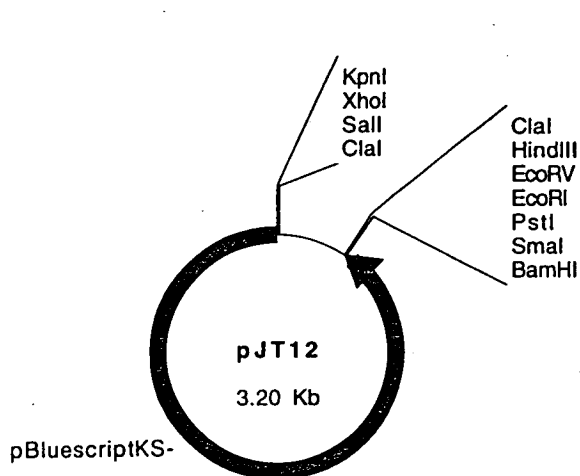
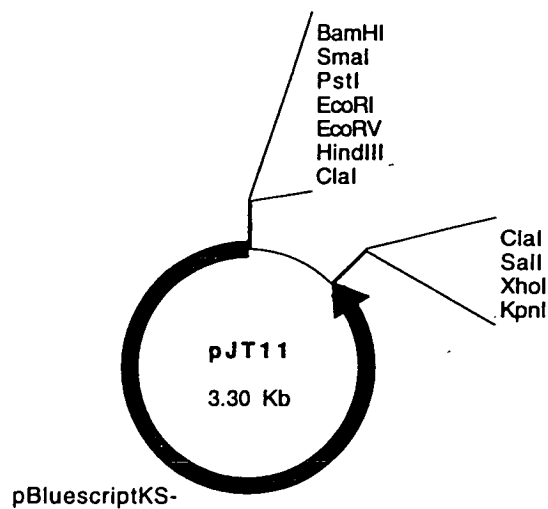
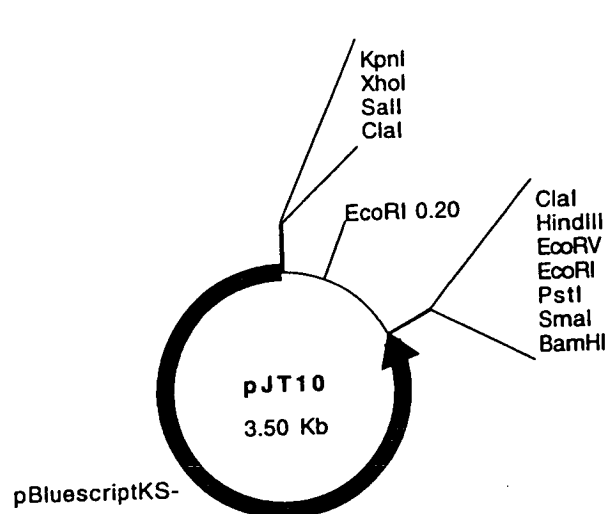


Enzymes that do not cut:
EcoRI, EcoRV, KpnI, ClaI.

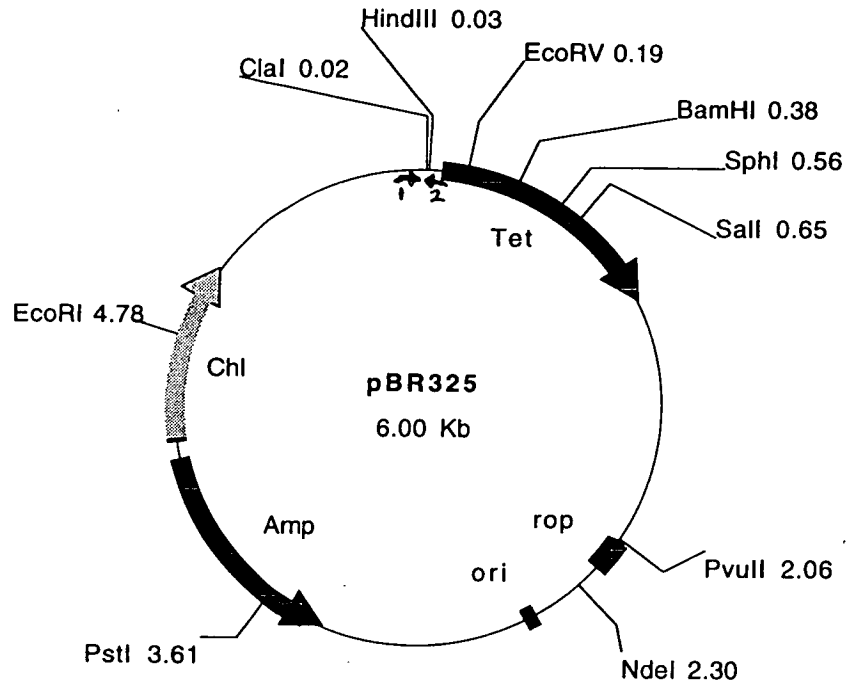
Appendix A1. Restriction map of transposon Tn5 (ChemWindow).



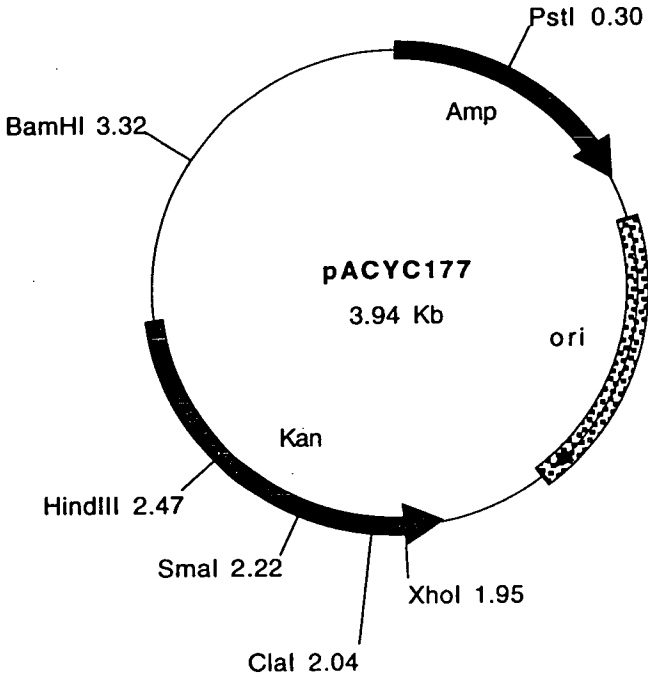
Appendix A2. Plasmids constructed for sequencing pZS163.



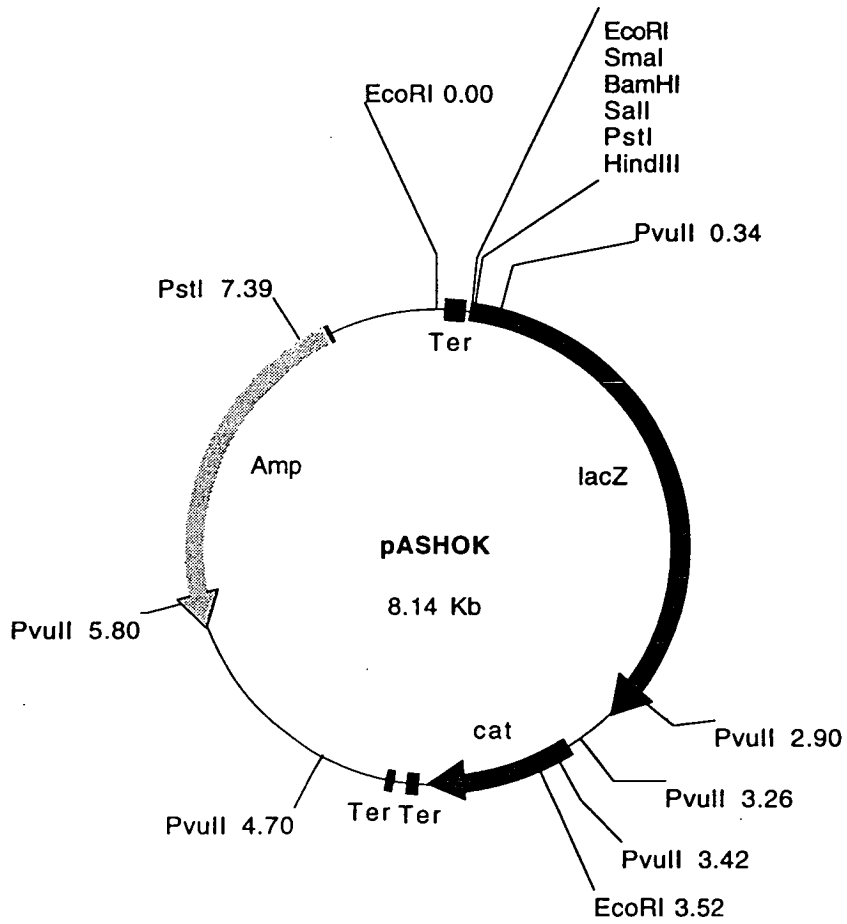
Appendix A3. Plasmids constructed for sequencing pJT170.



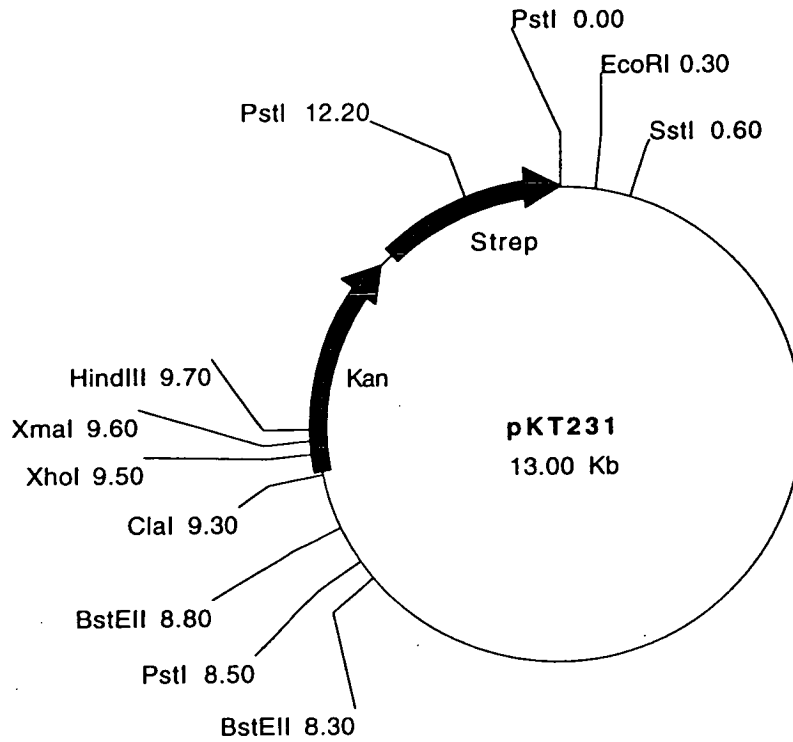
Appendix A4. Map of pBR325.



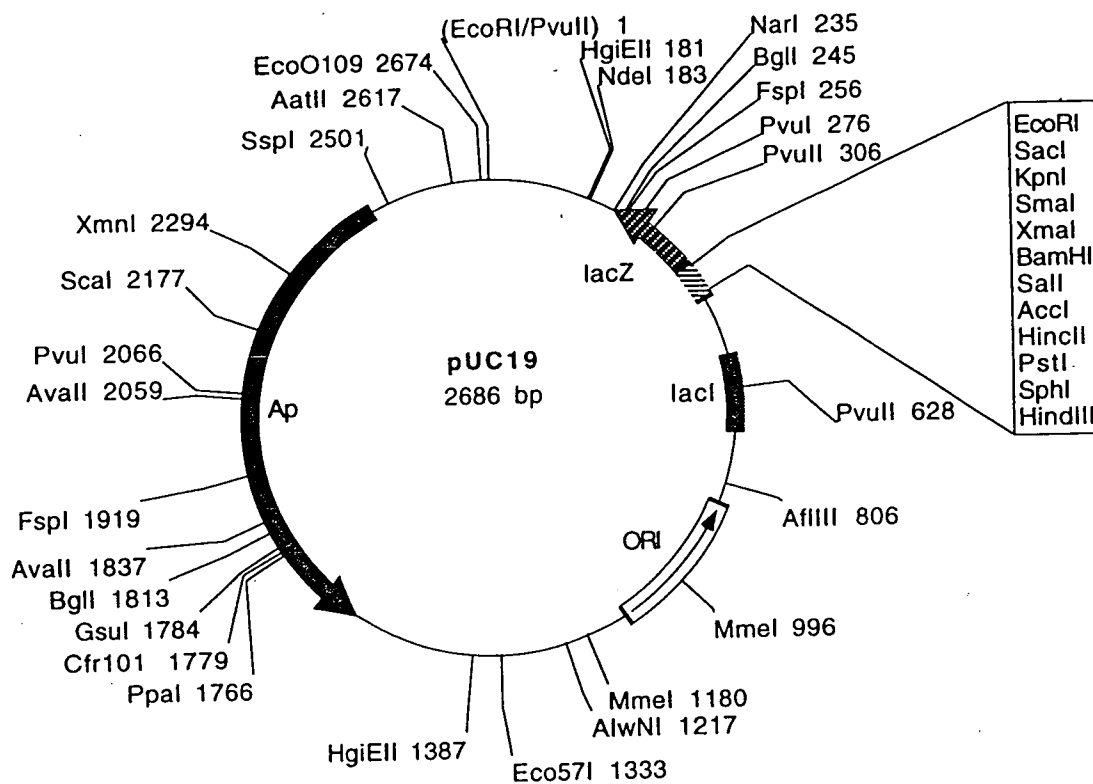
Appendix A5. Map of pACYC177.



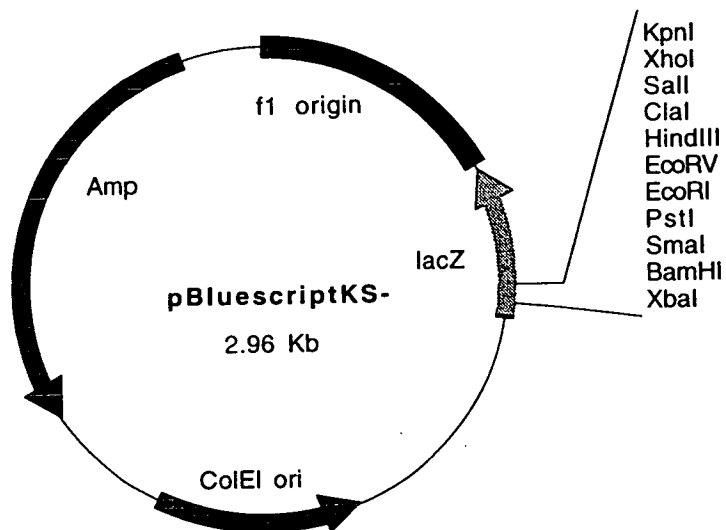
Appendix A6. Map of pASHOK.



Appendix A8. Map of pKT231.



Appendix A9. Map of pUC19.



Appendix A10. Map of pBluescript KS⁺.